

**A Systematic Analysis of Two-Component Systems
of *Streptomyces* spp.**

Rebecca Lo

A thesis submitted for a Biomolecular sciences research degree of
Doctor of Philosophy
University of East Anglia
School of Biological Sciences

May 2019

© This copy of the thesis has been supplied on condition that anyone who consults it is understood to recognise that its copyright rests with the author and that use of any information derived there from must be in accordance with current UK Copyright Law.

Abstract

Found in all domains of life, two-component systems (TCSs) are signal transduction pathways which are canonically composed of a membrane bound sensor kinase (SK) and a cognate response regulator (RR). Upon stimulation, the SK relays the signal to the RR through transfer of a phosphate group to a conserved aspartate residue. The active RR~P is then able to modulate gene expression in response to the initial stimulus. This output could be the regulation of metabolite production, development or movement for example.

Streptomyces species encode a high number of TCSs which reflects the multitude of environmental challenges they must face. *Streptomyces* species are prolific producers of bioactive natural products (NPs) and account for over half of the clinically used antibiotics. Many TCSs have been shown to regulate antibiotic biosynthesis including the global regulators MtrAB and AfsQ1/Q2. The newly emerging model organism *S. venezuelae* possesses 59 TCSs and a predicted 30 NP biosynthetic gene clusters. In this work, a library of TCS operon deletion mutants were generated through PCR targeting and CRISPR/Cas9 gene editing. High throughput screening of this library as well as a more targeted approach through analysis of potential regulons has been utilised in an effort to characterise these mutants. In this study, through analysis of adjacent genes, a TCS was identified to regulate tunicamycin resistance (TunRS; Sven15_3170/71).

Another TCS which mediates antibiotic resistance is VanRS, in response to vancomycin. Vancomycin is a glycopeptide antibiotic widely used in clinics to treat infections caused by Gram-positive bacteria such as *Staphylococcus aureus* and *Clostridium difficile*, for example. With the emergence and spread of vancomycin resistance, it is important to understand not just the mechanism of resistance but also the mechanism of recognition. This is with the aim to develop a means of sequestering recognition and resistance. It is currently unclear whether vancomycin binds directly to the SK (VanS) or first binding and forming a complex with another cell component. Here, work has been presented on the purification of the membrane protein VanS with the aim of elucidating the mechanism of vancomycin and VanS interaction.

The study of TCSs shows us how bacteria link their external surroundings with adaptive responses. The study of TCSs allows us to better understand not just how bacteria perceive their surroundings but could be used as a means to activate biosynthetic gene clusters of desirable products such as bioactives. With many TCSs in the genus *Streptomyces* uncharacterised, TCSs were rewired in an effort to activate antibiotic production through the RR AfsQ1 via the non-cognate SK VanS, which is involved in vancomycin resistance. The *in vitro* and *in vivo* analyses carried out in this investigation to test the effects of these chimeras, have produced results which are inconclusive in determining whether the use of vancomycin is able to activate antibiotic production through an AfsQ1-dependent pathway.

Acknowledgements

Firstly, I would like to thank my supervisor, Professor Matt Hutchings for all the encouragement, ideas and help to both get me through my PhD and development into a researcher. Additionally, thank you to my secondary supervisor, Dr Tom Clarke for giving me so much advice and support particularly in the protein purification arena which without your help I would have been even more lost.

To everyone in the Hutch Lab, both past and present, I am eternally grateful for all your kindness and support. Thank you to Elaine! I always describe you as being fairy-like because you're simply magical. Thank you, John and Rhiannah. You have both taught me so much not just in science but in all aspects of life. In meeting you, I feel I have gained not just friends for life but family. Thank you, Nicolle, for being an amazing example and mentor, Rebecca for all your help on bioassays, Sarah for all the qRT-PCR advice, Jake for putting up with me calling you 'lil' bro and Neil and Mahmoud for all your advice. From the John Innes Centre, a special thank you to Govind for all the bioinformatics help and analysis and also the Biological Chemistry Department over my internship and during my resubmission period. I would definitely have lost my mind without your guidance and support.

To my family, thank you does not begin to demonstrate my gratitude and love for you all. I am so very sorry for all the grief I have put you through. Thank you for always supporting me and sticking with me through thick and thin. Joshua, your birth in the final months of my PhD gave me the push I needed to finish. To my father, I know you are smiling down at me. Whenever I feel lost, I need only think of what you would say. Finally, I need to thank Joanna. My oldest and dearest friend for being so accepting and generous. I hope to be as great a friend to you as you have been to me.

In the last four years, I have encountered so many amazing people who have made my journey smoother and helped me overcome a lot of difficulties. Thank you all; I think you all know who you are. You've made such a huge impact on my life and in making me who I am today.

Abbreviations

1G	10% Glycerol
2G	20% Glycerol
4G	40% Glycerol
acyl-D-Ala-D-Ala	acyl-D-alanyl-D-alanine
ACT	Actinorhodin
Ala	Alanine residue
amp	Ampicillin
ampR	Ampicillin resistance
AMP	Adenosine monophosphate
ANTAR	AmiR and NasR transcriptional anti-terminator regulator domain
apr	Apramycin
APS	Ammonium persulphate
aprR	Apramycin resistance
Arg	Arginine residue
ARR	Atypical response regulator
Asn	Asparagine residue
Asp	Aspartate residue
<i>bld</i>	Bald gene
BGC	Biosynthetic gene cluster
bp	Base pair
BTAD	Bacterial transctional activation domain
CA	Catalytic and ATPase domain
cAMP	Cyclic-adenosine monophosphate
CDA	Calcium-dependent antibiotic
c-di-AMP	Cyclic-di-adenosine monophosphate
cml	Chloramphenicol
cmlR	Chloramphenicol resistance
CRISPR	Clustered regularly interspaced short palindromic repeats
crRNA	CRISPR RNA

CSR	Cluster situated regulator
D-Ala-D-Ala	D-alanyl-D-alanine
D-Ala-D-Lac	D-alanyl-D-lactate
D-Ala-D-Ser	D-alanyl-D-serine
Dhp	Dimerisation and phosphotransfer domain
DSB	Double stranded break
DUF	Domain of unknown function
EMSA	Electrophoretic mobility shift assays
FIS	Factor of inversion stimulation
FPLC	Fast protein liquid chromatography
GAF	cGMP-regulated cyclic nucleotide phosphodiesterases, adenylate cyclases, and the bacterial transcriptional regulator FhlA
Gly	Glycine residue
GMP	Guanosine monophosphate
cGMP	Cyclic-guanosine monophosphate
c-di-GMP	Cyclic-di-guanosine monophosphate
His	Histidine residue
HisKA	Histidine kinase domain A
HK	Histidine kinase
HPt	Histidine phosphotransferase
HR	Homologous recombination
HTH	Helix-turn-helix
dH ₂ O	Distilled water
H ₂ O ₂	Hydrogen peroxide
HWE	H, W and E amino acid residues within conserved boxes of the kinase core
hyg	Hygromycin
hygR	Hygromycin resistant

IMHK	Intramembrane histidine kinase
KO	Knockout
NO	Nitric oxide
HAMP	Histidine kinases, Adenylyl cyclases, Methyl-accepting chemotaxis proteins, and Phosphatases
kan	Kanamycin
kanR	Kanamycin resistance
kanS	Kanamycin sensitivity
Leu	Leucine residue
LGT	Lateral gene transfer
LSE	Lineage specific expansion
Lys	Lysine residue
MCP	Methyl-accepting chemotaxis proteins
MM	Minimum medium
MRE	Methicillin resistant <i>Enterococcus</i>
MRSA	Methicillin resistant <i>Staphylococcus aureus</i>
NHEJ	Non-homologous end joining
NRPS	Non-ribosomal peptide synthase
nt	Nucleotide
OD	Optical density
<i>oriT</i>	Origin of transfer
OE	Overexpression
PAM	Protospacer adjacent motif
PAS	Period circadian, aryl hydrocarbon receptor nuclear translocator, and single-minded proteins
PCR	Polymerase chain reaction
PDC	PhoQ/DcuS/CitA
PKS	Polyketide synthase
pRLxxx	Plasmids from this work
Pro	Proline
<i>pyr-redox</i>	Pyridine nucleotide-disulphide oxidoreductase
<i>ram</i>	Rapid aerial mycelium

RLxxxx	Primers from this work
REC	Receiver domain
RED	Undecylprodigiosin
RPSBLAST	Reverse PSI-BLAST
RR	Response regulator
RT	Room temperature
SapB	Spore associated protein B
SALP	SsgA like proteins
SARP	<i>Streptomyces</i> antibiotic regulator protein
Ser	Serine residue
SffA	SpoIIIE/FtsK family protein A
sgRNA	Synthesised guide RNA
SFM	Soya flour mannitol media
SK	Sensor kinase
TCS	Two-component system
TEMED	Tetramethylethylenediamine
thio	Thiostrepton
thioR	Thiostrepton resistance
Thr	Threonine residue
TM	Transmembrane
TPR	Tetratricopeptide
tracrRNA	Trans-activating crRNA
TSS	Transcriptional start site
USP	Universal stress protein
UTR	Untranslated region
van	vancomycin
<i>whi</i>	White genes
<i>wbl</i>	<i>whiB</i> -like
WT	Wild-type
yCPK	Yellow cryptic polyketide (coelimycin P2)

Table of Contents

Abstract	2
Acknowledgements	4
Abbreviations	5
Table of Contents	9
Table of Figures	14
Table of Tables	27
1. Introduction	29
1.1 Two-Component Systems	30
1.1.1 Sensor Kinases	31
1.1.1.1 Sensor and Transmembrane Domain	33
1.1.1.2 Signal Transduction Domains	36
1.1.1.3 Kinase Core	38
1.1.2 Response Regulators	40
1.1.2.1 REC domain	40
1.1.2.2 Effector domain	41
1.1.2.3 Transcriptional Activators	41
1.1.2.4 Protein binding, enzymatic activity and transporters	44
1.1.3 Evolution of new TCSs and the impact on partnering of SKs and RRs	45
1.1.3.1 Evolution of TCSs	45
1.1.3.2 Specificity of pairing between SKs and cognate RRs	46
1.1.4 Regulation of TCSs	47
1.1.4.1 Phosphatase activity	47
1.1.4.2 TCS expression	48
1.1.5 TCS variants	49
1.1.5.1 Orphans	49
1.1.5.2 Hybrid TCSs	50
1.1.5.3 Multiple component systems	52
1.1.6 Potentials of TCSs to be used as antibiotic targets and targets for antibiotic production	52
1.2 <i>Streptomyces</i>	54
1.2.1 Streptomyces: nature's pharmaceuticals	55
1.2.2 Life cycle	57

1.2.3 Secondary metabolite production.....	63
1.2.3.1 Actinorhodin.....	65
1.2.3.2 Undecylprodigiosin	66
1.2.3.3 Cryptic polyketide	67
1.2.3.4 Calcium-dependent antibiotic.....	71
1.3 TCSs of <i>Streptomyces</i>.....	72
1.3.1 Global regulators.....	73
1.3.1.1 MtrAB	73
1.3.1.2 AfsQ1/Q2	75
1.3.2 Stress Regulators.....	79
1.3.2.1 PhoPR.....	79
1.3.2.2 CseBC.....	80
1.3.2.3 VanRS	82
1.3.3 Specific Antibiotic Regulator.....	84
1.3.3.1 AbsA1/A2.....	84
1.4 Aims and Objectives.....	85
2. Material and Methods.....	87
2.1 Strains, culture conditions and storage	87
2.1.1 Strains and vector generation	87
2.1.2 Growth of strains and storage.....	130
2.1.3 Preparation of <i>Streptomyces</i> spores.....	132
2.1.4 Glycerol stocks.....	133
2.1.5 Centrifugation	133
2.2 Genetic Manipulation.....	133
2.2.1 DNA/RNA preparation	133
2.2.1.1 Plasmid preparation.....	133
2.2.1.2 Cosmid Preparation	133
2.2.1.3 <i>Streptomyces</i> genomic DNA preparation	134
2.2.1.4 RNA purification.....	135
2.2.2 Genetic Manipulation and Analysis Techniques.....	136
2.2.2.1 DNA/RNA analysis.....	136
2.2.2.2 Polymerase chain reaction (PCR).....	136
2.2.2.3 General restriction digest.....	136
2.2.2.4 Vector dephosphorylation	136
2.2.2.5 Ligations.....	137
2.2.2.6 Gibson Assembly	137
2.2.2.7 Preparation of competent cells	137

2.2.2.8 Chemical transformation	138
2.2.2.9 Electroporation transformation	138
2.2.2.10 Agarose gel electrophoresis	138
2.2.2.11 DNA extraction from agarose gel	139
2.2.3 PCR targeted gene editing	139
2.2.4 Gene editing through CRISPR/Cas9	143
2.2.5 RNA analysis	148
2.2.5.1 Reverse transcription	148
2.2.5.2 qRT-PCR	148
2.3 Protein Methodology	149
2.3.1 Protein preparation	149
2.3.1.1 Protein overexpression in <i>E. coli</i> and cell lysis	149
2.3.1.2 Cell lysis (<i>Streptomyces</i>)	149
2.3.1.3 Measuring protein concentration through Bradford assay	150
2.3.2 Protein Analysis	150
2.3.2.1 SDS-PAGE	150
2.3.2.2 Coomassie blue staining	150
2.3.2.3 Immuno-blot analysis	151
2.3.2.4 Phos-tag assay	151
2.3.2.5 Ponceau S staining	152
2.3.3 Protein purification from overexpression in <i>E. coli</i>	152
2.3.3.1 Overexpression and Lysis	152
2.3.3.2 Membrane protein separation	152
2.3.3.3 Purification with Ni ²⁺ NTA agarose beads	153
2.3.3.4 Purification with Ni ²⁺ His-Trap columns of VanS from <i>E. coli</i>	153
2.3.3.5 Sepharose size exclusion separation	154
2.3.4 Post purification protein treatment	154
2.3.4.1 Buffer exchange	154
2.3.4.2 Enterokinase treatment	154
3. Generation of a TCS deletion library in <i>S. venezuelae</i>	156
3.1 Chapter Overview	156
3.2 Introduction	156
3.3 Results.....	158
3.3.1 <i>In silico</i> analysis of the TCSs of <i>S. venezuelae</i>	158
3.3.1.1 Genome wide TCSs and related proteins	158
3.3.1.2 Paired TCSs of <i>S. venezuelae</i>	162
3.3.1.3 Conservation of TCSs	169

3.3.1.4 Adjacent genes of these TCSs	176
3.3.2 Generation of a TCSs deletion library.....	178
3.3.2.1 PCR targeting	179
3.3.2.2 CRISPR/Cas9	180
3.3.2.3 TCSs to be deleted.....	183
3.3.3 Characterisation of TCS deletion mutants	184
3.3.3.1 $\Delta 1773/74$	184
3.3.3.2 $\Delta 3170/71$	186
3.3.3.3 $\Delta 3682/83$	189
3.4 Discussion	190
3.4.1 Distribution of TCSs within the genome.....	190
3.4.2 Generating a paired TCS deletion library	191
3.4.3 Characterisation of specific deletion mutants	192
3.4.4 Characterisation of deletion library.....	194
3.4.5 Further characterisation of TCSs.....	195
4. Exploring purification methods of a full-length SK.....	197
4.1 Chapter overview.....	197
4.2 Introduction	197
4.3 Results.....	200
4.3.1 Generation of VanS overexpression vector.....	200
4.3.2 Overexpression of VanS	201
4.3.3 Truncation of VanS-His	204
4.3.4 Purification and storage of His-GST-VanS.....	208
4.3.5 Cleavage of GST and His tag.....	215
4.4 Discussion	216
5. Rewiring TCS Systems; A SK jigsaw puzzle	219
5.1 Chapter overview.....	219
5.2 Introduction	219
5.3 Results.....	221
5.3.1 Design of Chimeras.....	223
5.3.2 Cloning and Expression	225
5.3.3 Phenotype in <i>S. coelicolor</i>	228
5.3.4 Effects on other <i>Streptomyces</i> spp.	233
5.3.5 Deletion of <i>afsQ2</i>	243
5.3.6 <i>in vitro</i> analysis of phosphor-transfer between chimera SKs and AfsQ1	251

5.3.7 <i>in vivo</i> analysis of phosphotransfer between chimera SKs and AfsQ1	257
5.3.7.1 CRISPR/Cas9 3XFLAG- tag <i>afsQ1</i>	258
5.3.8 Quantifying Gene Expression	262
5.4 Discussion	268
6. Summary and Discussion.....	275
References	279
Supplementary Material.....	325

Table of Figures

Figure 1. 1: Typical membrane bound SK and intracellular RR configuration, where upon stimulus recognition the SK autophosphorylates and transfers a phosphoryl group to the RR allowing an output response. The typical output domain of RRs is a DNA binding domain allowing regulation of genes to combat the stimulus. Here the RR has bound to the promoter region (arrow) and activating gene expression in doing so. 31

Figure 1. 2: Example of a classical sensor kinase (SK) structure. A) SK embedded in membrane with extracytoplasmic sensor domain; B) Homodimer of only dimerisation and phosphotransfer domain (Dhp) and catalytic and ATP binding domain (CA), blue denotes one monomer of the CA domain and one of the helices of the Dhp domain, D α 1 and green another monomer whilst red denotes helix 2 (D α 2) of each Dhp domain of each monomer. The dashed line represents the line of symmetry between the monomers (Taken from Xie, *et al.* 2012). 32

Figure 1.3: Sequence alignment analysis of HAMP domains from different SKs from different bacteria. The two protomers are linked by a short sequence which after folding runs the length of the protomer. This linker sequence begins with a conserved Gly residue (highlighted in green). The red highlighted amino acids form the a and d position of the heptad repeats. 37

Figure 1.4: Sequence alignment analysis of kinase cores-Dhp and CA domains of HKs. Conserved sequence motifs H, N, G1, F, G2, and G3 boxes are highlighted in magenta boxes. Helices are highlighted in yellow, and β -strands in green (Taken from Wang, 2012). 40

Figure 1. 5: Distribution of the most common effector domains of response regulators (RR) in bacteria. A) Distribution of total effector domains across bacteria with their representative RR domain structure in ribbon form. Unlabelled output domains (clockwise from AraC) are as follows: Spo0A (dark blue), ANTAR (cyan), CheW (pink), CheC (white), GGDEF+EAL (orange), HD-GYP (yellow) (Taken from Galperin, 2010). B) Distribution of effector domains across bacterial phyla and archaea including the subdivisions of Proteobacteria (alpha, beta, gamma and delta). Effector domains are as labelled: single-domain (white), OmpR (maroon), NarL (bisque), NtrC (blue), combined LytR, ActR, YesN/AraC, and Spo0A (purple), CheB (magenta), combined c-di-GMP signaling (WspR, PleD, PvrR, FimX, and RpfG, orange), and enzymatic (HisK and PP2C output domains, green) families within each taxonomic group. The grey bars indicate combined fractions of all other RR families (Taken from Galperin, 2010). 43

Figure 1.6: Lifecycle of *S. coelicolor* grown on solid substrate. A dormant spore under favourable conditions germinates forming germ tube/s which proliferate into vegetative hyphae. The extension and branching of hyphae form a network which extract nutrients from surrounding substrate allowing the growth of the colony. Later when conditions are less favourable, there is a switch from vegetative growth

to aerial growth. Septa formation along the length of the aerial hyphae allows separation of compartments which later form the walls of separated spores (Edited from Flårdh and Buttner, 2009). 57

Figure 1.7: Regulation of actinorhodin through expression of SARP ActII-ORF4. Region upstream of *actII-ORF4* is shown in yellow which includes *actII-ORF3* and the intergenic region. Numbers below show distance from transcription start site (+1) as defined by Gramajo, *et al.*, (1993). Short coloured lines refer to binding sites of regulatory proteins with as experimentally determined by the following: LexA: Iqbal, *et al.*, (2012); DasR; Rigali, *et al.*, (2008), AdpA; Ohnishi, *et al.*, (2005), DraR; Yu, *et al.*, (2012), AfsQ1; Wang *et al.*, (2012), Rok7B7; Heo, *et al.*, (2008) and AtrA; Uguru., *et al.*, (2005). Regulatory proteins above the central genes applies negative regulation on *actII-ORF4* transcription and bottom row applies positive regulation. Signaling that controls the DNA binding activity of transcription regulators is shown and the state of regulation shown with blue arrows for positive regulation and red blunt arrows for negative regulation. 65

Figure 1.8: An overview of regulation of undecylprodigiosin (RED) biosynthesis by known extracellular signaling proteins and known and unknown stimuli. The serine/threonine kinases (green boxes) and the TCS SKs (deep orange) embedded in the membrane (grey), upon stimulus association, phosphorylates (light blue dotted arrows) the cytosolic transcriptional regulators (pale orange) which bind to the promoter regions and promote expression (black arrows) of regulation genes involved in RED biosynthesis, *afsS* and *redZ* or exert repression (red blunt arrows) on expression. The biosynthesis of RED is indicated in dark blue broken arrow. 67

Figure 1.9: CPK biosynthesis cluster and proposed pathway through which the coloured structurally novel compound coelimycin P1 is generated. A) *S. coelicolor* CPK biosynthetic cluster of genes. Type I modular PKS core genes are shown in red, regulatory genes both putative and characterised are in blue, the predicted genes encoding proteins involved in generating the precursor which is loaded into the polyketide synthase (PKS) synthase are shown in green, pink denotes post-PKS editing enzymes and black denotes a putative export protein. Taken from (Gomez-Escribano, *et al.*, 2012). B) Schematic view of the proposed mechanism through which coelimycin P1 is assembled (Gomez-Escribano, *et al.*, 2012). 68

Figure 1.10: The yellow pigmented cryptic polyketide (yCPK) biosynthesis expression is regulated by an interplay between butyrolactone signaling, TCS signaling (orange) and from other antibiotics produced by *S. coelicolor* (actinorhodin and undecylprodigiosin), resulting in the expression of the SARP regulator CpkO (green). Black (solid) arrows demonstrate positive regulation, black dashed arrow refers to positive regulation exerted by SARP regulator, blunt red arrows denote inhibition or repression, blue dotted arrows represent phosphotransfer. 70

Figure 1.11: CDA BGC with the SARP encoding *cdaR* and the CSR encoding genes *absA1* and *absA2*, that encode a TCS, and the three peptide synthases (PSI-

III) labelled. In addition are genes encoding enzymes for transport and the assembly of the peptide and post-assembly modifications. 71

Figure 1.12: TCS AfsQ1/Q2 regulation. A) Position of *afsQ1*, *afsQ2*, *afsQ3* and the divergently expressed *sigQ* in the *S. coelicolor* genome of approximately 8.7 million base pairs encoding a RR, SK, lipoprotein and sigma factor respectively. (Taken from StrepDB) B) Consensus sequence binding site of AfsQ1 predicted by Weblogo using alignment of 20 identified binding sites (Taken from Wang, *et al.*, 2013B). C) Predicted regulation network exerted by AfsQ1 based on the consensus sequence binding site showing global regulation on morphological development and metabolite production, both primary and secondary. An interlink with global regulator GlnR is also shown. Arrows demonstrate positive regulation, arrows ending in circles show negative regulation, double lined arrows show dual regulation and broken arrows show indirect control (Taken from Wang, *et al.*, 2013B). 72

Figure 1. 13: Operon of *phoPR* in genome of *S. coelicolor* and two of its regulons, the divergently expressed *phoU* and *pstABCS* which encodes phosphate specific transport system. 79

Figure 1.14: Model of cell envelope stress response activation through TCS CseBC activating expression of sigma factor E which results in the expression of cell envelop related genes after the HK CseC senses cell envelop stress (Taken from Hutchings, *et al.*, 2006). 81

Figure 1.15: The VanRS regulon consists of only 4 transcriptional units in *S. coelicolor* (Hutchings, *et al.*, 2006). 82

Figure 2. 1: Cloning strategy of PCR targeting. A) Design of primers to amplify aprR cassette (*aac(3)IV* along with FLP-recombinase (FLP) recognition targets (FRT)) through binding at P1 and P2 with overhangs corresponding to flanking regions to gene of interest. B) The amplified cassette possesses the flanking regions (FR), P1/P2, FRT and aprR. C) This is transformed into BW25113/pIJ790 that already has the cosmid (containing gene of interest) transformed in. The addition of arabinose induces λ RED genes which facilitate recombination of the linear DNA with the cosmid. D) This cosmid containing the aprR cassette is extracted and transformed into ET12567/pUZ8002. This is then conjugated into *Streptomyces* where through another recombination event leads to replacement of gene of interest with the aprR cassette. 140

Figure 2. 2: Cloning strategy to generate a gene deletion in *Streptomyces* using the CRISPR/Cas9 system developed by Cobb, *et al.*, 2015. A) Constructing a deletion vector using pCRISPomyces-2 by insertion of protospacer into the BbsI site (forming a synthetic guide RNA (sgRNA) which is the crRNA and the tracrRNA fused together) and homology region (flanking region to the gene of interest). B) After conjugation into *Streptomyces*, the expressed Cas9 enzyme binds with sgRNA. Upon a match of the crRNA (protospacer sequence) and the genomic DNA, the DNA is cleaved forming a DSB. The vector is selected for using apr due

to the AprR cassette. C) The DSB can then be repaired through homologous recombination (HR) with the homology sequence inserted into the vector. After HR, the vector can then be lost through growth at a higher temperature (37-39°C) due to temperature sensitive replication region of pGS5 and also removal of apr selection. 142

Figure 2.3: PCR analysis strategy of CRISPR/Cas9 generated deletion mutants where flanking PCR refers to primer pairs situated outside the original homology amplification flanking sequence, external PCR refers to primer pairs within the original homology flanking sequence and internal PCR where one primer of the pair is situated within the gene deleted. 148

Figure 3.1: Signal transduction proteins identified in *S. venezuelae* through analysis using P2RP (Barakat, *et al.*, 2013). Classic TCSs includes typical TCSs (1 SK and 1 RR adjacently encoded) and multiple components (2 SK and 1 RR). Orphan SK and RRs refers to SKs and RRs without known partners, respectively. 2 hybrid SKs were identified, one in the same operon as a RR and the other not. 1 Hpt protein encoding gene (*sven15_0954*) was identified to be located in the same operon as a SK. One-component systems refer to proteins with input and output domains in a single protein often with no phosphotransfer domains. 160

Figure 3.2: Distribution of TCSs and orphan SKs within the genome. Taking the start of the ORF of each SK (both of paired TCSs and orphan kinases), the number of SKs within 10^5 base pair frame of the genome was calculated. The positioning of these bars in the X axis denotes the midpoint of the 10^5 bp frame. These frames were shifted by 10^4 bp. For *sven15_2343-45* and *sven15_4209-11*, *sven15_2343* and *sven15_4210* was taken as reference. 161

Figure 3.3: Alignment of protein sequences of SKs from paired TCSs with multiple SKs to a single RR. A) *Sven15_2343* and *Sven15_2344*; B) *Sven15_4210* and *Sven15_4211*. Alignment conducted using Clustal Omega. * refers to conservation of residue, : refers to conservation of strongly similar properties, . refers to conservation of weakly similar properties. 167

Figure 3.4: Analysis of RR (from paired TCSs) effector domain protein families. NarL and OmpR refer both to DNA binding domains, CheY which just has a known REC domain, TrxB with possesses two pyr-redox domains, and unclassified which as yet, no known structure has been identified in other studied proteins. 169

Figure 3.5: Conservation of TCS in over 100 Actinobacteria genomes (Chandra and Chater, 2013). Boxes coloured in represent different orders and families of Actinobacteria. Magenta-Streptomycineae, turquoise- Catenulisporineae, powder blue- Glycomycineae, indigo- Micromonosporineae, purple- Pseudonocardineae, chartreuse green- Streptosporangineae, seafoam green- Frankineae, red-Corynebacterineae, lime green- Propionibacterineae, pink- Kineosporineae, green-yellow-Micrococcineae, brown-Actinomycineae, Teal green- Bifidobacteriales, peach-Acidimicrobineae, light green-Rubrobacteridae, light yellow-Coriobacterideae, Neon blue- *B. subtilis*, orange- *E. coli*. Amongst the magenta,

from left to right boxes represent *S. lividans*, *S. viridochromogenes*, *S. scabiei*, *S. sviveus*, *S. avermitilis*, *S. griseoflavous*, *S. coelicolor*, *S. griseus*, *S. hygrosopicus*, *S. pristinaespiralis*, *S. roseosporus*, *S. albus*, *S. claviligeus* and *Kitasatospora setae*. Yellow highlighted genes are HKs. 171

Figure 3.6: PCR confirmation of deletion of $\Delta 3148/49$ ($\Delta cseBC$) through use of CRISPR/Cas9. A) PCR strategy using primers RLOTCSKO296F, RLOTCSKO297F paired with RLOTCSKO301R for external and internal PCR, respectively. Expected (Exp) sizes of wild-type (WT) and successful deletion (del) are shown. B) Results of external (top row) and internal (bottom) PCR. Numbers refer to independent mutant colonies in comparison to WT. 181

Figure 3.7: PCR confirmation of deletion of $\Delta 7022/23$ through use of CRISPR/Cas9. A) PCR strategy using primers RLOTCSKO371F, RLOTCSKO372F paired with RLOTCSKO374R for external and internal PCR, respectively. Expected (Exp) sizes of wild-type (WT) and successful deletion (del) are shown. B) Results of external (top row) and internal (bottom) PCR. Numbers refer to independent mutant colonies in comparison to WT. 182

Figure 3.8: *S. venezuelae* wild-type (both plates to the left) and the three independent $\Delta 1773/74$ mutants cultured on MYM agar for 2 days. Top row shows the base of the plates and bottom row shows top view. 185

Figure 3.9: *S. venezuelae* wild-type (left) and $\Delta 1773/74$ mutant (right) cultured on MYM for 3 days. 185

Figure 3.10: Assay of *S. venezuelae* wild-type and the isogenic $\Delta 3170/71$ mutant in the presence of tunicamycin at different concentrations (0, 1, 3, 5, 10, 20 and 50 μ l of a 1 mg/ml stock) on each disk. Van refers to vancomycin (10 μ l of 10 μ g/ml) and methanol refers to 50 μ l of methanol. All disks were dried before application to plate. Confluent lawns were prepared by spreading a cotton bud soaked in 10^7 spores over the entire plate. 187

Figure 3.11: Differential RNA sequencing data for *sven15_3169-3171* at 8 hrs, 12 hrs, 16 hrs and 20 hrs after growth of *S. venezuelae* wild-type in liquid MYM (Munnich, *et al.*, 2016). *S. venezuelae* numbers shown here reflect the gene numbers from a different annotation of the same species (NRRL B-65442) genome; *sven_3238* refers to *sven15_3169*, *sven_3239* refers to *sven15_3170* and *sven_3240* refers to *sven15_3171*. 188

Figure 3.12: Colony morphology of *S. venezuelae* and 3 independent $\Delta 3682/83$ mutants grown on MM for 7 days. 190

Figure 3.13: Neighbouring genes of the *sven15_3682/82* with predicted functions annotated (edited from Marchler-Bauer *et al.*, 2007). 191

Figure 4.1: Conservation of *vanRS* regulon within Streptomycineae based on ActinoBLAST results using *S. coelicolor* as reference (Chandra and Chater, 2014). Boxes filled in magenta show presence of homologue. 198

Figure 4.2: Cloning of *vanS* into pGS-21a. A) Overexpression vector pGS-21a (Genscript) with its multi-cloning site containing *NcoI* and *HindIII* which when cloned into yields a N-terminal His and GST tagged VanS and when cloned into *NdeI* and *HindIII* yields a C-terminally tagged VanS once expressed. The *NdeI* site overlaps with the transcriptional start site (TSS). The red boxes represent the hexa-His tags; B) Restriction digest of *vanS* (expected size of 1100 bp) from pGS-21a. pRL100 refers to N-terminally hexa-His tagged *vanS* and pRL100 refers to C-terminally hexa-His tagged *vanS*. Red arrow denotes excised *vanS*, blue arrow denotes linear pGS-21a and green arrow denotes undigested pRL100 vector. 201

Figure 4.3: Overexpression of VanS after 4 hrs of induction using IPTG ranging from 0 mM to 2 mM. A) Coomassie stained SDS-PAGE gel of His-GST-VanS overexpression in RL001 (BL21 pRL100); B) Coomassie stained SDS-PAGE gel of His-GST-VanS overexpression in RL002 (BL21 pRL101). For both A) and B) lanes from left to right are BL21 pGS-21a (-ve control), BL21 pET-28a-AntA (+ve control), RL001/2 induced with 0 mM, 0.25 mM, 0.5 mM, 0.75 mM, 1 mM or 2 mM IPTG. C) Western blot analysis of VanS overexpression from RL001 and RL002 using HRP conjugated His antibody. Lanes from left to right are BL21 pGS-21a (-ve), RL001 induced with 1 mM IPTG, 10-fold dilution of RL001 with 1 mM IPTG, RL002 with 1 mM IPTG induction, 10-fold dilution of RL002 with 1 mM IPTG, BL21 pET-28a-AntA (+ve). Arrows denote expected migration of VanS proteins at 68 kDa (Blue for His-GST-VanS) and 42 kDa (Red for VanS-His). Band running through whole gel ~30 kDa is likely caused by intensity luminescence refracting off the film covering gels in the exposure process. 203

Figure 4.4: SDS-PAGE analysis of VanS-His fraction location through ultracentrifugation of lysate to pellet insoluble protein. Supernatant, containing soluble proteins was extracted (soluble fraction) and pellet was resuspended in Tris buffer containing 0.5% sarkosyl (insoluble fraction) before pelleting of cell debris. Lanes from left to right excluding protein size reference ladder are BL21 pGS-21a insoluble fraction, BL21 pGS-21a soluble fraction, BL21 pET-28a-AntA insoluble fraction, BL21 pET-28a-AntA soluble fraction, RL002 0 mM IPTG insoluble fraction, RL002 0 mM IPTG soluble fraction, RL002 1mM IPTG insoluble fraction, RL002 1 mM IPTG soluble fraction. Black arrow shows expected size of VanS-His and red arrow shows overexpression of VanS-His. 204

Figure 4.5: Purification of VanS-His from the soluble protein fraction through use of FPLC. A) Purification elution profile. Lime green line displays the gradient of imidazole concentration in each fraction of the elution, with 300 mM as the maximum. Dark blue line represents the UV absorbance in mAU as the protein is eluted from the column which is presented in the Y axis. Collected fractions are listed in the X axis. B) Eluted fractions from the purification process analysed through SDS-PAGE. The lanes from left to right are flow through protein was

loaded on the column, fraction A2, A7, A8, A9, A10, A12, A13. Arrow denotes VanS-His purified protein of expected size 42 kDa. 205

Figure 4.6: Intact mass spectrometry of VanS-His protein expressed from pRL101 vector in BL21. Mass spectrometry was carried out on protein purified from fraction A3 from the purification shown in figure 4.5. The deconvoluted spectrum measured peak masses are 31476.04 and 31781.2. Y axis shows relative abundance of protein and X axis shows the size of the protein isoform. Expected full-length protein size is 42 kDa. 207

Figure 4.7: Predicted cleavage site of VanS-His based on intact mass spectrometry most abundant peak size of 31.435 kDa and presence of His-tag. Sizes indicated on the right are calculated from the C-terminus. 208

Figure 4.8: Coomassie blue stained SDS-PAGE analysis of overexpression of mutants VanS with L89V, A91G and LA90:91VG substitutions after 4 hrs induction with 1 mM IPTG. RL005 and RL008 express VanS with L89V mutation; RL006 and RL009 express VanS with A91G mutations and RL007 and RL0010 express VanS with LA90:91VG mutation; strains RL005-RL007 express VanS with a N-terminal His tag; RL008-10 with C-terminal His-tags; -ve is BL21 pGS-21a. The expected VanS size is 42 kDa shown with red arrow but expressed protein shown with black arrow. 208

Figure 4.9: SDS-PAGE analysis of His-GST VanS fraction location through ultracentrifugation of lysate to pellet insoluble protein. Supernatant, containing soluble proteins was extracted (soluble fraction) and pellet was resuspended in Tris buffer containing 0.5% sarkosyl (insoluble fraction) before pelleting of cell debris. Lanes from left to right excluding protein size reference ladder are BL21 pGS-21a insoluble fraction, BL21 pGS-21a soluble fraction, BL21 pET-28a-AntA insoluble fraction, BL21 pET-28a-AntA soluble fraction, RL001 0 mM IPTG insoluble fraction, RL001 0 mM IPTG soluble fraction, RL001 1mM IPTG insoluble fraction, RL001 1mM IPTG insoluble fraction overflow, RL001 1 mM IPTG soluble fraction. 209

Figure 4.10: Purification of His-GST-VanS from the insoluble protein fraction through use of FPLC. A) Purification elution profile. Lime green line displays the gradient of imidazole concentration in each fraction of the elution (300 mM maximum). Dark blue line represents the UV absorbance in mAU as the protein is eluted from the column which is presented in the Y axis. Collected fractions are listed in the X axis. B) Eluted fractions from the purification process analysed through SDS-PAGE and consequent anti-His immune blotting. The lanes from left to right are resuspended insoluble protein of crude lysate (CL), flow through (FT), A6, A11, A13, A15, B14. Arrow denotes His-GST-VanS purified protein which was expected to be 68 kDa. 210

Figure 4.11: Purification of His-GST-VanS through size exclusion. Protein first purified through His-affinity FPLC then further purified by feeding through a Superdex 75 pregrade gel filtration column. A) purification profile. Dark blue line

shows the UV absorbance as protein was eluted and the collected fractions are shown in the X axis. B) Coomassie blue stained acrylamide gel image after SDS-PAGE and subsequent Western blot using His antibodies. Lanes from left to right for B) and C) are fractions spanning the peak of A) C12, C6, C3, C2, C1, B1, B2, B3, His-GST-VanS after His affinity FPLC purification before loading onto the gel filtration column. Arrows shows expected band of His-GST-VanS. 211

Figure 4.12: Effects of Triton X-100 and sarkosyl on the purification of His-GST-VanS. Purification by use of His affinity FPLC. A) SDS-PAGE analysis; B) Anti-His protein immuno-blot. The different lanes labeled are CL= crude lysate where post lysis and ultracentrifugation, pellet has been resuspended in detergent overnight; FT refers to flow through from His-trap column; W1 is the first wash of column after lysate has been loaded; F1-F7 refer to fractions taken from elution step. Arrows denote expected band of His-GST-VanS. 213

Figure 4.13: Overexpression of His-GST-VanS from vector pRL100 in different expression strains of *E. coli*. After 4 hours of induction using 1 mM IPTG induced overexpression, cells were harvested and analysed through Anti-His immune blotting. Strains tested were RL001, RL003 (C41 pRL100) and RL004 (C43 pRL100). Arrow denotes positioning of 68 kDa protein band. 214

Figure 4.14: His-GST-VanS (10 µg) incubation with enterokinase to cleave GST tag from VanS under different conditions. A. Overnight incubation at 4°C and 37°C with 5U enterokinase. B. Incubation using different ratios of purified protein to enzyme. P is the protein (His-GST-VanS) only, P + B refers to the protein and buffer, B + E is buffer and enterokinase, and P + B + E refers to protein, enterokinase buffer and enterokinase. The arrows denote expected size of His-GST-VanS and His-GST and VanS if enterokinase cleavage is successful. 215

Figure 5.1: Alignment of SKs AfsQ2 and VanS of *S. coelicolor* using Clustal Omega. * refers to conservation of residue, : refers to conservation of strongly similar properties, . refers to conservation of weakly similar properties. The domains are highlighted as follows, blue text denotes sensor domains, red text denotes TM helices (as predicted by ExPasy TMPred), underlined text denotes HAMP domain (as predicted by P2RP; Barakat, *et al.*, 2013), green text denotes Dhp domain and orange/brown text denotes CA domain. The different boxes highlight the conserved regions, with the red boxes showing the H box, the blue boxes showing the N box and the green boxes showing boxes G1, G2 and G3. 222

Figure 5.2: Design of VanS-AfsQ2 chimera SKs. A) Schematic of the two TCSs VanSR and AfsQ1/Q2 alongside with designed chimera, demonstrating the desired result. B) Schematic of the designs of the chimeras, where Chimera 1 and 2 have been altered by exchanges of domains and Chimeras 3-5 have residue changes only in the Dhp domain of VanS. C) Residue changes in the Dhp domain of Chim 3-5. These residue changes have been highlighted in the alignment. Chimera 3 possesses changes highlighted in red, Chimera 4 possesses the changes highlighted in red and purple and Chimera 5 has all the changes highlighted in red, purple and green. EnvZ

has been shown in the alignment as a comparison between the residues changed between EnvZ and RstB in the rewiring work carried out by Skerker, *et al.*, (2008).
225

Figure 5.3: Confirmation of cloning A) *chim1* and B) *chim2* into pAU3-45 through restriction digest with XbaI and EcoRI. The expected sizes of *chim1* and *chim2* fragments are 1412 bp and 1349 bp, respectively. Arrow depicts the excised chimera fragments.
226

Figure 5.4: PCR confirmation of chimeras (Chim1-5) integrated into *S. coelicolor* M145 genome. The amplification of *chim1* (expected size of 1541 bp) and *chim2* (expected size of 1478 bp) were carried using primers pAU3-45F/R. The amplification of *chim3*, *chim4* and *chim5* and the empty vector pMS82 were carried out using pMS82F/R. The expected size of the amplified fragments for *chim3,4* and 5 is ~1500 bp.
227

Figure 5.5: Expression of chimeras in M145 with different concentrations of vancomycin. Mycelia was harvested after 3 days of growth on SFM. A) Anti-His was used to visualise Chim1 and 2 proteins. B) Anti-StrepII was used to visualise Chim3-5 proteins. All concentrations in µg/ml. Red arrow represents Chim1 (42.7 kDa), black is Chim2 (41 kDa) and purple is Chim3-5 (39.5 kDa).
228

Figure 5.6: *S. coelicolor* M145 strains containing Chim1-5 grown on SFM with different concentrations of vancomycin (0, 10, 50 and 100 µg/ml) for 5 days at 30°C.
229

Figure 5.7: Effect of chimeras on M145 colony morphology after 11 days of growth on MM supplemented with low levels of glutamate (7.5 mM) as sole nitrogen source and vancomycin (10 mg/ml).
230

Figure 5.8: Comparison of homologues of AfsQ operon with SigQ across four *Streptomyces* species (*S. lividans* (Sliv), *S. venezuelae* (Sven) and *S. formicae* (KY5)) against *S. coelicolor* (Sco). Amino acid identity was measured through use of NCBI BLASTp alignment.
231

Figure 5.9: Protein sequence alignment of A) AfsQ2 and B) AfsQ1 homologues from *S. coelicolor* (Sco), *S. venezuelae* (Sven) and *S. formicae* (KY5) using Clustal Omega. The domains of AfsQ2 are highlighted as follows, blue text denotes sensor domains, red text denotes TM helices (as predicted by ExPASy TMPred), underlined text denotes HAMP domain (as predicted by P2RP; Barakat, et al., 2013), green text denotes Dhp domain and yellow text denotes CA domain. The REC domain of AfsQ1 is shown in purple and the DNA binding domain in orange.
235

Figure 5.10: Alignment of the Dhp domain region where changes were made between Chim3-5 between AfsQ2 homologues of *S. coelicolor* and *S. lividans* (Sco/Sliv), *S. venezuelae* (Sven) and *S. formicae* (KY5). Altered residues between the chimeras are colour coded. Red residues are altered residues in Chim3; Chim4

residues altered are those in red and purple and Chim5 altered residues are the green, purple and red residues. 236

Figure 5.11: The effects of Chim1 and Chim2 in *S. lividans* with and without vancomycin (10 µg/ml). Strains were grown on SFM agar for 7 days. All scale bars show 2 mm. Sliv refers to *S. lividans*, ::pAU3045 refers to *S. lividans* with empty vector pAU3-45 integrated, ::Chim1 and ::Chim2 refer to *S. lividans* with *chim1* and *chim2* integrated at the ϕ C31 site. 237

Figure 5.12: The effects of Chim3 and Chim4 on *S. lividans* with and without vancomycin (50 µg/ml). Strains cultured on SFM for 7 days. Sliv refers to *S. lividans*, ::pMS82 refers to *S. lividans* with empty vector pMS82 integrated, ::Chim3 and ::Chim4 refer to *S. lividans* with *chim3* and *chim4* integrated at the ϕ BT1 site. 237

Figure 5.13: Analysis of bioactivity of *S. venezuelae* strains containing Chim3-5 against (A) *E. coli* Top 10 and (B) *C. albicans* (clinical isolate). *S. venezuelae* strains were spotted on to the MYM plate with (0.5 µg/ml) and without vancomycin and grown for 3 days before indicator strains were inoculated into SNA and overlaid onto the plate around the growing *Streptomyces*. 239

Figure 5.14: Analysis of bioactivity of *S. formicae* KY5 strains containing Chim3-5 against *E. coli* Top10. KY5 strains were spotted on to the MYM plate with (0.5 µg/ml) and without vancomycin and grown for 7 days before indicator strains were inoculated into SNA and overlaid onto the plate around the growing *Streptomyces*. 241

Figure 5.15: PCR confirmation of *S. coelicolor* M145 Δ *afsQ2*. Three sets of PCRs were carried out in the analysis, flanking PCR where primers amplify the region surrounding *afsQ2* (RLO0129F/131R), internal PCR where one primer is situated within *afsQ2* (RLO0130F/131R) and a third PCR where one primer is within the homology region originally amplified and one primer is outside of this region (RLO0129F/133R). The expected (exp) sizes of these PCRs are shown. WT refers to M145, and 1-4 refer to the four independent apramycin sensitive strains tested. 244

Figure 5.16: Growth of M145 and M145 Δ *afsQ2* in MM in triplicate with low (7.5 mM) and high (75 mM) levels of glutamate for 24 hrs. Cultures (50 ml) were grown in 250 ml conical flasks, aerated with springs. 246

Figure 5.17: *S. coelicolor* M145 and isogenic Δ *afsQ2* strains cultured on MM supplemented with 7.5 mM and 75 mM of glutamate as sole nitrogen source with 0 and 10 µg/ml. All strains were spotted (5 µl) onto plates in the same orientation as schematic. The numbers are represented as follows: 1 = M145 (WT or Δ *afsQ2*), 2 = ::pMS82, 3 = ::truncated *afsQ1*(*ermE**), 4-6 = ::Chim3 (independent strains), 7-9 = ::Chim4 (independent strains). 247

Figure 5.18: Colony morphology comparison of Chim4 in *S. coelicolor* M145 Δ *afsQ2* (M145 Δ *afsQ2*) grown on MM for 9 days with 7.5mM glutamate with 10 μ g/ml vancomycin. C4.1-3 refer to isogenic strains. Three colonies are shown per plate. Each plate contained approximately 15-30 colonies. 249

Figure 5.19: Bioassay comparison of *S. venezuelae* and isogenic Δ *afsQ2* grown on MYM with (10 μ g/ml) and without vancomycin. *S. venezuelae* strains were spotted on to the plate and grown for 3 days before indicator strains were inoculated into SNA and overlain. 250

Figure 5.20: Confirmation of overexpression vectors. Primer RLO147F was used in all the amplifications and binds to the T7 promoter of pGS-21a. This was paired with primers amplifying from within the gene inserted. For *c-afsQ2* (expected (exp) size: 750 bp), primer RLO144R was used; *c-chim2* (exp size: 465 bp), *c-chim3- c-chim5* (exp size: 423 bp) and *c-vanS* (exp size: 423 bp), primer RLO144aR was used, for *afsQ1* (exp size: 520 bp), primer RLO146R and for confirming *vanR* (exp size: 552 bp), primer RLO145R was used. 252

Figure 5.21: Anti-His immuno-blot analysis of the overexpression of cytoplasmic regions of SKs, AfsQ2 (Q2), VanS (VS) and chimeras (C2-5) and RRs, VanR (VR) and AfsQ1 (Q1). The expected sizes of each from the first lane (C2) to lane 8 (VS) are as follows: 30.83 kDa, 30.31 kDa, 30.3 kDa, 30.31 kDa, 26.03 kDa, 32.78 kDa, 25.7 kDa, 30.34 kDa. Cultures of each overexpression strain were induced with 1 mM IPTG and induced for 4 hrs before harvesting of cells. 253

Figure 5.22: Anti-His immuno-blot analysis of the overexpression of cytoplasmic regions of SKs, AfsQ2 (Q2), VanS (VS) and RR, VanR (VR). Two AfsQ2 overexpression strains were used, both overexpressing N-terminally His-tagged cAfsQ2. The expected sizes of each overexpressed protein is 25.7 kDa (VanR), 30.34 kDa (c-VanS) and 32.78 kDa (c-AfsQ2). Cultures of each overexpression strain were induced with 1 mM IPTG and induced for 4 hrs before harvesting of cells. 254

Figure 5.23: Purified protein from His-affinity FPLC. Purified samples were snap frozen and stored at -20°C without and with 10% glycerol (G). Proteins purified are c-Chim2 (C2; 30.83 kDa), c-Chim3 (C3; 30.31 kDa), c-Chim4 (C4; 30.3 kDa), c-Chim5 (C5; 30.31 kDa), AfsQ1 (Q1; 26.03 kDa), c-AfsQ2 (Q2; 32.78 kDa), VanR (VR; 25.7 kDa) and VanS (VS; 30.34 kDa). 255

Figure 5.24: Collected fractions from overexpression and purification of AfsQ1 (Q1), c-AfsQ2 (Q2), VanR (VR) and c-VanS (VS) analysed through anti-His immuno-blot. After 1 mM IPTG overexpression induction for 4 hrs, harvested cells were lysed through passage through French press twice (1000 psi). The cell debris was separated from the soluble proteins through centrifugation (10 mins, 10000 rpm, Accupsin 1R with a Ch. 007379 rotor), the supernatant was loaded on the His-Trap column. Column and protein was washed with 40 ml buffer (no imidazole) before eluting with buffer containing different concentrations of imidazole. 256

Figure 5.25: Gene sequence of *afsQ1* after insertion of a N-terminal 3 X FLAG tag (red) through CRISP/Cas9 editing. The protospacer used is shown in green and PAM sequence in bold blue text. To remove the recognised cleavage sequence of Cas9, the PAM sequence was altered 33G>A generating a silent mutation. The amplification of the *afsQ1*, insertion of FLAG sequence and mutation was conducted using primers RLOCC009F-14R and Gibson Assembled into p-CRISPomyces-2. 258

Figure 5.26: Immuno-blot using M2 anti-FLAG antibodies to visualise 3XFLAG tagged AfsQ1 expression over 20 hrs of growth in liquid MYM, where samples were removed every 4 hrs from 8hrs after inoculation. This was carried out in duplicate. Arrow shows represents expected size of AfsQ1 (28 kDa). 260

Figure 5. 27: Growth curve of *S. venezuelae* wild-type (WT) and F-AfsQ1 (FLAG) in MYM over 48 hrs. Non-capped error bars are wild-type and capped are F-AfsQ1. Error bars show standard error. An OD₆₀₀ below 1 was measured using 1 ml sample in a 10 mM path length cuvette. From this growth rate and duplication time were calculated. Samples with an OD₆₀₀ of above 1 were measured through diluting the sample and scaling up. Cultures and samples were taken in triplicate. The growth rate and duplication time are both not significantly different (One-sample T-test; $p < 0.05$, $|t|$ (growth rate) = 1.042 < 4.303; $|t|$ (duplication) = 1.087 < 4.303). 260

Figure 5.28: Analysis of phosphorylation state of AfsQ1 in F-AfsQ1 background with Chim3 and Chim4 in the presence and absence of vancomycin. Strains were grown on MM with 7.5 mM glutamate as sole nitrogen source. The – and + refer to growth with vancomycin (0.5 µg/ml) or without. A) Coomassie stained SDS-PAGE acrylamide gel of whole cell lysate of samples. Red arrows show expected position of protein of AfsQ1. B) Western blot (anti-FLAG) Phos-tagged SDS-PAGE. Blue arrows show phosphorylated AfsQ1 and Black arrow shows unphosphorylated AfsQ1. 262

Figure 5.29: Amplification plots generated from standards for each of the targets (*sigQ*, *actII-ORF4* and *redZ*) and also the reference gene (*hrdB*). Standards used were amplification of targets using primers RLO161F-168R (Table 2.3). All standards were <400 bp. From the size of amplicon, the number of copies of DNA was calculated. Standards used ranged from 10000000 to 10 copies of DNA. Standards were carried out in duplicate and each standard is represented by one coloured line in each graph. With red lines representing 10000000 copies, orange showing 1000000 copies, light green showing 100000 copies, green showing 10000 copies, cyan showing 1000 copies, blue showing 100 copies, purple showing 10 copies and magenta showing just water. The horizontal line shows the threshold value, which was decided by eye to omit noise. 264

Figure 5.30: CT values were plotted against the number of copies from standards (blue). Lines of best fit were drawn. Orange points represent the data points of the non-standard (purified cDNA) samples. Each purified cDNA sample was amplified in triplicate. Standards were obtained from diluting amplified *hrdB*, *redZ*, *sigQ* and

actII-ORFIV using primers RLO161F-168R (Table 2.3) from 10000000 to 10 copies. 265

Figure 5.31: Comparison of the expression of targets: *sigQ*, *actII-ORF4* and *redZ* in M145 Δ *afsQ2* strains with and without chimera proteins when grown in the absence (blue bars) or presence of vancomycin (10 μ g/ml; orange bars). Errors bars show are standard deviation of the samples expression levels. Expression levels is shown as fold change as normalised to *hrdB* expression. 266

Table of Tables

Table 1.1: Number of HKs and RRs predicted in the <i>Streptomyces</i> species in comparison to the total number of genes encoded within the genome (Edited from Rodríguez, <i>et al.</i> , 2013).	73
Table 1. 2: Amino acid identity of the components MtrA, MtrB and LpqB, which form an essential TCS in Mycobacterium, across actinobacterial family of species. (Taken from Hoskisson and Hutchings, 2006).	74
Table 2.1: DNA plasmids and constructs generated throughout study.	87
Table 2. 2: Strains used throughout study.	92
Table 2. 3: Primers and oligonucleotides used as protospacers in CRISPR/Cas9 gene editing used throughout study. All hexa-His tag sequences are underlined, restriction sites are italicised and in lower case, four nucleotides were added to allow binding of restriction enzymes (shown in lower case) and primer sequences ending in F and R refer to forward or reverse direction during amplification.	102
Table 2. 4: Culturing media used throughout study.	130
Table 2. 5 Antibiotics and concentrations used throughout study.	132
Table 3. 1: TCSs of <i>S. venezuelae</i> NRRL B-65442 with structural analysis using P2RP analysis (Barakat, <i>et al.</i> , 2013). RR-N refers to N terminal REC domain; HisKA and HisKA_3 refer to the kinase domain families as described by Pfam; Phy refers to phytochrome region; PspC refers to Phage shock protein C domain; Pyr-redox refers to pyridine nucleotide-disulphide oxidoreductase domain.	162
Table 3. 2: Genes surrounding TCSs of <i>S. venezuelae</i> which may give an indication as to their functions.	176
Table 3. 3: TCSs found in secondary metabolite clusters as predicted by antiSMASH (Weber, <i>et al.</i> , 2015). PKS refers to polyketide synthase and NRPS refers to non-ribosomal peptide synthase.	177
Table 3.4: List of TCSs deletions in <i>S. venezuelae</i> generated using the PCR targeting method.	179
Table 3.5: Number of independent deletions made per mutant using CRISPR/Cas9 gene editing.	183
Table 3.6: Remaining TCSs of <i>S. venezuelae</i> to be deleted to complete library of deletions and stage of generation.	184
Table 4.1: Buffer composition of the different buffers used in different His affinity FPLC purifications of His-GST-VanS, where solubilisation buffer refers to buffer	

used to resuspend pellet after ultracentrifugation of lysate, buffer 1 refers to buffer used to wash protein on His-trap column and also used in elution mixed with buffer 2 which contains imidazole. 212

Table 5. 1: PCR efficiencies of the genes amplified including reference gene (*hrdB*) and tested genes (*sigQ*, *redZ* and *actII-ORFIV*). PCR efficiency calculated according to protocol of Mygind, *et al.*, 2002. 268

1. Introduction

Bacteria are the most successful living organisms on earth. They have colonised every niche environment from temperature extremes of the poles to thermal vents, pH opposites of soda lake to the human stomach and the highest pressures found in the depths of the Mariana trench (Carpenter, *et al.*, 2000; Deshmukh, *et al.*, 2011; Rampelotto, 2013; Hauptmann, *et al.*, 2014). Whilst some environments are stable and unchanging, some environments are prone to change. Whatever, the conditions, there are groups of bacteria which have evolved to survive and thrive in these environments. In all cases, bacteria must be able to sense any changes or stresses in their surroundings or internally within the cell before mounting the appropriate responses. Bacteria utilise a range of methods to register and respond to these signals from autoinducers of quorum sensing (Nealson and Hastings, 1979; Miller and Bassler, 2001; Hense and Schuster, 2015), to use of secondary messengers such as cAMP, c-di-AMP, cGMP and c-di-GMP in signaling cascades to regulate processes such as biofilm formation (Zhang, 1996; Gomelsky, 2011; Gomelsky and Galperin, 2013) or specific signal transduction kinases. These include histidine/aspartate, serine/threonine and tyrosine kinases (Shah, *et al.*, 2008; Grangeasse, *et al.*, 2012; Cousin, *et al.*, 2013; Shi, *et al.*, 2014). The most prevalent and best studied of these in bacteria are histidine/aspartate kinases found in two-component systems (TCSs; section 1.1).

The number of TCSs found in a genome is thought to reflect the differing stimuli the bacteria are exposed to. Pathogens exposed to stable surroundings possess fewer TCSs in their genomes (Alm, *et al.*, 2006), for instance *Porphyromonas gingivalis* W83, an oral bacterium, possesses only 4 TCSs (Mattos-Graner and Duncan, 2017). In contrast, soil dwelling *Streptomyces* species possess far more. The model organism *S. coelicolor* possesses 68 TCS operons in the genome (P2RP database; Barakat, *et al.*, 2013).

Streptomyces (section 1.2) is the largest genus in the Actinobacteria phylum (Hong, *et al.*, 2009). They are antibiotic factories, producing over 60% of clinically used antibiotics (Procópio, *et al.*, 2012). They undergo complex lifecycles, initially beginning life as dormant spore, which germinates and undergoes vegetative

growth before changing to aerial growth when conditions are less favourable. Aerial hyphae undergo cell division to form chains of spores (section 1.2.2).

The study of TCSs in *Streptomyces* has shown them to regulate physiological changes, primary metabolism and secondary metabolism. However, despite the sheer number of TCSs found in *Streptomyces*, only a small proportion have been characterised (section 1.3). Here, I discuss what is currently known about the TCSs in *Streptomyces* and their regulons and different means to further progress and facilitate these studies.

1.1 Two-Component Systems

TCSs are signal transduction pathways found across all domains of life but predominantly in bacteria. It is thought the gain of TCSs into archaeal and eukaryotic genomes was through numerous independent lateral gene transfer (LGT) events (Koretke, *et al.*, 2000; Kim and Forst, 2001). The basic premise of a TCS is two protein components, a sensor kinase (SK) and a response regulator (RR), which sense the external stimulus and relays this signal to the inside of the cell resulting in an output to combat the stress. In a canonical system, a stimulus, such as turgor pressure or membrane damage, is registered by the SK, triggering phosphorylation at a conserved histidine (His) residue. The conserved His, found within the H box motif, gives these types of SKs the name histidine kinase (HK). From herein, all SKs discussed are HKs. This phosphoryl group is then passed to a conserved aspartate (Asp) residue in the RR. Phosphorylation of the RR causes conformational changes which can either activate or deactivate the output signaling of the RR (Figure 1.1; Stock, *et al.*, 2000; Mascher, *et al.*, 2006; Gao, *et al.*, 2007; Mitrophanov and Groisman, 2008). Adaptive response regulation can be executed through DNA, RNA or ligand binding or the RR may possess a domain with enzymatic activity (Zschiedrich, *et al.*, 2016). However, there are often variations to this pathway which may involve additional SKs or RRs, or accessory proteins (section 1.1.5).

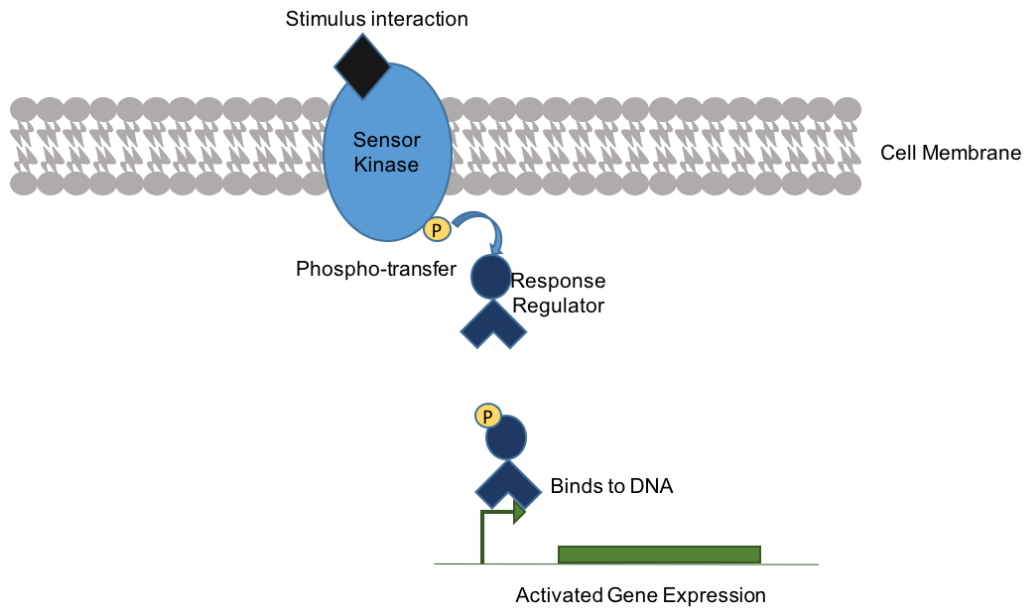


Figure 1. 1: Typical membrane bound SK and intracellular RR configuration, where upon stimulus recognition the SK autophosphorylates and transfers a phosphoryl group to the RR allowing an output response. The typical output domain of RRs is a DNA binding domain allowing regulation of genes to combat the stimulus. Here the RR has bound to the promoter region (arrow) and activating gene expression in doing so.

1.1.1 Sensor Kinases

SKs are modular proteins. An example structure of a SK monomer is displayed in figure 1.2A. Their role is to recognise a specific extra- or intra-cellular stimulant and relay it as a signal to the RR. In the case of extracellular signal recognition (other signals discussed in section 1.1.1.1), there is typically an extracellular sensor domain which is anchored to the membrane through transmembrane (TM) helices. This is connected to the cytoplasmic located domains of the SK through a signal relay domain such as a HAMP domain, so named for their identification in histidine kinases, adenylyl cyclases, methyl-accepting chemotaxis proteins, and phosphatases (Wang, 2012). Other domains also serve this function such as PAS (in period circadian, aryl hydrocarbon receptor nuclear translocator, and single-minded proteins) domains or GAF (cGMP-regulated cyclic nucleotide phosphodiesterases, adenylate cyclases, and the bacterial transcriptional regulator FhlA) domains (section 1.1.1.1 and section 1.1.1.2). The signal is then passed to the kinase core (section 1.1.1.3) which is composed of a highly conserved C-terminal catalytic and ATP binding (CA) domain, also known as the H-ATPase

domain and a less highly conserved dimerisation and histidine phosphotransfer (Dhp) domain (Gao and Stock, 2009). The CA domain catalyses the transfer of a phosphoryl group from ATP to the conserved His residue within the Dhp domain. The phosphate group can then be transferred to the RR.

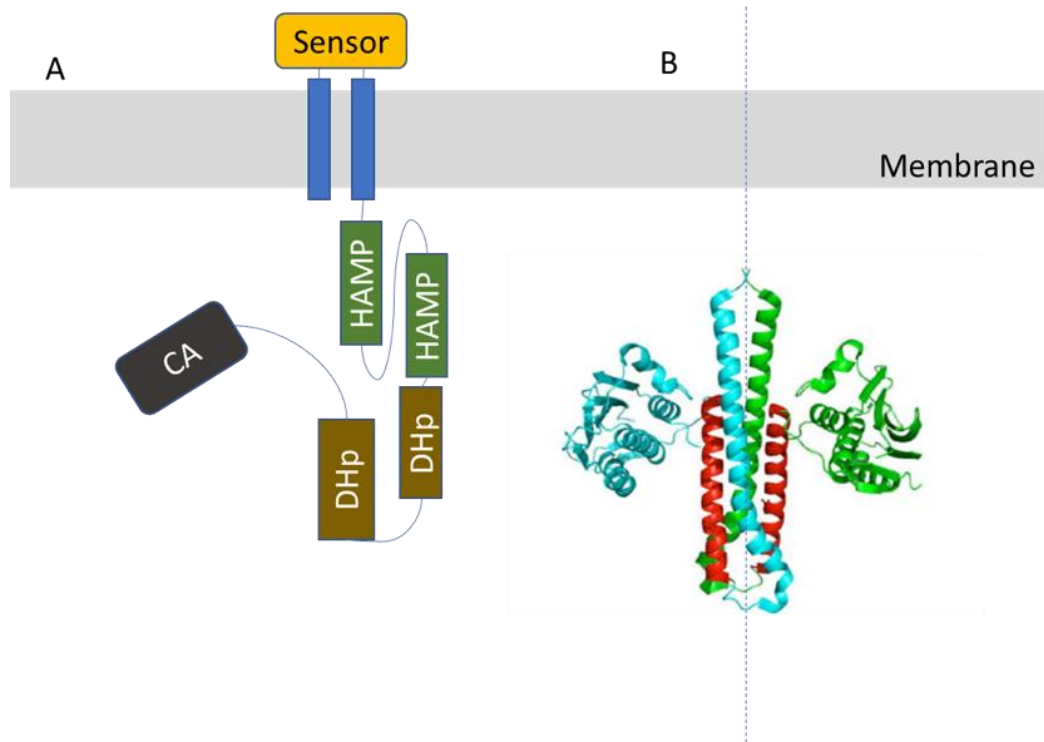


Figure 1. 2: Example of a classical sensor kinase (SK) structure. A) SK embedded in membrane with extracytoplasmic sensor domain; B) Homodimer of only dimerisation and phosphotransfer domain (Dhp) and catalytic and ATP binding domain (CA), blue denotes one monomer of the CA domain and one of the helices of the Dhp domain, D α 1 and green another monomer whilst red denotes helix 2 (D α 2) of each Dhp domain of each monomer. The dashed line represents the line of symmetry between the monomers (Xie, *et al.* 2012).

Typically, SKs function as homodimers as seen in figure 1.2B. A well-studied example is PhoR, part of the TCS PhoPR which is involved in regulating virulence in *Mycobacterium tuberculosis* (Ryndak, *et al.*, 2008; Xing, *et al.*, 2017). More recently a class of SKs (referred to as HWE/HisKA2) has been identified which has been shown to be stable in higher oligomeric states (Herrou, *et al.*, 2017). The HWE class of HKs are characterised by the absence of the F box within the kinase core (Figure 1.4). The class name HWE is derived from the histidine (H), tryptophan (W) and glutamate (E) residues in the N and G1 box (Karniol and Vierstra, 2004). The atypical HK, ExsG, identified initially in *Rhizobium* NT-26, is part of this family and has been demonstrated to be stable as a homohexamer

(Wojnowska, *et al.*, 2013). In addition to forming oligomers, SKs may also function as monomers. The SK EL346 of *Erythrobacter litoralis* HTCC2594 is active as monomer (Rivera-Cancel, *et al.*, 2014). The light-oxygen-voltage (LOV) sensor domain interacts with the dimerisation domain upon photoactivation. The conformational change releases the CA domain allowing kinase activity (Rivera-Cancel, *et al.*, 2014). Another case is DcuS of *Escherichia coli*, where if the PAS domains of the two DcuS monomers act as a hinge. When the PAS domains are dimerised, the kinase domains do not interact and are in the inactive state (Monzel, *et al.*, 2013).

SKs can possess purely kinase activity or both kinase and phosphatase activity to regulate the activity of the RR when the original stimulus signal dwindles and reset the system (section 1.1.4). Other forms of regulation exerted by SKs also exist such as binding to other SKs to sequester phosphorylation of cognate RRs as exemplified by GacS and RetS studied in *Pseudomonas aeruginosa* (Goodman, *et al.*, 2009).

1.1.1.1 Sensor and Transmembrane Domain

The sensor domain is highly variable in structure in contrast to the highly conserved domains of the core kinase. Sensor domains can be divided into three types. Firstly the classical, where two TM domains anchor a sandwiched extracytoplasmic sensor domain, this is the most common and the extracytoplasmic sensor domain can take many different structures; second, multiple TM helices with no clear sensor domain that are thought to monitor membrane associated stresses such as cell envelope stress; lastly, the sensor domain is cytoplasmic which has been associated with internal stimuli or signals which can diffuse through the membrane (Gao and Stock, 2009).

Classical sensor domains are characterised by the separation of the cytoplasmic core kinase (seen in all SKs) and the extracytoplasmic or periplasmic sensor domain which can be between 50-300 amino acids (Mascher, *et al.*, 2006). The number of anchoring TM helices can be two or more. Some of the best studied TCSs fall within this category including EnvZ and EnvZ-type SKs (e.g PhoQ of the TCS PhoPQ) and NarX and NarQ type sensors (Baraquet, *et al.*, 2006; Mascher,

et al., 2006). The structure of the sensory domain can be subdivided further. One division is the PDC group which is so named from the first SKs to be identified in their respective groups (Gao and Stock, 2009): PhoQ (responds to acidic pHs and cation concentrations; Prost, *et al.*, 2007), DcuS (responds to C₄ decarboxylates; Janausch, *et al.*, 2002) and CitA (reponds to citrate; Kaspar and Bott, 2002). This group of sensors contain the PDC fold which is composed of five central anti-parallel β -sheets encompassed by α helices on either side (Cheung and Hendrickson, 2010). PhoQ, which is involved in pathogenesis in *Salmonella* and other Gram negatives, is repressed by divalent ions and a neutral pH, but activated in acidic conditions, low levels of divalent ions or by cationic antimicrobial peptides (Mascher, *et al.*, 2006; Prost, *et al.*, 2007; Hicks, *et al.*, 2015). The sensor domain of PhoQ is made up of an $\alpha\beta$ core, an acid residue rich patch made up by α -helices, α_4 and α_5 and β -strands, 5 and 6 which form a scaffold that bind divalent cations and antimicrobial peptides (Waldburger and Sauer, 1996; Hicks, *et al.*, 2015). In the presence of high levels of divalent ions or neutral pH, the sensor domain is anchored to the membrane by divalent cation salt-bridges formed between the acidic patch and the membrane phospholipids. However, with acidic conditions or a fall of divalent ions from millimolar to micromolar concentrations, the previously acquiescent and exposed α_4 and α_5 , helices take on a flexible conformation. This switch also causes a conformational change to the core of the domain releasing the acidic patch of the protein from the cationic salt bridges formed between the protein and the membrane allowing activation of the SK (Hicks, *et al.*, 2015).

Another type is made up of purely α -helices, among this group is TorS and NarX, whilst others may be made of entirely β -folds such as RetS (Wang, 2012). The sensor domain of TorS is composed of 6 anti-parallel α -helices, which form two four-helix bundles. Helix α_3 and α_6 run the length of the bundle and connect the two four-helix bundles (Moore and Hendrickson, 2009). The NarX sensor domain possesses four anti-parallel helices which possess kinks in each helix (Cheung and Hendrickson, 2009). Where NarX binds directly with nitrate and nitrite, TorS interacts with trimethylamine-N-oxide through TorT, a periplasmic binding protein (Baraquet, *et al.*, 2006; Moore and Hendrickson, 2009). RetS is a

hybrid TCS with SK and RR domains. Along with another hybrid SK, LadS, they belong to a 7TM family of receptors. RetS possesses two ligand binding sites. One of these is composed of β -sandwich fold that is structurally similar to a new class of carbohydrate binding proteins (Jing, et al., 2010; Borland, et al., 2016).

The second group is the least common of the three types. This group is characterised by the lack of an obvious sensor domain and between 2-20 TM helices that are linked by very short linkers (Mascher, et al., 2006). In *E. coli*, EnvZ is a classical SK. EnvZ of *Xenorhabdus nematophilus* lacks a periplasmic domain. Interestingly, when EnvZ_{Xn} was heterologously expressed in *E. coli* $\Delta envZ$, it was able to complement the phenotype (Tabatabai and Forst, 1995).

This group is also referred to as intramembrane sensing HKs (IMHKs), a term which was first used to describe the cell envelope stress sensors of *Bacillus subtilis* (Mascher, et al., 2003). The cell envelope stress sensors discovered in *B. subtilis* are LiaS, BceS, and YvcQ (Mascher, et al., 2003). These three were characterized by the similarities of <400 amino acid sequence with only two TM helices (Mascher, 2006). Later other LiaS-like SKs were found to also be associated with recognition of antibiotics. BceS-like HKs are coupled with an ABC transporter within the regulons. The transporter is thought to facilitate removal of harmful compounds such as antibiotics which may have diffused through the cell membrane (Joseph, et al., 2002; Mascher, 2006). A similar SK is VanS (section 1.3.2.3), which has a similar structure but has a longer linker between the two TM helices of 20-30 amino acids. This is thought to be sufficient in differentiating IMHKs from VanS, which is considered to be a classical HK (Hutchings, et al., 2006; Mascher et al., 2006). Other IMHKs possess higher numbers of TM helices; from the 4-6 of DesK-like HKs which respond to membrane fluidity due to temperature (Aguila, et al., 1998) to those of more than 10 including CbrAB of *P. aeruginosa* which responds to carbon/nitrogen ratios (Nishijyo, et al., 2001).

The third type is the second most abundant after classical SKs. Within this group, some SKs are membrane integral, some are anchored to the membrane through connection to membrane integral proteins or may be entirely cytosolic (Mascher, et al., 2006). KdpD is an example of a membrane integral SK of this group and is anchored by 4 TM helices. In *E. coli* KdpD activates the RR KdpE

which switches on the expression *kdpFABC* which constructs the high-affinity K⁺ uptake ATPase in response to turgor pressure or osmolality induced stress. This SK possesses a complex structure with a large N-terminal input domain (approximately 400 amino acids) which contains a Walker A and Walker B motif that make up an ATPase as well as a universal stress protein (Usp) domain and a C-terminal kinase core (Mascher, *et al.*, 2006). Deletion of the 4 TM helices reduced but did not abolish activity of the SK (Rothenbücher, *et al.*, 2006). It is thought that the TM helices brings the two terminals into the right position for interaction (Mascher, *et al.*, 2006).

CheA represents the second group of cytoplasmic SKs which is anchored to the membrane through another integral membrane protein. CheAY form a very well investigated TCS involved in regulation of the flagella motor construct of enteric bacteria such as *E. coli*. CheA is connected to the membrane but methyl-accepting chemotaxis proteins (MCPs) (Mascher, *et al.*, 2006).

The final type is the purely cytosolic SKs. KinA is one such example and is one of the five SKs of the RR SpoF (section 1.1.5.3). KinA possesses 3 PAS domains with uncertain function. (Marscher, *et al.*, 2006; Mitrophanov and Groisman, 2008). It is thought that PAS domains are involved in formation of a tetramer for autokinase activity to be possible (Kiehler, *et al.*, 2017). Many cytosolic SKs possess PAS and GAF domains, in some cases, these are required for sensing, others for signal relay (1.1.1.2) and others for binding molecules (Marscher, *et al.*, 2006; Gao and Stock, 2009; Wang, 2012; Zschiedrich, *et al.*, 2016).

1.1.1.2 Signal Transduction Domains

Once the signal is recognised by the sensor domain, the signal must be transduced to the kinase core and relayed to the RR. There are a number of domains through which this is achieved including the HAMP and PAS domains which are widely distributed in SKs at approximately 31% and 33% (Szurmant, *et al.*, 2007; Gao and Stock, 2009; Wang, 2012), the GAF domain at approximately 10% (Szurmant, *et al.*, 2007) and also coiled-coils which may be situated in the cytoplasm following the TM domain (Bhate, *et al.*, 2015). As previously discussed,

the PAS and GAF domains may bind proteins and also take on a sensory role, it has also been suggested that the HAMP domain may take on a similar role through being able to bind other proteins and interact with other proteins which possess sensor domains (Szurmant, *et al.*, 2007).

HAMP domains are typically formulated by two protomers and function as dimers, however, the *P. aeruginosa*, soluble receptor Aer2 was found to possess a trimer HAMP unit (Airola, *et al.*, 2010). Each unit forms a four-helix bundle connected by a long linker which runs the length of the protomer forming two parallel bundles. The start of this linker is usually a highly conserved glycine (Gly) residue. The individual bundles are made of two sets of two helices (H α 1 and H α 2) connected by approximately 14 residues (Hulko, *et al.*, 2006; Airola, *et al.*, 2010; Wang, 2012). Each turn of the helix is formulated by heptad repeats whereby the first and fourth or a and d positions are occupied by hydrophobic residues (Figure 1.3). These residues face towards the inside of the protein complex when the SKs form dimers. The packing of bundles can differ between HAMP domains (Wang, 2012) and the stacking of the bundles is thought to take on a more ordered or less ordered state. The less ordered the structure, the more splayed the arrangement of the helices bundles. It has been proposed that the HAMP domain undergoes a helix rotation to transfer the signal (Hulko, *et al.*, 2006). It has been shown that when one helix moves outwards the other moves inwards (Mohnair, *et al.*, 2014; Bhate, *et al.*, 2015) suggesting helical tilts play an important role in passing of the signal. The whole structure of the HAMP domain is very symmetrical while the kinase core in the autokinase state is asymmetric, so a signal conversion must occur (Bhate, *et al.*, 2015).

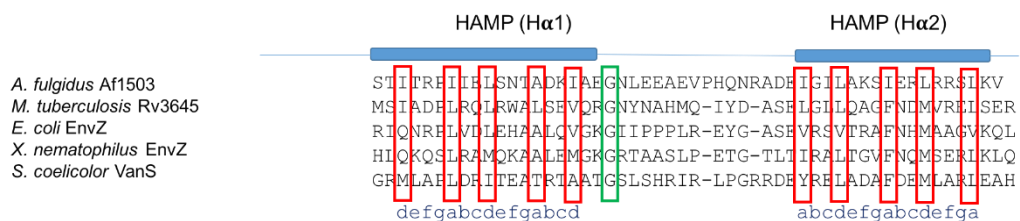


Figure 1.3: Sequence alignment analysis of HAMP domains from different SKs from different bacteria. The two protomers are linked by a short sequence which after folding runs the length of the protomer. This linker sequence begins with a conserved Gly residue (highlighted in green). The red highlighted amino acids form the a and d position of the heptad repeats.

The sequence of HAMP domains can be highly variable whether between different SKs or orthologous SKs between species (Figure 1.3). An example of this is seen in Figure 1.3, whereby the HAMP domains of SK EnvZ from *E. coli* and *X. nematophilus* and SKs of different bacteria with different functions such as VanS from *S. coelicolor* which recognises vancomycin. Despite sequence variations, HAMP domains have been shown to be exchangeable between different SKs. Hulko, *et al.*, (2006) demonstrated that the exchanging of HAMP domain of the mycobacterial adenylyl cyclase of Rv3645, which requires dimerisation for function, with the HAMP domain of a TM receptor protein Af1503 of *Archaeoglobus fulgidus* did not abolish function but increased the V_{\max} by 2.2-fold.

In addition to the HAMP domain, the sensory PAS and GAF domains, described above, are also thought to have signal transducing function in some HKs and undergo a conformational change that acts as a switch for the kinase core (Casino, *et al.*, 2014). GAF and PAS domains demonstrate high sequence variability and plasticity allowing them to have dual function (Gao, and Stock, 2009). Analysis of SK sequences is insufficient on the whole to deduce whether PAS and GAF domains function as signal transducers, function in partnership with other domains as a sensor or serves as the sensor themselves (Mascher, *et al.*, 2006; Gushchin, *et al.*, 2017). DcuS possesses two PAS domains, one extracellular and one cytoplasmic, and functions in association with the succinate transporter DcuA in aerobic conditions but with antiporter DcuB in anaerobic conditions. In the absence of C_4 decarboxylates, the cytoplasmic PAS domain has a closed conformation which inhibits kinase activity, however, in the presence of C_4 decarboxylates, it switches to an open conformation resulting in kinase activity (Monzel, *et al.*, 2013). In *S. coelicolor* only six TCSs possess PAS domains and seven contain GAF domains, with only one containing both (Hutchings, *et al.*, 2004). PAS domains, unlike PDC domains, have more of an intrinsic affinity for dimerisation (Gao, *et al.*, 2009).

1.1.1.3 Kinase Core

The kinase core is comprised of the Dhp domain (also called Histidine kinase domain A, HisKA) and the CA domain. The Dhp domain is the site of

autophosphorylation of the SK and phosphotransfer between the SK and RR. If the SK possesses intrinsic phosphatase activity, this is also the site of dephosphorylation of the RR. The Dhp domain is formed through two helices referred to as D α 1 and D α 2. These are antiparallel coiled-coils and upon dimerisation form a bundle of 4 helices (Figure 1.2). The His residue which becomes autophosphorylated is absolutely conserved within HKs and is situated within the H box of D α 1 (Figure 1.4). This conserved His is the first of seven amino acids which are all well conserved to aid in the phosphotransfer event. Residue 2 is often an Asp or Glu residue which serves as a hydrogen bond acceptor. In the fourth position is usually a lysine (Lys) or arginine (Arg) which can associate with the reactive phosphoryl group. The fifth position occupied by asparagine (Asn) or threonine (Thr) followed by a proline (Pro). These allow flexibility and helix bending allowing the the helix to adopt different conformations during the reactions (Figure 1.4; Wang, 2012; Bhate, *et al.*, 2015).

Much of the helices are tightly associated, with more plasticity around the conserved His residue. The Pro and Thre residues within the H box have been shown to be essential for phosphatase activity in the SK, VicK from *Streptococcus mutans*, as are the HAMP and PAS domains (Wang, *et al.*, 2013A).

The other part of the kinase domain is the CA domain or H-ATPase domain, which binds ATP. This is linked to the Dhp domain via a flexible loop to the CA domain (Bhate, *et al.*, 2015). When the Dhp domain is brought closer, the His residue acts as nucleophile to autophosphorylate. The CA domain structure is highly conserved with an N, G1, F, G2 and G3 box (Figure 1.3). Structurally, the domain is composed of 2 layers of $\alpha\beta$ folds, where one layer is of 5 stranded β -sheet and another of three α -helices, (Wang, 2012).

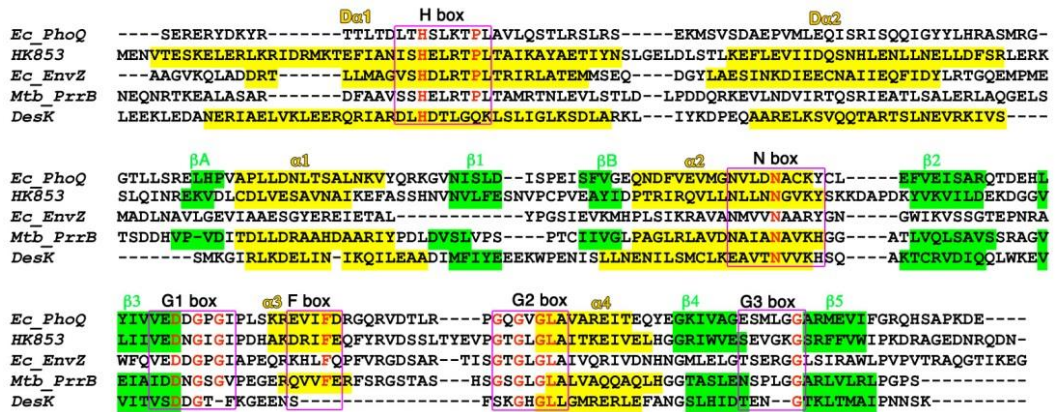


Figure 1.4: Sequence alignment analysis of kinase cores-Dhp and CA domains of HKs. Conserved sequence motifs H, N, G1, F, G2, and G3 boxes are highlighted in magenta boxes. Helices are highlighted in yellow, and β -strands in green (Taken from Wang, 2012).

It has been noted that different positions of the kinase core undergo symmetry changes during signal binding, autophosphorylation and RR binding. In the top part, above the proline, symmetric to asymmetric conformational changes occur in the change between phosphatase and kinase activity. In the mid portion of the core, positioning remains stable and the lower part of the interhelical loop, demonstrates high variability in its position and handedness (Bhate, *et al.*, 2015). In contrast, the LuxPQ complex, asymmetric conformation of the dimers causes an inhibition of kinase activity (Gao and Stock, 2009).

1.1.2 Response Regulators

RRs are relatively simple in comparison to SKs, because they contain only two domains: the receiver domain (REC), identified when the first bacterial RR was sequenced, and the effector or output domain. (Stock, *et al.*, 1985; Galperin, 2006).

1.1.2.1 REC domain

The REC domain, like the CA domain of SKs, is composed of $\alpha\beta$ folds but with five core β -sheets surrounded by 5 α -helices in an alternating corrugated fashion. The conserved reactive Asp residue which becomes phosphorylated resides in the C-terminus of β_3 situated within an acidic cluster of residues which binds divalent cations. These facilitate the phosphotransfer reaction. In addition to the acid pocket, other regions are essential in phosphotransfer and these can differ

between classes of RRs. In PhoP/OmpR type RR, the $\alpha_4\beta_5\alpha_5$ was found to be directly involved in phosphorylation-induced RR dimerisation. Disruption to this site affects not just dimerisation but also DNA binding in PhoB; phosphorylation of PhoP/OmpR type RRs cause a change in conformation which favours dimerisation at the same interface of $\alpha_4\beta_5\alpha_5$ (Mack, *et al.*, 2009). Perturbation of the $\alpha_1\alpha_5$ surface did not cause any such effects; however, this was found to be the mediator of phosphorylation and dimerisation in NarL/LuxR (also referred to as NarL/FixJ) type RRs (Leonard, *et al.*, 2013; Trajtenberg, *et al.*, 2014). Similarly, phosphorylation of NtrC allowed triggered activation through dimerisation (Gao, *et al.*, 2007). It has been shown that phosphorylation of VraR, a NarL/LuxR type RR that mediates vancomycin resistance in *Staphylococcus aureus* changes the structure from a closed to open conformation (Leonard, *et al.*, 2013). A similar effect was also speculated for Spr1814 from *Streptococcus pneumoniae* (Park, *et al.*, 2013) and in the case of CheB, in the unphosphorylated state, the REC domain prevents access to the methyltransferase active site (Gao, *et al.*, 2007).

1.1.2.2 Effector domain

REC domains in RRs are usually coupled with an effector domain, however, in some cases this is not the case (Figure 1.5) making it ambiguous as to what purpose they serve. Additionally, analysis of sequence and homology is not an immediate indicator of regulatory function as few mutations are necessary for change in recognition sequence and hence regulation targets (Galperin, 2010). Studying effector domains has revealed that RRs may be responsible for more than DNA binding (63%; Gao and Stock, 2009) but also RNA binding to change expression levels. Additionally, some RRs possess domains with enzymatic activity, protein binding domains or transporter domains (Galperin, 2010).

1.1.2.3 Transcriptional Activators

The best studied DNA binding transcriptional activator RRs are the PhoP/OmpR type, NarL/LuxR type, NtrC/DctD and LytR/AgrA types. Approximately 50% of RRs form dimers, with all OmpR family RRs forming dimers to bind the target DNA sequence (Gao and Stock, 2010; Capra and Laub,

2012). From Figure 1. 5, it can be seen that the winged helix motifs of PhoPR type RR is most common in bacteria, this holds true for the proteobacteria, cyanobacteria and thermotogae. However, in Actinobacteria, this is not the case. Here, NarL/LuxR type helix turn helix (HTH) RRs are predominant.

Where PhoP/OmpR and NarL/LuxR type RRs possess only two domains (REC and DNA binding effector domain), NtrC/DctD family of RRs possess three domains. In addition to the REC domain, it also possesses a factor of inversion stimulation (Fis) domain and an AAA⁺ ATPase domain. FIS domains have HTH motifs and serve to activate transcription and recombine sequences through binding at specific enhancer sites (Kostrewa, *et al.*, 1991). Whilst the FIS domain binds DNA, the AAA⁺ ATPase domain binds to sigma factor 54 (σ 54) in RNA polymerase generating an open complex (Gao, *et al.*, 2007). The FIS domain is not only found in conjunction with the AAA⁺ ATPase domain, in ActR/PrrA type RR, only the FIS domain is linked to the REC domain. Other HTH motif domains include MerR, which is commonly associated with responses to oxidative stress, heavy metals and antibiotics (Brown, *et al.*, 2003), YcbB found in RR GlnL (formerly YcbB; Satomura, *et al.*, 2005; Galperin, 2006), AraC, ArsR and Spo0A (Galperin, 2010). The LytR/AgrA type are the only type to not possess solely α helices in the binding motif. Instead it possesses 10 β -folds and a single α helix (Sidote, *et al.*, 2008). This has been shown to have a novel mechanism of DNA interaction.

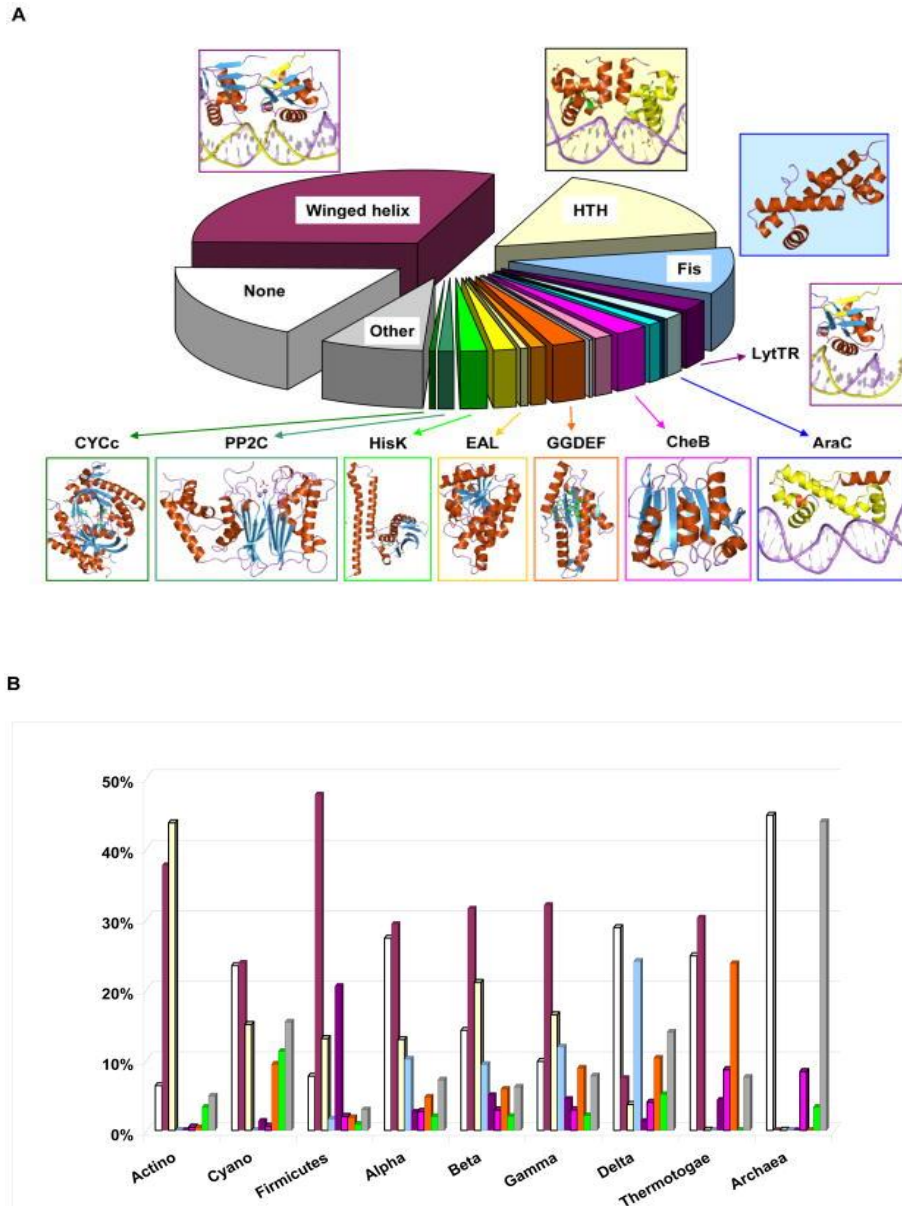


Figure 1. 5: Distribution of the most common effector domains of response regulators (RR) in bacteria. A) Distribution of total effector domains across bacteria with their representative RR domain structure in ribbon form. Unlabelled output domains (clockwise from AraC) are as follows: Spo0A (dark blue), ANTAR (cyan), CheW (pink), CheC (white), GGDEF+EAL (orange), HD-GYP (yellow) (Taken from Galperin, 2010). B) Distribution of effector domains across bacterial phyla and archaea including the subdivisions of Proteobacteria (alpha, beta, gamma and delta). Effector domains are as labelled: single-domain (white), OmpR (maroon), NarL (bisque), NtrC (blue), combined LytR, ActR, YesN/AraC, and Spo0A (purple), CheB (magenta), combined c-di-GMP signaling (WspR, PleD, PvrR, FimX, and RpfG, orange), and enzymatic (HisK and PP2C output domains, green) families within each taxonomic group. The grey bars indicate combined fractions of all other RR families (Taken from Galperin, 2010).

Unlike with DNA binding domains, only one type of RNA binding domain has been identified which is the ANTAR (AmiR and NasR transcriptional anti-terminator regulator domain). The ANTAR domain consists of three helices which

contain 5 strictly conserved residues that are exposed: three alanines (Ala), one Ala or serine (Ser) and an aromatic residue (O'Hara, *et al.*, 1999; Ramesh, *et al.*, 2012). ANTAR domains alone are able to dimerise but phosphorylation of the RR EutV by EutW triggered dimerisation which improves RNA binding affinity (Ramesh, *et al.*, 2012). The ANTAR domain of AmiR and NasR have been shown to prevent termination of transcription through binding to nascent RNA upstream of the terminator. It is thought this is to prevent formation of a termination stem loop and thus preventing the RNA polymerase from dropping off during translation (O'Hara, *et al.*, 1999).

1.1.2.4 Protein binding, enzymatic activity and transporters

Different protein binding domains have been identified, most notably the chemotaxis RRs, combining the REC domain with CheW effector domain in CheV-type RRs (Galperin, 2006). In addition to this, PAS, GAF, TPR (tetratricopeptide) and histidine phosphotransferase (Hpt) domains can also function as protein binding domains in RRs (Galperin, 2006). TPR domains are also found in proteins such as RapF which is an anti-activator and serves to sequester expression of target genes of ComA, a RR that regulates genetic competence genes in *B. subtilis*, through blockage of its DNA binding site (Bongiorni, *et al.*, 2005; Baker, *et al.*, 2011). The TPR domain was identified in the RR DVU2937 in Gram-negative sulphate-reducing bacteria *Desulfovibrio vulgaris* (Heidelberg, *et al.*, 2004).

In addition to the domains mentioned, the RRs RssB and PhyR possess protein binding domains which have anti-sigma factor and anti-anti-sigma factor activity, respectively. RssB~P inhibits SigS, which is a master stress regulator in *E. coli* (Becker, *et al.*, 2000). PhyR~P binds to the anti-sigma factor NepR of SigEcfG (Galperin, 2010; Herrou, *et al.*, 2010).

As mentioned earlier, the NtrC/DctD family of RRs possess an AAA⁺-ATPase domain, other ATPase domains are also found including the MinD/ParA (cell division protein) and PilB (secretion ATPase) families. In addition to ATPases, a plethora of other enzymatic cellular reactions are directly associated with RR domains including diguanylate cyclase activity in GGDEF-type output domain, c-di-GMP-specific phosphodiesterase activity from EAL domain of VieA,

kinase and phosphatase activity to name only a few (Galperin, 2006; Galperin, 2010).

Finally, an increasing number of RRs have been identified that possess transporter activity to move molecules across membranes including sugars, nitrate, formate, and other ions (Galperin, 2010). However, many of these output domains seem to be clade specific.

1.1.3 Evolution of new TCSs and the impact on partnering of SKs and RRs

As has been discussed so far, TCSs are very diverse, whether it is the structure of the SK or RR, their input signaling or their output signaling target and mechanism. To this end, the evolution of TCSs was and is highly important.

1.1.3.1 Evolution of TCSs

Analysis of total TCSs in genomes have shown that typically the number of TCSs roughly correlates with the square of the genome size (Galperin, 2005; Capra and Laub, 2012). The genome size and lifestyle of the bacterium also plays a large role, with the reduced genome size of parasites with highly specific and stable environments containing significantly less TCSs, whereas, bacteria living in diverse environments being exposed to ever changing conditions require more TCSs to allow adaptive responses. *S. coelicolor*, for instance which is a soil dwelling bacteria has approximately 1% of its genome (8183 genes) composed of by HKs. Another soil dwelling bacterium, *Dechloromonas aromatic* RCB, which is a Gram-negative anaerobe of the Betaproteobacteria, one of the eight classes of the Proteobacteria phylum, possesses 3933 genes and 105 of these are HKs. On the other side of the spectrum, the pathogen *M. tuberculosis* H37Rv has a genome size of 4202 genes and only 14 of these genes are HKs (Alm, *et al.*, 2006).

The gain of a new TCS has been attributed to two avenues: lineage specific expansion (LSE), where there is a duplication event or reshuffling and lateral gene transfer (LGT), where genes are transferred from one species to another (Alm, *et al.*, 2006). In a 2006 study by Alm, *et al.*, nearly 5000 HKs from 207 sequenced genomes were analysed. In this study, classification of whether a TCS was attained via LGT or LSE was based on identifying homologues and building family trees. If the closest homologues are distributed within the closest relatives, these were

categorised as being derived from LSE. If the closest homologs were identified in distant branches, these were classed as having been gained through LGT. The gain of new TCSs may be evenly balanced between LSE and LGT as is seen in *Bradyrhizobium japonicum*, or may be biased towards one of these methods such as for *P. aeruginosa* which has gained the majority of its new TCSs from LGT and for *S. coelicolor* which have evolved new TCSs from LSE (Alm, *et al.*, 2006). As TCS expansion in *S. coelicolor* has largely been attributed to lineage specific means, this may explain why streptomycete RR effector domains appear to be largely restricted to transcriptional regulation (Galperin, 2006).

The gain of new TCSs through LGT is thought to be more likely to preserve the positioning of the genes in their adjacent position or closely within a regulon, however, those gained through duplication events are more likely to cause separations (Alm, *et al.*, 2006).

After a duplication event, there must be cross-phosphorylation between the parent TCS and the replicated TCS. The duplication could result in the higher concentration of the mother and daughter genes, which would have a higher energy cost on the cell to produce. It could also reduce the signaling in the cell, particularly if the activation of signaling is a low concentration of the substrate, SKs without substrate could dephosphorylate the RR~P within the cell, thus reducing the signaling (Rowland and Deeds, 2014). After duplication events, the buildup of mutations and reshuffling events can change the function and recognition of TCSs to generate new TCSs. In addition to reshuffling and duplication, hybridisation can also occur, generating hybrid TCSs (Section 1.1.5.2). This can occur at stop codons or independently of this. Reshuffling and hybridisation are both thought to be very rare events however (Capra and Laub, 2012). In the process of mutation build up, the two components may gain or lose functions and pseudogenes may also be formed. In some cases, this may result in multiple RRs being activated by a single SK or multiple SKs regulating a single RR (section 1.1.5.3).

1.1.3.2 Specificity of pairing between SKs and cognate RRs

As the signal recognition for these is so specific, so too must the interaction between the SK and its cognate RR as ‘cross-talk’ - the phosphorylation of a RR by

a non-cognate SK, could be deleterious. Studies have shown that cross-talk can take place both *in vitro* and *in vivo* (Verhamme *et al.*, 2002; Skerker, *et al.*, 2005). Skerker, *et al.*, (2005) demonstrated in phosphotransfer assays that a purified HK~P could transfer the phosphoryl group to purified RRs when the reaction was left to run for an hour, however, in a short period of time (10s) only the cognate RR was phosphorylated suggesting a much higher affinity and kinetic preference. Verhamme *et al.*, (2002) showed that in a $\Delta ntrB$ strain, its cognate RR NtrC could be phosphorylated by other SKs. Another study which demonstrates this, was conducted by Rick, *et al.*, (2014), who showed that overexpression of the RR AbrA2 in an $\Delta abrA1$ (HK) background was lethal. Other SKs or phospho-donors may have phosphorylated AbrA1 as the result mirrored that of a phosphomimetic AbrA2 strain (Rico, *et al.*, 2014). However, these studies also show that cross-talk is extremely rare if seen at all in wild-type bacteria (Bijlsma and Groisman, 2003). In addition to cross-phosphorylation being rare, many SKs possess phosphatase activity which reduces the effects of any cross-talk.

1.1.4 Regulation of TCSs

As discussed earlier, TCSs are not the sole signal transduction pathways in bacteria. Ser/Thr/Tyr protein kinases are also highly prevalent. Where Ser/Thr/Tyr kinases generate phosphoesters, SKs generate phosphoramidates. The hydrolysis of the latter possesses significantly more negative free energy; the high energy state generated is suitable for phosphoryl-transfer particularly as equilibrium favours the unphosphorylated state when considering the ADP/ATP ratio within cells (Stock *et al.*, 1990; Stock, *et al.*, 2000). Similarly, the phosphorylated Asp residue possesses an extremely high energy state which is able to drive conformational changes in protein structure (Stock, *et al.*, 2000). Half-lives of RR~P can range from seconds to hours; some RRs possess autophosphatase activity rendering the half-life shorter (Weiss and Magasanik, 1988).

1.1.4.1 Phosphatase activity

Whilst HK's phosphorylate RRs, many also possess phosphatase activity to switch off the response once the signal abates. The vancomycin sensing HK VanS is a good example in *Streptomyces*. The VanRS TCS senses vancomycin and

responds by activating inducible vancomycin resistance (*van*) genes. An *S. coelicolor* Δ *vanS* mutant constitutively expresses the *vanRSJKHAX* resistance genes because VanR is constitutively phosphorylated by acetyl phosphate and cannot be dephosphorylated by VanS (Hutchings, *et al.*, 2006). In addition to SKs and RRs possessing phosphatase activity, dephosphorylation can also be facilitated by auxiliary proteins which can be highly specific to the TCS. An example of this interaction is seen in the chemotaxis pathway in *Escherichia coli*, where CheA phosphorylates CheY which is dephosphorylated by CheZ. The dimeric CheZ was shown to only bind the phosphorylated version of CheY (Blat and Eisenbach, 1994; Blat and Eisenbach, 1996).

1.1.4.2 TCS expression

In addition to the maintenance of phosphorylation state, expression levels of the TCS genes plays a large part in the regulation of TCS activity. To maintain a basal level of the SK and RR, there is usually a constitutive promoter which can be strong or weak. This may also be paired with a second promoter which has an inducible, autoregulatory function and this has been well studied in the PhoP/PhoQ system in *Salmonella*, *Yersinia* and *E. coli* (Soncini, *et al.*, 1995; Kato, *et al.*, 1999). In *Streptomyces*, the negative regulator of antibiotic biosynthesis TCS AbsA1/A2, possesses two promoters. One of these promoters regulates expression of both *absA1* and *absA2* and the other promoter only for the expression of *absA2*, the RR (Santos-Beneit, *et al.*, 2013).

When a strong constitutive promoter is regulating TCS expression, the immediate signal intensity could elicit expression of the target regulons. However, under the regulation of a weak promoter, the expression of target genes would require positive feedback regulation on the TCS itself to generate the same amount of RR~P (Mitrophanov, *et al.*, 2010). Furthermore, with different levels of RR~P within the cell, the extent of regulation of target genes can change. Promoters with binding sites of a higher affinity may be targeted with a lower RR~P present but those with a lower affinity may not be targeted until a higher threshold is reached (Groisman, 2016). Positive feedback control can maintain levels of TCSs when the SK or RR or both possess phosphatase activity (Goulian, 2010). The autoregulation exerts a form of ‘memory’ for the system for recurrence of the stimulus. Study of

PhoB/PhoR which responds to phosphate depletion in *E. coli* has shown that in response of a second phosphate depletion, the expression response of target genes is activated at a faster rate due to the higher levels of RR in the cell than for cells which encounter phosphate starvation for the first time (Gao and Stock, 2013; Gao, *et al.*, 2017). Whilst rare, there are also studied instances of negative feedback where the RR either dependent or independently of phosphorylation state, can repress its expression. Examples include the CovS/CovR system from *Streptococcus pyogenes* (Gusa and Scott, 2005; Goulian, 2010).

1.1.5 TCS variants

So far only canonical TCSs have been discussed in detail but for many TCSs this is not the case. Some TCSs have multiple components whether accessory and adaptor proteins or additional HK and RRs. Some TCS proteins are orphans which have no function, or its cognate RR is situated elsewhere in the genome and for both, their function has been retained. Here, these variants will be discussed further.

1.1.5.1 Orphans

Orphaned components are TCS genes which are not situated in an operon with a cognate partner gene. These may have arisen through rearrangement or duplication events which resulted in operon duplications and the subsequent loss of an SK or RR gene or simply duplication of a single TCS genes. The maintenance of these genes within the genome, usually signifies some selective advantage as mutations can quickly build resulting in the status of pseudogenes or loss of the gene completely (Capra & Laub, 2012).

Some orphan RRs display loss or change in the some of the five most conserved residues of REC domain rendering it no longer phosphorylatable, resulting in an atypical RR (ARR). In *Streptomyces venezuelae*, the ARR JadR1 regulates the expression of the jadomycin biosynthetic gene cluster (BGC) in a phosphorylation independent manor. Structurally it is an OmpR family RR with a winged HTH motif, and it possesses the conserved Asp residue which typically accepts the phosphoryl group, but it lacks two of the conserved Asp residues in the terminus of the β 1 strand which would bind the divalent ions. Instead, jadomycin B and a late stage molecule in the biosynthesis pathway binds to JadR1 to form a

negative feedback loop (Hong, *et al.*, 2007; Wang, *et al.*, 2009). Another ARR involved in antibiotic regulation is PapR6 which mediates pristinamycin production by binding upstream of one of the four operons (*snaFE1E2GHIJK*) encoding its biosynthesis in *Streptomyces pristinaespiralis*. Here PapR6 lacks four of the five conserved residues (Dun, *et al.*, 2015). As mentioned, ARRs typically display a loss of the five main conserved residues, within the REC domain. These are situated within the phosphorylative pocket. BldM (discussed further in section 1.2.2) is an ARR which is able to heterodimerise with another orphan RR, WhiI. Where, these five residues are intact in WhiI (Molle and Buttner. 2000), BldM does not possess three of the five conserved residues (Ainsa, *et al.*, 1999). In *Helicobacter pylori*, there are only three HKs and five RRs. Two of these RRs are essential for growth and another if deleted causes severe physiological defects (Schär, *et al.*, 2005). Both HP1043 and HP1021 are orphan ARRs, with HP1043 being essential. In the traditional phosphorylative pocket of HP1043, the Asp amino acid is replaced by a Lys residue. However, another Asp residue (D52) is thought to be moved towards this pocket as a consequence. Furthermore, D52 is adjacent to S51. A homologue of HP1021, in *Helicobacter hepaticus*, a Ser residue replaces the phosphorylated Asp residue (Schär, *et al.*, 2005). This leads to the question of whether in these ARRs, whether serine is the phosphorylated residue or whether D52 is the phosphor-acceptor in HP1021, or whether these RRs are activated in a phosphorylation independent manner.

1.1.5.2 Hybrid TCSs

Besides SK and RR signaling, there are ‘hybrids’. Some signal transduction proteins possess sensor domains of a SK and also domain or domains of a RR. There are two types of these hybrid systems. The first are one-component systems which possess a sensor domain and an effector domain. An example of this is RocR of *B. subtilis* which possesses a PAS domain and an HTH type DNA binding domain (Calogero, *et al.*, 1994; Ulrich, *et al.*, 2005). RocR senses high arginine concentrations and activates expression of genes involved in the utilisation of arginine as a sole nitrogen source (Calogero, *et al.*, 1994). These typically do not

have phosphotransfer domains. One-component systems are thought to be the ancestors of TCSs (Ulrich, *et al.*, 2005).

Where the one-component system is a single protein, this second type requires other proteins to relay the signal. These are referred to as phosphorelay systems. Here, after autophosphorylation, the chemical signal is transferred to the REC domain (within the same protein) which then passes on to either a HPt domain, HPt protein or other phospho-acceptor and transfer proteins which then shuttles the signal to the terminal RR. This type of pairing has been shown to have reduced specificity compared to typical TCS signaling (Cheng, *et al.*, 2014).

One of the best studied examples of a phosphorelay system is sporulation control in *B. subtilis*. KinA and KinB are two HKs which ultimately activate the RR, Spo0A. Acting as intermediates in the pathway are the HPt proteins Spo0F and Spo0B (Perego, 1998; Perraud, *et al.*, 1999). In a multistep system such as this, there are more targets of regulation. Rap A and RapB are both phosphatases that regulate Spo0F and are their expression is also subjected to regulation by physiological conditions. Additionally, another phosphatase, Spo0E regulates the RR, Spo0A (Perraud, *et al.*, 1999).

In the instance of ArcB in *E. coli*, the protein possesses multiple domains. The phosphoryl group can be shuttled from the initial His residue to the Asp residue of the REC domain to the His residue of the HPt domain before the Asp residue of the RR, ArcA. In this system, the reactive phosphoryl group can also be passed directly from the His to the Asp of the RR. This is thought to be connected to anaerobic and aerobic conditions (Matsushika and Mizuno, 1998; Perraud, *et al.*, 1999).

Whilst phosphorelay systems are less specific, one-component systems are thought to have the issue of reduced signaling as they can also be tethered to the membrane meaning for DNA binding to occur the chromosome must diffuse to the protein. Additionally, they possess a 1:1 ratio of SK: RR, rather than the typical higher RR: SK ratio (Raghavan & Groisman, 2010). Eukaryote TCSs are predominantly hybrid systems. It is argued that this is perhaps due to greater stability and a less transient and labile interaction (Capra and Laub, 2012).

1.1.5.3 Multiple component systems

As described earlier (section 1.1.5.1) with orphan components derived from duplication events, in some cases, orphan kinases retain kinase activity against the original cognate RR (Capra & Laub, 2012). This is exemplified in *B. subtilis*, where the RR Spo0F can be phosphorylated by five orphan SKs, KinA/B/C/D/E (Stephenson & Hoch, 2002). These five kinases retain the residues surrounding the His and Asp residues of the SK and RR, respectively, which confer the specificity between the protein pairings but have very dissimilar sensor domains allowing recognition of different stimuli as shown by the varying levels of sporulation under different growth conditions in the null mutants (LeDeaux, *et al.*, 1995; Bijlsma and Groisman, 2003).

Another example is AbrC1/C2/C3 found in *S. coelicolor* and *S. lividans*. Here again there are multiple SKs to a single RR and the RR is transcribed independently of the SKs. The AbrC TCS regulates antibiotic production, with Δ *abrC1* mutants overproducing antibiotics, whereas, Δ *abrC2* has a less severe effect suggesting complementary roles of these SKs (Rodríguez, *et al.*, 2015).

In addition to multiple SKs or RRs, auxillary proteins may also be present. These proteins may be involved in stimulus perception, fine-tuning, cross-talk, or signal integration (Island & Kadner, 1993; Kato & Groisman, 2004; Eguchi *et al.*, 2007; Fleischer *et al.*, 2007; Paul *et al.*, 2008; Heermann and Jung, 2010). Examples include CseBC and PhoPR, both of which are discussed in section 1.3.2.

1.1.6 Potentials of TCSs to be used as antibiotic targets and targets for antibiotic production

Thus far, many TCSs and their variants spanning different bacteria phyla have been briefly discussed demonstrating their importance in the regulation of essential functions and also the control of adaptive responses when bacteria are exposed to extra- and intra-cellular changes. Furthermore, the fact that they are ubiquitously found in bacteria but not humans allows TCSs to be viewed as potential targets for anti-infectives (Barrett and Hoch, 1998; Watanabe, *et al.*, 2008; Shor and Chauhan, 2015; Tiwari, *et al.*, 2017).

Many TCSs are involved in virulence signaling (e.g. EnvZ/OmpR and PhoPQ of *Salmonella enterica*; Feng, *et al.*, 2003; Bijlsma and Groisman, 2005) or resistance (e.g. VanRS of *Enterococcus faecalis* and *S. aureus*; Evers and Courvalin, 1996; Périchon and Courvalin, 2009) and some TCSs are essential for viability (e.g. MtrAB in *M. tuberculosis*; Zahrt and Deretic, 2000). All of these would be suitable targets of antibiotics or antibiotic adjuvants. The deletion of PhoP in *M. tuberculosis* has been shown to be an effective vaccine strategy in mice and guinea pigs, more so than the BCG (*Bacillus Calmette-Guérin*) vaccine (Martin, *et al.*, 2006). Many compounds have been identified which inhibit TCSs including bis-phenol which targets VanS and EnvZ (Domagala, *et al.*, 1998) or thiazole derivatives which can inhibit autophosphorylation of VanS in *E. faecium* and phosphorylation and desphosphorylation of Algr2 in *P. aeruginosa* (Roychoudhury, *et al.*, 1993; Ulijasz and Weisblum, 1999; Tiwari, *et al.*, 2017). In both the former cases, preventing sensing of vancomycin would prevent activation of the vancomycin resistance genes being expressed and hence allow vancomycin to be used against previously resistant pathogenic strains.

The conservation of the kinase core makes it an attractive target when selecting antibacterial hits for further study as it could target not just one specific TCS, but multiple, thus increasing the difficulty for resistance to occur. However, there is also sequence conservation between the kinase domain of HKs found in prokarya and archaea as well as kinases found in eukarya (Tiwari, *et al.*, 2017). There is also a high degree of similarity between the ATP binding pocket of HKs and several human family proteins including the Hsp90 (heat shock protein) chaperone (Bem, *et al.*, 2015; Tiwari, *et al.*, 2017).

Inhibitors have also been identified which the RR, rather than the SK. WalRK is almost ubiquitous in Firmicutes. Due to multiple independent discoveries of this TCS in different species, this is also referred to as VicRK. The walrycins were identified in a high throughput screen to specifically identify inhibitors of WalR, the RR (Gotoh, *et al.*, 2010). Walrycin A is thought to enter *E. coli* more readily, whereas walrycin B has greater entry efficiency into *B. subtilis* and *S. aureus*. Walrycins alter the equilibrium between monomeric and dimeric forms of the RR, favouring the dimeric form. This inhibitor bound dimeric form is unable to

bind promoters in stark comparison to WalR dimers formed in the absence of the inhibitor (Gotoh, *et al.*, 2010).

In addition to targeting TCSs as an anti-infective, TCSs can be used as a means to activate the production anti-infectives, other therapeutics or compounds which may be useful to us in other means. The signaling circuitry could be remodeled to activate secondary metabolite biosynthetic pathways of compounds. In a review by Ninfa (2010), rewiring of TCSs through different means has been discussed such as grafting additional domains to SKs or RRs to extend signaling capabilities or to change sensor domains of SKs of the same family to manipulate output. Skerker, *et al.*, (2008) demonstrated by exchanging as few as three residues within the Dhp domain of the SK was sufficient to change the specificity of one SK to recognise the RR of another SK of which those three residues matched with. Another means to change the output is through deletion of modules within the SK as demonstrated by Bidart, *et al.*, (2012) in deletions of segments of the previously described ArcB SK, differences in metabolic flux under anoxic conditions, which could be utilised for the production of reduced biochemicals.

Many TCSs are well studied for their involvement in the activation of antibiotic biosynthesis such as PhoPR (Section 1.3.1.1) which was discussed earlier for its high conservation across bacterial families and also importance in *M. tuberculosis* virulence and AfsQ1/Q2 (Section 1.3.1.2), a global regulator in *Streptomyces*. As stated before, the model organism *S. coelicolor* possesses more than 60 complete TCSs in its genome and many more HKs. *Streptomyces* as a genus are well characterised for their complicated lifecycle as well as producing an incredible array of different secondary metabolites making it an ideal genus in the study of TCSs and rewiring of TCSs for the activation of metabolite production especially from cryptic gene clusters.

1.2 *Streptomyces*

The first streptomycete is thought to have evolved around 450 million years ago (Chater, 2006), but the genus was not proposed until 1943 by Waksman and Henrici when streptomycin, the first effective treatment for tuberculosis was identified by the Selman Waksman's laboratory (Anderson and Wellington, 2001;

Kresge, *et al.*, 2004). Today the genus has expanded to contain more than 600 species (Sousa and Olivares, 2016).

As a genus *Streptomyces* are Gram-positive bacteria with a high GC content (69-78%) and are found ubiquitously in nature but most commonly as soil dwelling saprophytes that give the ground its earthy aroma (Korn-Wendisch and Kutzner, 1992). This characteristic soil smell, that is particularly pungent after rain is the smell of geosmin (not solely produced by *Streptomyces*), is one of the many secondary metabolites *Streptomyces* synthesise (Gerber and Lechevalier, 1965). They are characterised for their complex lifecycle (section 1.2.2), first beginning life as thermo-resistant spores that germinate under favourable conditions to form branching lateral vegetative mycelia then later differentiate into aerial mycelia that form septa compartmentalising copies of chromosomes and later mature into dormant spores. During growth of the colony whilst the peripheral hyphae extend the colony in the vegetative stage, the centre of colony undergoes the switch to aerial growth and sporulation. It is thought this process is fed by the apoptosis of substrate mycelia releasing nutrients to the hyphae on the surface (Chater, 2011; Celler, *et al.*, 2016).

1.2.1 Streptomycetes: nature's pharmaceuticals

Streptomyces are a vastly important genus which has shaped modern medicine. Since the discovery of streptomycin from *S. griseus*, thousands of compounds have been isolated and found to possess bioactivity (Antoraz, *et al.*, 2015; Raja & Prabakarana, 2011). In fact, over 60% of clinically used antibiotics were discovered in *Streptomyces* (Watve, *et al.*, 2001; Esnault, *et al.*, 2017). It has been estimated that the genus has the potential to produce in the order of 10^4 antimicrobial compounds (Watve, *et al.*, 2001). In addition to antibacterials, many of these compounds are used as antifungals, antivirals, immunosuppressants, antihypertensives, and antitumorals (Procópio, *et al.*, 2012).

In addition to producing compounds utilised in a clinical setting, *Streptomyces* are also highly important in agriculture. Being ubiquitously found in soil, many studies have been conducted to investigate the role *Streptomyces* may play and their potential to interact and influence plants (Tarkka, *et al.*, 2008; Seipke,

et al., 2012; Chater, 2016; Sousa and Olivares, 2016; Tokala, *et al.*, 2016; Viaene *et al.*, 2016). The filamentous lifestyle of *Streptomyces* is thought to enable these bacteria to enter the rhizosphere of nearby plant roots as well as penetrating into the roots themselves as endophytes or as parasites (Coombs and Franco, 2003; Seipke, *et al.*, 2012). This is particularly well demonstrated by Clark and Matthews (1987) who presents scanning electron images of *S. ipomoea*, a plant pathogen spreading into the parenchymal cells of a sweet potatoe plant. Armed with the capability to produce a wealth of bioactive enzymes and compounds, *Streptomyces* can produce plant promoting growth factors such as auxin and anti-infectives to prevent invasion of phytoparasites such as chitinases or cell-wall degrading enzymes to promote and protect the plant (Hoster, *et al.*, 2005; Cordovez, *et al.*, 2015; Sousa and Olivares, 2016).

Streptomyces can also encourage growth of other symbiotic microorganisms. *Streptomyces* sp. AcH 505 is a mycorrhization helper bacterium, so called as it facilitates bacterial-fungal-plant symbiosis. AcH 505 produces auxofuran which promotes fungal growth and also an inhibitor of mycelial growth, a naphthoquinone antibiotic WS-5995 B (Riedlinger, *et al.*, 2006; Lehr, *et al.*, 2009). Only resistant strains are able to grow, thus selecting for symbiotic fungi (Tarkka, *et al.*, 2008; Lehr, *et al.*, 2009). In addition to production of antibiotics to prevent pathogens from colonising, they are also able to induce plant defense responses and hence prime the plant. Kurth, *et al.*, 2014 showed that inoculation of AcH 505 with oak suppressed infection by powdery mildew. The investigation showed that Ach 505 elicited the jasmonic acid, salicylic acid, jasmonate/ethylene and abscisic acid plant defence pathways. *Streptomyces* are also implicated in a number of other symbiotic relationships, such as in Attine and *Allomerus* ants, marine sponges and fungi to name but a few. Many reviews and investigations discuss these relationships (Kroiss, *et al.*, 2010; Barke, *et al.*, 2011; Seipke, *et al.*, 2012; Kaltenpoth, *et al.*, 2014).

Whilst most *Streptomyces* species are non-pathogenic, a few cause disease. An example presented above was *S. ipomoea* which causes soft rot in sweet potatoes. The most commonly studied plant pathogen within this genus is *S. scabies* which as the name implies is the common cause of potatoe scab disease (Loria,

et al., 2006). Analysis into the mechanism behind plant pathogenicity has shown that *Streptomyces* can produce many phytotoxins. *S. scabies* has been shown to produce a coronatine-like phytotoxin (Bignell, *et al.*, 2010; Bignell, *et al.*, 2013). Besides plant pathogens, there are two human pathogens named *S. sudanensis* and *S. somaliensis* which are capable of causing severe and debilitating deep tissue and bone infections (Quintana, *et al.*, 2008; Kirby *et al.* 2012).

1.2.2 Life cycle

Streptomyces spores are spore forming bacteria but their spores are distinctly different to endospores of *Bacillus*, being far less able to survive stress conditions; furthermore, spores of *Streptomyces* are not entirely lacking of all metabolic activity (Elliot and Flärdh, 2012). On solid media, these spores darken, swell, establish polarity and germinate (Figure 1.6). This protrusion of hyphal tubes occurs through apical growth and tip extension.

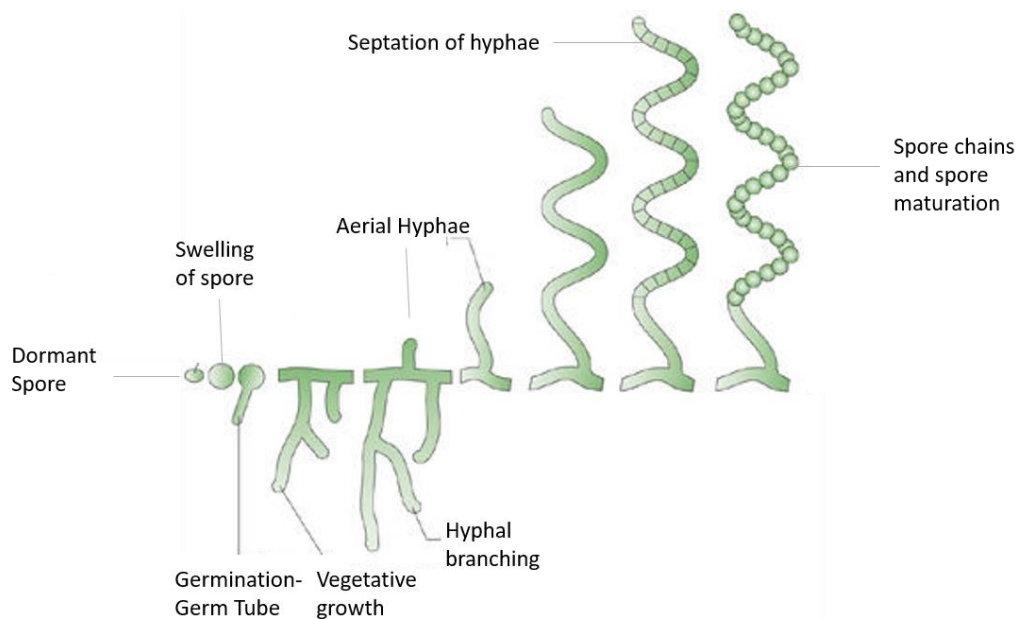


Figure 1.6: Lifecycle of *S. coelicolor* grown on solid substrate. A dormant spore under favourable conditions germinates forming germ tube/s which proliferate into vegetative hyphae. The extension and branching of hyphae form a network which extract nutrients from surrounding substrate allowing the growth of the colony. Later when conditions are less favourable, there is a switch from vegetative growth to aerial growth. Septa formation along the length of the aerial hyphae allows separation of compartments which later form the walls of separated spores (Edited from Flärdh and Buttner, 2009).

For germination to begin, aqueous conditions have been shown to be the bare minimum for *S. viridochromogenes* (Hirsch, and Ensign, 1976). Whereas, for

S. antibioticus, divalent cations (e.g. Ca^{2+}) and endogenous spore reserves are all that are required to initiate germination (Hardisson, *et al.*, 1978). However, with the addition of mechanical spore envelop disruption, heat shock or addition of required nutrients (e.g. peptidoglycan residues, yeast or glucose) speeds up the process (Hirsch, and Ensign, 1976; Mikulik, *et al.*, 1977; Shah, *et al.*, 2008; Bobek, *et al.*, 2017). In fact, heat shocking is a routinely used technique to synchronise spore germination (Kaiser, *et al.*, 2000).

The cues and mechanisms which lead to the initiation of germination remains ambiguous. This change from dormancy to vegetative growth requires the coordination of a number of genes to both detect the suitable growth environment and to begin germination. Within a spore's primordial soup lies a cocktail of stable mRNAs, functional ribosomes and translational apparatus as well as pre-synthesised hydrolases for spore wall reconstitution (Mikulik, *et al.*, 1984; Mikulik, *et al.*, 2002; Bobek, *et al.*, 2017). To maintain these components in a stable state, they reside in trehalose, a disaccharide sugar of glucose. The trehalose both stabilises the mixture as well as acts as an energy source in the early stages of germination (Elbein *et al.*, 1974; Crowe, *et al.*, 1984; Bobek, *et al.*, 2004; Bobek, *et al.*, 2017). The mRNA strands awaiting translation, express at least 15 different proteins; in fact, RNA and protein synthesis is detectable in the first 5 mins of germination (Mikulik, *et al.*, 1984; Mikulik, *et al.*, 2002).

During the germination process, the spore undergoes three steps: darkening, swelling and hyphal protrusion. The darkening step is the loss of refraction (Hardisson, *et al.*, 1978). The divalent ions are thought to bind to the calcium binding proteins and also to carboxyl units of peptidoglycan and polyphosphate groups of teichoic acid on the spore wall (Thomas and Rice, 2014; Bobek, *et al.*, 2017). The second phase of swelling requires an exogenous carbon source and swelling results in a diameter increase of over 1.5 times the original spore size (Hardisson, *et al.*, 1978). Throughout germination (initiation, darkening and swelling), the spore is rehydrated through osmosis which results in the reactivation of the previously inactive proteins including trehalase which breaks down trehalose as an additional source of energy (Elbein *et al.*, 1974; Crowe, *et al.*, 1984; Bobek, *et al.*, 2017). Furthermore, the release of the pigments from their complexes formed

with ribosomal precursors in *S. granaticolor* (Mikulik, *et al.*, 1984), activates ribosomes allowing translation to occur. The energy attained is also used in the first DNA replication event which occurs briefly before or simultaneously with the emergence of one or two germ tubes (Bobek, *et al.*, 2017). The germ tubes protrude at the sites marked by the SsgA protein (Traag and van Wezel, 2008).

In *S. granaticolor*, over 320 proteins are synthesised before the first DNA replication (Mikulik, *et al.*, 2002). Some of the earliest genes to be switched on are a group called the resuscitation promoting factors (*rpf*). These are cell wall lytic enzymes which aid in the hyphal germ tube formation. *S. coelicolor* encodes five of these factors, RpfA-E. These factors, whilst not essential, greatly affect the viability of spores when the encoding genes are deleted but individual gene deletions did not demonstrate any defects beyond delayed germination (Sexton, *et al.*, 2015). SwlA is another hydrolytic enzyme which, when removed, displayed similar effects to the *rpf* deletions (Haiser, *et al.*, 2009). Another key player in germination is cyclic-AMP (cAMP). Mutants lacking the cAMP receptor protein (Δcrp) or adenylate cyclase (Δcya) which cannot synthesize cAMP are defective in germination (Derouaux, *et al.*, 2004).

It has also been shown that spores can secrete autoregulatory compounds such as germicidin from *S. viridochromogenes* which demonstrates inhibitory effects at a concentration as low as 200pM (Peterson, *et al.*, 1993). Secreted compounds can also have different effects on different species. Xu and Vetsigian (2017) observed that *S. viridochromogenes* supernatant exhibits inhibitory or promoting effects on the germination of *S. coelicolor* and *S. venezuelae* spores, respectively. Another identified inhibitor is staurosporine is produced by *Streptomyces* sp. TP-A0274 (Onaka, *et al.*, 2002) which can block muropeptide-promoted spore germination has been suggested to be able to inhibit germination of other spores such as those belonging to *Bacillus* spp (Shah, *et al.*, 2008).

To add another layer of complexity, there are differences between the germination strategy adopted between species. Some species germinate in a synchronous style, such as *S. granaticolor* and *S. viridochromogenes* whilst in some, a proportion of spores will germinate and signal to others to germinate or to remain dormant as is seen in *S. coelicolor* and *S. venezuelae*, where some

spores abort growth soon after germination (Bobek, *et al.*, 2017; Xu and Vetsigian, 2017).

In the spores of dormant and germinating *S. coelicolor* spores, the antibiotic actinorhodin, actinorhodinic acid and γ -actinorhodin was identified; the exact role of these is unclear, whether for competition against other bacteria or signaling (Čihák, *et al.*, 2017). The expression of genes involved in the biosynthesis of actinorhodin is likely to be repressed during germination. SigQ (Sigma factor Q) sees the greatest expression level increase (18 fold) within the first 30 mins of germination in *S. coelicolor* (Bobek, *et al.*, 2014). SigQ is an antagonist of the RR AfsQ1 which is a positive regulator of antibiotic biosynthesis (Shu, *et al.*, 2009; Bobek, *et al.*, 2014; Bobek, *et al.*, 2017).

The germ tube or tubes emerge from the inner spore wall through the outer rodlet layer (Glauert and Hopwood, 1961); following this event, the cell biomass rapidly increases through the metabolism of environmental nutrients. Hydrolytic enzymes are secreted to break down polymeric substrates for absorption. During this phase of development, hyphae grow through tip extension and can branch to form new hyphae.

The coiled-coil protein DivIVA plays an instrumental role in establishment of polarity and growth (Flärdh, 2003). Other coiled-coil proteins such as Scy and FilP localise to the forefront (Holmes, *et al.*, 2013). The organization at the polar tip is referred to as tip organizing centre (TIPOC) or polarisome (Holmes, *et al.*, 2013). FilP offers the plastic growing tip mechanical scaffolding support through formation of a cis-interconnecting network. The interaction between FilP and DivIVA establishes a gradient, increasing towards the extending tip (Fuchino, *et al.*, 2013). Where FilP plays a cytoskeletal reinforcement role, Scy serves as a recruitment protein, localizing other proteins involved in the establishment and action of polar growth. Another function of Scy is the assertion of apical dominance; preventing hyphal branching directly behind the growing tip (Holmes, *et al.*, 2013). The deposition of DivIVA behind the growing tip has also been found to establish new branching hyphae along the lateral walls (Hempel, *et al.*, 2008). This is also facilitated by SwlB and SwlC, lytic transglycosylase and endopeptidase

enzymes, respectively, that cleave cell walls allowing new growth (Haiser, *et al.*, 2009).

The regulation of the polarisome is thought to be through phosphorylation of different proteins. Current thoughts are that these are largely Ser/Thr/Tyr kinases. The Ser/Thr kinase AfsK has been shown to phosphorylate DivIVA and colocalise to the growing hyphal tips; in the absence of AfsK, there is an increase in hyphal length, whereas in mutants where AfsK is constitutively active and phosphorylates DivIVA, the strain presented a hyper-branching phenotype (Hempel, *et al.*, 2012).

In this phase of development, the hyphae are multinucleated and compartmentalized through formation of vegetative crosswalls which are continuous with the cell wall and distantly spaced, as well cross membranes that are continuous with the extracellular membrane. Microscopy carried out by Yagüe, *et al* (2016) showed these membranes not to be permeable to nucleic acid stains. The membranous compartmentalisation is thought to support bacteria which have multicellular growth, particularly with programmed cell death seen in substrate mycelia (Celler, *et al.*, 2016; Yagüe, *et al.*, 2016).

When conditions in the environment are less favourable, there is a switch from vegetative growth to aerial growth; it is also during this phase that secondary metabolite production is activated. The switch to form aerial hyphae involves breaking through the surface tension and generating unbranched hyphae. The erection of aerial hyphae is largely governed by *bld* genes. The deletion of these genes results in a ‘bald’ phenotype whereby there is a lack of aerial mycelia formation. BldD is a transcription regulator which regulates ~167 transcription units (den Hengst, *et al.*, 2010). These include *bldN*, encoding a sigma factor involved in aerial mycelia formation which regulates the atypical response regulator BldM. BldM can homodimerise or heterodimerise with another ARR WhiI to regulate two different subsets of genes (Al-Bassam, *et al.*, 2014).

BldD also controls the secretion of surfactant proteins to form a hydrophobic sheath. The hydrophobic sheath that surrounds the aerial hyphae is made up of three classes of proteins: SapB (spore associated protein B), chaplins and rodlins. On rich media production of SapB, a lantibiotic-like peptide, is

essential for aerial hyphae formation; SapB is encoded by the rapid aerial mycelium (*ram*) formation gene cluster that is convergently regulated by the RR RamR (Willey, *et al.*, 2006; Capstick, *et al.*, 2007). As yet, no HK has been identified for the orphan RR RamR. The orphan HK OhkA has been linked to morphological development as an $\Delta ohkA$ mutant demonstrated increased levels of SapB transcription but reduced levels of other developmental genes including: *bldM*, *bldN*, *whiG*, *whiH*, *whiI* and *whiE* (Lu, *et al.*, 2011). In addition to SapB, chaplins, which self-assemble into long filaments which are organised into paired rodlets by rodlines also make up the hydrophobic coating. In minimal media a SapB independent pathway is activated whereby, only chaplins and rodlines make up the sheath (Elliott, 2003; Flärdh & Buttner, 2009).

The aerial hyphae grow through tip extension much like vegetative hyphae but they do not branch. ParA is recruited to the polarisome and interacts with Scy. Through the transient recruitment of ParA, there is a change in oligomeric state of Scy. There interaction between the two proteins causes a reciprocal inhibition to oligomerize to form higher order structures (Ditkowski, *et al.*, 2013). As the ratio of ParA to Scy increases, Scy breaks down and ParA polymerises to form long filaments which spiral down the hyphae. Later, ParA, an ATPase protein, forms a complex with ParB, a DNA binding protein which binds to *parS* sites at the origin of DNA replication, *oriC* (Jakimowicz, *et al.*, 2007).

The elongation of these pre-sporulation cells is arrested through the control of WhiA and WhiB, and then the switch to septation (Flärdh, *et al.*, 1999). The white (*whi*) genes are so called because *whi* mutants lack the grey-brown WhiE spore pigment, which indicates the maturation of spores. Along with the *bld* mutants these were the first developmental mutants to be discovered.

The partitioning of these cells through septa formation is via the formation of Z-rings by FtsZ. During early sporulation, *ftsZ* is greatly up-regulated by WhiA/B/G/H/I. It is thought that FtsZ levels then far exceed the threshold for polymerisation, which together with SsgA/B proteins, facilitates arrangement into helices along the length of the aerial hyphae (Flärdh, *et al.*, 2000; Willemsse, *et al.*, 2011). The Z-rings are anchored to the membrane and stabilized by a number of

proteins including the dynamins (DynA/B), SepF1/2/3, FtsW/I (Mistry, *et al.*, 2008; Schlimpert, *et al.*, 2017).

Other SsgA-like proteins (SALPs) are involved in spore development. These include SsgC which is an antagonist of SsgA, SsgD which facilitates thick spore wall formation, SsgE and SsgF separate individual spores and SsgG controls regular localization of division sites (Bobek, *et al.*, 2017).

Septa form through annular ingrowth within the cells. As the walls close in the folds become the two new cell walls of the spores (Wildermuth & Hopwood, 1970). FtsK, a DNA translocase, moves the nucleoids into their respective compartments. This is thought to be in concert with SmeA (small membrane protein) and SpoIIIE/FtsK family protein A (SffA; Ausmees *et al.*, 2007).

The nucleoids condense as the spores mature. Spore walls become thickened. This process is largely orchestrated by the *Streptomyces* spore wall synthesizing complex which is comprised of MreB, Mbl, MreC, MreD, Pbp2 and Sfr (Heichlinger *et al.*, 2011; Kleinschnitz *et al.*, 2011; McCormick, *et al.*, 2012). The remodeling of the cell wall also requires cell wall hydrolases, including SwlA, B, C and RpfA (Haiser, *et al.*, 2009).

In the late stage of sporulation, spores must go into a dormant phase. The mechanism remains elusive, but the expression of the metallophosphatase, MtpS and calcium binding proteins is thought to play a role in spore dormancy (Lamp, *et al.*, 2013).

1.2.3 Secondary metabolite production

There is much debate as to exact purpose of antibiotics for their producers. It has been proposed as a means of inter and intra-species competition, defense during programmed cell death, and signaling; many reviews have debated this issue (Linares, *et al.*, 2006; Cornforth and Foster, 2015). Regardless of the reasoning behind its use in bacteria, since their discovery, antibiotics have revolutionised medicine and medical practice as we know it by allowing patients to recover from infections and to prevent infections during surgery and chemotherapy.

Sequence analysis on available *Streptomyces* genomes predict species of the genus to possess in the region of 20 to 60 secondary metabolite BGCs; the model organism *S. coelicolor*, encodes 29 BGCs in its linear chromosome and

another two on the plasmid SCP1 (Nett, *et al.*, 2009), *S. venezuelae* has 30 predicted BGCs and there are at least 45 in *S. formicae* (Holmes, *et al.*, 2018). Many of their secondary metabolites have antibacterial or antifungal activity and early efforts to identify new antibiotics revolved around isolating microbes from soil samples and screening for zones of inhibition when grown with selected pathogens (Kresge, *et al.*, 2004).

Since their discovery, much effort has been made to find new antibiotics for human use and to understand their regulation and mechanism. *S. coelicolor* is one of the best characterized model organisms for this genus. (Liu, *et al.*, 2013). Prior to completion of sequencing of *S. coelicolor*, gene clusters giving rise to six structurally distinct groups of metabolites were identified to be produced but analysis of the genome showed that *S. coelicolor* possesses sixteen other gene clusters (Rutledge and Challis, 2015). Five known antibiotics of *S. coelicolor* are actinorhodin (ACT), undecylprodigiosin (RED), calcium dependent antibiotic (CDA), cryptic polyketide (CPK) and methylenomycin. The first four are encoded in the linear chromosome whilst the methylenomycin is encoded by one of the two plasmids, SCP1.

Antibiotic biosynthesis can be encoded by a single BGC or split into several BGCs and regulation of these BGCs is often mediated by cluster specific regulators (CSRs) and global regulators. CSRs may have pleiotropic effects through cross pathway regulation or simply regulate a single BGC. Some CSRs are also *Streptomyces* antibiotic regulatory proteins (SARPs) which possess a HTH N-terminal motif that bind to heptameric repeat sequences spaced 4-15 nucleotides apart and often around the -35bp region of the promoter (Arias *et al.*, 1999; Sheldon *et al.*, 2002). One of the founding SARP members, ActII-ORF4, is a pathway specific regulator but SARPs can also be pleiotropic regulators as is exemplified by AfsR (Wietzorrek and Bibb, 1997; Tanaka, *et al.*, 2007; Garg and Parry, 2010; Liu, *et al.*, 2013). Below, ACT, RED and CPK biosynthesis and their regulation are briefly discussed particularly regarding what is known of environmental signaling through TCSs, both negative and positive regulation.

1.2.3.1 Actinorhodin

ACT is an aromatic polyketide antibiotic, which was first identified for its weak bacteriostatic activity against *S. aureus* (Brockman, *et al.*, 1950). The BGC contains 22 genes (Fernández-Moreno *et al.*, 1994; Itoh, *et al.*, 2007). Its biosynthesis involves a type II polyketide synthase (PKS) which generates the basic carbon backbone, from which post-PKS modifications such as cyclisation are made.

ACT production is elicited by the SARP ActII-ORF4. ActII-ORF4 binds to the repeat consensus sequence of TCGA upstream of the five transcription units that encode ACT biosynthesis enzymes. In addition to ActII-ORF4, there is one other cluster situated gene regulator, *actR*. This encodes a TetR family regulator which represses the expression of the *actA* operon, encoding a transporter system for ACT. ACT biosynthesis intermediates binding to ActR relieve this repression (Tahlan, *et al.*, 2008).

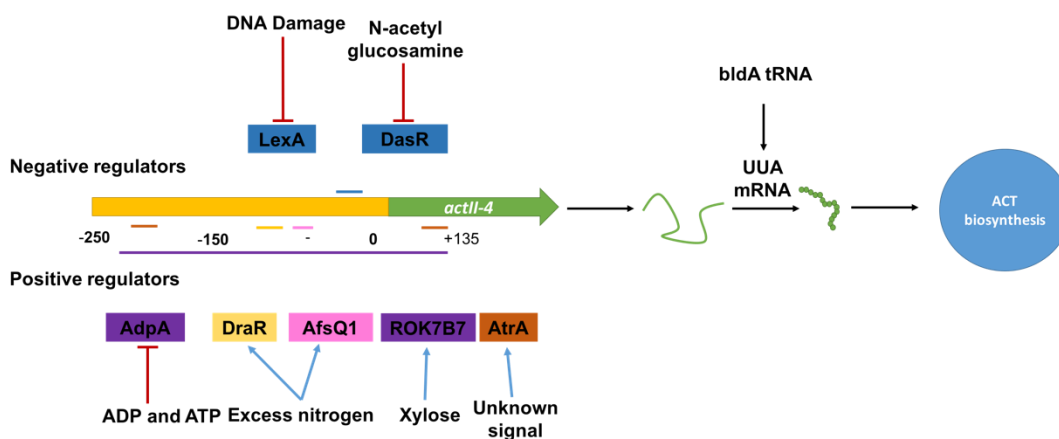


Figure 1.7: Regulation of actinorhodin through expression of SARP ActII-ORF4. Region upstream of *actII-ORF4* is shown in yellow which includes *actII-ORF3* and the intergenic region. Numbers below show distance from transcription start site (+1) as defined by Gramajo, *et al.*, (1993). Short coloured lines refer to binding sites of regulatory proteins with as experimentally determined by the following: LexA: Iqbal, *et al.*, (2012); DasR; Rigali, *et al.*, (2008), AdpA; Ohnishi, *et al.*, (2005), DraR; Yu, *et al.*, (2012), AfsQ1; Wang *et al.*, (2012), Rok7B7; Heo, *et al.*, (2008) and AtrA; Uguru., *et al.*, (2005). Regulatory proteins above the central genes applies negative regulation on *actII-ORF4* transcription and bottom row applies positive regulation. Signaling that controls the DNA binding activity of transcription regulators is shown and the state of regulation shown with blue arrows for positive regulation and red blunt arrows for negative regulation.

The expression of *actII-ORF4*, at both the transcriptional and translational levels is heavily regulated (Figure 1.7). AdpA (BldH) is a pleiotropic regulator of both aerial mycelium formation with RamR (Nguyen, *et al.*, 2003) and antibiotic production. It activates expression of *actII-ORF4* and inhibits the expression of the

antibiotic down-regulator WblA (Lee, *et al.*, 2013). ACT biosynthesis is also subject to direct regulation by a number of two-component systems; AfsQ1/Q2 (section 1.3.1.2) and DraR/K, in response to nitrogen levels, PhoP/R, in response to phosphate starvation, AbsA global repressor of antibiotic synthesis, MtrA (1.3.1.1), a highly conserved RR within Actinobacteria and RapA1/2 and AbrC1/2/3 which are as yet uncharacterized. The AbrA1/2 and CutR/S are also implicated in suppression and inhibition of ACT biosynthesis (Rodríguez, *et al.*, 2013). The translation of *actII-ORF4* requires a rare codon (TTA) in which *bldA* encodes the tRNA of, suggesting another link to developmental regulation (Fernández-Moreno *et al.*, 1991).

1.2.3.2 Undecylprodigiosin

The red pigment from which RED is thus named is a concoction of a least four different prodiginines with undecylprodigiosin and butylcycloheptylprodiginine being predominant (Kieser, *et al.*, 2001). As can be seen from figure 1-8, numerous environmental factors can elicit the activation of RED biosynthesis. Two CSRs are responsible for its biosynthesis. RedZ is an NarL type ARR. Also, like *actII-ORF4*, *redZ* it is a direct target of AfsQ1, DasR and MtrA binding (Figure 1-8; Liu, *et al.*, 2013). In late exponential and stationary phase, RedZ levels build up but RedD, the second CSR does not accumulate until much later. RedZ switches on *redD* expression but *redD* also contains the rare leucine codon encoded by *bldA*. RedD is a SARP and like ActII-ORF4 it is encoded by a small gene less than 300bp (White and Bibb, 1997; Liu, *et al.*, 2013). The buildup of RED seems to form a negative feedback loop on expression. It is thought that RED interacts with RedZ, the ARR to autoregulate its biosynthesis (Wang, *et al.*, 2009).

In addition to TCS regulation, RED production is also modulated by the global regulator AfsR. Multiple serine/threonine kinases are able to phosphorylate AfsR, the best studied of which is AfsK which is activated by S-adenosyl-L-methionine (SAM; Lee, *et al.*, 2002; Lee, *et al.*, 2006). AfsR phosphorylation greatly enhances DNA binding ability whilst ATPase activity conversion of ATP

the final module. ScoT is a type II thioesterase that does not get expressed till an hour after the other biosynthetic genes under the tested conditions of the study conducted by Nieselt, *et al.*, (2010). ScoT is thought to be an editing enzyme following the expansion of the core carbon chain (Kotowska, *et al.*, 2002; Kotowska, *et al.*, 2014). The expression of *cpkA*, *B* and *C* begins during the change between vegetative and aerial growth (Pawlik, *et al.*, 2007). The five modules process a precursor generated by the products of *cpk α* , *cpk β* , *accA1* and *cpkK*. Gomez-Escibano, *et al.*, (2012) proposed a mechanism to which the antibiotic coelimycin P1 is generated from this cluster of genes (Figure 1.9).

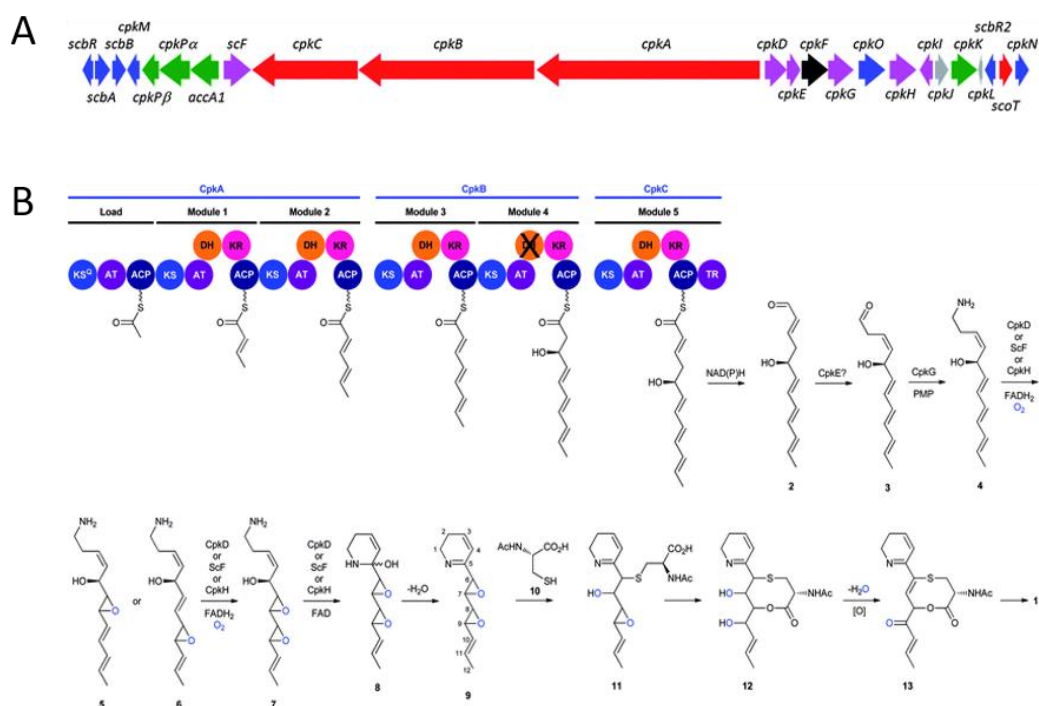


Figure 1.9: CPK biosynthesis cluster and proposed pathway through which the coloured structurally novel compound coelimycin P1 is generated. A) *S. coelicolor* CPK biosynthetic cluster of genes. Type I modular PKS core genes are shown in red, regulatory genes both putative and characterised are in blue, the predicted genes encoding proteins involved in generating the precursor which is loaded into the polyketide synthase (PKS) synthase are shown in green, pink denotes post-PKS editing enzymes and black denotes a putative export protein. Taken from (Gomez-Escibano, *et al.*, 2012). B) Schematic view of the proposed mechanism through which coelimycin P1 is assembled (Gomez-Escibano, *et al.*, 2012).

Two SARPs are present within the CPK BGC: CpkN and CpkO. CpkO possesses an N terminal SARP domain but the C-terminus is undefined (Liu, *et al.*, 2013). Additionally, the *scb* genes and *cpkM* also encode regulators. The function of CpkM is yet unknown but BLASTp analysis showed the closest related proteins to be HKs. Further analysis showed that there are only two domains, an HATPase

domain and Dhp domain (Barakat, *et al.*, 2013). However, within the cluster there are no RRs.

The *scb* genes are related to γ -butyrolactone (GBL) signaling. *scbA* is divergent from *scbR*; *scbA* and *scbB* encode GBL synthases generating GBL signaling molecules SCBs, whereas *scbR* encodes a repressor molecule of the pathway binding to the promoters of *cpkO* and the bidirectional promoter of *scbR* and *scbA* (Takano, *et al.*, 2001). In addition to the promoters within the cluster, *scbR* has been shown to be able to bind to many other promoters through EMSAs including *cdaR*, *afsK* and *gapI* (Li, *et al.*, 2015B). As a GBL receptor it is also able to bind SCBs.

It is thought that SCB accumulates throughout growth, either through low level expression of *scbA* or via exogenous SCBs, and reaches a threshold to bind to ScbR. Binding of ScbR to SCBs causes an alleviation of repression on *scbA* allowing levels to build. This increase in ScbA to ScbR ratio allows formation of a heterodimer which then binds to a site upstream of *scbA*, causing increased expression of ScbA resulting in further sequestering of ScbR repression on other promoters, including *cpkO* (Takano, *et al.*, 2001; Gottelt, *et al.*, 2010; Liu, *et al.*, 2013). A second proposed mechanism of action is that the change in ratio between SCBs and ScbR is sufficient to alleviate the repression of the the ScbR targets (van Wezel and McDowall, 2011).

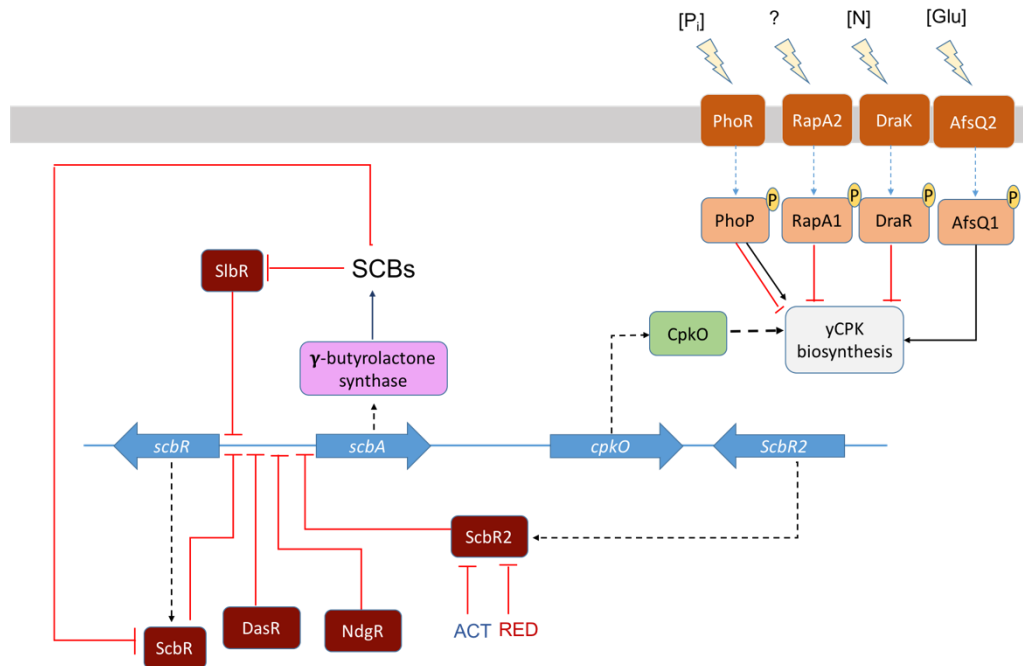


Figure 1.10: The yellow pigmented cryptic polyketide (yCPK) biosynthesis expression is regulated by an interplay between butyrolactone signaling, TCS signaling (orange) and from other antibiotics produced by *S. coelicolor* (actinorhodin and undecylprodigiosin), resulting in the expression of the SARP regulator CpkO (green). Black (solid) arrows demonstrate positive regulation, black dashed arrow refers to positive regulation exerted by SARP regulator, blunt red arrows denote inhibition or repression, blue dotted arrows represent phosphotransfer.

Another dimension to the cluster's regulation is *scbR2*. ScbR2 is a pseudo-GBL receptor, which does not bind ScbA. However, it binds to the promoters of *redD* and *adpA* as well as to promoters of genes within ACT and RED BCGs and also within exogenous BCGs including angucylin and hence modulating both antibiotic production and morphogenesis (Xu, *et al.*, 2010; Wang, *et al.*, 2014). $\Delta scbR2$ has been shown to abolish production of ACT, RED and CDA but increased production yCPK and the overexpression of ScbR2 increases their production (Gottelt, *et al.*, 2010; Xu, *et al.*, 2010). However, ACT and RED represses ScbR2 activity by preventing repression of *cpkO* (Xu, *et al.*, 2010; Figure 1.10). Whilst ScbR2 does not bind ScbA it binds the same promoter region of *scbA* as ScbR does. The $\Delta scbR$ resulted in the expression of *scbR2* throughout growth, whereas, $\Delta scbA$ abolished expression of *scbR2* (Gottelt, *et al.*, 2010).

In addition to butyrolactone signaling and repression exerted by the antibiotic ACT and RED, yCPK is also subjected to regulation by other pathways including TCS signaling. Of the ones described here, AfsQ1 is the only positive regulator and there are consensus binding sites of *cpkO*, *cpk α* and *cpk β* (Wang, *et al.*, 2013B).

Figure 1.10 shows the TCS PhoPR to exert negative and positive regulation, as the exact regulation of PhoP on yCPK pathway remains ambiguous. PhoP has been shown to transiently downregulate the levels of *cpk* gene expression (Rodríguez-García, *et al.*, 2007). This may be due to PhoP repressing the expression of ScbA (Allenby, *et al.*, 2012) and hence the expression of *cpkO* is affected. However, ChIP-Seq (Chromatin immunoprecipitation sequencing) also shows binding enrichment at three sites within *cpkB* and *cpkC*. Allenby, *et al.*, (2012), has suggested to exert positive regulation on yCPK.

1.2.3.4 Calcium-dependent antibiotic

In comparison to the other three antibiotics discussed so far, the regulation of CDA remains elusive in many respects. CDA is a cyclic lipopeptide antibiotic composed of 11 amino acid residues cyclized by linkage to connected to 2,3-epoxyhexanoyl fatty acid side chain (Kempter, *et al.*, 1997; Hojati, *et al.*, 2002). It is synthesised from three large, non-ribosomal peptide synthases (*psI/II/III*; Figure 1.11). Additionally, within the regulon are fatty acid synthases, and enzymes involved precursor assembly and latter post peptide synthesis editing (Hojati, *et al.*, 2002).



Figure 1.11: CDA BGC with the SARP encoding *cdaR* and the CSR encoding genes *absA1* and *absA2*, that encode a TCS, and the three peptide synthases (PSI-III) labelled. In addition are genes encoding enzymes for transport and the assembly of the peptide and post-assembly modifications.

Within the cluster is the SARP encoded by *cdaR*. CdaR switches on the biosynthetic genes. Regulation of *cdaR* expression by the TCS AbsA1/A2 is the best understood (Li *et al.*, 2013). AbsA2 is global negative regulator of antibiotic production (Brian, *et al.*, 1996). The SK, AbsA1 possesses both phosphatase and kinase activity. In the absence of signaling, AbsA1 dephosphorylates AbsA2. However, in the presence of the corresponding ligand, the phosphorylated AbsA2 has a greater affinity to binding and repressing *cdaR* expression and hence negative regulation is demonstrated (Anderson *et al.*, 2001). The negative regulation of

AbsA2~P binding may override any positive regulation exerted by CdaR binding (Ryding, *et al.*, 2002). Other TCSs involved in the regulation of CDA biosynthesis include the AfsQ1/Q2, AbrC1/C2/C3 and AbrA1/A2. AfsQ1 and AbrC3 are positive regulators of *cdaR* whereas, AbrA2 is a negative regulator (Yepes, *et al.*, 2011; Wang, *et al.*, 2013B; Rico, *et al.*, 2014).

1.3 TCSs of *Streptomyces*

In section 1.1.1.3, the number of TCSs relative to genome size and bacterial niche was discussed. Typically, HKs or RRs form approximately 1% of the number of genes within a genome. However, bacteria exposed to greater environmental diversity possess higher numbers of TCSs. For instance, the well studied *E. coli*, which can be found in the gut of warm-blooded animals encodes 4140 genes and 29 of these are HKs, another 32 are RRs and 1 hybrid TCS (Oshima, *et al.*, 2002). In comparison the number of genes in *Streptomyces* is much higher but taking *S. coelicolor* as an example, which possesses nearly twice as many genes as *E. coli*, there are more than three times the number of SKs and RRs encoded within the genome (Table 1.1). This highlights the importance of TCSs in allowing streptomycetes to recognise and respond to vast environmental diversity they face.

The TCSs of *E. coli* are far better characterised than the TCSs of any *Streptomyces* species (Oshima, *et al.*, 2002). As TCSs can be well conserved, homologues of different TCSs can be annotated across species. However, owing to streptomycetes having more TCSs than many well studied bacterial species (e.g. *E. coli*) and many TCSs being conserved only within the Actinobacterial family or within the *Streptomyces* genus, annotations of TCSs in streptomycete genomes are rare. Among the known TCSs of *Streptomyces*, the best understood are discussed below. Many of these are involved in the regulation of antibiotic biosynthesis which has brought attention to their study.

Table 1.1: Number of HKs and RRs predicted in the *Streptomyces* species in comparison to the total number of genes encoded within the genome (Edited from Rodríguez, *et al.*, 2013).

Organism	HK	RR	Total number of genes
<i>Streptomyces bingchenggensis</i> BCW-1	125	117	10022
<i>Streptomyces scabeiei</i> 87.22	108	95	8746
<i>Streptomyces violaceusniger</i> Tu 4113	106	99	8985
<i>Streptomyces coelicolor</i> A3(2)	100	87	8152
<i>Streptomyces avermitilis</i> MA-4680	91	72	7684
<i>Streptomyces griseus</i> NBRC 13350	83	80	7136
<i>Streptomyces</i> sp. Sirex AA-E	76	73	6357
<i>Streptomyces cattleya</i> NRRL 8057	63	59	7475
<i>Streptomyces hygroscopicus</i> 5008	61	75	9108

1.3.1 Global regulators

1.3.1.1 MtrAB

MtrAB is a global regulating TCS that is highly conserved throughout the Actinobacteria phylum. It has been characterised in *M. tuberculosis*, *Corynebacterium glutamicum*, *S. coelicolor* and *S. venezuelae*. It is the only essential TCS in *M. tuberculosis* but is not essential in *Streptomyces* or in *C. glutamicum* (Zahrt and Derectic, 2000; Möker, *et al.*, 2004; Brocker and Bolt, 2006; Som, *et al.*, 2016; Som, *et al.*, 2017). MtrA (*M. tuberculosis* regulator A) is the RR in this system and MtrB, the SK.

MtrA_{MT} (MtrA from *M. tuberculosis*) regulates expression of *dnaA* and *dnaN*, encoding the DNA replication initiator and DNA polymerase III stabilising protein, respectively, and binds to *oriC*, sequestering the origin to prevent further DNA replication. Direct interaction of MtrA with the DnaA protein may facilitate the binding of MtrA~P (phosphorylated MtrA) to *oriC*. This occurs in the post replication period of the cell (Purushotham, *et al.*, 2015). MtrA is thought to stop further DNA replication and move the cycle towards cell division. MtrB_{MT} (MtrB from *M. tuberculosis*) localises to the cell membrane in a FtsZ (cell division initiator) dependent but phosphorylation independent manner and has also been shown to interact with Wag31 (DivIVA), FtsI and PknA/PknB (Protein kinase A and B; Ser/Thr kinases), which are all involved in controlling cell division and shape (Kang, *et al.*, 2005; Plocinska, *et al.*, 2012; Plocinska, *et al.*, 2014).

Table 1. 2: Amino acid identity of the components MtrA, MtrB and LpqB, which form an essential TCS in Mycobacterium, across actinobacterial family of species. (Taken from Hoskisson and Hutchings, 2006).

Actinobacterium	Amino acid identity to <i>M. tuberculosis</i> MtrA (%)	Amino acid identity to <i>M. tuberculosis</i> MtrB (%)	Amino acid identity to <i>M. tuberculosis</i> LpqB (%)	Source
<i>Mycobacterium leprae</i>	98	88	87	http://www.Sanger.ac.uk
<i>Mycobacterium avium</i>	99	87	86	http://www.Sanger.ac.uk
<i>Nocardia farcinica</i>	89	63	40	http://nocardia.nih.go.jp/
<i>Thermobifida fusca</i>	76	49	25	http://www.ncbi.nlm.nih.gov
<i>Corynebacterium diphtheriae</i>	70	53	26	http://www.Sanger.ac.uk
<i>Corynebacterium glutamicum</i>	72	53	29	http://www.ncbi.nlm.nih.gov
<i>Streptomyces avermitilis</i>	74	49	25	http://avermitilis.ls.kitasato-u.ac.jp/
<i>Streptomyces coelicolor</i>	74	49	23	http://www.Sanger.ac.uk
<i>Streptomyces scabies</i>	64	50	25	http://www.Sanger.ac.uk
<i>Leifsonia xyli</i>	67	41	25	http://www.ncbi.nlm.nih.gov
<i>Propionibacterium acnes</i>	57	40	24	http://www.ncbi.nlm.nih.gov
<i>Rhodococcus equi</i>	39	29	42	http://www.Sanger.ac.uk

To add an extra dimension, there is a third component, the genetically linked lipoprotein, LpqB, which in *M. smegmatis* has been shown to interact with the sensor domain of MtrB to mediate signaling (Nguyen, *et al.*, 2010). An *M. smegmatis* Δ *lpqB* mutant demonstrated multidrug sensitivity. Additionally, it displayed *Streptomyces*-like filamentous growth with polyploidy. A similar phenotype was also exhibited by an *mtrA* transposon insertion inactive mutant in *M. smegmatis* (Nguyen, *et al.*, 2010). *lpqB* is highly conserved as the third gene in the *mtrAB-lpqB* operon in Actinobacteria. This may indicate its importance for the effective functioning of MtrA/B TCS signalling. Analysis of the amino acid identity (Table 1.2) shows that identity of MtrA is highly conserved with a degree

less for MtrB and even less for LpqB, indicating that potentially, the function of LpqB within the TCS could be limited or lost across species and genus.

More recently, MtrA has been studied in *Streptomyces*. MtrA has been found to be a positive regulator of antibiotic production. The deletion of *mtrB* induced overproduction (>30-fold increase in comparison to wild-type) of chloramphenicol in *S. venezuelae* (Som, *et al.*, 2017). In addition to MtrA regulating secondary metabolite production, the $\Delta mtrB$ mutant demonstrated growth defects when grown on solid media (Som, *et al.*, 2017). Further analysis of MtrA gene targets using ChIP-seq shows that it binds to sites in 21 of the 29 BCGs in *S. coelicolor* including upstream of *actII-ORF4* and *redZ* (Som, *et al.*, 2017) suggesting that MtrA may switch on ACT and RED production. The fact that MtrA is essential in the pathogen *M. tuberculosis* and also regulates antibiotic production in *Streptomyces* makes it a very attractive TCSs for further study, whether as a target for antibiotics or to be used to activate antibiotic production. It is particularly interesting that Som, *et al.*, (2017) showed that despite there being only 75% similarity between MtrA_{TB} and MtrA_{Sven}, MtrA_{TB} was able to switch on chloramphenicol production in *S. venezuelae*. Heterologous expression of global regulator RRs or RRs which demonstrate specific antibiotic biosynthesis regulation could be used as a strategy of activating antibiotic production.

In addition to the regulation of antibiotics in *Streptomyces*, it has been found to play a critical role in the regulation of development. Deletion of *mtrA* resulted in a conditional bald phenotype in *S. coelicolor*, *S. lividans* and *S. venezuelae* that was dependent on the medium these were cultured on very similar to deletion mutants of *sapB*, or chaplins or *bld* genes (Zhang, *et al.*, 2017).

1.3.1.2 AfsQ1/Q2

As was described earlier in section 1.2.3, AfsQ1/AfsQ2 plays a significant role in antibiotic biosynthesis regulation. The TCSs encoded by *afsQ1*, *afsQ2* is in the same operon as *afsQ3* (Figure 1.12) which encodes a lipoprotein much like the lipoprotein LpqB being linked to MtrAB described in 1.3.1.1 and the CseA lipoprotein being linked to CseBC. AfsQ123 is also similar to CseABC (1.3.2.2), because both are genetically linked to an ECF sigma factor, in this case encoded by and divergent from *sigQ* (Wang, *et al.*, 2013B).

The TCS was identified when a DNA fragment containing *afsQ1* was heterologously expressed in *S. lividans*. In doing so, silent pathways were activated and production of the antibiotics actinorhodin (ACT) and undecylprodigiosin (RED) were induced (Ishizuka, *et al.*, 1992). Wang, *et al.*, (2013) showed through conducting EMSAs that AfsQ1 binds specifically to the SARPs of ACT (*actIII-ORF4*), RED (*redZ*) and CDA (*cdaR*) clusters. As mentioned earlier, it also regulates CPK biosynthesis. However, where AfsQ1 regulates CSR genes in the ACT, RED and CDA biosynthesis, in the CPK cluster, it regulates the expression of biosynthetic structural genes *cpkA* and *cpkD* genes (Wang, *et al.*, 2013B). The deletion of *afsQ1* resulted in decreased levels of CpkA and CpkD but interestingly an increase in the predicted coelimycin P1 precursor molecule synthesis gene *accA1* and the post-PKS editing enzyme encoding gene *scF* (Chen, *et al.*, 2016).

Where deletion of *afsQ1* or *afsQ* (*afsQ1/Q2*) resulted in reduced levels of antibiotics produced, the deletion of *sigQ* resulted in hyper-production of antibiotics (Shu, *et al.*, 2009). Where SigQ antagonises AfsQ1 stimulated antibiotic biosynthesis, AfsQ1 has been shown to positively regulate expression of *sigQ* (Wang, *et al.*, 2013B). The mechanism through which SigQ inhibits antibiotic production is still unclear.

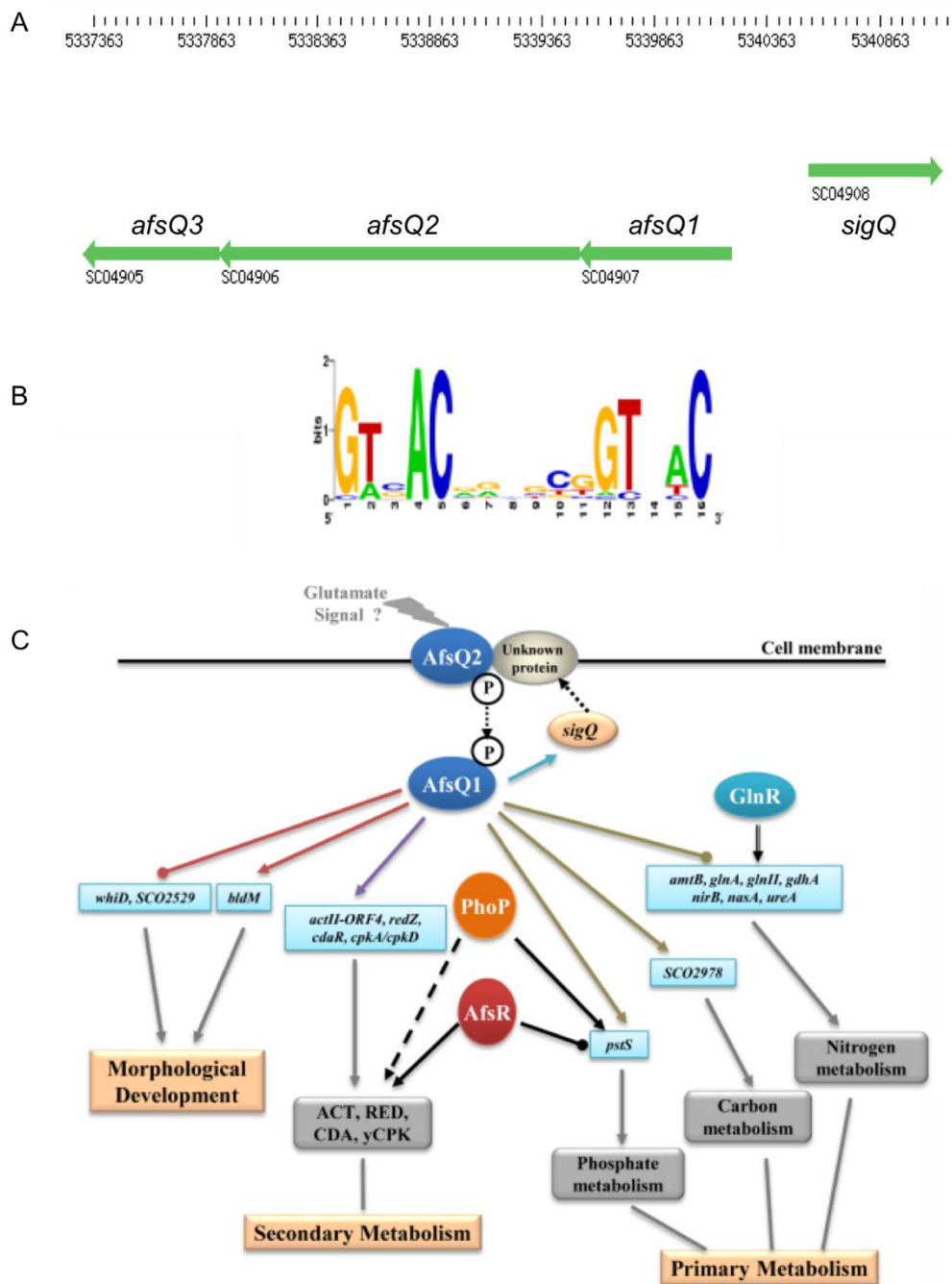


Figure 1.12: TCS AfsQ1/Q2 regulation. A) Position of *afsQ1*, *afsQ2*, *afsQ3* and the divergently expressed *sigQ* in the *S. coelicolor* genome of approximately 8.7 million base pairs encoding a RR, SK, lipoprotein and sigma factor respectively. (Taken from StrepDB) B) Consensus sequence binding site of AfsQ1 predicted by Weblogo using alignment of 20 identified binding sites (Taken from Wang, *et al.*, 2013B). C) Predicted regulation network exerted by AfsQ1 based on the consensus sequence binding site showing global regulation on morphological development and metabolite production, both primary and secondary. An interlink with global regulator GlnR is also shown. Arrows demonstrate positive regulation, arrows ending in circles show negative regulation, double lined arrows show dual regulation and broken arrows show indirect control. (Taken from Wang, *et al.*, 2013B)

Where some RRs can be phosphorylated by other phosphodonors such as in the case of AbrA1/A2 (Sergio, *et al.*, 2014), the study by Shu, *et al.*, (2009) reintroduced *afsQ1* into the Δ *afsQ* mutant but this did not restore the wild-type (WT) phenotype, suggesting that AfsQ2 is the only phosphodonor of AfsQ1. In work conducted by Daniel-Ivad, *et al.*, (2017), phosphomimetic AfsQ1 (*afsQ1*_{D52E}) was constitutively expressed under the control of *ermE** promoter in environmental strains resulted in cryptic secondary metabolites being produced. However, in some cases, this was lethal. To this end, the study generated a thiostrepton-inducible *afsQ1*_{D52E} construct which led to them isolating siamycin from environmental isolate WAC00263. In this study novel antibiotics were discovered which were found to be effective against Gram-positive bacteria including vancomycin-resistant *Enterococcus* (VRE) and a clinically isolated strain of MRSA.

While antibiotics biosynthetic pathways were activated by the expression of *afsQ1* in *S. lividans*, Δ *afsQ1* and Δ *afsQ2* mutant of *S. coelicolor* showed no detectable phenotype until they were grown on minimal media (MM) with 75mM glutamate as the sole nitrogen source where there was a severe impairment in ACT and RED production (Ishizuka, *et al.*, 1992; Shu, *et al.*, 2009), suggesting that AfsQ1 is activated in response to nitrogen excess. Recently, a glutamate sensing TCS in *S. coelicolor* was identified, GluR/K. In experiments conducted by Li, *et al.*, (2017), the extracellular domains of both GluK and AfsQ2 were analysed for binding with glutamate and a structural analogue, glutamine. In this study, GluK was found to specifically interact with glutamate but AfsQ2 interacted with neither glutamate nor glutamine. As yet the signal for AfsQ2 remains illusive. However, in the presence of excess nitrogen, AfsQ1 modulates nitrogen assimilation by competing for binding with GlnR for the promoter regions of *glnA* and *nirB*. GlnR is a RR that positively regulates glutamine synthase (*glnA*) and a nitrogen reductase encoded by *nirB*. In excess nitrogen, AfsQ1 acts as a repressor for both of these genes (Wang, *et al.*, 2013B).

Through analysis of 20 known binding sites of AfsQ1, Wang, *et al.*, (2013B) calculated a consensus sequence for AfsQ1 (Figure 1.12). Using the elucidated GTnAC repeat sequence with a 6bp spacing and applying it throughout the genome sequence, a map of genes regulated by the RR showed that it is a global

regulator which in addition to modulating antibiotic production, is also involved in changes in morphological development, primary metabolism and secondary metabolism (Wang, *et al.*, 2013B; Figure 1.12).

1.3.2 Stress Regulators

1.3.2.1 PhoPR

PhoPR senses and responds to low phosphate levels in the environment and switches on the expression of genes with the purpose of phosphate scavenging. As discussed earlier, PhoP is also involved in controlling antibiotic production. When phosphate levels are high (>0.5mM), the equilibrium is swayed towards primary metabolism (Vining, 1992). Under these circumstances, PhoR (SK) is thought to possess phosphatase activity and dephosphorylates PhoP. Under phosphate limitation, PhoR phosphorylates PhoP, switching on the *pho* operon. The Pho operon includes an alkaline phosphatase (*phoA*), a porin (*phoE*) and a phosphate binding protein (*phoS*). The binding site of PhoP is termed the PHO box and is a degenerate repeat sequence of GTTCACC in *S. coelicolor* (Sola-Landa, *et al.*, 2005; Sola-Landa, *et al.*, 2008).



Figure 1. 13: Operon of *phoPR* in genome of *S. coelicolor* and two of its regulons, the divergently expressed *phoU* and *pstABCS* which encodes phosphate specific transport system.

Divergent from *phoPR* is the *phoU* gene and the phosphate-specific transport (*pst*) genes, *pstABCS* (Figure 1.13). In *E. coli*, PhoU and the Pst system modulates the sensing of the phosphate signal. Under phosphate starvation, PhoR is liberated and phosphorylates PhoP (Oganesyanyan, *et al.*, 2005; Liu, 2013; Zhu, *et al.*, 2014).

In addition to the Pho operon, the PHO box can be found scattered throughout the genome. As mentioned earlier, it also regulates CDA production by directly binding to the SARP gene *cdar*. The deletion of *phoPR* causes a drop in ACT and RED expression, however, none of these biosynthetic clusters contain the PHO box. Instead PhoP competes with AfsR for the *afsS* promoter site in an

overlapping region. Both compete to activate *afsS* expression (Santos- Beneit, *et al.*, 2011a).

Beyond antibiotic up-regulation, PhoP also regulates cell morphology and development. It has been shown that PhoP positively regulates many of the *bld* genes, including *bldA*, *bldC*, *bldD*, *bldK* and *bldM* (Allenby, *et al.*, 2012). It also mediates changes in cell wall structure through activation of genes which can decorate the cell wall teichoic acids with glucose and galactose (Allenby, *et al.*, 2012).

Besides being a positive regulator, PhoP also serves as a repressor of gene expression. Binding of PhoP at the -35bp region has been shown to be a positive regulator, however, it has been noted that binding at the -11bp region of genes, PhoP acts as a negative regulator (Sola-landa, *et al.*, 2008; Santos-Beneit, *et al.*, 2011b). During phosphate limitation PhoP activates phosphate assimilation pathways and down regulates nitrogen assimilation pathways (Allenby, *et al.*, 2012) through the repression of *glnR*. However, this is a reciprocal exchange as GlnR also serves to negatively regulate PhoP (Yao & Ye, 2016). PhoP also represses expression of *glnRII* and *glnA* through competition with GlnR (Martin, *et al.*, 2017). In addition to nitrogen collation, PhoP also negatively regulates genes encoding key players in the oxidative phosphorylation pathway including genes in NADH dehydrogenase complex, F-type ATPase, cytochrome C and B oxidase complexes and the succinate dehydrogenase (Allenby, *et al.*, 2012). This demonstrates how much of a master regulator PhoPR is in regulation of bacterial primary and secondary metabolism.

1.3.2.2 CseBC

SigE (RNA polymerase sigma factor E) was the first extracellular function (ECF) sigma factor to be identified in *S. coelicolor* (Lonetto, *et al.*, 1994). The transcription of *sigE* is completely dependent on the TCS CseBC (control of sigma factor E) as was demonstrated by the identical phenotypes of $\Delta sigE$ and $\Delta cseB$ (RR) mutants (Paget, *et al.*, 1999A; Paget, *et al.*, 1999B).

SigE has been predicted to bind to 138 gene promoters to regulate normal cell wall homeostasis during growth (Zhou, *et al.*, 2011A). Amongst these proteins

are cell wall management enzymes which are activated when cell wall integrity is compromised.

Activation of the CseBC TCS can be achieved by the presence of numerous different antibiotics which target late cell wall biosynthesis, including vancomycin (Hong, *et al.*, 2002). Besides damage through antibiotic targeting, it is also thought that during germination, and shortly following, the repair from hydrolase activity (e.g SwlC and RpfA) is mediated by SigE (Bobek, *et al.*, 2014). However, the exact interaction of the stimulus with the SK CseC has not been identified.

Another component this system is the accessory lipoprotein, CseA. As with the MtrAB and AfsQ1/Q2 TCSs, the operon contains a gene encoding a lipoprotein. In a $\Delta cseA$ mutant, there is up-regulation of *sigE* expression (Hutchings, *et al.*, 2006) and CseA is thought to negatively interact with CseC (Figure 1.14) to fine-tune its signaling in a manner similar to MtrB and LpqB in *Mycobacterium*.

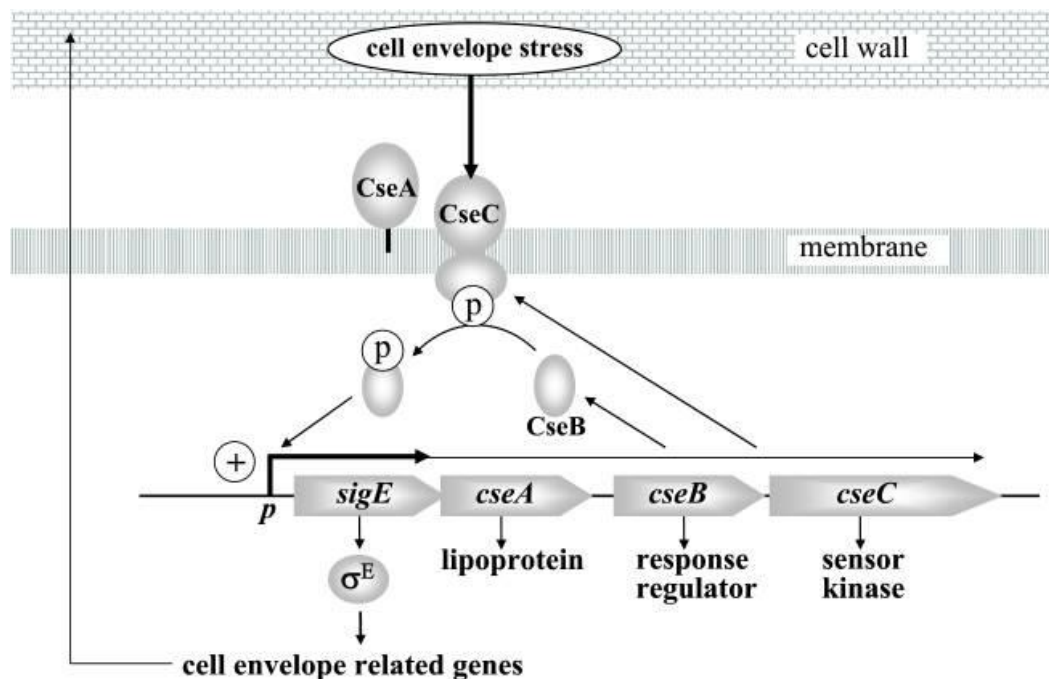


Figure 1.14: Model of cell envelope stress response activation through TCS CseBC activating expression of sigma factor E which results in the expression of cell envelope related genes after the HK CseC senses cell envelope stress (Taken from Hutchings, *et al.*, 2006).

1.3.2.3 VanRS

VanRS reacts to is vancomycin, a glycopeptide antibiotic that inhibits cell wall biosynthesis through competitively binding to the acyl-D-alanyl-D-alanine (acyl-D-Ala-D-Ala) side chain of the muramyl pentapeptide precursor of bacterial peptidoglycan. There are multiple types of vancomycin resistance. The change of D-Ala-D-Ala to D-alanyl-D-lactate (D-Ala-D-Lac) in the terminal sugar of peptidoglycan precursors is found in three types of resistance: VanA-, VanB- and VanD-type whilst the other three types documented, VanC-, VanE- and VanG-type, result in a terminal change to a serine (D-Ala-D-Ser; Fong and Drlica, 2007). These different modes were studied in vancomycin resistant *Enterococcus* species (VRE). *S. coelicolor*, is vancomycin resistant but sensitive to teicoplanin, another glycopeptide antibiotic that binds to peptidoglycan precursors. This is comparative to VanB-type resistance as characterised in VRE (Hong, *et al.*, 2004).

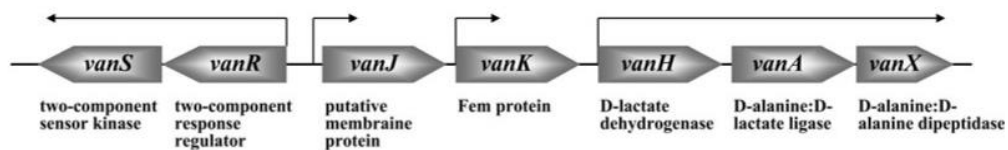


Figure 1.15: The VanRS regulon consists of only 4 transcriptional units in *S. coelicolor* (Hutchings, *et al.*, 2006).

VanRS is not a pleiotropic or global regulator. Instead this TCS is situated within its own regulon and controls the expression of only four transcriptional units. In *S. coelicolor* these are *vanRS*, which encode the TCS, *vanJ*, *vanK* and *vanHAX* (Figure 1.15; Hong, *et al.*, 2004). With vancomycin induction, VanS phosphorylates VanR which activates all four target promoters. The VanHAX enzymes cleave the terminal amino acid on the D-Ala-D-Ala dipeptide of peptidoglycan precursors and converts it to a D-Ala-D-Lac depsipeptide. This change reduces the affinity of vancomycin to bind by more than 1000-fold (Bugg, *et al.*, 1991). VanK is another protein crucial to vancomycin resistance in *Streptomyces*, however, VanK and its homologues are absent in other resistant pathogens. It is a member of the Fem family of proteins which add the Gly cross bridge amino acids between stem peptides in the cross-linked peptidoglycan. FemX is an essential enzyme that recognizes D-Ala-D-Ala containing substrates but cannot cross-link D-Ala-D-Lac containing precursors. Instead, following

vancomycin exposure, VanK adds the single Gly cross-bridge residue to the D-Ala-D-Lac containing peptidoglycan precursors and this allows formation of cross-links in the mature peptidoglycan. As FemX does not recognise the modified precursor, it becomes redundant when the *van* genes are switched on (Hong, *et al.*, 2005). VanJ is not essential for resistance to vancomycin but is essential for resistance against teicoplanin; it has been suggested that VanJ may modify or degrade lipid II with D-Ala-D-Ala. As teicoplanin does not induce expression of the *van* genes, resistance to teicoplanin is only achieved when vancomycin was also present (Novotna, *et al.*, 2012).

In the absence of an inducer, VanS acts as phosphatase and dephosphorylates VanR~P. Unlike AfsQ1, which only has one phosphor-donor, VanR has another which is acetyl phosphate. This small molecule phosphodonor is formed as part of central metabolism, in the interconversion of acetate to acetyl coA and its physiological role, if any, is unclear (Hutchings, *et al.*, 2006).

Multiple models for the interaction between vancomycin and VanS have been proposed. One is the direct and sole binding of the antibiotic to the sensor domain of the VanS protein. Another is the formation of a complex between vancomycin and its lipid II target which then binds to and activates VanS. A third suggested that there is an intermediate elicited by vancomycin stress (Hong, *et al.*, 2008). In 2010, Koteva, *et al.*, created a photoaffinity probe linked with vancomycin and biotin. From purifying and immuno-blotting they showed binding of VanS to vancomycin which also correlated with *vanHAX* expression. To further support this, it has been shown that sulfation of vancomycin reduces recognition of VanS to vancomycin (Kalan *et al.*, 2013). Later, Kwun, *et al.*, (2013) showed that desleucyl vancomycin (an altered vancomycin glycopeptide that no longer binds to cell wall precursors) in place of vancomycin did not result in the expression of *van* genes, indicating that the glycopeptide no longer bound to VanS. This study also showed that an increased ratio of D-Ala-D-Lac to D-Ala-D-Ala, reduced the expression of *van* genes. From these two studies, the current model stands at binding of vancomycin to the vancosamine sugars on peptidoglycan precursors to form a complex, which then binds to VanS and activates signaling (Kwun, *et al.*, 2013).

1.3.2.4 DraRK

DraRK has been briefly discussed for its involvement in antibiotic regulation in *S. coelicolor* in section 1.2.3. Deletion mutants of either *draR* or *draK* genes result in the reduction of ACT production and an increase of RED and yCPK production when grown on minimal medium (MM) and MM with 75 mM glutamate, respectively (Yu, *et al.*, 2012). The activation of ACT and repression of yCPK were found to be through the pathway specific regulators *actII-ORF4* and *kasO*, however, repression of RED production was independent of a RED pathway specific regulator (Yu, *et al.*, 2012). DraRK is also linked with primary metabolism regulation. It has been postulated that DraR positively regulates the expression of genes involved in pyruvate generation and negatively regulates genes involved in lipid biosynthesis for storage (Yu, *et al.*, 2012).

Due to a repression of yCPK in MM with high glutamate levels, DraRK has been linked to AfsQ1/Q2, however, more recently DraRK has been found to be sensitive to low pHs. In conditions where pH is lower than 5, the sensor domain of DraR takes on a more ordered conformation and when pH is higher, the sensor domain takes on a less ordered conformation (Yu, *et al.*, 2014). Additionally, in deletion mutants of *draRK*, the strain is unable to recover after acid shocking (Yu, *et al.*, 2014). These findings link well with earlier work conducted by Kim, *et al.*, (2007) which shows that pH shocking induces antibiotic production. In acidic conditions, DraK is triggered and phosphorylates DraR which activates genes involved in pH shock recovery, primary metabolism and antibiotic production or repression in *S. coelicolor*.

1.3.3 Specific Antibiotic Regulator

1.3.3.1 AbsA1/A2

As previously discussed in AbsA2 is a negative regulator of antibiotic production in *Streptomyces*. AbsA2~P is the active form and represses antibiotic production through the pathway specific regulators, *actII-ORF4*, *redZ* and *cdaR* (McKenzie and Nodwell, 2007). The half-life of AbsA2~P is 68.8 mins which is much less than the approximately 5 hrs of acyl-phosphates, however, as many RRs typically have intrinsic phosphatase activity, this would explain the difference

(Sheeler, *et al.* 2005); furthermore, this time allows AbsA2~P to maintain stable regulation of target genes.

AbsA1 possesses a non-conventional structure. The kinase is predicted to have 5 TM domains, with four clustered towards the N terminus and a fifth only 82 residues from the C-terminus. There is not an obvious sensor domain. Between the TM domains are the conserved H, N and G2 boxes, however, the G1 and F boxes are lacking. This structure indicates that another mechanism of phosphorylation is employed (Sheeler, *et al.*, 2005).

1.4 Aims and Objectives

TCSs are the first line of response for bacteria. They allow bacteria to recognise and respond to their surrounding environment and to changes within the cell. Among bacteria *Streptomyces* species are arguably some of the most interesting and important to humans both agriculturally and medically. However, our understanding of TCS signaling networks in *Streptomyces* bacteria is still quite poor. In section 1.3, the best characterised TCSs of *Streptomyces* have been described, however, of these only VanS, PhoR, DraK and GluK have known activators. Among these, whilst vancomycin has been well established as the stimulus of VanS, the mechanism by which it senses vancomycin is unknown. As the extracellular sensor domain of VanS is formulated by two loops, it is unclear as to whether vancomycin binds directly or via another protein.

Many TCSs have been characterised through deletion of their coding genes. In many cases, the absence of both genes caused the up- or down-regulation of target genes which led to the elucidation of genes they regulated. The deletion of 4 of the 11 TCSs of *M. tuberculosis*, gave rise to strains which displayed a higher level of virulence than WT (Parish, *et al.*, 2003). Two whole genome deletion libraries have also been generated in *B. subtilis*. One strain is erythromycin resistant and the other kanamycin resistant (Koo, *et al.*, 2017). These strains were then put under many screens for sporulation, competence and utilisation of carbon and nitrogen sources (Koo, *et al.*, 2017). Another deletion library was also made in *E. coli* (Baba, *et al.*, 2006). In 2002, Oshima, *et al.*, created a TCS deletion library in *E. coli* before analysing the number of up- and down-regulated genes and doubling

times, as well as other phenotypes. Generation of a TCS deletion library in a *Streptomyces* species, would be a good starting point for characterising the TCSs of in this genus. *S. venezuelae* would be a good choice to generate a TCS deletion library because of its rapid progression through development and its ability to sporulate in liquid almost to completion (Glazebrook, *et al.*, 1990), which is a rare trait among *Streptomyces* strains. The complete genome has been sequenced by the John Innes Centre and a wealth of microarray data is readily available (Pullan, *et al.*, 2011).

The regulation of antibiotic production in *S. coelicolor* has been discussed in section 1.2.3. This has been studied for many decades and despite many antibiotics having been discovered, it is clear through genome mining, that *Streptomyces* possess many BGCs which were not known before. To activate these silent pathways, different strategies have been used and also briefly discussed above such as heterologously expressing a phosphomimetic allele of the antibiotic production regulator AfsQ1 (Daniel-Ivad-2017), deletion of SKs, RR or the complete TCS, or through acid shocking (Yu, *et al.*, 2014). These methods have been demonstrated to work. However, another method which could be explored is through rewiring of TCSs. Changing of domains of different SKs or RRs could be a means of activating silent pathways or charactering TCSs within BGCs where the signaling mechanism is unknown.

In this work, I hope to lay the groundwork of piecing together how the TCSs help *Streptomyces* bacteria regulate and navigate through their complex lifecycles and environment as well as develop a means through which silent pathways can be activated. To achieve this, I aim to:

- Generate a TCSs deletion library in *S. venezuelae* and begin characterization of these deletion mutants (Chapter 3)
- Purify VanS to characterise its interaction with vancomycin (Chapter 4)
- Manipulate the interaction between SK and cognate RR through rewiring of VanS and AfsQ2 (Chapter 5).

2. Material and Methods

2.1 Strains, culture conditions and storage

2.1.1 Strains and vector generation

All bacterial strains and plasmids are listed in tables 2.2 and 2.1 respectively and the primers used to generate these plasmids or strains are listed in table 2.3. Tables have been split into strains and vectors used for cloning or strains specific to chapters within this work.

Table 2.1: DNA plasmids and constructs generated throughout study.

Plasmid	Description	Markers	Source
Plasmids used as controls and for cloning			
pGS-21a	Genscript high copy number overexpression and purification vector (SD0121)	ampR	Genscript
pET-28a	Expression vector with T7 <i>lac</i> promoter, adds N-terminal His tag, thrombin cleavage site, internal T7 epitope tag, C-terminal His tag	kanR	EMD Biosciences
pET-28a-AntA	pET-28a derivative containing the <i>antA</i> coding sequence cloned into the <i>NdeI/HindIII</i> sites	ampR	Seipke, <i>et al.</i> , 2014
pGemT-Easy	Parental vector for TA cloning of PCR products	ampR	Promega
pAU3-45	pSET-152 derivative <i>Streptomyces</i> integrative vector in ϕ C31 site	thioR and aprR	Bignell, <i>et al.</i> , 2005

pUZ8002	RK2 derivative with a mutation in <i>oriT</i>	kanR	Kieser <i>et al.</i> , 2000
pIJ773	<i>aac(3)IV oriT bla</i> (contains apramycin (apr) resistance cassette)	aprR	Gust <i>et al.</i> , 2002
pIJ790	<i>araC-Parab, Y, β, exo, cat, repA1001ts, oriR101</i>	cmlR	Gust <i>et al.</i> , 2002
pMS82	<i>Streptomyces</i> integrative vector into ϕ BT1 site	aprR	Gregory, <i>et al.</i> , 2003
pSS170	pMS82 derivative with <i>apr</i> promoter removed	hygR	Schlimpert, unpublished
pCRISPomyces-2	<i>oriT, reppSG5(ts), oriColE1, sSpcas9</i> , synthetic guide RNA cassette	aprR	Cobb, <i>et al.</i> , 2015
Vectors generated for work described in Chapter 4			
pRL100	pGS-21a derivative with <i>vanS</i> coding sequence cloned into <i>NcoI/HindIII</i> for over expression of His-GST-VanS	ampR	This work
pRL101	pGS-21a derivative with <i>vanS</i> coding sequence cloned into <i>NdeI/HindIII</i> for over expression of VanS-His	ampR	This work
pRL102	pGS-21a derivative with <i>vanS</i> mutant coding sequence cloned into <i>NdeI/HindIII</i> for over expression of His-VanS (L89V)	ampR	This work

pRL103	pGS-21a derivative with <i>vanS</i> mutant coding sequence cloned into <i>NdeI/HindIII</i> for over expression of His-VanS (A91G)	ampR	This work
pRL104	pGS-21a derivative with <i>vanS</i> mutant coding sequence cloned into <i>NdeI/HindIII</i> for over expression of His-VanS (LA90:91VG)	ampR	This work
pRL105	pGS-21a derivative with <i>vanS</i> mutant coding sequence cloned into <i>NdeI/HindIII</i> for over expression of VanS-His (L89V)	ampR	This work
pRL106	pGS-21a derivative with <i>vanS</i> mutant coding sequence cloned into <i>NdeI/HindIII</i> for over expression of VanS-His (A91G)	ampR	This work
pRL107	pGS-21a derivative with <i>vanS</i> mutant coding sequence cloned into <i>NdeI/HindIII</i> for over expression of VanS-His (LA90:91VG)	ampR	This work

Vectors generated for work described in Chapter 5			
pRL111	pAU3-45 derivative with <i>chim1</i> cloned into <i>XbaI/EcoRI</i>	aprR/thioR	This work
pRL112	pAU3-45 derivative with <i>chim2</i> cloned into <i>XbaI/EcoRI</i>	aprR/thioR	This work
pRL113	pMS82 derivative with <i>chim3</i> cloned into <i>HindIII/KpnI</i>	hygR	This work
pRL114	pMS82 derivative with <i>chim4</i> cloned into <i>HindIII/KpnI</i>	hygR	This work
pRL115	pMS82 derivative with <i>chim5</i> cloned into <i>HindIII/KpnI</i>	hygR	This work
pRL116	pGS-21a derivative with c- <i>chim2</i> (N-terminal His tag)	ampR	This work
pRL117	pGS-21a derivative with c- <i>chim3</i> (N-terminal His tag) cloned in with <i>NdeI</i> and <i>HindIII</i>	ampR	This work
pRL118	pGS-21a derivative with c- <i>chim4</i> (N-terminal His tag) cloned into <i>NdeI</i> and <i>HindIII</i>	ampR	This work
pRL119	pGS-21a derivative with c- <i>chim5</i> (N-terminal His tag) cloned into <i>NdeI</i> and <i>HindIII</i>	ampR	This work
pRL120	pGS-21a derivative with c- <i>vanS</i> (N-terminal His tag)	ampR	This work

	cloned into <i>NdeI</i> and <i>HindIII</i>		
pRL121	pGS-21a derivative with c- <i>afsQ2</i> (N-terminal His tag) cloned into <i>NdeI</i> and <i>HindIII</i>	ampR	This work
pRL122	pGS-21a derivative with <i>afsQ1</i> (N-terminal His tag) cloned into <i>NdeI</i> and <i>HindIII</i>	ampR	This work
pRL123	pGS-21a derivative with <i>vanR</i> (N-terminal His tag) cloned into <i>NdeI</i> and <i>HindIII</i>	ampR	This work
pRL124	pGS-21a derivative with <i>chim2</i> (N-terminal His tag) cloned into <i>NdeI</i> and <i>HindIII</i>	ampR	This work
pRL125	pGS-21a derivative with <i>chim3</i> (N-terminal His tag) cloned into <i>NdeI</i> and <i>HindIII</i>	ampR	This work
pRL126	pGS-21a derivative with c- <i>chim4</i> (C-terminal His tag) cloned into <i>NdeI</i> and <i>HindIII</i>	ampR	This work
pRL127	pGS-21a derivative with c- <i>chim5</i> (C-terminal His tag) cloned into <i>NdeI</i> and <i>HindIII</i>	ampR	This work
pRL128	pGS-21a derivative with c- <i>vanS</i> (C-terminal His tag)	ampR	This work

	cloned into <i>NdeI</i> and <i>HindIII</i>		
pRL129	pGS-21a derivative with c- <i>afsQ2</i> (C-terminal His tag) cloned into <i>NdeI</i> and <i>HindIII</i>	ampR	This work
pRL130	pGS-21a derivative with <i>afsQ1</i> (C-terminal His tag) cloned into <i>NdeI</i> and <i>HindIII</i>	ampR	This work
pRL131	pGS-21a derivative with <i>vanR</i> (C-terminal His tag) cloned into <i>NdeI</i> and <i>HindIII</i>	ampR	This work

Table 2. 2: Strains used throughout study.

Strain	Description	Resistance	Source
<i>E. coli</i> strains used for cloning, overexpression and constructing mutants			
TOP10	F ⁻ <i>mcrA</i> Δ(<i>mrr-hsdRMS-mcrBC</i>) Φ80 <i>lacZ</i> ΔM15 Δ <i>lacX74 recA1</i> <i>araD139</i> Δ(<i>ara leu</i>) 7697 <i>galU galK</i> <i>rpsL</i> (StrR) <i>endA1</i> <i>nupG</i>		Invitrogen
BL21	F ⁻ <i>ompT gal dcm lon</i> <i>hsdS_B</i> (<i>r_B⁻ m_B⁻) λ(DE3 [<i>lacI lacUV5-T7 gene 1 ind1 sam7 nin5</i>])</i>		Studier & Moffat, 1986

Rosetta™ (DE3)	F ⁻ <i>ompT hsdSB(rB-mB-)</i> <i>gal dcm</i> (DE3) pRARE (CamR)		Novagen
C41	F ⁻ <i>ompT gal dcm hsdSB(rB⁻ mB⁻)</i> (DE3)		Lucigen
C43	F ⁻ <i>ompT gal dcm hsdSB(rB⁻ mB⁻)</i> (DE3)		Lucigen
ET12567	<i>dam- dcm- hsdM-</i> strain with pUZ8002	kanR/cmlR	MacNeil <i>et al.</i> , 1992
BW25113	F ⁻ , DE(<i>araD-araB</i>)567, <i>lacZ4787(del)::rrnB-3, LAM, rph-1,</i> DE(<i>rhaD-rhaB</i>)568, <i>hsdR514</i> strain with pIJ790	cmlR	Datsenko & Wanner, 2000
<i>Streptomyces</i> wild-type strains used			
M145	<i>S. coelicolor</i> WT strain, SCP1-, SCP2-		
Sliv	<i>S. lividans</i> WT		
Sven	<i>S. venezuelae</i> NRRL B-65442 WT strain		
KY5	<i>S. formicae</i> WT		
<i>S. venezuelae</i> TCS deletion strains from Chapter 3			
	PCR targeting method- genes deleted in <i>S. venezuelae</i> NRRL B-65442 were replaced with apramycin resistance cassette		
Δ138/139	<i>S. venezuelae</i> Δ138/139:: <i>apr</i>	aprR	This work
Δ1732/33	<i>S. venezuelae</i> Δ1732/33:: <i>apr</i>	aprR	This work
Δ1916/17	<i>S. venezuelae</i> Δ1916/17:: <i>apr</i>	aprR	This work

$\Delta 2143/44$	<i>S. venezuelae</i> $\Delta 2143/44::apr$	aprR	This work
$\Delta 2151/52$	<i>S. venezuelae</i> $\Delta 2151/52::apr$	aprR	This work
$\Delta 2695/96$	<i>S. venezuelae</i> $\Delta 2695/96::apr$	aprR	This work
$\Delta 2739/40$	<i>S. venezuelae</i> $\Delta 2739/40::apr$	aprR	This work
$\Delta 3232/33$	<i>S. venezuelae</i> $\Delta 3232/33::apr$	aprR	This work
$\Delta 3326/27$	<i>S. venezuelae</i> $\Delta 3326/27::apr$	aprR	This work
$\Delta 3393/94$	<i>S. venezuelae</i> $\Delta 3393/94::apr$	aprR	This work
$\Delta 3472/73$	<i>S. venezuelae</i> $\Delta 3472/73::apr$	aprR	This work
$\Delta 3682/83$	<i>S. venezuelae</i> $\Delta 3682/83::apr$	aprR	This work
$\Delta 5286/87$	<i>S. venezuelae</i> $\Delta 5286/87::apr$	aprR	This work
$\Delta 5323/24$	<i>S. venezuelae</i> $\Delta 5323/24::apr$	aprR	This work
$\Delta 5393/94$	<i>S. venezuelae</i> $\Delta 5393/94::apr$	aprR	This work
$\Delta 5397/98$	<i>S. venezuelae</i> $\Delta 5397/98::apr$	aprR	This work
$\Delta 5426/27$	<i>S. venezuelae</i> $\Delta 5426/27::apr$	aprR	This work
$\Delta 5435/36$	<i>S. venezuelae</i> $\Delta 5435/36::apr$	aprR	This work
$\Delta 5634/35$	<i>S. venezuelae</i> $\Delta 5634/35::apr$	aprR	This work

$\Delta 56345/46$	<i>S. venezuelae</i> $\Delta 56345/46::apr$	aprR	This work
$\Delta 5973/74$	<i>S. venezuelae</i> $\Delta 5973/74::apr$	aprR	This work
$\Delta 5985/86$	<i>S. venezuelae</i> $\Delta 5985/86::apr$	aprR	This work
$\Delta 6082/83$	<i>S. venezuelae</i> $\Delta 6082/83::apr$	aprR	This work
$\Delta 6349$	<i>S. venezuelae</i> $\Delta 6349::apr$	aprR	This work
$\Delta 6350$	<i>S. venezuelae</i> $\Delta 6350::apr$	aprR	This work
$\Delta 6371/72$	<i>S. venezuelae</i> $\Delta 6371/72::apr$	aprR	This work
TCS in frame deletion mutants unmarked in <i>S. venezuelae</i> NRRL B-65442 generated using CRISPR/Cas9 gene editing method			
$\Delta 1397/98$	<i>S. venezuelae</i> $\Delta 1397/98$		This work
$\Delta 1773/74$	<i>S. venezuelae</i> $\Delta 1773/74$		This work
$\Delta 1949/50$	<i>S. venezuelae</i> $\Delta 1949/50$		This work
$\Delta 3170/71$	<i>S. venezuelae</i> $\Delta 3170/71$		This work
$\Delta 3148/49$	<i>S. venezuelae</i> $\Delta 3148/49$		This work
$\Delta 3364/65$	<i>S. venezuelae</i> $\Delta 3364/65$		This work
$\Delta 3393/94$	<i>S. venezuelae</i> $\Delta 3393/94$		This work
$\Delta 3682/83$	<i>S. venezuelae</i> $\Delta 3682/83$		This work

$\Delta 3736/37$	<i>S. venezuelae</i> $\Delta 3736/37$		This work
$\Delta 3785/86$	<i>S. venezuelae</i> $\Delta 3785/86$		This work
$\Delta 3821/22$	<i>S. venezuelae</i> $\Delta 3821/22$		This work
$\Delta 3873/74$	<i>S. venezuelae</i> $\Delta 3873/74$		This work
$\Delta 4209/10/11$	<i>S. venezuelae</i> $\Delta 4209/10/11$		This work
$\Delta 4373/74$	<i>S. venezuelae</i> $\Delta 4373/74$		This work
$\Delta 4474/75$	<i>S. venezuelae</i> $\Delta 4474/75$		This work
$\Delta 5214/15$	<i>S. venezuelae</i> $\Delta 5214/15$		This work
$\Delta 5286/87$	<i>S. venezuelae</i> $\Delta 5286/87$		This work
$\Delta 5306/07$	<i>S. venezuelae</i> $\Delta 5306/07$		This work
$\Delta 5349/50$	<i>S. venezuelae</i> $\Delta 5349/50$		This work
$\Delta 6686/87$	<i>S. venezuelae</i> $\Delta 6686/87$		This work
$\Delta 7022/23$	<i>S. venezuelae</i> $\Delta 7022/23$		This work
$\Delta 7155/56$	<i>S. venezuelae</i> $\Delta 7155/56$		This work
$\Delta 7219/20$	<i>S. venezuelae</i> $\Delta 7219/20$		This work
Strains used in Chapter 4			

BL21 pET-28a-AntA	BL21 with pET-28a-AntA	ampR	Seipke, <i>et al.</i> , 2014
BL21 pGS-21A	BL21 with pGS-21a	ampR	This work
RL001	BL21 with pRL100	ampR	This work
RL002	BL21 with pRL101	ampR	This work
RL003	C41 with pRL100	ampR	This work
RL004	C43 with pRL101	ampR	This work
RL005	BL21 with pRL102	ampR	This work
RL006	BL21 with pRL103	ampR	This work
RL007	BL21 with pRL104	ampR	This work
RL008	BL21 with pRL105	ampR	This work
RL009	BL21 with pRL106	ampR	This work
RL010	BL21 with pRL107	ampR	This work
Strains used in Chapter 5 * 1-3 refers to biological replicates			
<i>Candida albicans</i>	Clinical isolate		Prof Neil Gow, University of Exeter
<i>B. subtilis</i>	Wild-type		Lab Stock
M145::pAU3-45	<i>S. coelicolor</i> M145 with pAU3-45 integrated into Φ C31 (single crossover)	aprR/thioR	This work
M145::Chim1.(1-3)	<i>S. coelicolor</i> M145 with pRL111 (<i>chim1</i>) integrated into Φ C31 (single crossover)	aprR/thioR	This work
M145::Chim2.(1-3)	<i>S. coelicolor</i> M145 with pRL112 (<i>chim2</i>) integrated into Φ C31 (single crossover)	aprR/thioR	This work
M145::pMS82	<i>S. coelicolor</i> M145 with pMS82 integrated into Φ BT1 (single crossover)	hygR	This work

M145::Chim3.(1-3)	<i>S. coelicolor</i> M145 with pRL113 (<i>chim3</i>) integrated into Φ BT1 (single crossover)	hygR	This work
M145::Chim4.(1-3)	<i>S. coelicolor</i> M145 with pRL114 (<i>chim4</i>) integrated into Φ BT1 (single crossover)	hygR	This work
M145::Chim5.(1-3)	<i>S. coelicolor</i> M145 with pRL115 (<i>chim5</i>) integrated into Φ BT1 (single crossover)	hygR	This work
M145 Δ <i>afsQ2</i>	<i>S. coelicolor</i> M145 Δ <i>afsQ2</i>		This work
M145 Δ <i>afsQ2</i> ::pMS82	<i>S. coelicolor</i> M145 Δ <i>afsQ2</i> with pMS82 integrated into Φ BT1 (single crossover)	hygR	This work
M145 Δ <i>afsQ2</i> ::Chim3.(1-3)	<i>S. coelicolor</i> M145 Δ <i>afsQ2</i> with pRL113 (<i>chim3</i>) integrated into Φ BT1 (single crossover)	hygR	This work
M145 Δ <i>afsQ2</i> ::Chim4.(1-3)	<i>S. coelicolor</i> M145 Δ <i>afsQ2</i> with pRL114 (<i>chim4</i>) integrated into Φ BT1 (single crossover)	hygR	This work
M145 Δ <i>afsQ2</i> ::Chim5.(1-3)	<i>S. coelicolor</i> M145 Δ <i>afsQ2</i> with pRL115 (<i>chim5</i>) integrated into Φ BT1 (single crossover)	hygR	This work
Sliv::pAU3-45	<i>S. lividans</i> with pAU3-45 integrated into Φ C31 (single crossover)	aprR/thioR	This work
Sliv::Chim1.(1-3)	<i>S. lividans</i> with pRL111 (<i>chim1</i>) integrated into	aprR/thioR	This work

	Φ C31 (single crossover)		
Sliv::Chim2.(1-3)	<i>S. lividans</i> with pRL112 (<i>chim2</i>) integrated into Φ C31 (single crossover)	aprR/thioR	This work
Sliv::pMS82	<i>S. lividans</i> with pMS82 integrated into Φ BT1 (single crossover)	hygR	This work
Sliv::Chim3.(1-3)	<i>S. lividans</i> with pRL113 (<i>chim3</i>) integrated into Φ BT1 (single crossover)	hygR	This work
Sliv::Chim4.(1-3)	<i>S. lividans</i> with pRL114 (<i>chim4</i>) integrated into Φ BT1 (single crossover)	hygR	This work
Sliv::Chim5.(1-3)	<i>S. lividans</i> with pRL115 (<i>chim5</i>) integrated into Φ BT1 (single crossover)	hygR	This work
Sliv Δ <i>afsQ2</i>	<i>S. lividans</i> Δ <i>afsQ2</i>		This work
Sliv Δ <i>afsQ2</i> ::pMS82	<i>S. lividans</i> Δ <i>afsQ2</i> with pMS82 integrated into Φ BT1 (single crossover)	hygR	This work
Sliv Δ <i>afsQ2</i> ::Chim3.(1-3)	<i>S. lividans</i> Δ <i>afsQ2</i> with pRL113 (<i>chim3</i>) integrated into Φ BT1 (single crossover)	hygR	This work
Sliv Δ <i>afsQ2</i> ::Chim4.(1-3)	<i>S. lividans</i> Δ <i>afsQ2</i> with pRL114 (<i>chim4</i>) integrated into Φ BT1 (single crossover)	hygR	This work
Sliv Δ <i>afsQ2</i> ::Chim5.(1-3)	<i>S. lividans</i> Δ <i>afsQ2</i> with pRL115 (<i>chim5</i>) integrated into Φ BT1 (single crossover)	hygR	This work

Sven::pMS82	<i>S. venezuelae</i> with pMS82 integrated into Φ BT1 (single crossover)	hygR	This work
Sven::Chim3.(1-3)	<i>S. venezuelae</i> with pRL113 (<i>chim3</i>) integrated into Φ BT1 (single crossover)	hygR	This work
Sven::Chim4.(1-3)	<i>S. venezuelae</i> with pRL114 (<i>chim4</i>) integrated into Φ BT1 (single crossover)	hygR	This work
Sven::Chim5.(1-3)	<i>S. venezuelae</i> with pRL115 (<i>chim5</i>) integrated into Φ BT1 (single crossover)	hygR	This work
Sven Δ <i>afsQ2</i>	<i>S. venezuelae</i> Δ <i>afsQ2</i> with pMS82 integrated into Φ BT1 (single crossover)		This work
F-AfsQ1	<i>S. venezuelae</i> 3x FLAG- <i>afsQ1</i>		This work
F-AfsQ1::pMS82	<i>S. venezuelae</i> 3x FLAG- <i>afsQ1</i> with pMS82 integrated into Φ BT1 (single crossover)	hygR	This work
F-AfsQ1::Chim3.(1-3)	<i>S. venezuelae</i> 3x FLAG- <i>afsQ1</i> with pRL113 (<i>chim3</i>) integrated into Φ BT1 (single crossover)	hygR	This work
F-AfsQ1::Chim4.(1-3)	<i>S. venezuelae</i> 3x FLAG- <i>afsQ1</i> with pRL114 (<i>chim4</i>) integrated into Φ BT1 (single crossover)	hygR	This work
F-AfsQ1::Chim5.(1-3)	<i>S. venezuelae</i> 3x FLAG- <i>afsQ1</i> with pRL115 (<i>chim5</i>) integrated into	hygR	This work

	ΦBT1 (single crossover)		
KY5::pMS82	<i>S. formicae</i> with pMS82 integrated into ΦBT1 (single crossover)	hygR	This work
KY5::Chim3.(1-3)	<i>S. formicae</i> with pRL113 (<i>chim3</i>) integrated into ΦBT1 (single crossover)	hygR	This work
KY5::Chim4.(1-3)	<i>S. formicae</i> with pRL114 (<i>chim4</i>) integrated into ΦBT1 (single crossover)	hygR	This work
KY5::Chim5.(1-3)	<i>S. formicae</i> with pRL115 (<i>chim5</i>) integrated into ΦBT1 (single crossover)	hygR	This work
RLOEVanR	BL21 pRL130	ampR	This work
RLOEAfsQ1	BL21 pRL1131	ampR	This work
RLOEc-VanS	BL21 pRL120	ampR	This work
RLOEc-AfsQ2	BL21 pRL121	ampR	This work
RLOEc-Chim2	BL21 pRL116	ampR	This work
RLOEc-Chim3	BL21 pRL117	ampR	This work
RLOEc-Chim4	BL21 pRL118	ampR	This work
RLOEc-Chim5	BL21 pRL119	ampR	This work

Table 2. 3: Primers and oligonucleotides used as protospacers in CRISPR/Cas9 gene editing used throughout study. All hexa-His tag sequences are underlined, restriction sites are italicised and in lower case, four nucleotides were added to allow binding of restriction enzymes (shown in lower case) and primer sequences ending in F and R refer to forward or reverse direction during amplification.

Primer	Primer sequence	Description
General Primers		
SP6	ATTTAGGTGACACTATAG	Sequencing of pGemT-Easy
T7	TAATACGACTCACTATAGGG	Sequencing of pGemT-Easy and pGS-21a
T7 term	GCTAGTTATTGCTCAGCGG	Sequencing of pGS-21a
pMS82F	GCAACAGTGCCGTTGATCGTGCTATG	Amplifies MCS of pMS82
pMS82R	GCCAGTGGTATTTATGTCAACACCGCC	
SpacerFor-2756	ACGCAGCTCCTTCGGCTTGAACGG	Amplifies region of protospacer sequence
SpacerRev-2756	AAACCCGTTCAAGCCGAAGGAGCT	
For-CRISP-2	AGGCTAGTCCGTTATCAACTTGAAA	Amplifies ~100bp up and downstream of XbaI site of pCRISPomyces-2
Rev-CRISP-2	TCGCCACCTCTGACTTGAGCGTCGA	
Chapter 3: Generation of a TCS deletion library in <i>S. venezuelae</i>		
<i>Asven15_1393/99</i>		
RLOTCSKO001	ACGCTGTCCGACTTCCTCGGCCTC	Protospacer
RLOTCSKO002	AAACGAGGCCGAGGAAGTCGGACA	
RLOTCSKO003F	GCTCGGTTGCCGCCGGCGTTTTTTAT CTAGAGTGAAGACCGCCGAGAAGACC ATGCCGCTGCTC	Homology Amplification
RLOTCSKO004R	GGACTGAACGGTCGTGCGCCCCGACGC AACGCCTGGTGAGTTCGTTACGTG	

RLOTCSKO005F	CTCACCAGGCGTTGCGTCGGGGCGCAC GACCGTTCAGTCCTTCATACCGTC	
RLOTCSKO006R	GCGGCCTTTTTACGGTTCCTGGCCTCTA GAGGATACGTCCACCAGCTCCAGTACA TCGCTCATGAG	
RLOTCSKO007F	GGTGTTCGCAGACATAACGGACTA	Confirmation and sequencing primers
RLOTCSKO008R	GGTACATCCTCCTGGTCATCGCTG	
RLOTCSKO009F	TCTGGAGGTGCAGGACGACATAGA	
RLOTCSKO010F	CATCTGCGCCATCGGCTTCTCGAC	
RLOTCSKO011R	GCGATGTTCAGAAGGGTGGTCTTG	
RLOTCSKO012F	CCTTCGGCGTTGTCTTCGGTGC	
RLOTCSKO013F	CCTGCGGGCTGTTGCGGTTGTA	
RLOTCSKO014R	TGACGCGGGTGCGGACAGAGAAG	
RLOTCSKO015R	GTGGAGGTGGTCTGGCGGTGTCTG	
<i>Asven15_1479/80</i>		
RLOTCSKO016	ACGCGTCGCCGTCGCCGCGCTGTT	Protospacer set
RLOTCSKO017	AAACAACAGCGCGGCGACGGCGAC	1
RLOTCSKO016a	ACGCTTCTGGATGGTCGGCACGCT	Protospacer set
RLOTCSKO017a	AAACAGCGTGCCGACCATCCAGAA	2
RLOTCSKO018F	GCTCGGTTGCCGCCGGCGTTTTTAT CTAGACAGGACCTGGAGCGAGCCGTC GATGACGTAG	Homology Amplification
RLOTCSKO019R	GAACCTTCATACGGACCGGGTCAGGTC ACGCCTCGGCGCTCCGCCGCCG	
RLOTCSKO020F	TCAGGTCACGCCTCGGCGCTCCACACG GAGGCCCGGTCCGTATGAAGGTTT	
RLOTCSKO021R	GCGGCCTTTTTACGGTTCCTGGCCTCTA GAGACCCTGCATATCGTGTGACGGGCA CCGAC	
RLOTCSKO022F	CTGGCGAAATGATCACCGGGTTCC	Confirmation and sequencing primers
RLOTCSKO023F	GTCGAGGCCCGTACCGAAGCATGG	
RLOTCSKO024F	CTGTCCACGTAGTGGTTGTCGTAC	
RLOTCSKO025F	GCTCGAAGCCCATCACCGTGAGCA	
RLOTCSKO026F	CATGACCAGGACCGAACTCCTCCG	

RLOTCSKO027F	GCACCCTCTTCGTGTTGTACGCG	
RLOTCSKO028R	GGGTTCTTCAGCCGGTCGTCGGTG	
RLOTCSKO029R	GGAGGCGTTCTCGTTCTTCAGCAC	
<i>Asven15_1773/74</i>		
RLOTCSKO030	ACGCCTGGTGCTGCGCCGGCGCTA	Protospacers
RLOTCSKO031	AAACTAGCGCCGGCGCAGCACCAG	
RLOTCSKO032F	GCTCGGTTGCCGCCGGGCGTTTTTAT CTAGAGAGAGGTCCGCCGTCACCTTGT CGGTGG	Homology Amplification
RLOTCSKO033R	TCCACCCTCGGACGTACCAGCGTGGCG CGTGGGTGTCAGCCGGGGATGAG	
RLOTCSKO034F	GCTGACACCCACGCGCCACGCTGGTAC GTCCGAGGGTGGAGTGACCG	
RLOTCSKO035R	GCGGCCTTTTTACGGTTCCTGGCCTCTA GACCCAGGTGCCGCTTGATGTTCTCCA GGAC	
RLOTCSKO036R	GTCCAGATCCTTATCCCGCGCATAAC	Confirmation and sequencing primers
RLOTCSKO037F	GAGTACGTCGTGCAGTCGCTGCGG	
RLOTCSKO038F	CGAGTCGACGAAGTCGCGCACGAAG	
RLOTCSKO039R	GACCACGGTCAGGGAGACGAGCAG	
RLOTCSKO040R	GCCGACGTCGCTCATCTCCTCCGA	
RLOTCSKO041F	CAGGGCGAGGAGGAGAAGCTCACC	
RLOTCSKO042F	GTCCAGATCCTTATCCCGCGCATAAC	
RLOTCSKO043R	GATGGTGCGGCTCTTGCCCGTCTC	
<i>Asven15_1949/50</i>		
RLOTCSKO044	ACGCCGGCTGCGGCTCATCGTCTT	Protospacer
RLOTCSKO045	AAACAAGACGATGAGCCGCAGCCG	
RLOTCSKO046F	GCTCGGTTGCCGCCGGGCGTTTTTAT CTAGAGTACGTCAGGTATGGCGGGATG CG	Homology Amplification
RLOTCSKO047R	GCCGGGACACCCCCGTCCCGCTCCTT ACGCCGTCCTCG	
RLOTCSKO048F	CGTAAGGAGCGGGACGGGGGGTGTCC CGGCCCGTCGGCTAC	

RLOTCSKO049R	GCGGCCTTTTTACGGTTCCTGGCCTCTA GACTGGTCAACACCTCCCGCACGATG	
RLOTCSKO050R	GTGGCCAGGAAGCTGTGGGAACTC	Confirmation and sequencing primers
RLOTCSKO051F	ACGACATGATCCGACTGCTGCTGG	
RLOTCSKO052F	CTCCTCGTGGCGGTGAAGACCTCG	
RLOTCSKO053R	GACGGCACGTTCTCGGCACGATC	
RLOTCSKO054F	CACGGTCTGTTCTCCACCCACTAC	
RLOTCSKO055F	ATGTCACCGCGTCAGGTCGTCATC	
RLOTCSKO056F	CGCTTGTCGTTGTCGAGCTGGTGC	
<i>Asven15_2534/35</i>		
RLOTCSKO057	ACGCGTTGCGCGAGGTCGCCATT	Protospacer
RLOTCSKO058	AAACAATGGGCGACCTCGCGCAAC	
RLOTCSKO059F	GCTCGGTTGCCGCCGGGCGTTTTTAT CTAGAGGACTCGCCGAACATACCCG ACCGGGAAC	
RLOTCSKO060R	CTCTCGACCGCTCGGCGGGTGGGCCGC ACCGTACGCCATTCGGG	Homology Amplification
RLOTCSKO061F	AATGGCGTACGGTGCGGCCACCCGCC GAGCGGTCGAGAGCTGACGGACC	
RLOTCSKO062R	GCGGCCTTTTTACGGTTCCTGGCCTCTA GATCGACCTTGGTCAGCTTGTACTGG	
RLOTCSKO063F	GTAGCTCTTCACGTTGACTCCGT	
RLOTCSKO064F	CTCCTCGCCAACGAACGGGAACTC	Confirmation and sequencing primers
RLOTCSKO065F	GCTGCCACTGAGACGAGTGATCCG	
RLOTCSKO066R	ATGACGGGCAGCGTGAAGGAGAC	
RLOTCSKO067F	GCTTCTACGCGGCGAACCTGGCC	
RLOTCSKO068R	AACTGCTGCCATCGCGTGCCTG	
RLOTCSKO069F	TCCCGATGGCTTCCTTAAGCGGAG	
<i>Asven15_3170/71</i>		
RLOTCSKO070	ACGCGTGCTGATGGATGTGCGCAT	Protospacer
RLOTCSKO071	AAACATGCGCACATCCATCAGCAC	
RLOTCSKO072F	GCTCGGTTGCCGCCGGGCGTTTTTAT CTAGACGTTGGAGAAGGCGGAGAGCC AGTCG	Homology Amplification

RLOTCSKO073R	CAGCAGCGTCACGGCGTCACCCAGAGT AGGGAAGGCGGATAGG	
RLOTCSKO074F	CCTACTCTGGGTGACGCCGTGACGCTG CTGTGGATCAAC	
RLOTCSKO075R	GCGGCCTTTTTACGGTTCCTGGCCTCTA GAGTCCACCCGCTCCGACTTCCTGCTG	
RLOTCSKO076F	CCCTCCGGGCGCAGATAGAAGC	
RLOTCSKO077F	GACGACGAAGGAATCTGATGTCCATC	
RLOTCSKO078F	GAGGAACATCAGGTGGTTGAGGAC	Confirmation and sequencing primers
RLOTCSKO079R	GAGGTGAGCGTGACCATAGACATC	
RLOTCSKO080R	CGATCCTTGACGCGGAGCCCGTAC	
RLOTCSKO081R	TACGGACGTGGTGGGCGAACTCC	
RLOTCSKO082R	CGCCACAAGACCGAACTGCTGCG	
<i>Asven15_3736/37</i>		
RLOTCSKO083	ACGCCGCTGCTGATCACCGGCGTT	Protospacer
RLOTCSKO084	AAACAACGCCGGTGATCAGCAGCG	
RLOTCSKO085F	GCTCGGTTGCCGCCGGCGTTTTTTAT CTAGAGTGAAGGCGTAGTCGCGGACG TTGTCCACAG	Homology Amplification
RLOTCSKO086R	CCCTTCTTCCGCGCCTCCGGGCGAATC CCGCTCGCGAACGAGGG	
RLOTCSKO087F	CGCGAGCGGGATTGCCCCGAGGCGC GGAAGAAGGGTCCGACAA	
RLOTCSKO088R	GCGGCCTTTTTACGGTTCCTGGCCTCTA GATTCATCATGCCTGCGACCGCCTCA CAC	
RLOTCSKO089R	CTTCCCAAGCTTATAGCGCGGGTTC	
RLOTCSKO090F	CTGCACGATTCATCACCCATCAGATC	
RLOTCSKO091F	CATGCTGCCGAAGCCCACGTACAC	Confirmation and sequencing primers
RLOTCSKO092R	GTTCTTGACGTCCAGGGCGTAGG	
RLOTCSKO093F	CGTAGCGGATGCCGAGCTTCTCG	
RLOTCSKO094F	GTGACCCGGTGGCAATGCCGAGA	
RLOTCSKO095R	CTCGAACACCCGGAAGAAGCGGTC	
<i>Asven15_3393/94</i>		

RLOTCSKO096	ACGCGTGCTGATGGACATCAGGAT	Protospacer
RLOTCSKO097	AAACATCCTGATGTCCATCAGCAC	
RLOTCSKO098F	GCTCGGTTGCCGCCGGGCGTTTTTAT CTAGACTCTGGACCACCAGGACGCCTT CGC	Homology Amplification
RLOTCSKO099R	CCAGCCCCATCGGCCTCAGGTCAGTTC ACGAGGTCCGACGTCATGCGGG	
RLOTCSKO100F	CGTCAAGTGACCTGAGGCCGATGGGG CTGGACGGGCGGG	
RLOTCSKO101R	GCGGCCTTTTTACGGTTCCTGGCCTCTA GAGAGTTGCCGCTGTTGCCGATCAGTC C	
RLOTCSKO102F	CGTCGGACCTCGTCAAGTGACCT	
RLOTCSKO103F	CATCCTGACCACGTTTCGACACCGAC	Confirmation and sequencing primers
RLOTCSKO104F	GAATCCAAGAAGCAGGAGACCCGG	
RLOTCSKO105R	GTTCGACCTGTCCGAGCACACG	
RLOTCSKO106F	GGACAACGCCTTCAGCCTGCTG	
RLOTCSKO107R	GAGGACCTTGGGCACGCGCTGAC	
<i>Asven_15 3472/73</i>		
RLOTCSKO108	ACGCAGACGTCGCCGAGGACGAAT	Protospacer set
RLOTCSKO109	AAACATTCGTCCTCGGCGACGTCT	1
RLOTCSKO108a	ACGCTTCGAGTTCCCCGAGCTGGT	Protospacer set
RLOTCSKO109a	AAACACCAGCTCGGGGAACCTCGAA	2
RLOTCSKO110F	GCTCGGTTGCCGCCGGGCGTTTTTAT CTAGAGCTCCGTGATGTAGCCGTTGAC CTGCTTC	Homology Amplification
RLOTCSKO111R	GGCCTGGAGTTCTAGGCCCCCATCCTC TCCCCGCCGTATATG	
RLOTCSKO112F	GGAGAGGATGGGGGCCTAGAACTCCA GGCCGGCGAGCAGCC	
RLOTCSKO113R	GCGGCCTTTTTACGGTTCCTGGCCTCTA GAGAAGTCGTGGCGGACACCGACGCG GTC	

RLOTCSKO114R	GTCCGGTTCGATGCGCGGGTACTTC	Confirmation and sequencing primers
RLOTCSKO115F	GAAGTAAAAGAACTCGGGCAGACCA	
RLOTCSKO116F	CATGATCGGGTTGAGGAGGACGGC	
RLOTCSKO117R	CGACGTACTCGTTGTCGCTGGTGTTTC	
RLOTCSKO118F	CTTGCCGATGAGGTGGACGTTCGC	
RLOTCSKO119F	GATCTTCTGACCGTGCTCGTCCG	
RLOTCSKO120F	GAAGTACCCGCGCATCGAACC GGAC	
RLOTCSKO121R	AAGACGGAGGCCGCGGCTGACG	
<i>Asven15_3682/83</i>		
RLOTCSKO122	ACGCGGCACCTTCCTCACCGGCAT	Protospacer
RLOTCSKO123	AAACATGCCGGTGAGGAAGGTGCC	
RLOTCSKO124F	GCTCGGTTGCCGCCGGGCGTTTTTTAT CTAGAGCATCGAACCGCCCTACTACAC CGCC	Homology Amplification
RLOTCSKO125R	TCGCCGGGGCCGCTGGACCTCACGGTG TCCGCCGCCGCTGAG	
RLOTCSKO126F	GGACACCGTGAGGTCCAGCGGCCCCCG GCGAGTGTCCGGTGGCATG	
RLOTCSKO127R	GCGGCCTTTTTACGGTTCCTGGCCTCTA GAGTCGAAGTCATCGGTTCGTTCTTGG GTCGT	
RLOTCSKO128F	GTTCACGGACTTCAGCGAGCGGCTC	
RLOTCSKO129F	CCCTGATCCTCGTCGAGCTCAGC	Confirmation and sequencing primers
RLOTCSKO130F	CCTTCGTAAAGTCTTGGATCCCCTTTCC	
RLOTCSKO131R	GTCGAAGTCATCGGTTCGTTCTTGG	
RLOTCSKO132F	GGGACGACATCCAGGTCCTCCTGG	
RLOTCSKO133R	GACATCGCGCCGGATCGCCTTGAAG	
RLOTCSKO134R	TACCTCGCGCTGTACTCGCTCTTC	
<i>Asven15_3736/37</i>		
RLOTCSKO135	ACGCGCCGTGCTCGATCTGCAGAT	Protospacer
RLOTCSKO136	AAACATCTGCAGATCGAGCACGGC	
RLOTCSKO137F	GCTCGGTTGCCGCCGGGCGTTTTTTAT CTAGAGCGAACAGGTCCGGGTCAAGC AGCTGTC	Homology Amplification

RLOTCSKO138R	CCGTAGCGCGGAGCCAAGGGCGCAGG TCCGTCCTCTCGGTC	
RLOTCSKO139F	TAGGACGGACCTGCGCCCTGGCTCCGC GCTACGGCGCATGCGGA	
RLOTCSKO140R	GCGGCCTTTTTACGGTTCCTGGCCTCTA GACGAACCTCCTCGACCGCATCTGCAA GAG	
RLOTCSKO141F	TGACCGGCGTGATGACGCTGGTAC	Confirmation and sequencing primers
RLOTCSKO142R	GTGCACGGTAAGGATGATCTCGGCG	
RLOTCSKO143F	ACCGTGGCCGAAACCGTGAGGATGT	
RLOTCSKO144R	GGCACCAGGAGACGAGCCTCTACC	
RLOTCSKO145	CTCGAAGAGGCCTTCTCGACATC	
RLOTCSKO146	GACCACGACGAGAACGTGTCGTACGA G	
RLOTCSKO147	TCCTCTCGGTCTCGCGCGGGATTC	
<i>Asven15_3821/22</i>		
RLOTCSKO148	ACGCGAGATGCGGGTCTACACCTA	Protospacer
RLOTCSKO149	AAACTAGGTGTAGACCCGCATCTC	
RLOTCSKO150F	GCTCGGTTGCCGCCGGGCGTTTTTTAT CTAGAGTGAAGCTCTTCCCGTCGGCCC TGGTC	Homology Amplification
RLOTCSKO151R	CAGCGCCGTACGCACGTCAGCTCAGCG TCGCACGAGGCCCGTTCGC	
RLOTCSKO152F	GGGCCTCGTGCGACGCTGAGCTGACGT GCGTACGGCGCTGGCATGCGTA	
RLOTCSKO153R	GCGGCCTTTTTACGGTTCCTGGCCTCTA GACCCGCTGGAACCTCCGACAACCTCAA C	
RLOTCSKO154F	CATGTATTCGCCCAGTTCTTCGAGC	
RLOTCSKO155F	GTCTGTCGCGTTCGTTCAACGCGATG	Confirmation and sequencing primers
RLOTCSKO156R	GGCTTCGACGACGTGAAGGAGG	
RLOTCSKO157R	CCGTCTTCGACGACTACCTCGACG	
RLOTCSKO158F	CTCCCCGTCCATCGTCGAGATCTCC	
RLOTCSKO159R	GGATCTAGCGTTGCTAGCTGATGAG	

RLOTCSKO160R	GCAGGGTGAAGGCGGCGATGATGAC	
<i>Asven15_3862/63</i>		
RLOTCSKO161	ACGCGAGCGACGAGTGTTTCGAGCA	Protospacer set 1
RLOTCSKO162	AAACTGCTCGAACACTCGTCGCTC	
RLOTCSKO161a	ACGCTGTCCTACATGCTTCGCAAG	Protospacer set 2
RLOTCSKO162a	AAACCTTGCGAAGCATGTAGGACA	
RLOTCSKO161b	ACGCCTTGCGAAGCATGTAGGACA	Protospacer set 3
RLOTCSKO162b	AAACTGTCCTACATGCTTCGCAAG	
RLOTCSKO163F	GCTCGGTTGCCGCCGGGCGTTTTTAT CTAGACTTCTACGAGCGGCTGGGTTTC CGTACGACG	Homology Amplification
RLOTCSKO164R	GTTTCATCAGCGGCCACGGCGTCCATG CCTCCAAGGTTATGCGGGCCC	
RLOTCSKO165F	ATAACCTTGGAGGCATGGACGCCGTGG GCCGCTGATGAACGTGTGAAG	
RLOTCSKO166R	GCGGCCTTTTTACGTTTCCTGGCCTCTA GAGGTTATGTGAACAACAGGTCAATG GGTCGTGATCCAG	
RLOTCSKO167F	TCCCGCATGGATGTCCCTTTCTACG	Confirmation and sequencing primers
RLOTCSKO168F	CGTCGAGGATGAGGAATCCTTCAGC	
RLOTCSKO169F	TGGAACGAGGAGAAGGACCCCTCC	
RLOTCSKO170R	GAGTGGCCTTCTTCACGTACTCCGTTC	
RLOTCSKO171F	CTTCGCCACCGACACCGCGTGGTC	
RLOTCSKO172R	CTGGAAGCACGGCATCGAGACGGC	
RLOTCSKO173R	ACCGTGGACAACGTAAAGATCCAGAA C	
<i>Asven15_3934/35</i>		
RLOTCSKO174	ACGCCCCACCTCGGCCGCATCTAT	Protospacer
RLOTCSKO175	AAACATAGATGCGGCCGAGGTGGG	

RLOTCSKO176F	GCTCGGTTGCCGCCGGCGTTTTTTAT CTAGAGTTGCCAGCTTCGGGAAGTAC GGGTC	Homology Amplification
RLOTCSKO177R	AGCAGTGGTGGGGTGCCTACGTGCTCA CCTTCCTGACCTGGGGATATCTGTC	
RLOTCSKO178F	CAGGTCAGGAAGGTGAGCACGTACGC ACCCACCACTGCTACTGTGCGTTG	
RLOTCSKO179F	GCGGCCTTTTTACGGTTCCTGGCCTCTA GAGGAGTTCTCGTACCACTGGGCGCT GTAG	
RLOTCSKO180F	GTTCCAGGAGACGGCGGTGAACG	Confirmation and sequencing primers
RLOTCSKO181F	GACCCTCACCTACCTCGACGACCA	
RLOTCSKO182F	GTCGAGGTTGAAGGCGCTGAGGTC	
RLOTCSKO183R	GCGGTCGATTTCGGTAGTACAGCTG	
RLOTCSKO184R	AGTTCCTCATGAAGAAGATCCTCTTC	
RLOTCSKO185R	GTGTCTGACACTGTGCGGTTGGAC	
RLOTCSKO186R	CTTGAAGGCGAAGCTGAAGGAGTC	
<i>Δsven15_4209/10</i>		
RLOTCSKO187	ACGCCCGCTGTGGCAGTGGGTGTT	Protospacer
RLOTCSKO188	AAACAACACCCACTGCCACAGCGG	
RLOTCSKO189F	GCTCGGTTGCCGCCGGCGTTTTTTAT CTAGACTTCGGCTGGCTGTGGACCTCG CTGAAGGAC	Homology Amplification
RLOTCSKO190R	CCTGACAGAGTGTGAGATGACCTTCTC TGCTCAGGGGGCCGGCTACGTC	
RLOTCSKO191F	GGCCCCCTGAGCAGAGAAGCTCATCTG ACACTCTGTCAGGTATGCGGAGT	
RLOTCSKO192R	GCGGCCTTTTTACGGTTCCTGGCCTCTA GAGAAGTCCTCGGTGGTCTCGCCGAAG TTCC	
RLOTCSKO193F	GCTTCGGCATTCCCTCTCCTCCTC	Confirmation and sequencing primers
RLOTCSKO194F	GTCGCAGTACGTGGAGGAGCAGTACG	
RLOTCSKO195F	GTCGGCTTCGTCTACGCGGTCGTCAG	
RLOTCSKO196R	GAAGTTCTTGTGCTTGCTGAGCTCGTG	

RLOTCSKO197F	CTGGCCAAGGAGAAGCTCCTCGAC	
RLOTCSKO198R	GTGGAGAGGTCGTTCCCGAAGGAC	
<i>Asven15_4209/11</i>		
Protospacer used: RLOTCSKO187/188		
RLOTCSKO199F	GCTCGGTTGCCGCCGGGCGTTTTTAT CTAGAGAACATCTCGGCGGTCTCGCGC TCGTG	Homology Amplification
RLOTCSKO200	GCTCAAGCGGCTCGTGCCGCGGTCCCC AGACTGCCGGTCGGGGACGGTC	
RLOTCSKO201	CGACCGGCAGTCTGGGGACCGCGGCA CGAGCCGCTTGAGCCGCTTGAG	
RLOTCSKO202	CCTGACAGAGTGTGATGAGCGCCCG CTCCCTTGATCCACACCCAC	
RLOTCSKO203	TGGATCAAGGGAGCGGGCGCTCATCTG ACACTCTGTCAGGTATGCGGAGT	
RLOTCSKO204	GCGGCCTTTTTACGGTTCCTGGCCTCTA GAAGGTTCCCGAGATGTTCCGGTAGG TG	
RLOTCSKO205R	GTTTTCCCTACCTGGGGGAGGAGGAG	
RLOTCSKO206F	GCCGTACAGCCCCATGTTCCGAA	Confirmation and sequencing primers
RLOTCSKO207F	GTTTCGGAACATGGGGGCTGTACGGC	
RLOTCSKO208F	CTCATGTGTCACCTTCTGTACGGAC	
RLOTCSKO209R	AGATGCCGGAGCCGAAGTACGTC	
RLOTCSKO210F	CTGGAGCTTGAGGATGCCCTGGAG	
RLOTCSKO211F	GTCGCCCAGGGGAAGAGGAAGATC	
RLOTCSKO212F	CTCCTCCTCCCCAGGTAGGGAAAAC	
RLOTCSKO213R	GCCGTACAGCCCCATGTTCCGAA	
<i>Asven15_4209/10/11</i>		
Protospacer used: RLOTCSKO187/188		
RLOTCSKO214R	CCTGACAGAGTGTGATGAGGTCCCC AGACTGCCGGTCGGGGACGGTC	Homology amplification, in conjunction with 199F and 192R
RLOTCSKO215F	GGTCCCCAGACTGCCGGTCGTCATCTG ACACTCTGTCAGGTATGCGGAGT	

RLOTCSKO216F	CCCTGCTAAAGGGACCGTAAGCAG	Confirmation primer
<i>Δsven15_4373/74</i>		
RLOTCSKO217	ACGCCTGCGGAACTGGCTGTACAA	Protospacer
RLOTCSKO218	AAACTTGTACAGCCAGTTCCGCAG	
RLOTCSKO219F	GCTCGGTTGCCGCCGGCGTTTTTTAT CTAGAGATCCACTCCGTGGTGATCTGC TGGGGCAGTG	Homology Amplification
RLOTCSKO220R	TCGGCTGAACCGGGTCAGACGCACCG ATCGTCACACGTTCCGGCAGGCC	
RLOTCSKO221F	GAACGTGTGACGATCGGTGCGTCTGAC CCGGTTCAGCCGACCCGGGTC	
RLOTCSKO222R	GCGGCCTTTTTACGGTTCCTGGCCTCTA GAGGTTGTCCGGTCACCCCGCCGAGAA AAC	
RLOTCSKO223F	ATGGGCGTACGAGAATCGATCATC	Confirmation and sequencing primers
RLOTCSKO224F	CTTCGGGACGATCACCTTCAGCTGC	
RLOTCSKO225R	GTCACCCACGCGAAAGACAACGG	
RLOTCSKO226F	CACAGGTAGCCGATGGCCACCTTG	
RLOTCSKO227R	ACCTGGTCTTCTTCTACTCCGGGATCA G	
RLOTCSKO228R	AGTCGGAGCTGCGGACACAGAAGG	
<i>Δsven15_5214/15</i>		
RLOTCSKO229	ACGCTGCGGGTGCTGCTCCCCGTA	Protospacer
RLOTCSKO230	AAACTACGGGGAGCAGCACCCGCA	
RLOTCSKO231F	GCTCGGTTGCCGCCGGCGTTTTTTAT CTAGAGCGAGAAGCGGCTGATGCTCG ACCTGC	Homology Amplification
RLOTCSKO232R	GTCTTCCGGAGGTCAGTTCCTTACGGC TTGCGGCCACCGCGCCGAAC	
RLOTCSKO233F	CGGTGGGCCGCAAGCCGTAAGGAACT GACCTCCGGAAGACCGCCGGT	

RLOTCSKO234R	GCGGCCTTTTTACGGTTCCTGGCCTCTA GACCTTCGGCAGCGTGAACATCTCCTC CAGGAG	
RLOTCSKO235F	GCTCGGCATCCTCAACTTCGTCCTG	Confirmation and sequencing primers
RLOTCSKO236F	GAGATGACGACGATCCGGGTGGTG	
RLOTCSKO237F	GACGACACCCTGAAGCGCCTGTG	
RLOTCSKO238R	CGTCTGTGGAGTTCACGCTGTAGACG	
RLOTCSKO239F	CACCATGCGTAAGCTGATCAGGAAC	
RLOTCSKO240R	GTGTAACCGATGTTGAGGTAGTGCTG	
<i>Asven15_5306/07</i>		
RLOTCSKO241	ACGCCTGGCCTGTGTCTCTACTA	Protospacer
RLOTCSKO242	AAACTAGTAGACGACACAGGCCAG	
RLOTCSKO243F	GCTCGGTTGCCGCCGGCGTTTTTAT CTAGACGAGGACATGTTCTGAAGTTC AGCCTGGACGTCC	Homology Amplification
RLOTCSKO244R	GGGGTCCTCACGAAGATCGGGCGTCC AAGGATAGGACGGGCGGGTGGGGTC	
RLOTCSKO245F	CCCGTCCTATCCTTCGACCCCGATCTT CGTGAGGACCCCTAGGGGTC	
RLOTCSKO246R	GCGGCCTTTTTACGGTTCCTGGCCTCTA GACAGGGCGAAGCCGATCAGCATCAC CAG	
RLOTCSKO247F	GCACTACATCCCGGTCCCAACC	Confirmation and sequencing primers
RLOTCSKO248F	CTTCCGGTCGATCCTCTCCGACGAG	
RLOTCSKO249F	GACGGCGACACGAAGGCTCTGGAC	
RLOTCSKO250R	CCATCAGGACGAGATGCCAGAACC	
RLOTCSKO251F	GTGGTCGTGGAGTGCCATCTGCAG	
RLOTCSKO252R	GAGATCGAGTACGTCCTGGTTCAC	
RLOTCSKO253R	GGTGGTTGAGGAAGCCGTTGGAGAC	
<i>Asven15_53049/50</i>		
RLOTCSKO254	ACGCCTGCCGTGCGCGTGATCCTT	Protospacer
RLOTCSKO255	AAACAAGGATCACGCGCACGGCAG	

RLOTCSKO256F	GCTCGGTTGCCGCCGGCGTTTTTTAT CTAGACTTGACGTAACCCGCCTCCTCC AGCAGAC	Homology Amplification
RLOTCSKO257R	CGGCGCTACGCCTCCAGATAGCAAGAT CGTCCGGGCCGTACCGGAAG	
RLOTCSKO258F	TACGGCCCCGACGATCTTGCTATCTGG AGGCGTAGCGCCGGCTCAC	
RLOTCSKO259R	GCGGCCTTTTTACGGTTCCTGGCCTCTA GACGTCGGAGAAAAGGGAGTTGGCCA TGG	
RLOTCSKO260F	ACCTCGTGACGTACGGCTCCCGAC	Confirmation and sequencing primers
RLOTCSKO261F	CTACTTCGTGGTGTCCGAGTGCGT	
RLOTCSKO262F	CGTACAGCTTGTTGTCCGGCGTTCTC	
RLOTCSKO263R	GACGGCCATTTTCGTCATGCCTTTCGAC TTC	
RLOTCSKO264F	TGTTCTGGACGACGCTCGGTTCCGGTG	
RLOTCSKO265R	CGACCGCGTACCTCTCCAGCTTCGC	
<i>Asven15_5558/59</i>		
RLOTCSKO266	ACGCCGCGACGAGCCGTTTCATCTA	Protospacer
RLOTCSKO267	AAACTAGATGAACGGCTCGTCGCG	
RLOTCSKO268F	GCTCGGTTGCCGCCGGCGTTTTTTAT CTAGACCATGACCTTGGCGATACCCC TGAGGA	Homology Amplification
RLOTCSKO269R	TGCGGCTAGGGCTCGATCAGTTCAGC CAGTCCCCCAGCATCTTCCG	
RLOTCSKO270F	TGCTGGGGGACTGGCTGGAAGTTCGATCG AGCCCTAGCCGCAGCCGTAGTCG	
RLOTCSKO271R	GCGGCCTTTTTACGGTTCCTGGCCTCTA GACTCACCAAAGCCAAGGCCCTGTGCT ACATCGTG	
RLOTCSKO272F	TTCGTCGCAGGTCAAAGGGCCTGGATG	Confirmation and sequencing primers
RLOTCSKO273F	GTCTGGAAGAACTCGGCCTGCACAGC	
RLOTCSKO274F	GTGATGATCGGCAGGTAGACCGCCATC	
RLOTCSKO275R	GCCTCCTCACGAGACCTAGACTCAGC	

RLOTCSKO276F	AGGATGATCGCACCCGAACCTCGATCAG	
RLOTCSKO277R	CAGGGAGACGACTCCTTGGCAAACCTG	
<i>Δsven15_0672/73</i>		
RLOTCSKO278	ACGCCCCCTGGGGTCAGGAGCTT	Protospacer
RLOTCSKO279	AAACAAGCTCCTGACCCCAAGGGGG	
RLOTCSKO280F	GCTCGGTTGCCGCCGGGCGTTTTTAT CTAGAACGCCGCCGAAGAAGATCCCG ACCTCG	Homology Amplification
RLOTCSKO281R	AGGGCCGTTCCAGCCAGCCATTCCATG TCCGCCACGCTAACCGGACC	
RLOTCSKO282F	TTAGCGTGGCGGACATGGAATGGCTGG GCTGAACGGCCCTCCTGGGCCGTGTC	
RLOTCSKO283R	GCGGCCTTTTTACGGTTCCTGGCCTCTA GAGAGGACCTGGAGTGCTGGAGCTTCC TC	
RLOTCSKO284F	CTTCGGGCTGGTCTCCTTCGAGGTG	Confirmation and sequencing primers
RLOTCSKO285F	CTTGAGCTGACCGTCGACGACGAG	
RLOTCSKO286F	GTTCGGCGTGGGTGTGACGAGCGAG	
RLOTCSKO287R	ACATCGTCGAGGCACACCCGACGTAC	
RLOTCSKO288F	CTCGCTTGAGATCAGTGTGCACGGATC	
RLOTCSKO289R	GGTTCTCGACGAGTTCGAGGGACAC	
<i>Δsven15_3148/49</i>		
RLOTCSKO290	ACGCGGCTTCCGCGTCACGGCCAT	Protospacer
RLOTCSKO291	AAACATGGCCGTGACGCGGAAGCC	
RLOTCSKO292F	GCTCGGTTGCCGCCGGGCGTTTTTAT CTAGACTCCTCATGGACGTCCTGAAGG TGCTCGCG	Homology Amplification
RLOTCSKO293R	CTGTTTCGTACGGCGGTGTCACATCGTG CGTGCCCTTCGGATCTCTGCGCGTG	
RLOTCSKO294F	TCCGAAGGGCACGCACGATGTGACAC CGCCGTACGAACAGCTGACCTCAGACG	
RLOTCSKO295R	GCGGCCTTTTTACGGTTCCTGGCCTCTA GAGGCTGGCGCTGGTCCTTCTACATCA ACCTG	

RLOTCSKO296F	AGCACGACTGGGTCCACAACGACTAC	Confirmation and sequencing primers
RLOTCSKO297F	GACGATCATGAACGATCTCGACC	
RLOTCSKO298F	GGTCATGATCAACACCCGGACCGAGTG	
RLOTCSKO299R	GTGATGGCGATCATCGGGCAGCTCATC	
RLOTCSKO300F	TGGATCCGATCGCGCTGCTCAAG	
RLOTCSKO301R	CAGCACCGGCAAGTACAAGATCTTC	
<i>Δsven15_3785/86</i>		
RLOTCSKO302	ACGCTCGTGACGACCGTTCTCATC	Protospacer
RLOTCSKO303	AAACGATGAGAACGGTCGTCACGA	
RLOTCSKO304F	GCTCGGTTGCCGCCGGGCGTTTTTAT CTAGACCGACCACCTGATCGTCATCGG CAAGG	Homology Amplification
RLOTCSKO305R	TCGCGCTCCTTGCGGGTCGGGTGATCA TCTCCTCATACTCCCGGCG	
RLOTCSKO306F	ACGTATGAGGAGATGATCACCCGACCC GCAAGGAGCGCGAAAGGGTTC	
RLOTCSKO307R	GCGGCCTTTTTACGGTTCCTGGCCTCTA GAGAGACTTTGAAGCCGTGACGCCAGT CATGG	
RLOTCSKO308F	ACCGTGCCCGCGCTGTTGCTCAAG	Confirmation and sequencing primers
RLOTCSKO309F	GTCGTCCAGGAAGCCCTGACGAACAC	
RLOTCSKO310F	CGTGAAGGGCTTCTCGCTCGGCATG	
RLOTCSKO311R	GCACTACGAGTAAAGATGCTCGTTTCG	
RLOTCSKO312F	TCGACACCGTCATCCTCACCTGTAC	
RLOTCSKO313R	GAGAGTAGGACGCCGCCGAACAATC	
RLOTCSKO314R	AGAACGTCGTGAGACAGTTCGGTC	
<i>Δsven15_4474/75</i>		
RLOTCSKO315	ACGCATCCGCCGCACGGACCAGTT	Protospacer
RLOTCSKO316	AAATAACTGGTCCGTGCGGGCGGAT	
RLOTCSKO317F	GCTCGGTTGCCGCCGGGCGTTTTTAT CTAGACTGCCGTGAACTCGACGTCCTC GCGGAC	Homology Amplification
RLOTCSKO318R	CTCACGCTTCTCCACCTCGTCTGTTCG ATTCGGCCGTCCGAGTTCG	

RLOTCSKO319F	GGACGGCCGAATGCGACAGACGAGGT GGAGGAAGCGTGAGGCGCCGCACTTA C	
RLOTCSKO320R	GCGGCCTTTTTACGGTTCCTGGCCTCTA GAGTCTACCGGGCGATCGGAACCCTGG TAATCGTC	
RLOTCSKO321F	CGACTGTCACAGGCGTGTACAGG	Confirmation and sequencing primers
RLOTCSKO322F	GTACCCGTACCACCTGTTCTGGCAG	
RLOTCSKO323F	GCTGTTCGTGGCGGAGGGGATCTTCG	
RLOTCSKO324R	GGAAGATCAGACGCATCGTGTTCGCGG AG	
RLOTCSKO325R	GCAAGCTCAACGAGTACCCGACCGAG	
RLOTCSKO326F	CACCAGCATGGTCCGCTGGAGCTC	
RLOTCSKO327R	CAGCAGCAGATGCACGAGGACGAGGA C	
<i>Asven15_4861/62</i>		
RLOTCSKO328	ACGCGAGGACGAGGGTCCCGGCAT	Protospacer
RLOTCSKO329	AAACATGCCGGGACCCTCGTCCTC	
RLOTCSKO330F	GCTCGGTTGCCGCCGGCGTTTTTTAT CTAGACTTCCTCGTGGGCACGGTCTAT CTCG	Homology Amplification
RLOTCSKO331R	GGTCCGGTTCGAACCCTACGGCTATCC AGGAGTTATCCGGGACGGAC	
RLOTCSKO332F	CCGGATAACTCCTGGATAGCCGTAGGG TTCGAACCGGACCGGCTCGTTC	
RLOTCSKO333R	GCGGCCTTTTTACGGTTCCTGGCCTCTA GAGTGAAGTCCTCCATCGTCAGCTTGC CCAC	
RLOTCSKO334F	GGGTACGGACGGAAGAGATCCCCGTT G	Confirmation and sequencing primers
RLOTCSKO335F	GCTACATCACGATCTTCGCGATGATC	
RLOTCSKO336F	GTCCTGCTGTTCGCGCTTGCGGTG	
RLOTCSKO337R	GACCTTCGAGATGCCAGCTTGTTTCAG	
RLOTCSKO338F	CATGTCAGACCCGTGACCCTCGAC	

RLOTCSKO339R	GATCCGGTTGTCTGAAGAGCAGCTTCAC	
<i>Δsven15_4999/5000</i>		
RLOTCSKO340	ACGCACGACGCCCGTGCCACACCT	Protospacer
RLOTCSKO341	AAACAGGGTGGGCACGGGCGTCGT	
RLOTCSKO342F	GCTCGGTTGCCGCCGGGCGTTTTTTAT CTAGAACACGAGGTGTACTTGCGCTCG ATGAAG	Homology Amplification
RLOTCSKO343R	GGGGCCGCCCTTCGGATTCACAGCACC TTGATCATGCCGACCAGCCTAG	
RLOTCSKO344F	TCGGCATGATCAAGGTGCTGTGAATCC GAAGGGCGGCCCTAGCGGAGCAGCA C	
RLOTCSKO345R	GCGGCCTTTTTACGGTTCCTGGCCTCTA GAGTCCCCTCGTACAAGCGGCTCACCC TGATG	
RLOTCSKO346F	AATCCGGGTCAGGCTAGCAGCACG	Confirmation and sequencing primers
RLOTCSKO347F	GGATGGAACGCGAACAGGCGGCG	
RLOTCSKO348F	CTTGTCCTTCTCGTAGACGAGTTC	
RLOTCSKO349R	GAACTCGGCTGGACCGACTCCGTC	
RLOTCSKO350F	GAAGGCGTTGTAGTCGACCTCGAT	
RLOTCSKO351R	AGTACGTCGAGCGGCTGTACGTG	
<i>Δsven15_6686/87</i>		
RLOTCSKO352	ACGCGTGTCCCTGGTGGCCTTCAT	Protospacer
RLOTCSKO353	AAACATGAAGCGCACCAGGGACAC	
RLOTCSKO354F	GCTCGGTTGCCGCCGGGCGTTTTTTAT CTAGACGTCCAGTACCGAGATCAGCCG CTCACG	Homology Amplification
RLOTCSKO355R	CCCCGCGGCGGTCAGTCCTCGGTGTCG ATGCTACGAGCCGGCGCGTATCG	
RLOTCSKO356F	CGGCTCGTAGCATCGACACCGAGGACT GACCGCCGCGGGGCCAGGCC	
RLOTCSKO357R	GCGGCCTTTTTACGGTTCCTGGCCTCTA GACATGACGCTAGGGCCGAAGGACCC GAGAGGTC	

RLOTCSKO358R	CTTGACGCGGTCTCGGTTTCGTAC	Confirmation and sequencing primers
RLOTCSKO359F	CTACGCCGGATTCCTGATGCTGGC	
RLOTCSKO360F	GTGCCTCCCGCCAGTACGTGAAGAAGC	
RLOTCSKO361R	CATGACCGTCTTCTTGCCGAGGGTC	
RLOTCSKO362F	CGGCTGTCTGAAGGACGGCACCTTC	
RLOTCSKO363F	ACTCCATCCAGAAGTCCAGGGTGTC	
RLOTCSKO364R	TCGCACGATCTCGTACGGGAGCTG	
<i>Asven15_7022/23</i>		
RLOTCSKO365	ACGCCTGAAGGAGAGCTCCGGATG	Protospacer
RLOTCSKO366	AAACCATCCGGAGCTCTCCTTCAG	
RLOTCSKO367F	GCTCGGTTGCCGCCGGCGTTTTTAT CTAGAGTTCCGCGTGTTCACGGATGC CGTGA	Homology Amplification
RLOTCSKO368R	CGTGCCGGACACACCCATGCGTCGCTT CCATCGGGGGTGATC	
RLOTCSKO369F	TGGAAGCGACGCATGGGTGTGTCCGGC ACGTCCGGCACGTAG	
RLOTCSKO370R	GCGGCCTTTTACGGTTCCTGGCCTCTA GATGTCCAGGAGGGGTTGGTGTGGT GATC	
RLOTCSKO371F	GTGCACCAGCGTGGAGATGGAG	Confirmation and sequencing primers
RLOTCSKO372F	TGTCCTTCGCGAACCATCCCGAG	
RLOTCSKO373F	GTGTGGCGTCGTGATGCAAGGGACGGT CTC	
RLOTCSKO374R	AGTGCTGGAGCCGGTCTTGATGCCGAC GAC	
RLOTCSKO375F	GTCGGCTGTGTATCGGGCGTGTATC	
RLOTCSKO376F	GTCATCCTTGAGGAGCACCCGCTGAAG	
<i>Asven15_7155/56</i>		
RLOTCSKO377	ACGCGCACGCGGGCGCGTCCGGTT	Protospacer
RLOTCSKO378	AAACAACCGGACGCGCCCGCGTGC	
RLOTCSKO379F	GCTCGGTTGCCGCCGGCGTTTTTAT CTAGAGTCTGGACATCCGGCACACCG ACTGCGGAG	Homology Amplification

RLOTCSKO380R	CGCCGAGACCAGACCGGTCATCGGAC CCGGGGTGTACGACCG	
RLOTCSKO381F	CCGGGTCCGATGACCGGTCTGGTCTCG GCGCACTGACGGCCGCGTA	
RLOTCSKO382R	GCGGCCTTTTTACGGTTCCTGGCCTCTA GAATGGAACCGTACTGTTGCGGTGGAT GTCTCTG	
RLOTCSKO383F	CTTCTCTTCTTCTGGTGGTCCCAG	Confirmation and sequencing primers
RLOTCSKO384F	CAAGACCTATGTGACCAGGCTGCTG	
RLOTCSKO385F	GCTACGAGTACCGGCTCACCGCCAAGG	
RLOTCSKO386F	CACTCCAGCACATAGCGCACTTTTACC	
RLOTCSKO387R	CGATGGGATCACCTCATCCAAGC	
RLOTCSKO388R	CGTCTGACGAAGATCGACCTG	
<i>Asven15_7219/20</i>		
RLOTCSKO389	ACGCGCCGACGACTACCTGACCAA	Protospacer
RLOTCSKO390	AAACTTGGTCAGGTAGTCGTCGGC	
RLOTCSKO391F	GCTCGGTTGCCGCCGGCGTTTTTTAT CTAGAGGTCTTCAGCGTGCGGTACATC GGCTC	Homology Amplification
RLOTCSKO392R	CTGACGGGTCGCGACGACCCCTGTGTA TCCGAAAGGGACCTTTC	
RLOTCSKO393F	GGATACACAGGGGTCGTCGCGACCCGT CAGGGTCAGATCAGG	
RLOTCSKO394R	GCGGCCTTTTTACGGTTCCTGGCCTCTA GACAACTGGCAGGGGAACGTCCAGTA CTTC	
RLOTCSKO395F	CTTCTCTCAGCGGTTTCGTTTACAC	Confirmation and sequencing primers
RLOTCSKO396F	GTCTGGTCCACAACCTCGTGGTGAAC	
RLOTCSKO397F	GTGTACTCCTCGTCGACGTCGAAC	
RLOTCSKO398R	TGTACGACGTCGACCCCTACGAGTAC	
RLOTCSKO399R	ACATCTGTCTGCTCGATCCACCGAAG	
RLOTCSKO400F	CTGCCAGTTGTCCTGCACGGTGAT	
<i>Asven15_5396</i>		
RLOTCSKO401	ACGCGGTGCCTTCTTCGTGGCGAT	Protospacer

RLOTCSKO402	AAACATCGCCACGAAGAAGGCACC	
RLOTCSKO403F 1	GCTCGGTTGCCGCCGGGCGTTTTTAT CTAGAGACGAGGAGACAGACGGTGGAGGGTTC	Homology Amplification
RLOTCSKO404R 1	CATCCACTCCTCCATGTCCACCTGTAC CGTCCCCCACC	
RLOTCSKO405F 2	ACGGTACAGGTGGACCTGTCCGGTCATG GAGGAGTGGATG	
RLOTCSKO406R	GCGGCCTTTTTACGGTTCCTGGCCTCTA GACGAAACGATCCGTGACGGAGCGTC AGC	
RLOTCSKO407F	CTGGTTGGGTGGCGGTGAAACACTG	Confirmation and sequencing primers
RLOTCSKO408F	GATCGTCCTGATGGACATCATGATG	
RLOTCSKO409F	GTGCCGATGAAGACCTCGAAGGGGTC C	
RLOTCSKO410R	CTCACCCGTCGTGTCGTCCTTGC	
RLOTCSKO411R	CACCCTTCTGGCAACAGTCCGTCAG	
RLOTCSKO412F	ATGGTGCAGAAGGCCAAGATCCTC	
<i>Asven15_4924/25</i>		
RLOTCSKO413	ACGCAGCGGAATGATCTCCTTCAT	Protospacer
RLOTCSKO414	AAACATGAAGGAGATCATTCCGCT	
RLOTCSKO415F	GCTCGGTTGCCGCCGGGCGTTTTTAT CTAGAGTCCTCGTCCGGATCCAGAACG ACCTCTC	Homology Amplification
RLOTCSKO416R	GTTGTCCCCCTAGACTCTCACCCGTTT ATCCAACACGCCCCG	
RLOTCSKO417F	GATGAACGGGTGAGAGTCTAGGGGGA CAACGGCGACGTTGGT	
RLOTCSKO418R	GCGGCCTTTTTACGGTTCCTGGCCTCTA GATTCTTCAGCTTGCGCAGCTGGTTGA AGTTG	
RLOTCSKO419F	TGACGAGCTGCCCTACATCGTTTCGAC	Confirmation and sequencing primers
RLOTCSKO420F	TCGAAGCTGGGCGAGGGGCTGTCGAA C	

RLOTCSKO421F	CAAGACGGATCTGCGGATCTCGGCCTA C	
RLOTCSKO422R	GTCCTCCACCAGGTCGTAGCAGGACTG	
RLOTCSKO423R	CTTGAGTGCTCAACGGTGCTCCTCAAG	
RLOTCSKO424F	GACAAGGGCATCAAGA ACTACGACGT C	
Chapter 4: Exploring purification methods of a full-length SK primers		
RL001F	<i>ccatgg</i> ATAGGCGCCCCGGTCTGAG	<i>vanS</i> amplification forward primer with <i>NcoI</i> overhang for N- terminal His tag
RL002R	<i>aagctt</i> TCACCTGCCGGTGTGCGGA	<i>vanS</i> amplification reverse primer with <i>HindIII</i> overhang for N- terminal His tag
RL003F	<i>catatg</i> GATAGGCGCCCCGGTCTGA	<i>vanS</i> amplification forward primer with <i>NdeI</i> overhang for C- terminal His tag
RL004R	<i>aagctt</i> CCTGCCGGTGTGCGGAGCGG	<i>vanS</i> amplification reverse primer with <i>HindIII</i> overhang for C- terminal His tag
RL029F	<i>aattcatatg</i> <u>CATCATCATCATCATGAT</u> AGGCGCCCCGGTCTGAGCGTC	<i>vanS</i> amplification forward primer

		with <i>NdeI</i> and hexa-His overhang for N-terminal His tag
RL030R	ttaaaagctfTCACTCCCTGCCGGTGTGCGG AGC	<i>vanS</i> amplification reverse primer with <i>HindIII</i> overhang for N-terminal His tag
RL032F	aattcatatgGATAGGCGCCCCGGTCTGAGC GTC	<i>vanS</i> amplification forward primer with <i>NdeI</i> overhang for C-terminal His tag
RL033R	ttaaaagctfTCAATGATGATGATGATGATG CTCCCTGCCGGTGTGCGGAGCGGC	<i>vanS</i> amplification reverse primer with <i>HindIII</i> and hexa-His tag overhang for C-terminal His tag
Chapter 5: Rewiring TCSs; A SK jigsaw puzzle		
Confirmation primers for <i>chim1</i> and <i>chim2</i> into pAU3-45		
RL005F	TCTAGAGACAGCCGTCTCCGAGCC	Forward amplification of <i>chim1</i> and <i>chim2</i>
RL006R	GTGGTGGTGGTGGTGGACCTGTC	Reverse amplification of <i>chim1</i>

RL007R	GTGGTGGTGGTGGTGCCTGC	Reverse amplification of <i>chim2</i>
pAU3-45F	GTAACGCCAGGGTTTTCCAGTCACGAC	Sequencing primers
pAU3-45R	GAGCGGATAACAATTTACACAGGAAACAGCTATGAC	
Confirmation primers for <i>chim3</i> , <i>chim4</i> and <i>chim5</i> in pMS-82		
pMS82F	GCAACAGTGCCGTTGATCGTGCTATG	Amplification in empty vector should yield ~350 bp
pMS82R	GCCAGTGGTATTTATGTCAACACCGCC	
Cloning cytoplasmic regions of chimeras and also RR into pGS-21a		
RL0025F	aattcatatgCATCATCATCATCATGTGCTTCCCTGTTGCTGATCGAGG	N-Terminal His tagged <i>afsQ1</i> (<i>NdeI</i>)
RL0026R	aattaagcttTCACTGAGGCGGATCCAGCCGTA	N-Terminal His tagged <i>afsQ1</i> (<i>HindIII</i>)
RL0027F	aattcatatgCCTTCCCTGTTGCTGATCGAGGAC	C-Terminal His tagged <i>afsQ1</i> (<i>NdeI</i>)
RL0028R	ttaaaagcttTCAATGATGATGATGATGATGCTGAGGCGGATCCAGCCGGTAGAC	C-Terminal His tagged <i>afsQ1</i> (<i>HindIII</i>)
RL0035F	aattcatatgCATCATCATCATCATGGCGAGGGGAAGCTGGACAC	c-Chim1 (<i>afsQ2</i>) N-terminal His tag (<i>NdeI</i>)
RLO036R	aattgaattcTCAGACCTGTCCCTTCGCGTCC T	c-Chim1 (<i>afsQ2</i>) N-terminal His tag (<i>HindIII</i>)
RLO037F	aattcatatgCATCATCATCATCATGGATCCCTCTCCCACCGCAT	c-Chim2-5 N-terminal His tag (<i>NdeI</i>)

RLO038R	aattgaattcTCACCTGCCGGTGTGCGGAGC GG	c-Chim2-5 N- terminal His tag (<i>Hind</i> III)
RLO039F	aattcatatgGGCGAGGGGAAGCTGGACAC	c-Chim1 (<i>afsQ2</i>) C- terminal His tag (<i>Nde</i> I)
RLO040R	aattgaattcTCAATGATGATGATGATGATG GACCTGTCCCTTCGCGTCCT	c-Chim1 (<i>afsQ2</i>) C- terminal His tag (<i>Hind</i> III)
RLO041F	aattcatatgGGATCCCTCTCCCACCGCAT	c-Chim2-5 C- terminal His tag (<i>Nde</i> I)
RLO042R	aattgaattcTCAATGATGATGATGATGATG CCTGCCGGTGTGCGGAGCGG	c-Chim2-5 C- terminal His tag (<i>Hind</i> III)
RLO049F	aattcatatgCATCATCATCATCATCGT GTGCTGATTGTCGAGGAC	<i>vanR</i> N-terminal His tag (<i>Nde</i> I)
RLO050R	ttaagaattcCTATCCACCGTCGCCGCCCGC CTG	<i>vanR</i> N-terminal His tag (<i>Hind</i> III)
RLO051F	aattcatatgCGTGTGCTGATTGTCGAGGAC GAGCCC	<i>vanR</i> C-terminal His tag (<i>Nde</i> I)
RLO052R	aattgaattcCTAATGATGATGATGATGATG TCCACCGTCGCCGCCCGCCTG	<i>vanR</i> C-terminal His tag (<i>Hind</i> III)
RLO144R	TTGTAGAAGCGGTCTGAAGAC	Confirmation primers for cloning cytoplasmic chimeras into pGS-21a
RLO144aR	AGGGACATGTCGACCTGTTC	
RLO145R	AACTGCTTCCTGGTCAACGC	
RLO146R	GTTCTTCGTCACGGTCATCG	
RLO147F	TAATACGACTCACTATAGGGGAAT	
N-terminal 3X FLAG tag of <i>afsQ1</i> in <i>S. venezuelae</i> wild-type		
RLOCC007	ACGCGCCTTTTCTGTTGCTGATCG	Protospacer
RLOCC008	AAACCGATCAGCAACAGAAAAGGC	Protospacer

RLOCC009F	GCTCGGTTGCCGCCGGCGTTTTTTAT CTAGAGAATGCTTCACACTGGTGTCCC GTG	Upstream homology arm with homology to pCRISPomyces- 2 vector and <i>3XFLAG</i>
RLOCC010R	GTCCTTGTAGTCCATTCTGTCGCATTCTG GCCGTCC	
RLOCC011F	TGCGACAGAATGGACTACAAGGACCA CGACGGCGAC	<i>3XFLAG</i> amplification with homology to homology arms
RLOCC012R	GTCGTCTTCGATCAGCAACAGAAAAGG CACGGGCAGCTTGTCGTCATCGTCCTT GTAGTC	
RLOCC013F	CTTTTCTGTTGCTGATCGAAGACGACG ACGCCATCC	Downstream homology arm with altered PAM sequence and homology to <i>3X FLAG</i> and pCRISPomyces- 2 vector
RLOCC014R	GCGGCCTTTTTACGGTTCCTGGCCTCTA GATTCTCCATGGCGATCGACAGACCG	
RLOCC017F	CGACTGTCACAGGCGTGTACAGG	Confirmation primers
RLOCC018R	CTGGAGGTCCTCGCCGTTCTTGGTG	
RLO102F	GCGCCTCGACGACTTCTACAAGGA	
RLO103F	TTCGGTCCGTGTGCCAAGAAGCTT	
RLO104F	CTCGCCGACGCTCATCCGTACCGT	
RLO105R	CTCACGGTTCAGCCAGTACGCGAT	
RLO106R	CACCGGGACCGTGGTCGTCCTGAT	
M145 Δ <i>afsQ2</i> generation		
RLO061	ACGCCGTGCCCGAGTCGCTGCGCA	Protospacers
RLO062	AAACTGCGCAGCGACTCGGGCACG	
RLO066F	TCGGTTGCCGCCGGCGTTTTTTATCTA GACCTGATACACCCCGGCTCGAAACT TT	Homology amplification

RLO067R	CGGCGTACGGTCATTCACTGAGGCGGA TCCAGCCGGTA	
RLO068F	GATCCGCCTCAGTGAATGACCGTACGC CGTCTGCCGGCC	
RLO069R	GCGGCCTTTTTACGGTTCCTGGCCTCTA GATACGTCTTTCACCAGGCCGTACGGG	
RLO0129F	TTCGGCGATGACCGTGACGAAGAA	Confirmation
RLO0130F	ACGTCTTCGACCGCTTCTACAAGGCGA	
RLO0131R	GACGAGCCGCACAGCAGGAACACC	
RLO0132R	AGGATCTCCACACCGGTCTGACC	
RLO0133R	GATCTCCACACCGGTCTGACCGTC	
RLO0134F	CGCTCCCTTTCCACCCCCGTGGAT	
RLO0135R	CCGCAAGATCTCCACACCGGTCTG A	
Sliv Δ <i>afsQ2</i> generation		
Same as M145 Δ <i>afsQ2</i> protospacers		Protospacers
RLOCC003F	GCTCGGTTGCCGCCGGCGTTTTTAT CTAGATCCTCGGTCGGTACTCGTTGA GC	Homology amplification
RLOCC004R	ACTACCGCCACCGCCAGAGCCACCTCC GCCTGAACCGCCTCCACCGTCACTGAG GCGGATCCAGCC	
RLOCC005F	GGTGGAGGCGGTTTCAGGCGGAGGTGG CTCTGGCGGTGGCGGTAGTGTCTGATG ACCGTACGCCGTCTGC	
RLOCC006R	GCGGCCTTTTTACGGTTCCTGGCCTCTA GAGGTACGTCTTTCACCAGGCCGTAC	
RLOCC006aR	GAACACTTCCTGTACACGGATGC	Confirmation primer
Sven Δ <i>afsQ2</i> generation		
RLOCC019	ACGCCAAGTCGCTGGCGGCCGAGA	Protospacer set 1
RLOCC020	AAACTCTCGGCCGCCAGCGACTTG	
RLOCC021	ACGCGCGCAGCCGCGTGAGGATGC	

RLOCC022	AAACGCATCCTCACGCGGCTGCGC	Protospacer set 2
RLOCC023F	GCTCGGTTGCCGCCGGCGTTTTTAT CTAGAAGTAGCGCAGCACCAGCATGG TCC	Homology amplification
RLOCC024R	ACGCCCGTAAGTGCGGCGCCTCACTCA CGCAGGGACGTCCAGCCGGTA	
RLOCC025F	TACCGGCTGGACGTCCCTGCGTGAGTG AGGCGCCGCACTTACGGGCGTAC	
RLOCC026R	GCGGCCTTTTTACGGTTCCTGGCCTCTA GACATCGTGTTTCGCGGAGATGCCGAAG	
RLOCC027F	GTGAGGTGGTAGGCGGTGGCGTAC	
RLOCC028F	ATCGAGGACGACGACGCCATCCGC	Confirmation and sequencing primers
RLOCC029F	GAGCACGACTACCTCGGGACTCG	
RLOCC030R	GAACGTGCAGACCAGCTGCGAGAGC	
RLOCC031F	GGAGGGCACGCTGCGGCTGA	
RLOCC032F	CAGGATCTCCGCGATCTCCGGATC	
RLOCC033R	ATCCACAGTCCGAGGTAGACCAGG	
RLOCC034R	TCAACGAGTACCCGACCGAGGAG	
RLOCC035F	CCTCGTGACGGACGCGTGATCGG	
RLOCC036F	CTAGGCCCCCGTTTCCCCCGTGAG	
RLOCC037R	CAGGCCACCCAGAACCTCCCGCTC	
qRT-PCR primers		
RLO161F	ATGCTCTTCTGGACCTCATCCAG	<i>hrdB</i>
RLO162R	GATCCACCAGGTGGCGTACGTGG	
RLO163F	ACGAGTACCCGACCGAGGAACTG	<i>sigQ</i>
RLO164R	GTAGTAGCGCAGGACCAGCATG	
RLO165F	GCATCGACAAGCTCACGGAACTC	<i>redZ</i>
RLO166R	GTGCACCAGTTCTTCGACCGAC	
RLO167F	AGCAATATCGCGCACCTGGAAGAG	<i>actII-ORF4</i>
RLO168R	GGTCTCGTTCAGCGGATGCG	

2.1.2 Growth of strains and storage

Liquid cultures of *E. coli* were routinely grown in 10-50 ml of Lennox broth at 250 rpm at 37°C unless otherwise stated. Liquid cultures of *S. coelicolor* (10-50 ml) were grown at 30°C, shaking at 250 rpm with specific media recipes given in later sections if applicable and aerated through use of springs or glass beads. Cultures grown on solid media were grown at the same temperatures listed above, unless otherwise stated. Where necessary, cultures were supplemented with antibiotics at concentrations listed in Table 2.5. Solid cultures of *Streptomyces* strains used for biomass isolation were grown on top of sterile cellophane discs, covering the media, which allow the organisms to grow while facilitating simple harvesting of the mycelium.

Table 2. 4: Culturing media used throughout study.

Media	Composition (g/L of media)
Lennox Agar	10 g Tryptone 5 g NaCl 5 g Yeast extract dH ₂ O –made to 1 L
For Solid media	15 g Agar
Soya Flour Media (SFM)	20 g Soya flour 20 g Mannitol 20 g Agar dH ₂ O –made to 1 L
Malt Yeast Maltose media (MYM)	4 g Maltose 4 g Yeast extract 10 g Malt extract 50/50 tap water/ dH ₂ O made to 1 L pH 7.3 – 7.4 2 ml R2 trace elements ^{*/**}
For Solid media	Agar 20 g
Minimal Media (MM)	0.5 g L-asparagine 0.5 g K ₂ HPO ₄

	0.2 g MgSO ₄ .7H ₂ O
	0.01 g FeSO ₄ .7H ₂ O
	10g Glucose**
	dH ₂ O made to 1 L
	pH 7.0 - 7.2
For Solid media	10 g agar
MM with 10 mM Glutamate	1.69 g Monosodium glutamate
	0.5 g K ₂ HPO ₄
	0.2 g MgSO ₄ .7H ₂ O
	0.01 g FeSO ₄ .7H ₂ O
	10g Glucose**
	dH ₂ O made to 1 L
	pH 7.0 - 7.2
For Solid media	10 g agar
MM with 75 mM Glutamate	12.68g Monosodium glutamate
	0.5 g K ₂ HPO ₄
	0.2 g MgSO ₄ .7H ₂ O
	0.01 g FeSO ₄ .7H ₂ O
	10g Glucose**
	dH ₂ O made to 1 L
For Solid media	pH 7.0 - 7.2
	10 g agar
2X YT	16g Difco bacto tryptone
	10g Difco bacto yeast extract
	5g NaCl
	dH ₂ O made to 1 L
TSB	30g Oxoid tryptone soya broth powder
	dH ₂ O made to 1 L
YEME	3g Difo yeast extract
	3g Oxoid malt extract
	5g Difco bacteriological peptone
	10g Glucose

340g Sucrose
dH₂O made to 1 L

*R2 trace elements: Per 1L, 40 mg ZnCl₂, 200 mg FeCl₃.6H₂O, 10 mg CuCl₂.2H₂O, 10 mg MnCl₂.4H₂O, 10 mg Na₂ B₂O₇.10H₂O and 10mg (NH₄)₆Mo₇O₂₄.4H₂O
**added after autoclaving

Table 2. 5 Antibiotics and concentrations used throughout study.

Antibiotic	Stock concentration (mg/ml)	Working concentration (µg/ml)	Overlay (mg/ml)
Ampicillin	100	100	
Apramycin	50	50	1.25
Chloramphenicol	30	30	
Hygromycin	50	25	1.25
Kanamycin	50	50	
Nalidixic acid	25	25	0.5
Thiostrepton	50	50	
Vancomycin	10	0.5-100*	

*For activation of chimeras 0.5 -100µg/ml was used depending on *Streptomyces* sp. To select for vancomycin resistance 10µg/ml was used.

2.1.3 Preparation of *Streptomyces* spores

Spores from a single colony were streaked out on agar plates, either using a loop or a sterile cotton bud to form a confluent lawn. *S. coelicolor* and *S. lividans* were grown on SFM agar for 5 days, typically before harvesting spores, *S. venezuelae* was grown on MYM-tap for 2-3 days and *S. formicae* on MYM-tap for 9 days. Spores were harvested by adding 2-3 ml of 20% glycerol (2G) to the plate and sloughing off the spores with a sterile cotton bud. The spores were filtered through the loosened cotton of the cotton bud. Spore stocks were stored at -20°C and -80°C.

2.1.4 Glycerol stocks

Glycerol stocks of *E. coli* were produced by taking 1 ml of *E. coli* overnight culture, pelleting cells and resuspending it in 1 ml of fresh, sterile, 1:1 Lennox, 40% glycerol (4G) mix. Glycerol stocks were stored at -20°C and 80°C.

2.1.5 Centrifugation

All DNA/RNA centrifugation steps were carried out using a benchtop Eppendorf Centrifuge 5424 where max speed is 14680 rpm. To concentrate *E. coli* cells of volumes 5-50 ml in falcon tubes, an Accuspin 1R with a Ch. 007379 rotor (Fisher scientific) at 4,000 rpm unless otherwise stated. To concentrate 1 L *E. coli* cultures, a Beckman Avanti J-20 centrifuge with JLA8.1000 rotor was used at 6000 rpm. For ultracentrifugation steps, the Beckman optima XL100k centrifuge was used with a Ti-40 fixed angle centrifuge at 42000 rpm.

2.2 Genetic Manipulation

2.2.1 DNA/RNA preparation

2.2.1.1 Plasmid preparation

Plasmid DNA was isolated with the Qiagen miniprep kits using 3-10 ml of overnight culture following manufacturers protocol. Exceptions include incubating matrix with PE buffer for 5-10 mins and elution with 50 µl of heated (50-65°C) water.

2.2.1.2 Cosmid Preparation

Cosmid DNA was isolated in two ways: either with the use of phenol chloroform or through the Promega wizard prep kit. The use of the latter method was carried out following the manufacturer's protocol.

For phenol extractions, 1-3 ml of *E. coli* overnight cultures were pelleted using a bench top centrifuge at 14680 rpm for 30 s. Pellets were resuspended in 100 µl of solution I (50 mM Tris-HCl, pH8; 10 mM EDTA) before the addition of 200 µl of solution II (200 mM NaOH; 1% SDS) and mixed through inversion. Solution III (150µl; 3 M potassium acetate, pH 5.5) was then added and again

mixed by inversion. Samples were centrifuged at full speed (Centrifuge 5424) for 5 mins at room temperature (RT). The supernatant was extracted and vortexed for 2 mins with 400 µl phenol/chloroform. This was followed by centrifugation, as above, for 5 mins. The upper aqueous phase was transferred to a fresh tube and a further cleaning step through addition of a further 400 µl of phenol/chloroform and vortexing before centrifugation as described. After removal of the aqueous phase, DNA was precipitated by mixing with 600 µl of iso-propanol and incubated on ice for 10 mins. Tubes were then centrifuged (as before) and pellets were washed in 70% ethanol before a further centrifugation step to pellet DNA. The sample tubes containing DNA pellets were left open at RT to dry before resuspension in 50 µl dH₂O heated to 50°C. Cosmids were then stored at -20°C.

2.2.1.3 *Streptomyces* genomic DNA preparation

Streptomyces cultures were grown overnight in a mixture of 50% TSB / 50% YEME media at 30°C shaking at 200 rpm. Cells were isolated by centrifugation at 14680 rpm for 30 s (0.5-2 ml culture). The pellet was resuspended in 500 µl Solution I (50 mM Tris/HCl, pH8; 10 mM EDTA). To lyse cells, 5µl of filter-sterilised lysozyme solution (40 mg/ml lysozyme and 20 mg/ml achromopeptidase) was added, gently mixed and incubated for 1 hr at 30°C. 10 µl of 10% SDS was then mixed into the samples before the addition of 500 µl (1:1 volume) of phenol/chloroform and vortexed for a minute. To separate the phases, the samples were centrifuged at 14680 rpm for 5 mins. The upper aqueous phase (containing the DNA) was removed and transferred to a fresh microfuge tube. The phenol/chloroform step was repeated until the upper phase was clear (i.e. protein free). With only the aqueous layer in a fresh microfuge tube, 1 ml of 100% ethanol was added followed by centrifugation as above. After removing the ethanol, the pellet was washed in 70% ethanol before repelleting through centrifugation for a further 2 mins at 14680 rpm. The DNA pellet was dried before resuspension in 50 µl sterile dH₂O. Aliquots of 10 µl diluted 1000-fold were stored at 4°C and for longer storage, undiluted samples were stored at -20°C.

2.2.1.4 RNA purification

All apparatus and surfaces used were treated with RNaseZAP (Sigma) and where appropriate was rinsed with double autoclaved water before autoclaving. All tubes which were not manufactured RNase free were double autoclaved. Mycelium was harvested from scraping off cellophane lined solid media at experimentally appropriate time points and immediately transferred to 2 ml round bottom tubes, flash frozen in liquid N₂ then stored at -80°C. Frozen mycelium was ground to a fine powder in tubes with added liquid N₂ over dried ice. Directly to the tube, 2 ml of TRI reagent (Sigma) was added to the grindings and mixed. Half the sample was transferred to new 2 ml tubes and snap frozen before storage at -80°C. The remaining samples were placed at RT for 10mins to allow the solutions to clear before the addition of 200 µl chloroform. The samples were then vortexed for 15 s before centrifugation (10 mins; 14500 rpm). The aqueous phase (upper phase containing RNA) was separated from interphase and lower phase (DNA and protein, respectively), and decanted into a new 2 ml tubes. The remainder of the protocol is based on Qiagen RNeasy® Mini Kit, with added DNase treatment (Qiagen RNase-Free DNase Set). To the RNA phase, 450 µl of RLT solution and 500 µl of 90% ethanol were added. This mixture was mixed gently through inversions passed through supplied treatment columns through centrifugation for 30s at 11500 rpm. The matrix was washed with 700 µl RW1 buffer before on column DNase treatment for 1 hr 30 mins (10 µl DNase mixed with 70 µl RDD) at RT. This was washed again with 500 µl RW1 buffer. The column was then further washed twice with RPE buffer (containing ethanol). Following discarding the flow through of the second wash, the column was centrifuged again for 2 mins and left at RT for 5 further minutes to allow column to dry. RNase-free water (60 µl) was heated to 50°C and added to the column for elution. Columns were incubated at 37°C for 10 mins before centrifugation; 10 µl was aliquoted from the sample and used for analysis and the remainder snap frozen and stored at -80°C. Thawed samples were DNase treated using TURBO™ DNase following manufacturer's instructions. To inactivate DNase, EDTA was added to final concentration of 15mM before heat inactivation for 10 mins at 75°C. To rid the sample of EDTA, RNeasy MinElute Cleanup Kit was used, again following all guidelines provided.

Elution volume was however, changed from 14 μ l to 50 μ l. DNase treatment was repeated with a further TURBO™ DNase followed directly by on column Qiagen RNase-Free DNase treatment during the clean-up procedure following manufacturers guidelines as above.

2.2.2 Genetic Manipulation and Analysis Techniques

2.2.2.1 DNA/RNA analysis

Nucleic acid concentrations were quantified using a NanoDrop ND2000c Spectrometer (Thermo Scientific).

2.2.2.2 Polymerase chain reaction (PCR)

GoTaq (Promega) or BioTaq polymerase (Bioline) were used for colony PCR and Q5 polymerase was used for high fidelity PCR and cloning in each case following the manufacturer's instructions unless otherwise stated. The primers used throughout are listed in table 2.3. Annealing temperature was calculated through lowest T_m (as calculated by Integrated DNA Technologies) of primer pair minus 2°C or through use of a gradient PCR.

2.2.2.3 General restriction digest

Reactions for cloning using a single or double restriction digest were routinely 60 μ l total volume and consisted of 6 μ l restriction digest enzyme compatible buffer, and 2 μ g of insert DNA or 5 μ g of vector DNA, 1 μ l of each enzyme (2 μ l for a single digest of vector DNA) and made to the final volume with dH₂O. Digestions were executed for between 2 hrs to overnight depending on the activity of the selected enzyme. After digesting vector DNA, these were incubated at 65°C for 20 mins (or as directed by manufacturer) to denature enzymes.

2.2.2.4 Vector dephosphorylation

To prepare vectors for ligation, after restriction digests, ends were dephosphorylated to prevent self-re-ligation. To the heat-inactivated digest mix, 1-2 μ l of shrimp alkaline phosphatase (NEB) was added. This was incubated for 2-

3hrs at 37°C. DNA was subsequently loaded onto an agarose gel for electrophoresis.

2.2.2.5 Ligations

Ligations were set up to a final volume of 20 µl using 1 µl T4 DNA ligase (New England Biolabs inc.), 4 µl of 5X ligase buffer, insert and vector DNA to a molar ratio of 3:1 with 100 ng vector DNA, typically. Ligations were carried out for either 1-3 hrs at RT or overnight at 4°C.

2.2.2.6 Gibson Assembly

To assemble multiple fragments into a vector, primers were designed to amplify each fragment with an overhang of between 12-15 bp. These overhangs complement the other fragments to be connected. As each fragment has 12-15 bp overhang, a total of 24-30 bp are complementary. Overhangs of 31 bp were added to complement the vectors. Restriction sites to be cloned into were designed to be kept intact should further cloning be required. Fragments were amplified using Q5 polymerase. The assembly mix was composed of 10 µl 2X Gibson Assembly master mix (New England Biolabs inc.), 100 ng of vector and followed a 3:1 vector to insert ratio for fragments >200 bp and for fragments <200 bp, a 6:1 ratio was implemented. Samples were incubated at 50°C for 30 mins, if only two fragments were being inserted and for inserts of ≥ 3 this was extended to 1 hr 30mins. Following incubation, 2 µl of the mix was chemically transformed into *E. coli* Top10.

2.2.2.7 Preparation of competent cells

An overnight *E. coli* culture inoculated from a colony was subcultured (1 in a 100) into 10 ml of Lennox media and incubated at 37°C, shaking at 200 rpm until an OD₆₀₀ (optical density at 600 nm at 1 cm path length) of 0.5-0.7 (exponential growth) was reached. These cultures were grown with antibiotics as appropriate. Cells were pelleted through centrifugation at 3,345 x g, 4°C for 5 mins. Supernatant was removed and gently resuspended on ice in sterile and chilled 100 mM CaCl₂ or 10% glycerol for chemically or electro-competent cells, respectively. Cells were

then pelleted again and resuspended again in the above solutions before a final pelleting centrifugation. Cells were then resuspended in 0.5 ml of 100 mM CaCl₂ with 10% glycerol or just 10% glycerol before separation into 100 or 50 µl, respectively. Competent cells were then snap frozen and stored at -80 °C or used immediately.

2.2.2.8 Chemical transformation

Aliquots of chemically competent *E. coli* cells were thawed on ice; 1-3 µl of plasmid DNA was then gently mixed in and left to incubate on ice for 20 mins. The samples were then incubated at 42 °C for 2 mins before returning to ice for a further 5 mins. Subsequently, 900 µl of Lennox media was added. The transformations were then allowed to recover at 37°C, shaken at 250 rpm for 30 mins to 1 hr. From this 50, 100 and 200 µl was then plated onto Lennox media with the appropriate antibiotics for selection. These were then incubated at 37 °C overnight (16 hrs) or for 24 hrs in the case of Gibson assembled vector transformations.

2.2.2.9 Electroporation transformation

Aliquots of electrocompetent *E. coli* cells were thawed on ice; typically, 0.5-1 µl (more DNA added if desalting had been carried out) of plasmid DNA was then added before transferring to an ice chilled electroporation cuvette. This was electroporated using the BioRad® Electroporator set to 200 Ω, 25 µF and 2.5 kV. The transformed cells were transferred into a fresh microcentrifuge tube with 900 µl of Lennox media and allowed to recover at 37°C shaken at 250 rpm for 30 mins to 1 hr. As with chemically transformed cells 50, 100 and 200 µl were plated with the appropriate antibiotics for selection. These too were then incubated at 37 °C overnight (16 hrs) or for 24 hrs in the case of Gibson assembled vector transformations.

2.2.2.10 Agarose gel electrophoresis

To separate DNA fragments and to determine size, DNA was subjected to gel electrophoresis through agarose gels. Gels were typically made to 1% (w/v)

agarose in 1x TBE buffer (90 mM Tris-HCl, 90 mM Boric Acid, 2 mM EDTA) with 3 µl ethidium bromide/100 ml of TBE. To separate fragments of similar sizes, a higher density gel was made, and a lower density gel was used in the event of analysis of DNA of >5000bp. Samples were mixed with 0.1 volumes of DNA-loading buffer (0.25% (w/v) bromophenol blue, 0.25% (w/v) xylene-cyanol blue, 40% (w/v) sucrose in water) and the gels were run in 1x TBE buffer at 120V for approximately 45 min. A 1Kb plus DNA ladder (Invitrogen) was run alongside the samples, and the DNA was visualised by exposure to UV light.

2.2.2.11 DNA extraction from agarose gel

After visualising DNA fragments using low level UV light, bands of the expected size of fragments were excised using a scalpel and DNA purified using Qiaquick Gel Extraction Kit (Qiagen), as per manufacturer's instructions. DNA were typically eluted in 50 µl sterile dH₂O.

2.2.3 PCR targeted gene editing

The PCR targeted gene editing method involves deletion of a gene by its replacement with a resistance cassette (e.g. apramycin (apr) resistance (aprR)). This replacement is achieved by fusing the resistance cassette with sequences flanking the gene/s of interest which allows homologous recombination (HR) once this DNA is conjugated into the cell. First primers are designed to amplify the resistance cassette with overhangs which complement the sequence immediately adjacent to the gene/s of interest. Through homologous recombination, the cassette replaces the gene within a cosmid. This cosmid, after extraction from *E. coli* is then conjugated into *Streptomyces* and through another round of HR results in gene deletion (Figure 2.1).

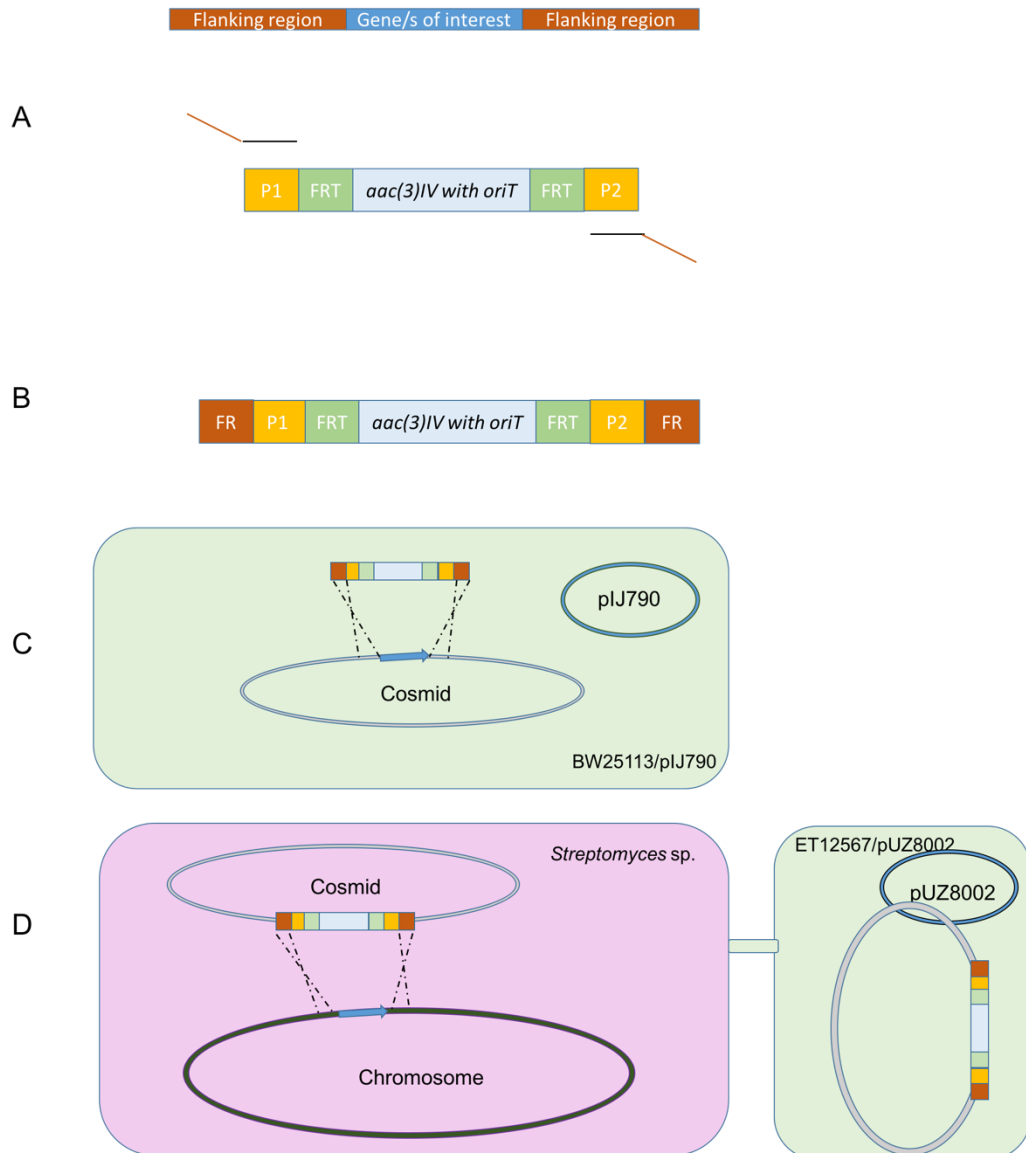


Figure 2. 1: Cloning strategy of PCR targeting. A) Design of primers to amplify aprR cassette (*aac(3)IV*) along with FLP-recombinase (FLP) recognition targets (FRT) through binding at P1 and P2 with overhangs corresponding to flanking regions to gene of interest. B) The amplified cassette possesses the flanking regions (FR), P1/P2, FRT and aprR. C) This is transformed into BW25113/pIJ790 that already has the cosmid (containing gene of interest) transformed in. The addition of arabinose induces λ RED genes which facilitate recombination of the linear DNA with the cosmid. D) This cosmid containing the aprR cassette is extracted and transformed into ET12567/pUZ8002. This is then conjugated into *Streptomyces* where through another recombination event leads to replacement of gene of interest with the aprR cassette.

The aprR cassette, containing *aac(3)IV* gene and an origin of transfer (*oriT*), of pIJ773 were amplified by PCR using primers specific for the disruption of the gene of interest. Details of the plasmids and how to design primers to generate in frame gene knockouts (KOs) were reported by Gust *et al.*, (2002). The forward primers consist of 39 nucleotides (nt) upstream of the gene of interest, terminating

in the translational start codon. This is connected to 20 nt of the 5' end (P1) of the aprR cassette. The reverse primer possesses 39 nt of the antisense sequence of the gene of interest ending in the translational stop codon and 19 nt of the 3' end (P2) of the aprR cassette (Figure 2.1). The PCR cycling conditions consisted of:

98°C	2 mins	1 cycle
98°C	45 s	} 10 cycles
50°C	45s	
72°C	2 mins	
94°C	45 s	} 15 cycles
55°C	45 s	
72°C	2 mins	
72°C	5 mins	1 cycle

These PCR reactions were carried out using Q5 polymerase adhering to manufacturers guidelines. PCR products were then analysed by agarose gel electrophoresis. A gel slice containing the amplified fragment of DNA was extracted and stored at -20 °C until use or used immediately.

Cosmids containing the wild-type gene to be targeted were obtained from the John Innes Centre (JIC, Norwich). An aliquot (~50 µl) of *E. coli* BW25113/pIJ790 electro-competent cells were transformed with ~2 µg of cosmid DNA. The cells were grown in 1 ml of LB for 1 hr before plating onto LB agar plates containing ampicillin (amp) and kanamycin (kan) to select for the incoming cosmid and chloramphenicol (cml) to select for the λRED recombinant plasmid pIJ790. The plates were incubated at 30°C overnight. Cosmids were confirmed by positive amplification of the gene of interest. Following confirmation, a colony was picked and inoculated into 10 ml Lennox containing antibiotic selection and incubated overnight at 30°C, shaking at 250 rpm. From this overnight culture a 1:100, overnight : fresh media was subcultured into in 10 ml Lennox with antibiotic selection. To this 100 µl 1M L-arabinose was added before incubating at 30°C for 4 hours at 250 rpm. The arabinose is essential as it induces the λRED genes on pIJ790 facilitating transformation with linear DNA.

These cells were then made electrocompetent (as described in section 2.3.2.7) and a 50 µl aliquot was electroporated with 2 µl of the deletion PCR product with flanking regions homologous to the gene of interest. These cells were then incubated for 1 hr at 37°C, shaken at 250 rpm and ultimately plated on to LB plates containing kan and apr to select for the cosmid and gene deletion, respectively. Each plate was then incubated overnight at 37°C to promote loss of the temperature-sensitive plasmid, pIJ790. Single colonies were then picked and incubated overnight at 37°C in 10ml Lennox containing appropriate antibiotics selection.

The PCR targeted cosmids were isolated from overnight cultures as described and checked by PCR for the gene disruption. Primers specific for the flanking wild-type region, or for the disruption cassette (P1 and P2), were used in combination, as well as checking by restriction digest (where appropriate), using appropriate enzymes, to check the disruption was successful.

S. coelicolor contains a methylation-sensing restriction system and as such it is essential to passage disruption cosmids through a non-methylating (dam- dcm) *E. coli* strain ET12567 before introduction into *Streptomyces*. ET12567 / pUZ8002 (Table 2.2) was transformed by electroporation with 2 µg of cosmid DNA and subsequently plated onto Lennox agar containing cml and apr. Plates were incubated overnight at 37°C and single colonies were selected and grown in 10 ml LB broth at 37°C overnight in the presence of the antibiotic selection as above, in addition to kan and amp. This was then subcultured into fresh Lennox medium with the same antibiotic selection (1:100) and incubated again at 37°C at 250 rpm for 4-6 hrs until an OD_{600nm} of 0.6-0.8 was reached. Cultures were centrifuged at 4000rpm for 5 mins. The supernatant was removed, and pellet was washed in fresh Lennox twice, spinning between washes. This is to remove the selection antibiotics. After further centrifugation, cell pellets were resuspended in 500 µl of LB broth. During the wash steps, 20-50 µl of *S. venezuelae* spores was mixed with 500 µl 2 x YT and incubated in a 55°C water bath for 10 mins. After allowing to cool, the *E. coli* cells and the spores were mixed and briefly centrifuged to pellet. Serial dilutions of 10⁰-10³ were plated onto SFM plates containing 10mM MgCl₂ and incubated at 30°C for 9 hrs or overnight at RT. Following this incubation period,

each conjugation plate was overlaid with 1 ml of sterile dH₂O containing nalidixic acid (nal) and apr to the concentration shown in table 2.5, to select for *Streptomyces* containing the cosmid for recombination. The overlay solution was distributed over the surface gently before allowing to dry. These were incubated at 30°C until colonies sporulated. Colonies were replica plated onto three different Lenox plates containing different selection. The first no selection, the second with kan and the third with apr. Double crossover events were selected using apr resistance and kan sensitivity (kanS) as the marked antibiotic cassette has now replaced the target gene in the chromosomal DNA and the cosmid has been lost. These colonies were then picked and purified for single colonies and replica plated a further two times to ensure of aprR and (kanS). Spore stocks were prepared for these double cross-over exconjugants and stored at -20°C.

2.2.4 Gene editing through CRISPR/Cas9

Developed by Cobb, *et al.*, (2015), the CRISPR/Cas9 gene editing method relies on the generation of a double stranded break (DSB) by the Cas9 enzyme and repair through HR. CRISPomyces-2 vector (Cobb, *et al.*, 2015) carries an aprR cassette, allowing for selection of vector, *cas9* gene from *S. pyogenes* that is under the control of a constitutive promoter, a temperature sensitive replication region in pGS5 allowing clearance of the vector after gene deletion, and trans-activating CRISPR RNA (tracrRNA) sequence, forming a ready fused synthetic guide RNA (sgRNA) sequence after a specific protospacer (later transcribed into CRISPR RNA (crRNA)) sequence is added to the vector (Figure 2.2). To generate a deletion vector, flanking homology regions to the gene of interest was inserted into the vector.

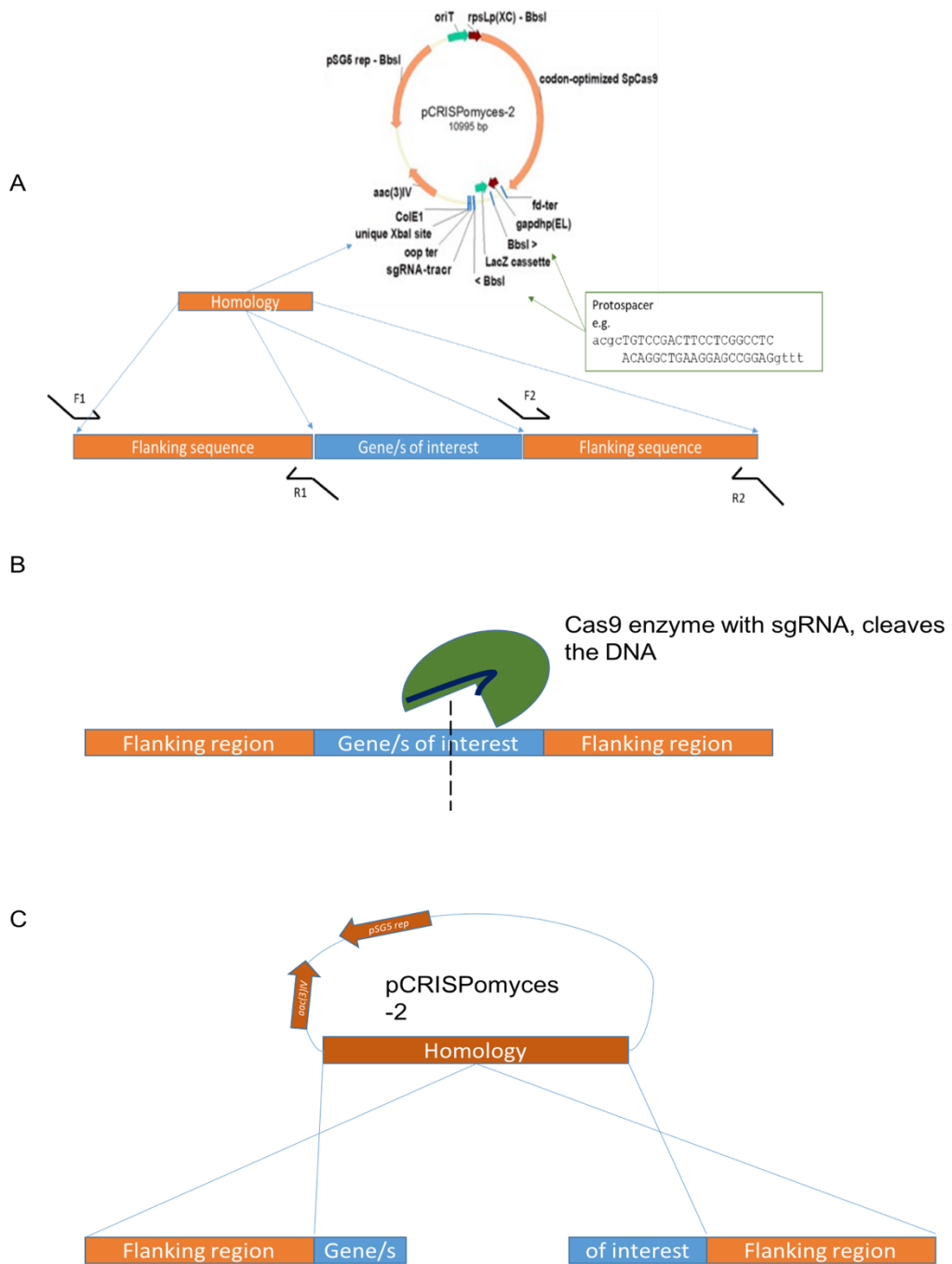


Figure 2. 2: Cloning strategy to generate a gene deletion in *Streptomyces* using the CRISPR/Cas9 system developed by Cobb, *et al.*, 2015. A) Constructing a deletion vector using pCRISPOmyces-2 by insertion of protospacer into the BbsI site (forming a synthetic guide RNA (sgRNA) which is the crRNA and the tracrRNA fused together) and homology region (flanking region to the gene of interest). B) After conjugation into *Streptomyces*, the expressed Cas9 enzyme binds with sgRNA. Upon a match of the crRNA (protospacer sequence) and the genomic DNA, the DNA is cleaved forming a DSB. The vector is selected for using apr due to the AprR cassette. C) The DSB can then be repaired through homologous recombination (HR) with the homology sequence inserted into the vector. After HR, the vector can then be lost through growth at a higher temperature (37-39°C) due to temperature sensitive replication region of pSG5 and also removal of apr selection.

The unique protospacer sequence was selected by eye and was chosen following the guidelines suggested by Cobb, *et al.*, 2015. These rules are:

1. Selection of a unique 20bp sequence that is immediately followed by a protospacer adjacent motif (PAM) sequence (NGG).
2. Sequence uniqueness was defined by BLASTN (NCBI) determination of the final 12 bp + NGG sequence through genome where all 4 possibilities of N were analysed
3. Protospacer was searched on the non-coding strand
4. The final 4 bp of the 3' end of protospacer contained largely purines

The uniqueness of the protospacer sequence took precedence and hence adhering to the purine guideline was not complete for most of the protospacer sequences chosen for each deletion construct.

The protospacer sequence was cloned into the *BbsI* site of pCRISPomyces-2 through golden gate assembly. Golden gate assembly utilises type II endonucleases ability to cleave outside of the recognition site to clone fragments into vectors with directionality. Multiple fragments can be assembled in one reaction, similar to Gibson Assembly. However, due to the restriction site being lost in the process of assembly, cleavage and assembly can occur simultaneously in one single reaction. The protospacer oligonucleotides were first annealed by heating to 95°C and ramped to 4°C at a rate of 0.1°C/s in a mix composed of 90 µl HEPES (30 mM, pH 7.8) and 5 µl of each of the forward and reverse strands of the protospacer (100mM). The annealed protospacer oligonucleotides (0.3 µl of 10-fold dilution) were added to the golden gate assembly mixture which also contained 100 ng of pCRISPomyces-2, 1 µl ligase, 2 µl ligase buffer and 1 µl *BbsI* before being made up to 20µl with water. The reaction mixture was then thermo-cycled as below:

37°C 10 mins
16°C 10 mins
Thermocycle first two steps 9 times
50°C 5 mins
65°C 20 mins
Storage at 4°C

Following thermocycling 1 µl of the golden gate assembled vector was transformed into chemically competent *E. coli* Top 10 before plating on Lennox solid media containing 40 µg/ml Xgal (5-bromo-4-chloro-3-indolyl-β-D-galactopyranoside) and 100 µg/ml IPTG for blue/white screening due to the presence of the lacZ gene in vector which is disrupted when the protospacer sequence is inserted, therefore, Xgal can no longer be cleaved. White colonies were selected, cultured overnight in Lennox media (10ml) and the DNA was harvested before sequencing with SpacerFor-2756 and SpacerRev-2756 (Table 2.3) to confirm the successful insertion of the protospacer sequence.

To incorporate the recombination template, primers were designed to amplify the flanking regions of >1000 bp of the deletion region and constructed by using Gibson Assembly (2.2.2.6). The protospacer containing vector was first digested using XbaI and dephosphorylated.

To confirm that the homology sequence had been successfully inserted, the region was sequenced using ForCRISP-2 and RevCRISP-2 primers (Table 2.3). The vector was then transformed into ET1256/pUZ8002 electrocompetent cells before conjugating into *Streptomyces*. As previously described *S. coelicolor* contains a methylation-sensing restriction system and hence passaging through *E. coli* ET12567 before introduction into *Streptomyces* was possible. However, *S. venezuelae* does not possess this system, notwithstanding, the vector was still transformed into *S. venezuelae* for use of the driver plasmid pUZ8002 for conjugation. *E. coli* ET1256/pUZ8002 strains possessing the vector were inoculated and grown overnight with cml, apr and kan selection. This was then subcultured 1:100 (culture: fresh media) into Lennox containing the aforementioned antibiotic selection. This was incubated for 4-6 hrs at 37°C at 250 rpm, until an OD_{600nm} of 0.6-0.8 was reached. Cells were then pelleted at 4000 rpm

for 5 mins and washed twice with 10 ml Lennox, spinning cells down (3 s using benchtop centrifuge 5424 quick spin) between each wash before a final pelleting of cells. These cells were then resuspended in 500 μ l of Lennox. During the wash steps, 10-50 μ l of *Streptomyces* spores were added to 500 μ l 2 x YT and incubated in a 55°C water bath for 10 mins to synchronise germination. After cooling, this was mixed through inversion with the concentrated and washed *E. coli* from before. Cells were gently pelleted through a short spin in the Eppendorf 5424 centrifuge for 5 s. Serial dilutions of 10^0 - 10^3 were plated onto SFM plates containing 10mM MgCl₂ and incubated at 30°C for 9 hrs for *S. venezuelae* or 16-20 hrs for *S. coelicolor*, *S. lividans* or *S. formicae*. After this incubation, 1 ml antibiotic solution (1ml sterile dH₂O containing nal and apr as depicted in table 2.5) was spread over the surface to select for *Streptomyces* colonies containing the deletion vector. After allowing to dry, plates were returned to incubate as before for between 5-10 days until colonies had sporulated. Colonies were picked and restreaked onto MYM-Apr for a single generation before growth at 37°C to remove the heat sensitive pCRISPomyces-2 vector. During the passaging process, mutants were confirmed through PCR analysis using crude lysates.

Crude lysates were generated through lysis of 400 μ l extracted from an overnight culture of *Streptomyces* exconjugant in 5 ml of MYM, incubated at 30°C, at 200 rpm. Cells were pelleted and resuspended in 200 μ l Buffer SET (75 mM NaCl, 25 mM EDTA pH 8, 20 mM Tris-HCL pH 7.5). To this 2 μ l of a lysis solution (40 mg/ml lysozyme and 20 mg/ml achromopeptidase) was added and mixed thoroughly. This was incubated at 30°C for 2 hrs and made up to 1 ml with sterile dH₂O. PCR analysis was carried out with primer pairs designed to amplify different regions of the edited region (Figure 2.3). For a deletion mutant, the three types of PCR analysis is shown in Figure 2.2, where flanking PCR primer pairs are outside of the homology region. This is also amplified and used for sequencing. External PCR primer pairs amplify the immediate region surrounding the deleted gene/s. One of these primers is used in conjunction with a primer complementary to a section found within the KO region, consequently no specific PCR product should be seen if KO was successful. Spore stocks were prepared for these confirmed deletion mutants and stored at -20°C.



Figure 2.3: PCR analysis strategy of CRISPR/Cas9 generated deletion mutants where flanking PCR refers to primer pairs situated outside the original homology amplification flanking sequence, external PCR refers to primer pairs within the original homology flanking sequence and internal PCR where one primer of the pair is situated within the gene deleted.

2.2.5 RNA analysis

2.2.5.1 Reverse transcription

Using Superscript II reverse transcriptase (RTII), following manufacture's guidelines, $\leq 2\mu\text{g}$ of pure RNA was reverse transcribed with $1\ \mu\text{l}$ (200 units) of RTII. Random primers ($300\ \text{ng}/\mu\text{l}$; Invitrogen), dNTPs ($10\ \mu\text{M}$ each; $1\ \mu\text{l}$) and approximately $2\ \mu\text{g}$ RNA were made up to $13\ \mu\text{l}$ with nuclease free water and incubated at 65°C for 5 mins before chilling on ice. To this $4\ \mu\text{l}$ of 5X first strand buffer and $2\ \mu\text{l}$ 0.1M DTT was added, gently mixed and further incubated for 2mins at 25°C before reverse transcriptase was added and mixed. The $20\ \mu\text{l}$ complete mix was then incubated at 25°C for 10mins, 42°C for 5 mins and finally at 70°C for 15 mins.

2.2.5.2 qRT-PCR

SYBR Green JumpStart Taq ReadyMix ($12.5\ \mu\text{l}$) was mixed with forward and reverse primers to a final concentration of $0.125\ \mu\text{M}$, MgCl_2 to a final concentration of $4\ \text{mM}$, $0.25\ \mu\text{l}$ of $20\ \text{mg}/\text{ml}$ BSA. This was made to $24\ \mu\text{l}$ with nuclease free water before $1\ \mu\text{l}$ of diluted (1: 2.5) first strand cDNA was added and mixed. Primers were designed for amplicons of between 90-150bp (Table 2.3). qRT-PCR was conducted in triplicate per cDNA sample.

To quantify the number of copies of mRNA, standards were generated ranging from 10^7 - 10^1 DNA copies from PCR amplicons amplified from

M145 Δ *afsQ2* genomic DNA. The standards were conducted in duplicate. With these values, a linear trendline was plotted and the equation of this line calculated.

The threshold was determined by eye and manual set. This was set to coincide with the linear part of each amplification curve, however to avoid artefact noise, this was set slightly higher when necessary. CT values (threshold cycle) is where the amplification curve meets the aforementioned threshold line. CT values were inputted into the equation generated from the trendline described earlier to calculate total copies of first strand cDNA and hence transcript. The values exceeding 1.5 times the median value of the calculated quantities were omitted.

2.3 Protein Methodology

2.3.1 Protein preparation

2.3.1.1 Protein overexpression in *E. coli* and cell lysis

Protein was overexpressed using *E. coli* BL21 carrying overexpression vectors. An overnight culture was subcultured (1:100) into fresh Lennox media containing the relevant antibiotic selection. Cultures were grown at 37°C at 250rpm. Once an OD_{600nm} of 0.4-0.5 was reached IPTG to a final concentration (unless otherwise stated) of 1mM was added. The cultures were then further incubated under the same conditions (unless stated) a further 4 hrs.

For protein trials, 1ml of culture was removed and pelleted, supernatant removed and resuspended in 100 μ l sample buffer (0.0625 M Tris-HCl (pH 6.8), 2% (w/v) SDS, 10% (v/v) glycerol, 5% (v/v) β -mercaptoethanol and 0.001% (w/v) Bromophenol blue). This was boiled for 5 mins before centrifuging at 14680 rpm for 3 mins. Samples were then loaded onto an acrylamide gel and SDS-PAGE was conducted.

Large volumes of cultures were grown for purification purposes. See purification section 2.3.3.

2.3.1.2 Cell lysis (*Streptomyces*)

Harvested mycelia were disrupted through grinding with a mortar and pestle on dry ice with added liquid nitrogen to maintain brittleness. Lysis was judged by production of a very fine powder.

2.3.1.3 Measuring protein concentration through Bradford assay

Using a 1 mg/ml stock of Bovine Serum Albumin (BSA) as a standard, 0, 1, 3, 5, 7 and 10 μ l was added to 200 μ l Bradford reagent and made up to 1ml using dH₂O in cuvettes of path length 1 cm. Samples were produced in the same way at suitable dilutions. After thorough mixing of all samples and standards, all were left for ~20 mins then measured at 595nm comparing sample absorbance to those of the known standards.

2.3.2 Protein Analysis

2.3.2.1 SDS-PAGE

All reagents and buffers for the sodium dodecyl sulphate (SDS) polyacrylamide gel electrophoresis (PAGE) gels were prepared as described by Laemmli (1970) with the following modifications. The acrylamide resolving gel was produced to a final concentration of 15% (50% final volume of 30% v/v acrylamide solution, 0.375 M Tris-HCl pH8.8 and 0.1% SDS), a stacking gel final concentration of 5% (12.5% final volume of 30% v/v acrylamide solution, 0.25 M Tris-HCl pH6.8 and 0.1% SDS) and both gel types were polymerised chemically using 50 μ l of 10% (w/v) ammonium persulphate (APS) and 10 μ l Tetramethylethylenediamine (TEMED) as supplied. Tris (2.5mM) Glycine (19.2mM) SDS (0.1%) buffer (TGS) was used as running buffer. Sample buffer concentrations were 0.0625 M Tris-HCl (pH 6.8), 2% (w/v) SDS, 10% (v/v) glycerol, 5% (v/v) β -mercaptoethanol and 0.001% (w/v) Bromophenol blue. SDS-PAGE was carried for 1 hr or until bromophenol blue was clear of the gel at between 150-200V.

2.3.2.2 Coomassie blue staining

To visualise all resolved protein bands, gels were stained with Instant Blue (Expedeon) in accordance with the manufacturer's instructions, typically leaving overnight to develop before destaining in dH₂O.

2.3.2.3 Immuno-blot analysis

Protein samples onto an SDS-PAGE gel and separated as above using prestained SDS-PAGE standards (BIO-RAD PageRuler™ Prestained Protein Ladder, 10 to 180 kDa) as a size marker. Proteins were transferred to a nitrocellulose membrane (BIO-RAD Immuno-Blot® PVDF Membrane), pre-soaked in methanol for 1-5 mins before adding transfer buffer (3 mM sodium carbonate, 10 mM sodium bicarbonate) to an approximate ratio of 1: 4. Following soaking, a BIO-RAD trans-blot SD semi-dry transfer cell, set up according to the manufacturer's instructions and run at 10 V for 1 hr. Following transfer, the nitrocellulose membrane was blocked, using 5% semi skimmed milk powder solution dissolved in Tris buffered saline (50 mM Tris, 0.85% (w/v) NaCl, pH 7.4) + 0.1% (v/v) Tween 20; TBST buffer) overnight or for 3hrs at 4°C. The membranes were incubated with 1/5000 of either Qiagen Penta-His HRP conjugate antibodies, Sigma monoclonal ANTI-FLAG® M2 antibody HRP conjugated antibodies or Novagen Strep•Tag® II HRP conjugate antibodies. The dilution was made with fresh 5% semi skimmed milk blocking buffer for 1 hour at RT and subsequently washed 3 times in TBST buffer for 5-10 mins a wash. Membranes were developed using the ECL system (GE Healthcare), exposed to X-ray film for between 5 mins to 1hr and developed using an Xograph automatic X-ray film processor.

2.3.2.4 Phos-tag assay

Powdered samples from grinding mycelia were kept on dry ice before adding Tris resuspension buffer (50 mM, pH 7.5, 150mM NaCl) with EDTA free protease inhibitors (Pierce™), DNase, and phosphatase inhibitor tablets (PhosSTOP™) to the manufacturers recommended amounts. The volume of buffer added reflected the amount of material harvested with approximately a 10:1 ratio of buffer volume to lysed matter. After resuspension, cell debris was pelleted, and supernatant transferred to a new tube and mixed in equal volume with Laemmli sample buffer. To equalise protein loading on gel, a Bradford assay was executed on remaining supernatant. Equalised protein was loaded onto Phos-Tag cast SDS-gels alongside 5 µl PAGE-ruler ladder with MnCl₂ (10 mM) at a ratio of 1:4. Phos-tagged gels were cast with the same as acrylamide gels detailed above but with the

addition of MnCl_2 (final concentration of 0.1mM) and Phos-tagTM AAL solution (final concentration of 50nM) in the resolving gel.

This was then subjected to electrophoresis at 200 V until the lowest band of the marker ladder reached the base of the gel. The gel was then incubated with gentle agitation in TGS transfer buffer containing EDTA (25 mM), 20% methanol, 0.1% SDS, 190 mM glycine, 1 mM EDTA) for 3 times 10 mins and then replaced with TGS transfer buffer without EDTA for a further 3 x10 mins. Proteins were then transferred to PVDF membrane through semi-dry electroblotting at 15 V for 1 hr 20 mins. Blocking and developing of dot was then executed as with the western blot protocol.

2.3.2.5 Ponceau S staining

To analyse the success of transfers, 20ml Ponceau S (0.1% (w/v) Ponceau S in 5% acetic acid) was added to the PVDF membrane and gently agitated for 10 mins.

2.3.3 Protein purification from overexpression in *E. coli*

2.3.3.1 Overexpression and Lysis

Cultures of IL volume were set up for overexpression and purification. Cells were pelleted at 6000 rpm for 20 mins. Pellets were transferred to a 50 ml falcon and stored at -20°C till use. Pellets were thawed on ice and resuspended in Tris based lysis buffer (50mM Tris and 150mM NaCl to which PierceTM EDTA free protease inhibitors (1 per 10ml), DNase (Sigma) and lysozyme (Sigma) (both ~10mg per 10ml was added). The volume of buffer used for resuspension was 10ml per 1L of the original overexpression culture. Lysis was then carried out by passaging through a French press (French Pressure Cell Press, Thermo Scientific, 40K cell) at 1000 psi, twice.

2.3.3.2 Membrane protein separation

For purification of membrane bound proteins, lysates were made to a volume of ~80ml using Tris based lysis buffer (without lysozyme) and ultracentrifuged at 42000 rpm for 1 hr. Supernatant was removed and pellet resuspended in sarkosyl containing resuspension buffer (50mM Tris and 150mM

NaCl, 1% sarkosyl (unless otherwise stated), Pierce™ EDTA free protease inhibitors (1 per 10ml) and agitated for 3hrs or overnight at 4°C. Cell debris was then pelleted through centrifugation (Accupsin 1R-Ch.007379 rotor) at 9000 rpm for 10 mins.

To determine whether proteins were located in the insoluble fraction, a pellet of harvested cells from overexpression (5 ml) was resuspended in 0.5 ml buffer composed of 100mM Tris and 50 mM NaCl at pH 8.0 and lysed through sonication on ice (4 times for 10 s). The cell debris and membrane bound proteins were pelleted through ultra-centrifugation (Sorvall MTX 150 Bench Micro-ultracentrifuge with S140-AT rotor) at 100000 rpm for 1 hr. Additional lysis buffer was added pre-centrifugation to meet safety requirements. After centrifugation, the supernatant was removed and prepared for SDS-PAGE analysis and the pellet was resuspended in 50 µl of buffer composed of 100 mM Tris, 50 mM NaCl, 0.5% sarkosyl at pH 8.0 before preparation for SDS-PAGE analysis.

2.3.3.3 Purification with Ni²⁺ NTA agarose beads

The supernatant was transferred to a fresh container and 50-100 µl of Ni²⁺ NTA agarose beads (Qiagen) were added per litre Lennox used for initial overexpression culturing (i.e. if initially 4 L of culture was grown for overexpression, 200-400 µl Ni²⁺ NTA agarose beads need to be added). Samples were incubated at 4°C mixing slowly for 1-2 hrs. The beads were then removed from the sample by centrifugation. These were then added to 1 ml propylene tubes (Qiagen) and washed with 20-30 ml of buffer A (50 mM Tris-HCl pH 7.3, 150 mM NaCl, 0.5% sarkosyl, RNase inhibitors). Following washes with buffer A, the sample is eluted from the beads using 1-2 ml of buffer B (buffer A + 300 mM imidazole).

2.3.3.4 Purification with Ni²⁺ His-Trap columns of VanS from *E. coli*

The clarified membrane protein fraction with debris removed was loaded onto a His-Trap column (GE-Healthcare HisTrap FF Crude) at 1 ml/min via ÄKTAFLC (GE Healthcare Life Sciences), washed with 30 ml of buffer 1 at a rate of 1 ml/min before being eluted using buffer 1 and 2 set at a gradient. During

the purification process the constituents of Buffer 1 and 2 were constantly changed to optimise the purification process. Typically, the constituents of buffer 1 was 50 mM Tris, 150 mM NaCl, pH 7.3. Full descriptions of conditions presented with data (table 4.1).

2.3.3.5 Sepharose size exclusion separation

Protein purified using with Ni²⁺ His-Trap columns were then passed through size exclusion Superdex 75 Pregrade column. Protein fractions collected from purification were buffer exchanged and concentrated into 3ml of storage buffer (50mM Tris, 10mM NaCl and 0.5% sarkosyl and RNase inhibitors) as explained in 2.3.4.1. Meanwhile, the Superdex column was rinsed first with 50 ml dH₂O (0.5 ml/min) and then 50ml of storage buffer (50mM Tris, 10mM NaCl and 0.5% sarkosyl and RNase inhibitors) at a rate of 0.5 ml/min. Into the column, the concentrated protein was injected manually with a syringe at a rate of approx. 0.5 ml/min. After protein is loaded, buffer used previously was again run through the column to elute. Fractions sizes were automated to 1.5 ml per fraction and 200 ml of buffer was used for elution. As this was conducted with the ÄKTAFPLC (GE Healthcare Life Sciences), fractions in accordance with the positioning of the peak/s were selected to be analysed though a coomassie blue stained acrylamide gel which had been subjected to SDS-PAGE.

2.3.4 Post purification protein treatment

2.3.4.1 Buffer exchange

The eluted protein was buffer exchanged using Amicon® Ultra 4 mL Centrifugal Filters of the following manufacturer's instructions into buffer A with 20mM NaCl and reduced sarkosyl (0.2%). Filters of 10, 30 and 50 kDa molecular weight exclusion were used depending on protein size.

2.3.4.2 Enterokinase treatment

Enterokinase from bovine intestine (Sigma) which recognises the peptide sequence N-X₁-Asp-Asp-Asp-Asp-Lys-X₂-C (where X₂ is any amino acid except proline) was used to cleave the His-GST tag from VanS. Purified protein sample was buffer exchanged into 50 mM Tris-HCl (pH 8.0), 50mM NaCl, 0.2% sarkosyl. His-GST-VanS (10, 20, and 30 µg) was incubated at 37°C overnight with 5-10 U

(where 1 U is amount of enterokinase required to cleave >95% of 1 μg of protein). Total volume was made typically to 30 μl (10-20 μg protein digestion) or 50 μl (30 μg protein digestion). Success of digest was judged through SDS-PAGE.

3. Generation of a TCS deletion library in *S. venezuelae*

3.1 Chapter Overview

In this chapter, an investigation into the TCSs of *S. venezuelae* NRRL B-65442 and the work undertaken to generate a TCS deletion library has been presented. In conducting *in silico* analysis on TCSs within the genome, analysing the distribution of the TCSs, class of RRs and domain structures, sheds some light on their roles in signaling. Furthermore, through assessing the conservation of each RR and SK, we can begin to infer how important or niche a role a TCS may play in *S. venezuelae*. For instance, in Actinobacteria the widely conserved TCSs, MtrAB and PhoPR are global and pleiotrophic regulators, respectively. However, further analysis is needed to ascertain their roles. To this end, a deletion library of TCSs was begun and is currently near completion with 10 of the 59 TCS operons still to be deleted. Some preliminary work has been carried out to characterise these mutants and the roles the TCSs serve. This library serves as a great platform to understand how *Streptomyces* are able to sense and respond to the changing environment they face.

3.2 Introduction

Since the discovery of streptothricin in 1942 (Waksman and Woodruff, 1942) and streptomycin in 1943 (Schatz, *et al.*, 1944), the genus *Streptomyces* was thrust into the limelight of research as important sources of antibiotics. Over the years, thousands of bioactive compounds have been identified (Bérdy, 2005).

In section 1.2.3, the regulation behind the production of ACT, RED, CDA, yCPK in *S. coelicolor* was described. The expression of many SARPS and CSRs are modulated by TCSs in response to changing external conditions. Furthermore, many BGCs encode one or more TCSs. For example, the yCPK BGC in *S. coelicolor* encodes 2 SKs and a RR (Weber, *et al.*, 2013). Deletion or insertion of additional copies of TCSs or part of these TCSs has led to production of antibiotics; this is exemplified in the identification of RR, AfsQ1 (section 1.3.1.2; Ishizuka, *et*

al., 1992). This demonstrates one facet of the importance in studying TCSs of *Streptomyces*.

In addition to modulating secondary metabolite production, TCSs also regulate primary metabolism (e.g. PhoPR), morphological development (e.g. AfsQ1/Q2 and MtraAB) and cell maintenance (e.g. CseBC), also discussed in section 1.2.3. TCSs have also been shown to be involved in quorum sensing and plant colonisation; RqpSR was recently identified to be involved in quorum sensing in *Burkholderia cenocepacia* (Cui, *et al.*, 2018) and RoxSR of *P. putida* in population density and redox state recognition and plant colonisation (Fernández-Piñar, *et al.*, 2008). As yet, no TCSs within *Streptomyces* have been linked to quorum sensing or plant colonisation. Studying TCSs would allow us to better understand how these bacteria perceive their environments, and from understanding their regulons, allow us to utilise or engineer these bacteria for purposes such as bioremediation (Schütze, *et al.*, 2014) or better colonisation of plants (Viaene, *et al.*, 2016) and hence potentially improve crop growth, for example.

As previously described a complete TCS deletion library has been generated for *E. coli* (Oshima, *et al.*, 2002; section 1.4). These mutants have been used to characterise the TCSs through transcriptome analysis as well as through phenotype microarrays (Oshima, *et al.*, 2002; Zhou, *et al.*, 2003). No other TCS deletion library has been described, however, for bacteria with few numbers of TCSs, such as in *M. tuberculosis*, all 11 complete TCSs have been deleted and characterised in different studies as reviewed by Cho and Kang (2015). Generation of a complete deletion library forms the basis of studying mass numbers of TCSs. This is particularly important for *Streptomyces* where many TCSs are clade specific and not homologous to many studied TCSs in other bacteria due to evolution of new TCSs largely due to LSE rather than HGT (Alm, *et al.*, 2006).

Within the vast *Streptomyces* genus, arguably the best studied species is *S. coelicolor*. The genetic study of this model organism has been ongoing for the last 60 years for antibiotic production, lifecycle and chromosome segregation (Chater, 2016). In addition to *S. coelicolor*, many other model organisms are used, some of which already discussed in section 1.2. These models include *S. granaticolor* and

S. viridochromogene for sporulation studies (Hardisson, *et al.*, 1978; Xu, and Vetsigian, 2017), *S. albus*, which has a particularly small genome of 6.4 million bp, has been used as a heterologous expression host (Zaburannyi, *et al.*, 2014) and *S. griseus* from which streptomycin was first isolated (Schatz, *et al.*, 1944). *S. venezuelae* is an emerging model organism which is a producer of chloramphenicol and depending on the strain can also produce jadomycin (NRRL B-65442; Forget, *et al.*, 2017) and pikromycin (ATCC 15439; He, *et al.*, 2016). Like *S. coelicolor*, *S. venezuelae* is genetically tractable. However, *S. venezuelae* has a faster growth cycle and readily sporulates to completion within liquid culture, allowing easier high throughput characterisation of mutant strains. Furthermore, despite being a producer of antibiotics, unlike *S. coelicolor*, it does not as readily synthesise these (Sekurova, *et al.*, 2016).

The study of TCSs within *Streptomyces* over the last twenty years has resulted in many TCSs being discovered, some already discussed here, however, with the sheer number of *Streptomyces* species and the number of TCSs their genomes possess, those discovered form only the tip of the iceberg. The research presented here, hopes to build on previous work of characterising individual TCSs by generation of a TCS deletion library in the model organism *S. venezuelae*, from which more TCSs can be better studied and hence characterised.

3.3 Results

3.3.1 *In silico* analysis of the TCSs of *S. venezuelae*

3.3.1.1 Genome wide TCSs and related proteins

S. venezuelae encodes 59 paired TCSs, one of which, OsaAB (Sven15_5286/87), has a hybrid SK possessing a HisKA domain as well as an HTH DNA binding domain in addition to the RR. There are also two others which possess two SKs to the one RR (Sven15_2343-45 and Sven15_4209-11). In this study, these have been grouped in as paired TCSs, for they all possess a least one SK and RR, creating a total of 59 TCSs. The hybrid SK encoded by *sven15_0344* was not included within this group for a separate RR was not identified adjacent to the SK.

These 59 paired TCSs were identified from running the genome through an online analysis tool, P2RP (Barakat, *et al.*, 2013), searching through genome annotations using the online tool StrepDB - The *Streptomyces* Annotation Server and confirmation by NCBI Protein Blast analysis. StrepDB currently contains over 10 *Streptomyces* genomes which are annotated to varying levels. It allows assessment of genes of interest as well as easy access to FASTA sequences of genes and proteins of interest.

P2RP, is an analysis tool which allows the search of complete genomes for regulatory proteins through analysis of known domains with input from SMART (Letunic and Bork, 2012) and Pfam (Finn, *et al.*, 2012) databases. Regulatory proteins are identified by using RPSBLAST (reverse PSI-BLAST) which searches a query sequence against SMART and Pfam database of profiles (Barakat, *et al.*, 2013). The program uses an E-value cut-off of 0.01 and a minimum of 50% identity per domain length (Ortet, *et al.*, 2012). Genes directly encoded adjacently to these TCSs were analysed through NCBI Protein Blast analysis and use of StrepDB.

This analysis of the genome showed that there are more than twice the number of one-component systems as there are TCSs (Figure 3.1). This is consistent with the research conducted by Ulrich, *et al.*, 2005, which argued that TCSs are evolutionary derivatives of one-component systems. Furthermore, in addition to the paired TCSs, 24 orphan HKs and 17 orphan RRs were identified (Figure 3.1). Whilst many of these HKs were listed as potentially incomplete in the analysis due to lack of an identifiable phosphorylatable His residue, some of these orphans may still be able to pair with some of the orphan RRs or RRs of paired TCSs as exemplified by Spo0F which can interact with 5 orphan SKs (section 1.1.5.3). Additionally, some RRs may be able to pair with SKs of paired TCSs, particularly as some of these RRs are in close proximity to paired TCSs such as *sven15_2691* to *sven15_2695/96* which encodes the MtrAB TCS.

Furthermore, the SK Sven15_0955 is transcriptionally linked to an Hpt protein (Sven15_0954). However, there was not a RR encoded directly up or downstream of this. Instead, 12 bp downstream of the Hpt protein is a multi-component regulatory protein (Sven15_0953) which through analysis with conserved domain BLAST revealed a DUF742 (domain of unknown function). The

SK in this system is predicted to have a NIT domain which is a nitrates and nitrites sensing domain. However, it also also predicted to be incomplete and lacks any TM helices. This system may have degraded over time and is no longer functional, however, this could also be linked to other components such as the orphan RR mentioned above or be connected to other proteins within the cell.

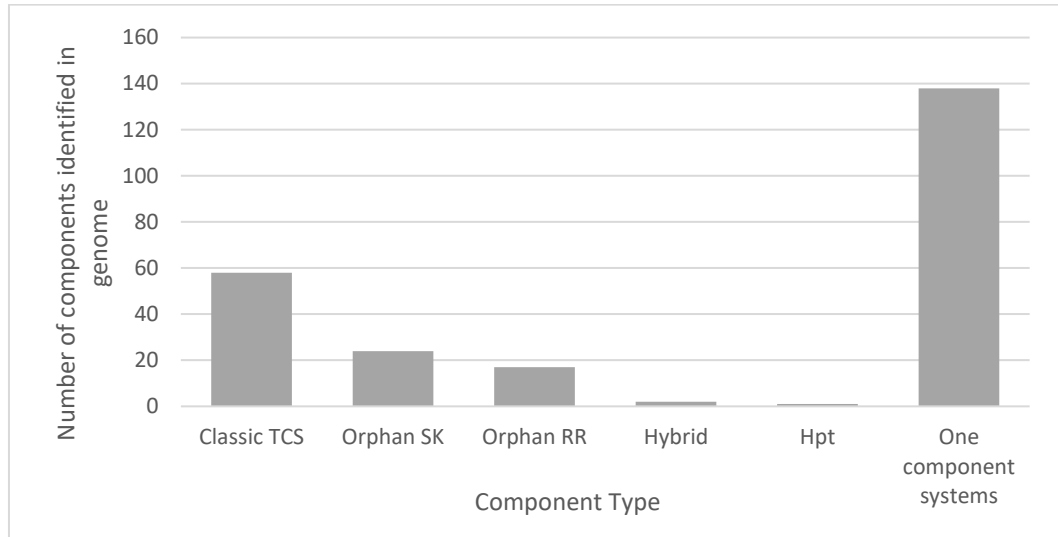


Figure 3.1: Signal transduction proteins identified in *S. venezuelae* through analysis using P2RP (Barakat, *et al.*, 2013). Classic TCSs includes typical TCSs (1 SK and 1 RR adjacently encoded) and multiple components (2 SK and 1 RR). Orphan SK and RRs refers to SKs and RRs without known partners, respectively. 2 hybrid SKs were identified, one in the same operon as a RR and the other not. 1 Hpt protein encoding gene (*sven15_0954*) was identified to be located in the same operon as a SK. One-component systems refer to proteins with input and output domains in a single protein often with no phosphotransfer domains.

As mentioned above there are two hybrid SKs, one which is paired with a RR, another which is not. *Sven15_0344* is predicted by P2RP (Barakat, *et al.*, 2013) to have 6 HAMP domains and a GAF domain in addition to the HisKA, HATPase and effector domain, whereas, *Sven15_5286* is predicted to have 11 HAMP domains, a GAF domain, HisKA, HATPase and effector domain. The high number of HAMP domains in both of these may be involved in signal transduction, however as there are no TM domains, these are likely to be cytosolic proteins or anchored to the membrane through integral membrane proteins. The GAF domains may serve as sensors in these two SKs.

Having identified the paired TCSs within the genome, the distribution of these genes within the genome was analysed. Using the start of the ORF of each SK as the reference point and in the cases where there are two SKs within the

operon, the ORF of the earliest point in the genome was selected. The number of TCSs within a frame of 10^5 bp was analysed and each frame was then shifted by 10^4 bp and the next 10^5 bp within that frame was analysed. These results are presented in Figure 3.2 which shows a concentration of TCSs in 3 points of the genome (~2 million bp, 4 million bp and 6 million bp into the chromosome). As there were multiple peaks, the orphan SKs were then factored in to see if the troughs were a result of loss of paired TCSs. From Figure 3.2, the presence of the aforementioned three peaks do not appear to have changed with the number of orphan SKs taken into consideration, however, there is a higher number of orphan kinases towards the end of the chromosome arm. The higher density of TCSs between certain points of the genome may be related to duplication events or through means of recombination. *Streptomyces* are well known for having unstable genomes, with duplication events thought to be largely at the ends of the chromosome in large blocks 15-126 genes (Chen, *et al.*, 2002; Zhou, *et al.*, 2012). In addition to duplications, the end of chromosomes have a higher frequency of deletions, amplifications and arm replacements (Redenbach, *et al.*, 1993; Fischer, *et al.*, 1997; Fischer, *et al.*, 1998; Uchida, *et al.*, 2003; Widenbrant, *et al.*, 2007). The termini of chromosomes are also highly variable between different species, whereas the core of chromosomes is largely maintained between species, albeit rearranged (Kirby, 2011). This may explain the higher proportion of orphans at the end of the chromosome relative the number of paired TCSs. The TCSs at the terminals of the chromosome may be deleted. Alternatively, if there was a duplication event at the terminals, components may not have been maintained together which could also result in the higher number of orphans.

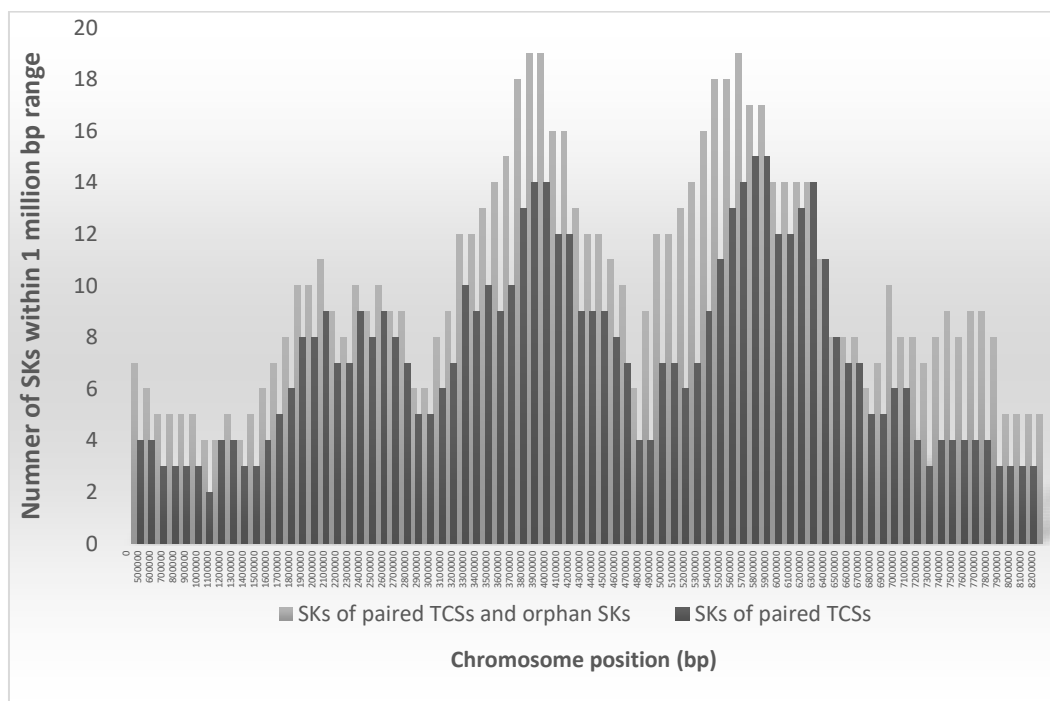


Figure 3.2: Distribution of TCSs and orphan SKs within the genome. Taking the start of the ORF of each SK (both of paired TCSs and orphan kinases), the number of SKs within 10^5 base pair frame of the genome was calculated. The positioning of these bars in the X axis denotes the midpoint of the 10^5 bp frame. These frames were shifted by 10^4 bp. For *sven15_2343-45* and *sven15_4209-11*, *sven15_2343* and *sven15_4210* was taken as reference.

3.3.1.2 Paired TCSs of *S. venezuelae*

For the remainder of this study, paired TCSs were focused upon for *in silico* analysis. Using P2RP (Barakat, *et al*, 2013), table 3.1 was constructed listing the paired TCSs and their counterparts and some structural analysis of these proteins. Most of the SKs are predicted to be anchored to the membrane, however, six have no predicted TM domains; these are: *Sven15_0546*, *Sven15_1398*, *Sven15_2151*, *Sven15_2344*, *Sven15_4979* and *Sven15_6349*. This infers that they are cytosolic TCSs or are anchored to the membrane through another protein.

Table 3. 1: TCSs of *S. venezuelae* NRRL B-65442 with structural analysis using P2RP analysis (Barakat, *et al.*, 2013). RR-N refers to N terminal REC domain; HisKA and HisKA_3 refer to the kinase domain families as described by Pfam; Phy refers to phytochrome region; PspC refers to Phage shock protein C domain; Pyr-redox refers to pyridine nucleotide-disulphide oxidoreductase domain.

Sven15	Component	Annotation	TM helices	Type
138	HK	1 HisKA_3, 1 HATPase_c	6	Classic
139	RR	LuxR family, HTH, RR-N		NarL

439	RR	RR-N		OmpR
440	HK	1 HAMP, 1 HisKA, 1 HATPase_c	1	Classic
545	RR	2 Pyr-redox, RR-N		TrxB
546	HK	Potentially incomplete SK; 1 cNMP binding, 1 HATPase_c	0	Classic
672	RR	LuxR family, HTH, RR-N		NarL
673	HK	1 HisKA_3, 1 HATPase_c	5	Classic
1397	RR	LuxR family, HTH, RR-N		NarL
1398	HK	1 GAF, 1 HisKA_3, 1 HATPase_c	0	Classic
1479	HK	1 HisKA_3, 1 HATPase_c	4	Classic
1480	RR	LuxR family, HTH, RR-N		NarL
1732	RR	LuxR family, HTH, RR-N		NarL
1733	HK	1 HisKA_3, 1 HATPase_c	6	Classic
1773	RR	LuxR family, HTH, RR-N		NarL
1774	HK	1 HisKA_3, 1 HATPase_c	4	Classic
1916	RR	LuxR family, HTH, RR-N		NarL
1917	HK	1 HisKA_3, 1 HATPase_c	4	Classic
1949	HK	1 HisKA_3, 1 HATPase_c	6	Classic
1950	RR	LuxR family, HTH, RR-N		NarL
2143	HK	1 HisKA_3, 1 HATPase_c	6	Classic
2144	RR	LuxR family, HTH, RR-N		NarL
2151	HK	1 HAMP, 1 HisKA, 1 HATPase_c	0	Classic
2152	RR	Phosphate regulon transcriptional regulatory protein PhoB; RR-N		OmpR
2343	HK	1 HisKA_3, 1 HATPase_c	5	Classic
2344	HK	1 PAS_4, 1 HisKA_3, 1 HATPase_c	3	Classic
2345	RR	RR-N		OmpR
2534	HK	1 HAMP, 1 HisKA, 1 HATPase_c	3	Classic
2535	RR	LuxR family, HTH, RR-N		NarL
2551	RR	LuxR family, HTH, RR-N		NarL
2552	HK	1 HisKA, 1 HATPase_c	3	Classic
2695	HK	MtrB; 1 HAMP, 1 HisKA, 1 HATPase_c	2	Classic
2696	RR	MtrA; RR-N		OmpR
2739	HK	1 HAMP, 1 HisKA, 1 HATPase_c	2	Classic
2740	RR	RR-N		OmpR
3148	RR	CseB, WH, RR-N		OmpR
3149	HK	CseC; 1 HAMP, 1 HisKA, 1 HATPase_c	2	Classic
3170	RR	LuxR family, HTH, RR-N		NarL
3171	HK	1 HisKA_3, 1 HATPase_c	4	Classic
3232	HK	1 HisKA_3, 1 HATPase_c	2	Classic
3233	RR	LuxR family, HTH, RR-N		NarL
3326	RR	LuxR family, HTH, RR-N		NarL

3327	HK	1 HisKA_3, 1 HATPase_c	6	Classic
3364	RR	LuxR family, HTH, RR-N		NarL
3365	HK	1 HisKA_3, 1 HATPase_c	4	Classic
3393	RR	LuxR family, HTH, RR-N		NarL
3394	HK	1 HisKA_3, 1 HATPase_c	4	Classic
3472	HK	1 HAMP, 1 HisKA, 1 HATPase_c	2	Classic
3473	RR	WH, RR-N		OmpR
3541	RR	LuxR family, HTH, RR-N		NarL
3542	HK	1 HisKA_3, 1 HATPase_c	6	Classic
3682	RR	WH, RR-N		OmpR
3683	HK	1 HAMP, 1 HisKA, 1 HATPase_c	1	Classic
3736	RR	LuxR family, HTH, RR-N		NarL
3737	HK	1 HisKA_3, 1 HATPase_c	6	Classic
3785	RR	LuxR family, HTH, RR-N		NarL
3786	HK	1 HisKA_3, 1 HATPase_c	5	Classic
3821	HK	LuxR family, HTH, RR-N		NarL
3822	RR	1 HAMP, 1 HisKA, 1 HATPase_c	2	Classic
3873	HK	PhoP; 1 HisKA, 1 HATPase_c	1	Classic
3874	RR	PhoR: WH, RR-N		OmpR
3934	RR	SenR; LuxR family, HTH, RR-N		NarL
3935	HK	SenS; 1 HisKA_3, 1 HATPase_c	5	Classic
4209	RR	LuxR family, HTH, RR-N		NarL
4210	HK	1 HisKA_3, 1 HATPase_c	4	Classic
4211	HK	1 HisKA_3, 1 HATPase_c	4	Classic
4373	HK	EsrS; PspC, 1 HATPase_c	6	Classic
4374	RR	EsrR; LuxR family, HTH, RR-N		NarL
4474	HK	AfsQ2; 1 HAMP, 1 HisKA, 1 HATPase_c	2	Classic
4475	RR	AfsQ1; WH, RR-N		OmpR
4861	HK	1 HAMP, 1 HisKA, 1 HATPase_c	2	Classic
4862	RR	WH, RR-N		OmpR
4924	RR	ChiR; LuxR family, HTH, RR-N		NarL
4925	HK	ChiS; 1 HisKA_3, 1 HATPase_c	4	Classic
4978	RR	RR-N		CheY
4979	HK	Potentially incomplete; 1 PAS, 1 HATPase_c	0	Classic
4999	HK	1 HisKA_3, 1 HATPase_c	5	Classic
5000	RR	LuxR family, HTH, RR-N		NarL
5214	RR	LuxR family, HTH, RR-N		NarL
5215	HK	1 HisKA_3, 1 HATPase_c	6	Classic
5286	HK	OsaA; 11 HAMP, 1 GAF, 1 HisKA, 1 LuxR family HTH	2	Hybrid
5287	RR	OsaB; RR-N		CheY

5306	RR	LuxR family, HTH, RR-N		NarL
5307	HK	1 HisKA_3, 1 HATPase_c	5	Classic
5323	RR	GluR; RR-N		OmpR
5324	HK	GluK; 1 HAMP, 1 HisKA, 1 HATPase_c	2	Classic
5349	RR	LuxR family, HTH, RR-N		NarL
5350	HK	1 HisKA_3, 1 HATPase_c	2	Classic
5393	HK	1 HisKA_3, 1 HATPase_c	4	Classic
5394	RR	LuxR family, HTH, RR-N		NarL
5397	RR	RR-N		Unclassified
5398	HK	Potentially incomplete; 1 HATPase_c	2	Classic
5426	RR	CutR; RR-N		OmpR
5427	HK	CutS; 1 HAMP, 1 HisKA, 1 HATPase_c	2	Classic
5435	HK	KdpD; 1 HisKA, 1 HATPase_c	4	Classic
5436	RR	KdpE; RR-N		OmpR
5558	HK	1 HAMP, 1 HisKA_3, 1 HATPase_c	3	Classic
5559	RR	LuxR family, HTH, RR-N		NarL
5634	RR	LuxR family, HTH, RR-N		NarL
5635	HK	1 HisKA_3, 1 HATPase_c	4	Classic
5645	RR	LuxR family, HTH, RR-N		NarL
5646	HK	1 HAMP, 1 HisKA_3, 1 HATPase_c	2	Classic
5973	RR	LuxR family, HTH, RR-N		NarL
5974	HK	1 HisKA_3, 1 HATPase_c	4	Classic
5985	HK	1 HisKA_3, 1 HATPase_c	4	Classic
5986	RR	LuxR family, HTH, RR-N		NarL
6082	RR	LuxR family, HTH, RR-N		NarL
6083	HK	1 HisKA_3, 1 HATPase_c	4	Classic
6349	HK	1 PAS_2, 1 GAF, 1 PHY, 1 HisKA, 1 HATPase_c	0	Classic
6350	RR	RR-N		CheY
6371	RR	RR-N		OmpR
6372	HK	1 HAMP, 1 HisKA_3, 1 HATPase_c	2	Classic
6686	RR	RR-N		OmpR
6687	HK	1 HAMP, 1 HisKA, 1 HATPase_c	2	Classic
7022	HK	1 HAMP, 1 HisKA, 1 HATPase_c	2	Classic
7023	RR	RR-N		OmpR
7155	HK	1 HisKA_3, 1 HATPase_c	5	Classic
7156	RR	LuxR family, HTH, RR-N		NarL
7219	RR	RR-N		OmpR
7220	HK	1 HAMP, 1 HisKA, 1 HATPase_c	2	Classic

Within table 3.1, some of the SKs were predicted to be potentially incomplete (Sven15_0546, Sven15_4979 and Sven15_5398) which is likely due to the analysis not being able to identify a phosphorylatable His residue. These may simply have degraded. However, another possibility is that these may have another residue or mode of phosphorylation as is seen in some ARRAs as described in section 1.1.5.1.

As stated before, two of the TCSs possess three components, two of which are HKs. Sven15_2343 and Sven15_2344 are separated by 103 bp and divergently expressed. The amino acid sequence of both were aligned showing very little if any homology (Figure 3.3A) despite both proteins being of very similar length. Sven15_4210 and Sven15_4211 are separated by 280 bp and encoded in *cis* (same strand) with 29 amino acids difference between the two proteins. However, when aligned using the program Clustal Omega (Larkin, *et al.*, 2007), both HKs show a high level of alignment in the C-terminal half of the protein (Figure 3.3B). These additional SKs suggest a gene duplication event. In the latter, both SKs possess 4 TM helices, the regions which differ are likely to be a result of mutation build up in the sensor domain of the SKs in the diversification process after expansion. In the case of the former which is very dissimilar, Sven15_2343 is predicted to have 5 TM domains whereas, Sven15_2344 only has 3 TM domains. However, the latter SK also possesses a PAS domain which as discussed before may function as a sensor, signal transduction or binding of ligands. In both these instances, experimental evidence is needed to determine which if not both of the SKs pair with the RR in the regulon.

A

Sven15_2343	-----MLRLPTVPALRRRCVDR-----WAGSPRALDV	26
Sven15_2344	VHEVSPPEQLSLAASLLDALPQAALLLDRDLRVVVRNRCTALLRLTDLDSLPGTDRDHVV	60
	* . * . * * * . * : * * * *	
Sven15_2343	VAALSAFGLMVLVDVPLGARA---DNSLTGVTATLVLAAGAATLVLRRLFPWLPYLVALG	82
Sven15_2344	DH---VAGLL--ARPEERRLLEESGTHGPVTRTTDYHLKDGRTLRRRRAPVLDGEELLG	115
	. * * : * * * . . : * * * . . : * * * * * * *	
Sven15_2343	LMGWLHELMIQFALYSIGRYRGRRAATAATLLYIAVAYGLFPLTPGWPARHGDTLSDFLS	142
Sven15_2344	HL-WLIEDV-----TRRGEAEGLYE	135
	: * * * . * : * * * : . . .	
Sven15_2343	LVVPIGVLAAGVGIAYRQDLVRALEVQRREAAARQAVQEERISVGRDVLVGLVRELTVL	202
Sven15_2344	QVRKLAAL-----ADDRAAFAGRALHELRTPLSTVL	166
	* : . * * * * : * * * * * *	
Sven15_2343	AVRAEVLAVRARGEAHRKDFEELADTARRAHLMLNETIVRRADRDAATPGLGLEAALAGE	262
Sven15_2344	SF-AELLDPAGG-PLSQEQASYVDAIRRNALRMRSVA-----ENLPRTAG-	210
	: . * * : * * * : : . . * : * * * : . . . * * * * *	
Sven15_2343	SERMGSPVELTVAEEAKALSPLRQAAVHR---VVQECLTNAAKHAPGLPVTVTITVEGP	318
Sven15_2344	---GGPV-----AEPRLGQVLVHELIERVVLEALQRAEGAGPY--ITAECPTVG	255
	* . *	
Sven15_2343	DLR-----IEV	324
Sven15_2344	PLIADAGMLTGAEELGNALRFTPEDGRVEVVGKAADHWITIEVGDDGIGVPLEYHEEI	315
	* * : *	
Sven15_2343	RNPLPKTPDPAP--VSTGTGLFSMEERVSMGGTLKARPEGDG---YAVTALLPTGLP	378
Sven15_2344	FTPFVRAPNARRGGYPGTGLGLAGALDTRVRLHGGTITVRDHDGRPGAVFTVRLPLGRAS	375
	. * : : * * . * * * . : * * * * : . . . * * * * *	
Sven15_2343	R	379
Sven15_2344	-	375

B

Sven15_4210	-----MASPRIPAAIRAPFEARTWRAFLYVLVGLPLGICWFALSIA	41
Sven15_4211	MSADLHPAESAGTSSTAGSAVAPRP--PKRTAYGKETWKEIVFLLSNLVTSLVGFVYAVV	58
	. : * * * * * : * : * * * : : * * * * * * * * * * * * * * * * *	
Sven15_4210	FVSTGAGLLITFLGVPILAGALAMCRGFGAVERARARALLDLDVKAPEPVRGTGGAFSW	101
Sven15_4211	SVVLGVGLSITVVGVLPLLALGLGARLIGRSEGRARALLGVEVAEFSRL-PKPGGFFGW	117
	* * . * * * * . : * * * * * . * . * * * * * * * * * * * * * * * *	
Sven15_4210	MGAMLKSGASWRHLLYAVLHMPWAVFSFSVSAFFGWGWLFTYPLWQVFPMPYAGQAGL	161
Sven15_4211	LWTSCLKDPVAWRTQLYGLIRLPWGIPTFTVALVSLIVLWP-----	157
	: : * * . : * * * * . : * * * * * : * * * * * : * * * * * * *	
Sven15_4210	QLYGDGTHGLYLDSPFEIAFTSFVGLLFVMAWPWLLRGCVAVDRLVSLGLGSPSR-LASR	220
Sven15_4211	-----VLFFLSRGLANADRGMRVGLLSPSDELERR	187
	. * : * * * . * * * : * * * * * * * * * * * *	
Sven15_4210	VTELESDRGLVVDTAADLRRIERDLHDGAQARLAALAMDGLAKEKLAEDPRAAAVLVD	280
Sven15_4211	IAELES DRGVVDTAADLRRIERDLHDGAQARLVALAMGLAKEKLLDDPETAAAMVD	247
	: : * * * * * : *	
Sven15_4210	EAHGEVKLALQELRDLARGIHPAVLTDRLDAALS AVASRCVAVPVSVDVLPARPVPAIE	340
Sven15_4211	EAHGEVKLALQELRDLARGIHPAVLTDRLSAAALS SVSARCTVPVKVTVDLTERPAEAI	307
	* *	
Sven15_4210	GIAYFTVSELLRNVTAHARARRAWDVWRSENRLMLQVRDDGVGGAVAVEGRSLSLSAR	400
Sven15_4211	GIAYFTVSELLQNVSKHSRARSASVDVWRTEDELLQVRDDGTGGARLDGGTGLAGLAER	367
	* *	
Sven15_4210	VGAVDGLVAVDSPAGGPTTIVTVELPWRA---	428
Sven15_4211	LGAVDGLLVLDSPGEGPTTITAEIPWRSRPSG	399
	: * * * * * : * : *	

Figure 3. 3: Alignment of protein sequences of SKs from paired TCSs with multiple SKs to a single RR. A) Sven15_2343 and Sven15_2344; B) Sven15_4210 and Sven15_4211. Alignment conducted using Clustal Omega. * refers to conservation of residue, : refers to conservation of strongly similar properties, . refers to conservation of weakly similar properties.

The RRs in table 3.1 were analysed to determine their effector domain families (Figure 3.4). In keeping with other Actinobacteria, as shown in figure 1.5, most effector domains were of the HTH (NarL) type. However, unlike the average of Actinobacteria, where the ratio between NarL and OmpR is fairly even, 59% are NarL and 31% are of the OmpR family. Similar to this, most of the orphan RRs are from the NarL family. This also holds true for *S. coelicolor*, *S. griseus*, *S. albus* and *S. avermitilis* when their genomes were analysed using P2RP (Supplementary material, S1). Interestingly, with the highly reduced genome size of *S. albus* subsp. *albus*, which only possesses one orphan RR, this is a NarL type RR.

Whilst the RRs of *S. venezuelae* are predominantly NarL and OmpR type, the other 10% is composed of CheY, TrxB, AmiR/NasR, and unclassified families. From this group TrxB is not typically associated with TCSs. Here the TrxB family effector of Sven15_0545 possesses two pyridine nucleotide-disulphide oxidoreductase (pyr-redox) domains. Pyr-redox domains are small NADH binding domains within a larger FAD binding. Both of these domains are predicted with an E-value of 0.0002 and 0.0009 which is a low match in comparison to other domains such as the NarL and OmpR types with E-values of 10^{-15} or lower. Further analysis would be needed to determine whether these domains are able to bind NADH or FAD. Whilst the functionality of this RR has not been determined, this RR has a homologue in *S. coelicolor*, however in *S. avermitilis* and *S. griseus*, there are no TrxB type RRs found. This is interesting as *S. avermitilis*, *S. griseus* and *S. venezuelae* share a more recent common ancestor than with *S. coelicolor* (Zhou, *et al.*, 2011B). Two potential explanations of this could be through loss of this TCS from *S. avermitilis* and *S. griseus* due to selection from not requiring this TCS or the gain of this type of TCS is through HGT. Analysis of the conservation of TCS genes could give an insight into the evolution of these TCSs and potentially their importance for species, genus, family or in a wider context of all bacteria.

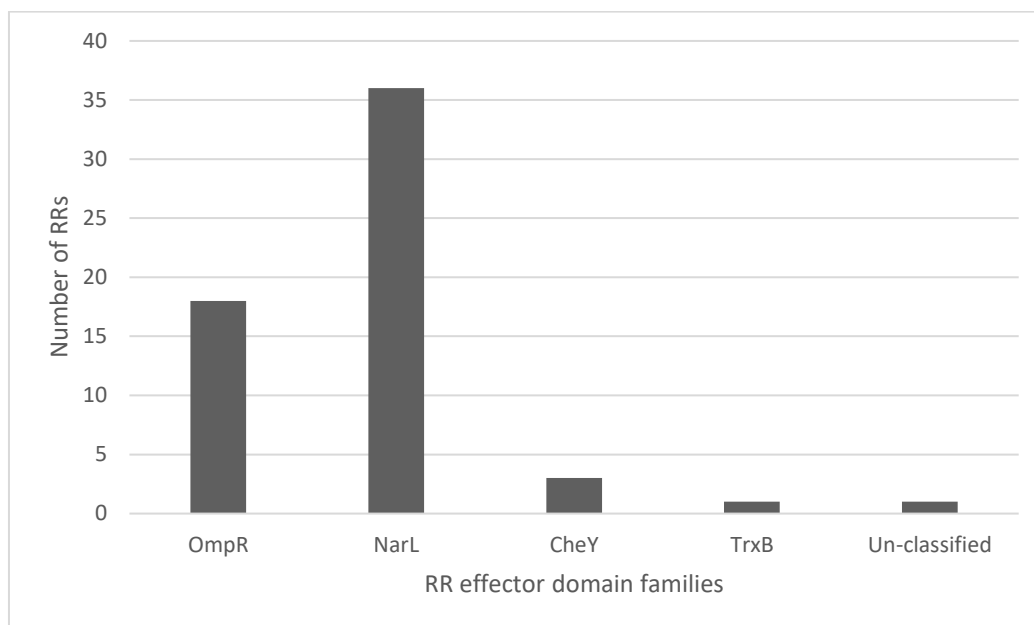


Figure 3. 4: Analysis of RR (from paired TCSs) effector domain protein families. NarL and OmpR refer both to DNA binding domains, CheY which just has a known REC domain, TrxB with possesses two pyr-redox domains, and unclassified which as yet, no known structure has been identified in other studied proteins.

3.3.1.3 Conservation of TCSs

Following the investigation of TCSs within the *S. venezuelae* genome, the genes encoding the individual components were analysed for their conservation within streptomycetes and within other Actinobacteria families to glean whether some TCSs are highly conserved across the phylum Actinobacteria or simply conserved within the *Streptomyces* genus or not conserved at all. This was achieved through use of the online tool ActinoBLAST (Chandra and Chater, 2014) which displays conservation through conducting reciprocal BLASTP analysis of the genes of *S. coelicolor* M145 against genomes of over 100 Actinobacteria (ActinoBLAST) and two other model organisms *B. subtilis* and *E. coli*. Representatives of the five orders and some of the major families within the order *Actinomycetales* are also displayed. Each order and family is represented by a different colour. Figure 3.5 displays the conservation of the paired TCS encoding genes. TCSs where homologues were not identified in *S. coelicolor*, were analysed using the same reciprocal BLASTP technique, by Dr Govind Chandra (JIC). Each box represents a different species and coloured boxes denote the presence of an orthologue. As

shown, few TCSs are conserved throughout the Actinobacteria phylum, but a greater number are conserved largely within the sub-order Streptomycineae.

Many of the TCSs located towards the peripheries (Sven15_0138/0139, Sven15_0439/0440, Sven15_0545/0546, Sven15_0672/0673, Sven15_7022/7023, Sven15_7155/7156 and Sven15_7219/7220) of the linear chromosome are not well conserved in the order or sub-order. With the terminals of chromosomes being more prone to change as described above, this may infer more species specific TCSs or more redundant TCSs, located towards the termini of the chromosomes.

However, this is not to say that TCSs genes located within the central regions of the chromosomes are all highly conserved. Only 25 TCSs were conserved in at least 13 of the 14 species of Streptomycineae. Amongst these 25 TCSs, only 12 are conserved beyond Streptomycineae in other Actinobacteria. Of these 12 TCSs, the most conserved are MtrAB, PhoPR and Sven15_3682/3683.

TCS component name	Sven15 gene	Component type	Streptomycineae	Micromonosporineae	Pseudonocardineae	Streptosporangineae	Frankineae	Corynebacterineae	Propionibacterineae	Micrococccineae	Actinomycineae	Bifidobacteriales	Rubrobacteridae	Coriobacteridae
	0138	HK												
	0139	RR												
	0439	RR												
	0440	HK												
	0545	RR												
	0546	HK												
	0672	RR												
	0673	HK												
	1397	RR												
	1398	HK												
	1479	HK												
	1480	RR												
	1732	RR												
	1733	HK												
	1773	RR												
	1774	HK												
	1916	RR												
	1917	HK												
	1949	HK												
	1950	RR												

3.3.1.4 Adjacent genes of these TCSs

Within the introduction, many genes which are regulated by different TCSs were discussed. Many of these are not encoded within an operon or close to any TCSs. For instance, global regulators such as MtrA or AfsQ1 are not encoded with all the genes they modulate, however, some TCSs are encoded within operons or clusters that they regulate the expression of. To this end, the genes surrounding the TCSs were assessed.

The genes directly adjacent to 4 of the unstudied TCSs are listed in table 3.2. The genes immediately surrounding most of the TCSs did not give an indication of what the role of the TCSs could be related to. Many of these genes encoded hypothetical proteins, membrane spanning proteins or transcriptional regulators, largely of the TetR and LysR families. Although only yielding potential regulatory roles, searching the genes around the TCSs has served as a starting point for inquiry and later investigation.

Table 3. 2: Genes surrounding TCSs of *S. venezuelae* which may give an indication as to their functions.

TCS (<i>sven15_</i>)	Adjacent genes	Potential Purpose or activation stimulus
1773/74	<i>sven15_1772</i> : RND multidrug efflux transporter; <i>sven15_1771</i> : quinolinate synthase	Regulation of the efflux of quinolinate synthesis or other substrates
2151/52	<i>sven15_2153</i> : proposed peptidoglycan lipid II flippase MurJ; <i>SVEN15_2154</i> : tRNA-dependent lipid II-amino acid ligase	Response to cell envelope stress-potentially against cell wall targeting antibiotics or more general salinity or pH stress.
3170/71	<i>sven15_3169</i> : putative TmrB protein-involved in tunicamycin resistance	Tunicamycin resistance
6349/50	<i>sven15_6351</i> : transcriptionally linked with the RR, possesses a GAF domain and a stage II sporulation protein E (SpoIIE) domain. SpoIIE interacts with FtsZ during septa formation of sporulation.	Regulation of sporulation

In addition to searching the genes located immediately adjacent to the TCS, TCSs located within BGCs were also analysed. Table 3.3 shows the TCSs located

in secondary metabolite clusters as predicted by antiSMASH (Weber, *et al.*, 2015). antiSMASH is an online tool which analyses genomes for BGCs by comparison of identified clusters of genes with genes of other known BGCs. The output of this analysis is a prediction of the number of BGCs in the genome, the similarity of genes within these clusters to the genes of the closest characterised BGC and also predicts the parameters of the cluster (i.e. where these clusters start and finish). Of the 30 predicted clusters in *S. venezuelae*, only 5 encoded TCSs. Two of these are identified within a cluster which has been predicted to produce a butyrolactone-type secondary metabolite. As described in yCPK regulation (section 1.2.3.3), butyrolactones can serve in activation of antibiotic biosynthesis. Whilst the BGCs of both chloramphenicol and jadomycin do not possess TCSs, GBL signaling is involved in the activation of jadomycin biosynthesis with JadR3 being a GBL receptor and JadW as a GBL synthase. These could potentially be related. This cluster encodes two proteins marked as ABC transporters, suggesting that the product of this cluster is exported out of the cell. The butyrolactone product may also be involved in quorum sensing (Biarnes-Carrera, *et al.*, 2015).

In section 1.2.3 type II PKSs were discussed, here *sven15_0439/40* is located within a predicted secondary metabolite cluster that shares 20% sequence identity with the BGC of the antibiotic thiotetronate Tu 3010; this cluster encodes a type III PKS, Type I PKS and non-ribosomal peptide synthase (NRPS) which synthesise the core scaffold of the antibiotic, from which other enzymes encoded in the cluster tailor the antibiotic.

Table 3. 3: TCSs found in secondary metabolite clusters as predicted by antiSMASH (Weber, *et al.*, 2015). PKS refers to polyketide synthase and NRPS refers to non-ribosomal peptide synthase.

TCS Genes	Anti-SMASH cluster number	Anti-SMASH cluster type
<i>sven15_439/40</i>	3	Type III PKS-Type I PKS-NRPS
<i>sven15_4978/79</i>	14	Butyrolactone
<i>sven15_4999/5000</i>	14	Butyrolactone
<i>sven15_5306/07</i>	17	Siderophore
<i>sven15_6082/83</i>	22	Ladderane-NRPS
<i>sven15_6686/87</i>	26	Melanin

The TCS encoding genes *sven15_5306/5307* were identified in a cluster predicted to synthesise a siderophore. The antiSMASH report showed two other siderophore biosynthetic clusters in the genome, showing a level of redundancy.

There are also TCSs located in the clusters 22 and 26 which are predicted to synthesise a ladderane molecule and melanin. There is 24% similarity of cluster 22 genes to the genes of skyllamycin, a cyclodepsipeptide that is produced by *Streptomyces* sp. Acta 2897. Whilst some of these percentage of gene similarities is low, these serve as a guide to the types of secondary metabolites these clusters produce and not the actual secondary metabolite. These predictions may give an indication of the type of metabolite production which may be affected if the TCSs regulate the expression of their biosynthetic genes.

3.3.2 Generation of a TCSs deletion library

Following analysis of the TCSs encoded by *S. venezuelae*, generation of a TCSs deletion library (deletion of both SK and RR genes) was decided upon, similar to the deletion library of *E. coli* (Oshima, *et al.*, 2002). In *Streptomyces*, a limited number of methods is available for deletion of genes. The most established being the Lambda Red mediated PCR targeting method established by Gust (2003). This method involves replacing target genes with an antibiotic resistance cassette (aprR) within a cosmid in *E. coli* which is later conjugated into *Streptomyces* where through another round of HR, the genes are exchanged with the cassette (Figure 2.1). Successful double recombinants are selected for using apramycin resistance and kanamycin sensitivity. This method results in marked deletions. The aprR cassette can be excised using FLP-recombinase, however, this still leaves a short scar sequence at the deletion site of 81 bp (Gust, 2003).

Another more recently developed method is through CRISPR/Cas9 gene editing. The use of CRISPR/Cas9 Gene editing in *Streptomyces* allows the deletion of stretches of DNA whether of genes or clusters without the insertion of a marker or scar. The basic premise of the technique is through generation of a targeted DSB which is then repaired through homologous recombination. The targeted DSB is achieved through incorporation of a sgRNA into the Cas9 (CRISPR associated

protein) which is then able to recognise the site complementary to the sgRNA called the protospacer. The excision is made upon recognition of the protospacer followed directly by a NGG PAM sequence. In this study, the vector pCRISPOmyces-2 created by Cobb, *et al.*, 2015 was used. The cloning strategy is demonstrated in figure 2.2.

Both methods were implemented in the generation of the deletion library. CRISPR/Cas9 gene editing was used to delete the TCSs which were not able to be deleted through used of PCR targeting. For both these methods unless otherwise stated double deletions (SK and RR) were made.

3.3.2.1 PCR targeting

The first method used to generate a library of TCS deletions was through the PCR targeting method. All primers were designed by Dr Mahmoud Al-Bassam and mutants were generated by members of the Hutchings group including Dr Mahmoud Al-Bassam, Dr John Munnoch, Elaine Patrick and myself. From this effort, the deletions as listed in table 3.4 were made. The number of exconjugants which were tested to be kanS and aprR are also listed.

The deletion of TCS genes *sven15_6549/50* have been separated to generate the mutants $\Delta 6349$ and $\Delta 6350$. This decision was made as these genes are encoded transcriptionally convergent, furthermore, as stated in table 3.3, *sven15_6350* is transcriptionally linked to *sven15_6351*, which encodes a protein possessing a SpoIIE domain. As the expression of the SK and RR of this system is not through the same promoter, two separate mutants were generated.

Table 3.4: List of TCSs deletions in *S. venezuelae* generated using the PCR targeting method.

TCS deletions	Number of independent mutants
$\Delta 138/139$	3
$\Delta 1732/33$	3
$\Delta 1916/17$	3
$\Delta 2143/44$	3
$\Delta 2151/52$	3
$\Delta 2695/96$	3
$\Delta 2739/40$	2
$\Delta 3232/33$	2

$\Delta 3326/27$	2
$\Delta 3393/94$	2
$\Delta 3472/73$	1
$\Delta 3682/83$	1
$\Delta 5286/87$	1
$\Delta 5323/24$	1
$\Delta 5393/94$	1
$\Delta 5397/98$	2
$\Delta 5426/27$	2
$\Delta 5435/36$	2
$\Delta 5634/35$	2
$\Delta 56345/46$	1
$\Delta 5973/74$	2
$\Delta 5985/86$	2
$\Delta 6082/83$	2
$\Delta 6349$	2
$\Delta 6350$	2
$\Delta 6371/72$	1

3.3.2.2 CRISPR/Cas9

From the PCR targeting method 26 TCS deletion mutants were generated. Some of these only yielded one successful double cross-over mutant. To generate the remaining mutants and to create more mutants where only one was successfully identified through PCR targeting, CRISPR/Cas9 was used. The work presented in this section was carried out solely by myself.

As discussed above the CRISPR/Cas9 gene editing technique used in this study was developed by Cobb, *et al.*, 2015. A number of TCS genes either overlapped or were very close to adjacent genes, so to prevent polar effects on surrounding genes, in frame deletions were made where short residual TCS gene sequences were retained. All primer sequences for amplification of the homology arms, primers used for sequencing and also PCR confirmation are presented in table 2.3.

After cloning homology sequences and protospacer sequences into pCRISPOmyces-2 and confirming them by sequencing, the vectors were introduced into *S. venezuelae*. After three generations of restreaking first on apr selective media (MYM) and then under non-selection, colonies were picked and colony PCRs were carried out using diluted crude lysates to determine the success of the CRISPR/Cas9 editing. As described before, three sets of PCRs were conducted to affirm the success of the deletion: internal, flanking and external. External PCR

primers are designed so that each primer is close to the gene of deletion yielding a fragment size of <800 bp if the deletion was made. Internal PCRs refer to one primer being situated outside of the genes deleted but within the originally amplified homology arms and the other primer within the gene, yielding no band if the deletion was successful and a band of less than 700 bp should the deletion be unsuccessful. Flanking PCRs are where the primer pair is situated outside the original homology sequence. These PCR products were over 2000-3000 bp if the deletion was successful and even larger if the wild-type genotype was retained. Due to the size of the product, these PCRs demonstrated a lower amplification efficiency with the lysates and would often need to be diluted down further.

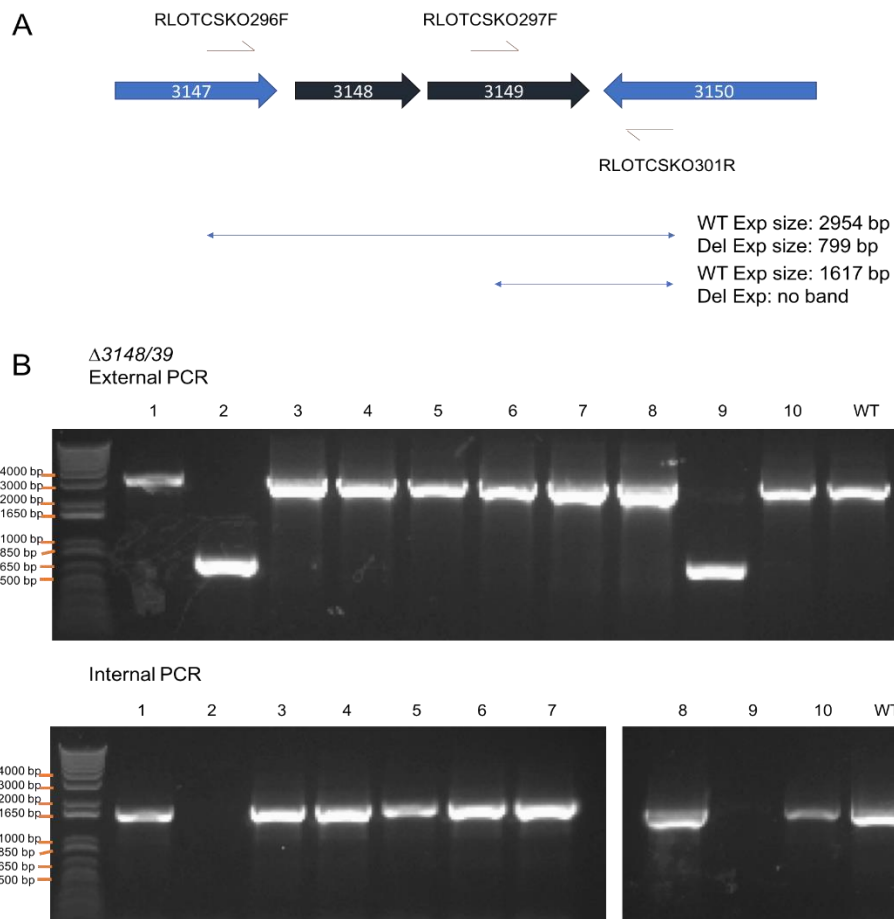


Figure 3.6: PCR confirmation of deletion of $\Delta 3148/49$ ($\Delta cseBC$) through use of CRISPR/Cas9. A) PCR strategy using primers RLOTCSKO296F, RLOTCSKO297F paired with RLOTCSKO301R for external and internal PCR, respectively. Expected (Exp) sizes of wild-type (WT) and successful deletion (del) are shown. B) Results of external (top row) and internal (bottom) PCR. Numbers refer to independent mutant colonies in comparison to WT.

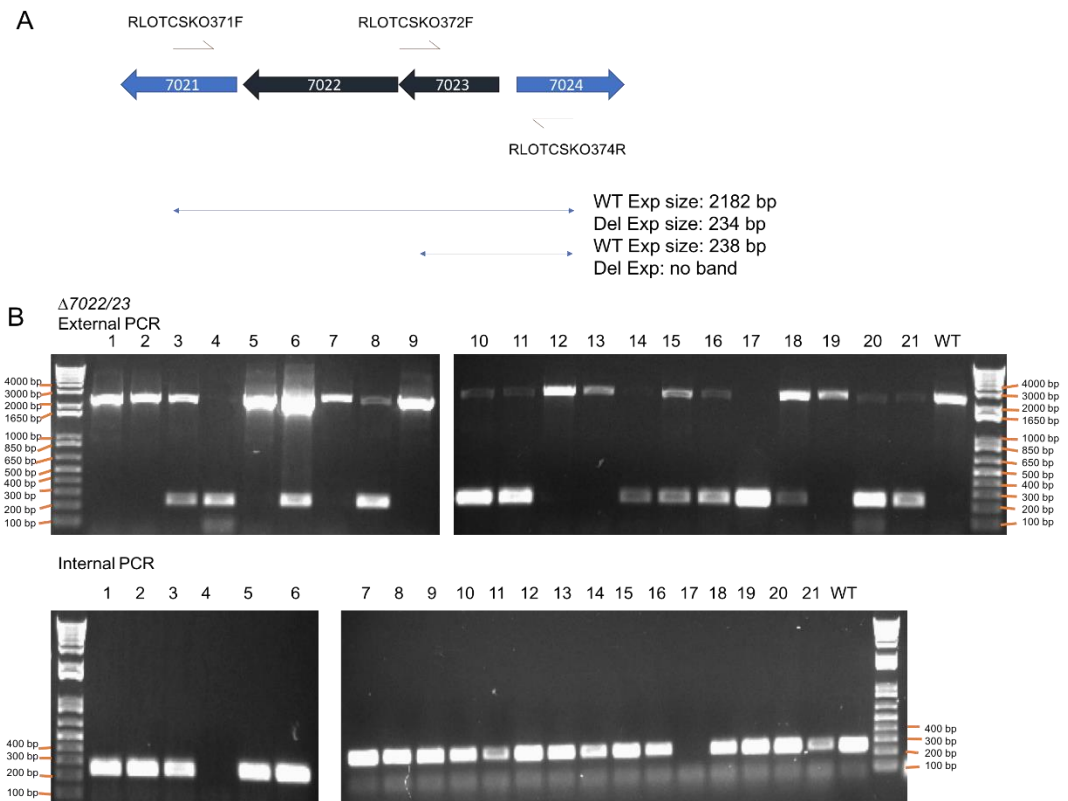


Figure 3.7: PCR confirmation of deletion of $\Delta 7022/23$ through use of CRISPR/Cas9. A) PCR strategy using primers RLOTCSKO371F, RLOTCSKO372F paired with RLOTCSKO374R for external and internal PCR, respectively. Expected (Exp) sizes of wild-type (WT) and successful deletion (del) are shown. B) Results of external (top row) and internal (bottom) PCR. Numbers refer to independent mutant colonies in comparison to WT.

Examples of internal and external PCRs are displayed in figures 3.6 ($\Delta 3148/49$) and 3.20 ($\Delta 7022/23$). From figure 3.19B colony number 2 was selected from this round of PCR and stocked and from figure 3.7B colonies numbers 4 and 17 were stocked. For colonies which have a faint WT band as seen in figure 3.6B mutant 9, PCRs were either repeated or other exconjugants selected for further rounds of PCR.

Table 3.5 lists the deletions made using CRISPR/Cas9. There are 3 deletions which match those in table 3.4 which are $\Delta 3393/94$, $\Delta osaAB$, and $\Delta 5286/87$. Typically, the frequency of finding successful deletion mutants ranged between 5% to 30%. Per each round of PCR screening, 10-20 colonies are selected.

Initial PCR tested deletions were also further confirmed through sequencing using primers described in table 2.3. Sequenced mutants include $\Delta 1773/74$, $\Delta 3393/94$ and $\Delta 3682/83$.

Table 3.5: Number of independent deletions made per mutant using CRISPR/Cas9 gene editing.

TCS deletions	Number of independent mutants
$\Delta 1397/98$	2
$\Delta 1773/74$	3
$\Delta 1949/50$	3
$\Delta 3148/49$ ($\Delta cseBC$)	3
$\Delta 3170/71$	2
$\Delta 3364/65$	1
$\Delta 3393/94$	3
$\Delta 3682/83$	3
$\Delta 3736/37$	2
$\Delta 3785/86$	3
$\Delta 3821/22$	3
$\Delta 3873/74$ ($\Delta phoPR$)	3
$\Delta 4209/10$	2
$\Delta 4209/10/11$	3
$\Delta 4373/74$ ($\Delta esrRS$)	2
$\Delta 4474/75$ ($\Delta afsQ$)	2
$\Delta 4999/5000$	3
$\Delta 5214/15$	1
$\Delta 5286/87$ ($\Delta osaAB$)	2
$\Delta 5306/07$	1
$\Delta 5349/50$	2
$\Delta 5558/59$	3
$\Delta 6686/87$	1
$\Delta 7022/23$	1
$\Delta 7155/56$	2
$\Delta 7219/20$	2

3.3.2.3 TCSs to be deleted

Currently, the deletion library has yet to be completed. Table 3.6 lists the remaining mutants as well as the status of these deletions. The initial search for TCSs within the *S. venezuelae* genome was through BLAST analysis, however, this did not result in 59 paired TCSs being identified. The remainder were identified later, through later implementation of P2RP (*sven15_0439/0440*, *sven15_0545/0546*, *sven15_2343-2345* and *sven15_3541/42*). This coupled with the fact that the high GC content of *Streptomyces* makes Gibson Assembly of pCRISPomyces-2 vectors difficult means $\Delta 2534/35$, $\Delta 3934/35$ and $\Delta 4209/11$ were not deleted in this project.

Table 3.6: Remaining TCSs of *S. venezuelae* to be deleted to complete library of deletions and stage of generation.

TCS deletions	Stage of deletion
$\Delta 0439/40$	Deletion vector not made
$\Delta 0545/46$	Deletion vector not made
$\Delta 0672/73$	No successful mutants identified
$\Delta 1479/80$	No successful mutants identified
$\Delta 2343/44/45$	Deletion vector not made
$\Delta 2534/35$	Deletion vector not made
$\Delta 3541/42$	Deletion vector not made
$\Delta 3934/35$	Deletion vector not made
$\Delta 4209/11^*$	Deletion vector not made
$\Delta 4924/25$	No successful mutants identified
$\Delta 5558/59$	No successful mutants identified

* $\Delta 4209/11$ has yet to be made but $\Delta 4209-11$ and $\Delta 4209/10$ has been made

For $\Delta 1479/80$, two independent protospacers have been designed and cloned into the deletion vector, however, after PCR testing over 40 colonies, no successful mutants have been identified. For the remaining two TCSs to be deleted ($\Delta 4924/25$ and $\Delta 5558/59$) despite also testing over 40 exconjugants of each, no successful mutants have been identified. The protospacer of these may need to be adjusted to improve efficiency. However, as the deletion of these three TCSs was previously attempted using PCR targeting, these TCSs may play an important role in survival of *S. venezuelae* which prevents their deletion from the genome.

3.3.3 Characterisation of TCS deletion mutants

3.3.3.1 $\Delta 1773/74$

In the process of generating the mutants and growing them for spore stocking, phenotypes differing from wild-type *S. venezuelae* were observed from $\Delta 1773/74$. Figure 3.8 and figure 3.9 shows the growth of $\Delta 1773/74$ on MYM media for 2 days and 3 days, respectively, in comparison to wild-type *S. venezuelae*. After 2 days of growth, more melanin is produced in the mutants than the wild-type. After growth for an additional day, droplets were seen on the surface of the mutants. These droplets were very viscous in consistency and were present only for a short time frame before dissipating. *S. venezuelae* wild-type was grown under the same conditions for the same amount of time and for longer to observe whether similar

droplets formed. Droplets were found on wild-type plates but not consistently and not to the same degree as in the mutants.

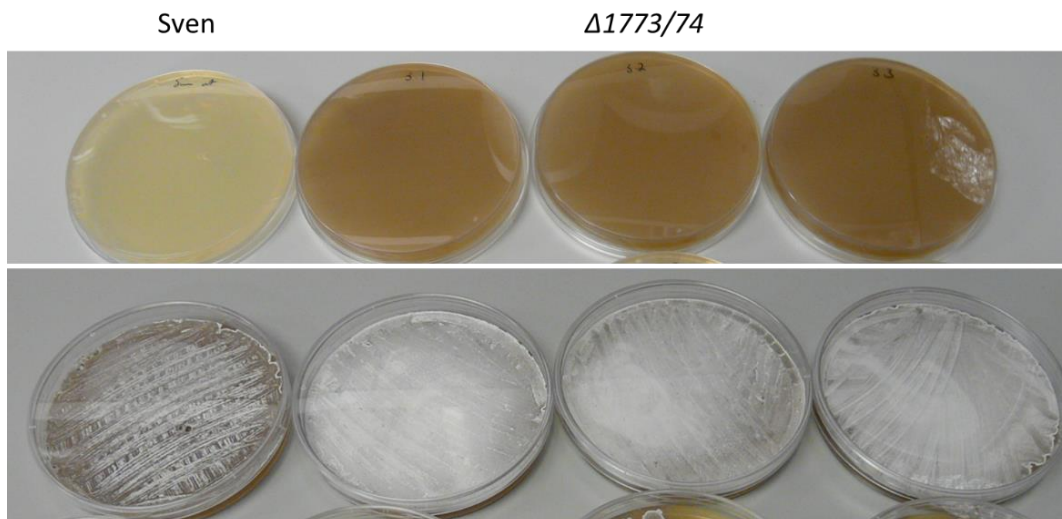


Figure 3.8: *S. venezuelae* wild-type (both plates to the left) and the three independent $\Delta 1773/74$ mutants cultured on MYM agar for 2 days. Top row shows the base of the plates and bottom row shows top view.

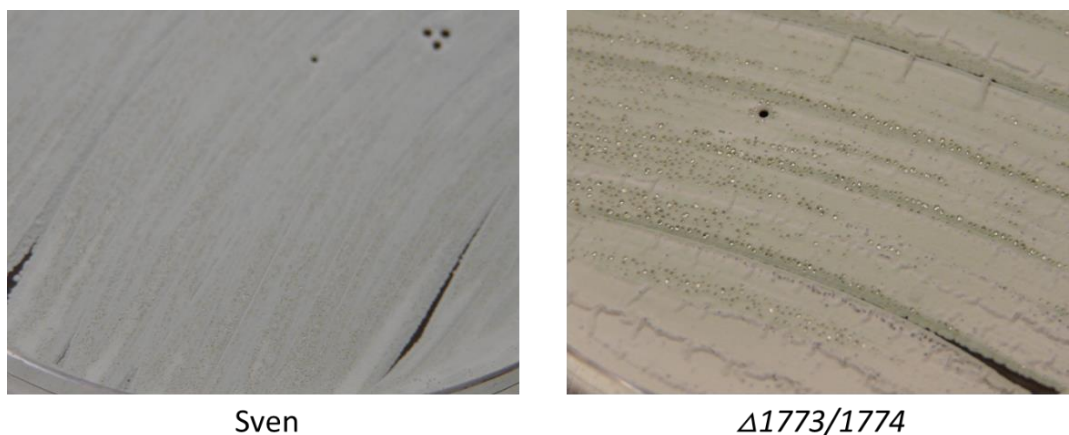


Figure 3.9: *S. venezuelae* wild-type (left) and $\Delta 1773/74$ mutant (right) cultured on MYM for 3 days.

The genes *sven15_1773/74* are quite well conserved within *Streptomyces*. Whilst this is not found within a secondary metabolite cluster, it could be regulating the efflux of metabolites. As discussed earlier, genes surrounding the TCSs were analysed (Table 3.2). Two genes of note neighbouring this TCS are an RND (resistance nodulation-division) efflux pump and a quinolinate synthase. RND transporters are a family of efflux pumps which can confer resistance to antibiotics. They can associate with other proteins that either span the membrane or in the case of Gram-negative bacteria, are periplasmic

proteins that aid in the capture and transport of substrates (Nikaido and Takatsuka, 2009). If the RND efflux pump is regulated by the TCS, this could explain the secretions. In addition to the RND transporter, another gene that could be under the regulation of the TCSs is the quinolinate synthase. Quinolinate is synthesised from aspartate in bacteria. It is also a precursor of the NAD cofactor (Sorci, *et al.*, 2013). Quinolinate is a colourless solid compound, this could be secreted if it is overexpressed following deletion of the TCS. It is unclear whether the TCS regulates the expression of these two genes. Further analyses such as electrophoretic mobility shift assays (EMSAs) and qRT-PCR could be used to test this. The latter would determine whether there is an expression difference between the wild-type and mutant and if so, an EMSA could be carried out to determine interaction between the RR and the gene promoters to see if the effect is direct.

3.3.3.2 $\Delta 3170/71$

The neighbouring gene of *sven15_3170/71*, is *tmrB* (*sven15_3169*) which encodes a membrane bound protein responsible for conferring resistance against the antibiotic tunicamycin. Tunicamycin is thought to enter the cell by binding to cell surface proteins and being transported into the cell. TmrB binds tunicamycin and is either thought to actively pump tunicamycin from the cell or interact with other pumps to do so (Noda, *et al.*, 1992; Noda, *et al.*, 1995).

With this information, a tunicamycin resistance assay with the mutants and wild-type *S. venezuelae* was carried out. Figure 3.10 shows that the mutant strains are more sensitive to tunicamycin than the wild-type as can be seen from the larger zones of inhibition surrounding the disks which contain increasing concentrations of tunicamycin. As tunicamycin was dissolved in methanol, methanol was used as a negative control. *S. venezuelae* is not resistant to vancomycin, which has been used here as a positive control, however, the lack of any zone of inhibition would suggest the vancomycin had degraded. This mutant is in the process of being complemented (data not shown).

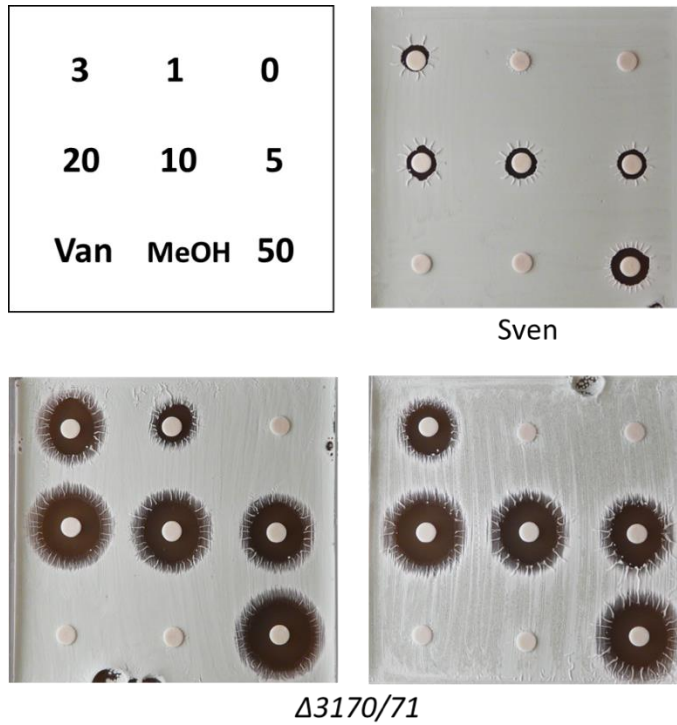


Figure 3.10: Assay of *S. venezuelae* wild-type and the isogenic $\Delta 3170/71$ mutant in the presence of tunicamycin at different concentrations (0, 1, 3, 5, 10, 20 and 50 μl of a 1 mg/ml stock) on each disk. Van refers to vancomycin (10 μl of 10 $\mu\text{g}/\text{ml}$) and methanol refers to 50 μl of methanol. All disks were dried before application to plate. Confluent lawns were prepared by spreading a cotton bud soaked in 10^7 spores over the entire plate.

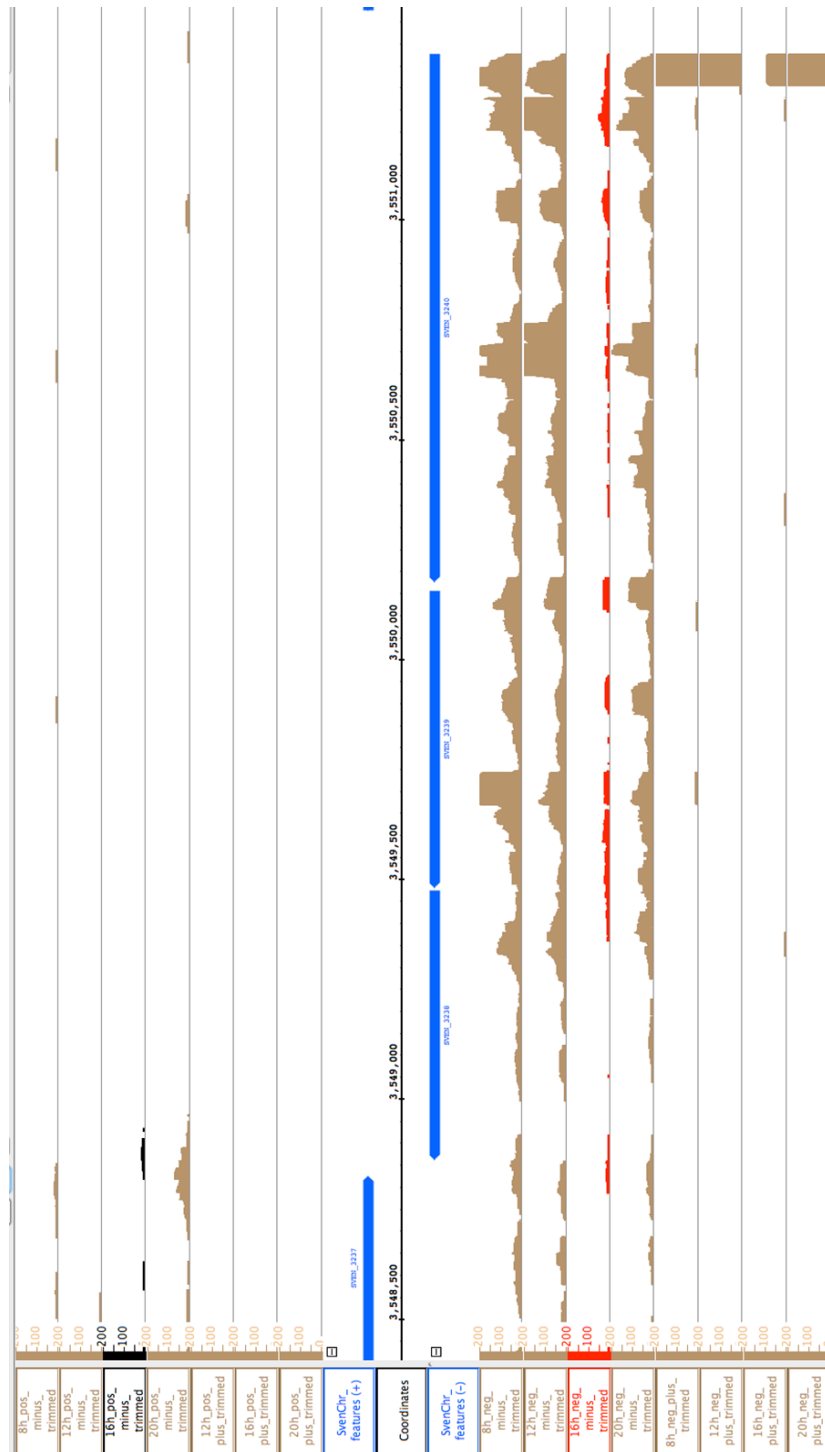


Figure 3.11: Differential RNA sequencing data for *sven15_3169-3171* at 8 hrs, 12 hrs, 16 hrs and 20 hrs after growth of *S. venezuelae* wild-type in liquid MYM (Munnoch, *et al.*, 2016). *S. venezuelae* numbers shown here reflect the gene numbers from a different annotation of the same species (NRRL B-65442) genome; *sven_3238* refers to *sven15_3169*, *sven_3239* refers to *sven15_3170* and *sven_3240* refers to *sven15_3171*.

Between the start and stop codon of the RR *sven15_3170* and *tmrB* are 3 bp. Whilst this is too short for a promoter sequence, the promoter of *tmrB* may overlap with *sven15_3170*. Therefore, the deletion of *sven15_3170* may result in

polar effects. Transcriptional start site data from differential RNA-seq data courtesy of Dr John Munnoch was hence analysed and shows that *tmrB* is expressed on a leaderless mRNA starting from the HK (Sven15_3171) through to *tmrB*. From the data, these genes are expressed throughout the time points, but is expressed at its lowest levels at 16 hrs (Figure 3.11). The 16 hr time point is associated with the change from vegetative growth to aerial growth in *S. venezuelae* grown in MYM liquid (Bush, *et al.*, 2013). This drop in expression may be a means for the cell to concentrate all resources to express the many genes required for this switch. Whether this is a change due to sigma factors required for the expression of this gene is unknown. The levels of both proteins (Sven15_3170/3171) already within the cell may be sufficient to initiate a resistance response should tunicamycin be present.

3.3.3.3 $\Delta 3682/83$

Another TCS of interest was the highly conserved Sven15_3682/83. This TCS is one of the most conserved across Actinobacteria with a similar level of conservation to MtrAB and PhoPR. Growth of the mutants on MYM, MM (Figure 3.12) and SFM did not give rise to any non-wild-type phenotypes. However, looking at the downstream genes of two glycosyl transferases, a transporter and transcriptional regulator (Figure 3.13), this TCS may be involved in regulating the synthesis of a metabolite by addition of sugar moieties. The TetR regulator could be sensing the abundance and repressing further biosynthesis whilst the transporter could be transporting the compound in or out of the cell. It is currently unclear as to the nature of this TCSs, however, the high conservation suggests a high demand for this system in the bacteria, warranting further investigation.

Sven



$\Delta 3682/83$

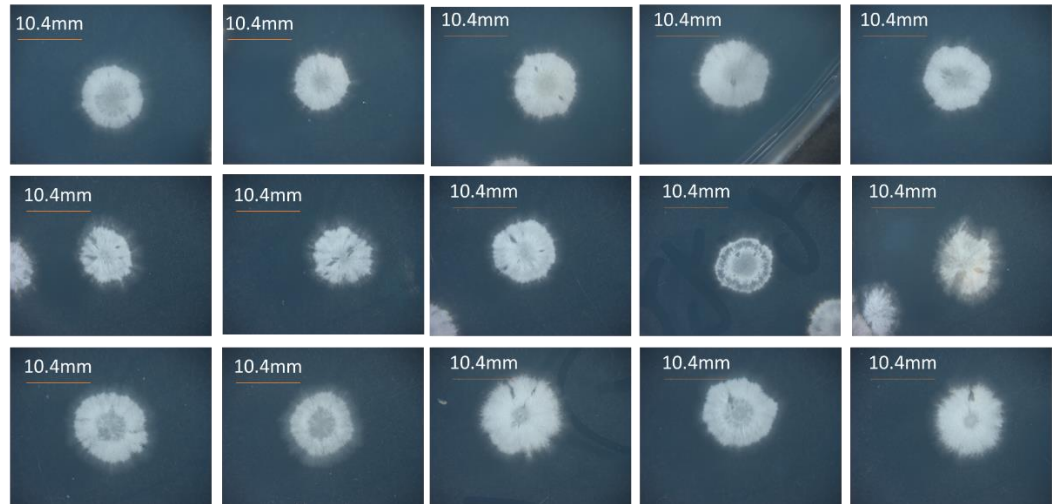


Figure 3.12: Colony morphology of *S. venezuelae* and 3 independent $\Delta 3682/83$ mutants grown on MM for 7 days.

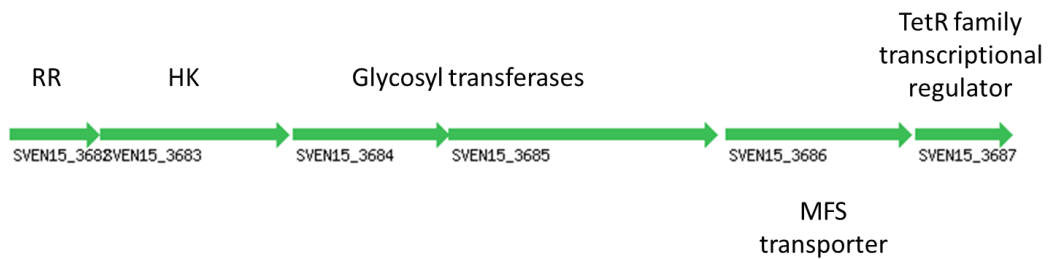


Figure 3.13: Neighbouring genes of the *sven15_3682/82* with predicted functions annotated (edited from Marchler-Bauer *et al.*, 2007).

3.4 Discussion

3.4.1 Distribution of TCSs within the genome

The number of orphan SKs and RRs is fairly even at ~60% and 40%, respectively, taking into account the total number of SKs and RRs, this difference is reduced to 53% and 47%. This is consistent with the research conducted by Williams and Whitworth (2010) who analysed the distribution of over 40000 TCSs proteins over 1405 bacterial replicons. As TCSs typically function as a pair this would explain the even distribution, the slightly higher number of orphan SKs to

RRs may be a random loss within the genome or be due to SKs containing more domains which would need an accumulation of more mutations for them to not be recognised in genome analysis. Another potential explanation could be that some of these SKs are functioning with other RRs within TCSs pairs. As is seen with two of the TCS pairs already mentioned (Sven15_4209-11 and Sven15_2343-45).

In the two instances where there are multiple components within system, Sven15_2343-2345 and Sven15_4209-4211, further experimental data would be needed to determine whether both SKs pair with the RR. Here $\Delta 4209/10$ and $\Delta 4209-11$ mutants have been made. $\Delta 4210/11$ and $\Delta 4209/11$ could also be made to test these. Mutants of the TCS Sven15_2343-2345 have yet to be made. Once these genes have been deleted, the mutants could be tested under a range of different conditions to see if any display a phenotype. If the RR is able to be phosphorylated by other phospho-donors within the cell, this may prove easier to test as the presence of the SK may dephosphorylate the RR. If no phenotype is obvious in both these instances, a phospho-transfer assay could be carried out with purified RR and cytoplasmic regions of the SKs, to identify if both SKs are able to phosphorylate the RR.

3.4.2 Generating a paired TCS deletion library

The use of the two different mutagenesis methods has allowed greater efficiency in disrupting the genes. Both methods utilised have different advantages. The use of CRISPR/Cas9 allowed scarless in-frame mutants to be made, whereas, the use of PCR targeting does not require identification of a unique protospacer sequence which may have different efficiencies. In the process of generating the mutants through use of CRISPR/Cas9, there was a large range in the efficiency. For some mutants, efficiency was as high as 30-50% when analysing the exconjugants. In other mutants, there was <5% efficiency. As few as 10 colonies have been tested and as many as 60 colonies to attain successful deletion mutants.

In the second method of CRISPR/Cas9 gene editing, a DSB break was made through the enzyme Cas9 under the guidance of the template gRNA. The DSB could be repaired by NHEJ or HR. In both repair mechanisms, the DNA sequence complementary to the template would be lost. *S. venezuelae* possesses the

conserved genes necessary for NHEJ (*sven15_4895* (*polK*), *sven15_4896* (*kuA*), *sven15_6252* (*ligC*), *sven15_6253* (*polC*), which unlike the described system of *E. coli* of Ku and LigD possesses more elements. This is in addition to the variably conserved NHEJ genes *sven15_0576* (*polO*) and p*Sven15_0093* (*kuB*), which Hoff, *et al.*, (2016) showed increased the sensitivity of the bacteria to DNA damage. The presence of the variably conserved subset of genes linked with the conserved genes may explain why NHEJ was so prevalent among the exconjugants.

Of the TCSs yet to be disrupted, a subset which have been targeted by both PCR targeting and CRISPR/Cas9 have the potential to be essential. As previously discussed *sven15_1479/80*, *sven15_4924/25* and *sven15_5558/59* are TCSs which are yet to be deleted despite using two deletion methods. To test whether these are essential genes, a second copy could be inserted into a phage integration site and PCR targeting could be repeated. This begs the question of whether any of the TCSs in *S. venezuelae* are essential. As the nature of TCSs is to sense different stresses, if the conditions of environment are highly favourable, it seems unlikely that deletion of any individual TCS would be lethal. MtrA has been shown to be essential in *Mycobacterium* due to regulation of *ftsZ* expression (Zahrt and Deretic, 2000), however, it is not essential in *Streptomyces* due to the nature of division of these bacteria.

3.4.3 Characterisation of specific deletion mutants

The TCS *Sven15_3682/3683* is more conserved in Actinobacteria than both the global and pleiotrophic regulating TCSs MtrAB and PhoPR, respectively. The high conservation suggests that this TCS plays an important role in regulation, whether this is in growth, development, primary or secondary metabolism or genome maintenance is unknown. The conservation analysis (figure 3.5) shows that this TCS is conserved in most orders of Actinobacteria but not in the suborder of Coriobacteriidae. The order of Coriobacteriales are non-motile, non-spore forming bacteria capable to living in anaerobic conditions. Gupta, *et al.*, (2013) identified one conserved signature indel that linked Coriobacteriales to Actinobacteria. This article was released a year after the suggestion that Coriobacteriales should not be part of the Actinobacteria phylum due to lack of conserved signature proteins of

Actinobacteria were present in the Coriobacteriales (Gao and Gupta, 2012). This demonstrates the significant differences between this suborder and the others compared in the ActinoBLAST conservation data (Figure 3.5; Chandra and Chater, 2014), causing more difficulty in finding out what this TCS is involved in. The deletion mutant $\Delta 3682/83$ did not present any unusual phenotypes when grown in rich or minimal media. However, if the analysis of the downstream genes is related to the TCS, analysis of the metabolomics of the strain in comparison to the wild-type is a potential route to deduce its function.

Whilst TCSs do not necessarily regulate adjacent genes, the approach of analysing these has allowed the identification of TunRS. From the dRNA-seq data, as the three proteins are expressed from one single transcript, it would be interesting to analyse whether TunR up-regulates the expression of the three genes or whether the basal level expression of the three is sufficient. Complementation of the TCS would be needed to analyse whether any polar effects were generated in the deletion process. If TunR up-regulates expression in the presence of tunicamycin, the promoter region could be used as an inducible promoter.

The other TCS mutant which demonstrated a phenotype was $\Delta 1773/74$. As discussed, it is unclear what the surface droplets might be. If quinolinate synthase expression is regulated by this TCS, potentially this could be the droplets, this could explain the potentially faster growth rate as well, however, this would need to be fully tested. If more quinolinate is present, more NAD co-factor could be generated resulting in faster growth and development to sporulation. In addition to its use in REDOX reactions, the cofactor is also required in the ribosylation of ADP in the regulation of DNA repair (Ziegler and Oei, 2001). To test whether the TCS is involved in quinolinate regulation, the droplets could be analysed through methods such as LCMS, however, the collection of a sufficient volume without collection of the spores would prove difficult. Another means to test could be assay with different DNA damaging agents to see if there is a drop or increase in viability.

Thus far, the TCS mutants corresponding to those found within antiSMASH predicted secondary metabolite clusters have yet to be analysed. However, these TCSs are not conserved across Actinobacteria or in *Streptomyces*. Whilst *Streptomyces* can possess very different secondary metabolite profiles, it is

important to note, that even the TCS thought to be found in the melanin biosynthesis cluster is also not well conserved. For the deletion mutants of these TCSs, it would be interesting to analyse the exudates to see whether there is a change in melanin production.

For the two TCSs situated within the predicted butyrolactone biosynthesis gene cluster, different *Streptomyces* spp. in addition to bacteria of other orders or families could be co-cultured or grown in close proximity, to determine whether there is a change in signaling or sensing of other bacteria (Hughes and Sperandio, 2008). In addition to butyrolactone, *S. venezuelae* is also predicted to possess two terpene biosynthesis clusters. It would be interesting to investigate whether any of the other mutants might react to terpenes produced by other bacteria, differently to wild-type. For instance, with the explorer phenotype witnessed when a volatile organic compound, first seen with yeast, is exposed to *S. venezuelae* (Jones, *et al.*, 2016). It would also be interesting to analyse whether the production of these terpenes or other volatile compounds may be affected.

3.4.4 Characterisation of deletion library

Over 20 of the deletion mutants have been screened on solid MYM and MM (data not shown), however, no significant phenotypes were observed. Other high throughput conditions of screening may be to co-culture the strains with other *Streptomyces* sp., grow with different stresses including the previously mentioned DNA damaging agents, high salinity, high temperature and cell wall damaging agents.

Analysis of the transcriptional data, as seen in figure 3.9, may allow a better understanding of when the TCS is expressed at the highest and lowest levels. Whilst this does not provide information as to the role of the TCS, it may give an indication of what stage of development the TCS could be related to. Furthermore, it would show whether adjacent genes are transcriptionally linked with the TCS regulon.

With *Streptomyces* being such prolific producers of secondary metabolites, whether the TCSs were identified within the clusters or not, analysis of the exudates through carrying out mass spectrometry on spent medium and also gaseous exudates would be a good means of analysis. As a means of testing whether more

chloramphenicol is produced in the deletion strains, growth besides *E. coli* or *B. subtilis* could be tested.

3.4.5 Further characterisation of TCSs

Generation of these mutants is the beginning of many experiments to try to elucidate their roles within *S. venezuelae*. Unlike *S. coelicolor*, which has long been established as a model organism, this relatively new emerging model organism, needs to be better characterised and has many advantages, including more rapid growth and differentiation in liquid medium. The characterisation of these TCSs may also allow better understanding of their role in other *Streptomyces* species or other actinobacteria. In doing so, it may also allow manipulation and utilisation of these TCS to modulate antibiotic production in this industrially important group of bacteria.

Other means in which the TCSs of *S. venezuelae* could be better studied in addition to analysis of the strains within the TCSs deletion library include cloning phosphomimetic RRs back into the strains and FLAG-tagging the RRs and conducting CHIP-Seq analysis. As not all TCSs may be stimulated under laboratory conditions, the addition of phosphomimetic RRs back into the deletion background may give rise to altered phenotypes or changed metabolomes. As seen with cloning a phosphomimetic allele of *afsQ1* into different environment *Streptomyces* strains, the effects may be lethal (Daniel-Ivad, *et al.*, 2017). This may be the case with some of these strains. In strains where a phenotype is observed, a FLAG-tagged allele of the RR could be cloned to conduct ChIP-seq analysis to determine what genes the RR may regulate.

In addition to characterisation of the paired TCSs within *S. venezuelae*, it would also be interesting to determine whether any of the orphan components are able to phosphorylate any of the other orphan components or are linked with any of the paired TCSs. To study this RRs and SKs (cytoplasmic regions) could be purified and have phospho-transfer assays performed whereby the SK is inoculated with radioactive ATP before addition of the RR to test for transfer. This type of *in vivo* analysis has been widely used in studies (Skerker *et al.*, 2005; Skerker, *et al.*, 2008; Pawelczyk, *et al.*, 2012).

Finally, to better understand environmental recognition led signal relay, it would be interesting to generate a deletion library of one-component systems. The analysis of the *S. venezuelae* genome using P2RP showed that there are 138 one-component systems within the genome, more than twice the number of paired TCSs. The domains among these one-component systems is highly diverse including BTAD (Bacterial Transcriptional Activation domain) which is found in SARPs. As one-component systems are thought to be more stable and have less transient signal transduction due to not relying on phosphotransfer, the output response to these stimuli may have more lasting effects. In understanding the signaling system within these fascinating bacteria we can piece together the complex network which may allow us to develop these bacteria into factories of secondary metabolite producers or as organic pesticides.

4. Exploring purification methods of a full-length SK

4.1 Chapter overview

This chapter presents work carried out in an attempt to purify full-length VanS, a membrane bound SK from *S. coelicolor*. This was carried out in an effort to determine the mode by which vancomycin activates VanS, i.e. through direct binding or through vancomycin binding to VanS once in a complex with a cell wall precursor. However, due to difficulties encountered in expression, purification, treatment and storage, this was not able to be achieved. Here, the different approaches taken have been shown and discussed.

4.2 Introduction

Vancomycin is a glycopeptide antibiotic first discovered in 1952 from a mud sample from Borneo containing *S. orientalis* (Levine, 2006). From resistance studies using *Staphylococcus*, after 20 passages there was only an increase of resistance of 4-fold by vancomycin in comparison to 1000-fold by penicillin (McGuire, *et al.*, 1955). Despite clinical trials showing vancomycin was effective against infections which other antibiotics available at the time could not treat, the discovery of new antibiotics (e.g. methicillin and cephalothin), also in the 1950s, coupled with toxicity issues saw vancomycin's use reserved as a last resort antibiotic or for patients who could not use β -lactams (Levine, 2006). It was not until the early 1980s that the use of vancomycin was revived for infections such as MRSA and methicillin resistant *Enterococcus* (MRE; Levine, 2006). However, by 1986, despite initial low resistance frequency displayed in trials, clinical resistance was emerging. Today many guidelines are clinically in place as to when vancomycin can be administered.

Different types of vancomycin resistance were noted in *Enterococcus* species, VanA-G types which have been briefly discussed in section 1.3.2.3. VanA and VanB type resistance in *Enterococcus* is not intrinsic like VanC type identified in *E. casseliflavus* and *E. gallinarum* (Cetinkaya, *et al.*, 2000). VanA and VanB

type resistance are both acquired through large mobile elements capable of being exchanged between different species (Arthur, *et al.*, 1993; Cetinkaya, *et al.*, 2000).

The resistance to vancomycin identified in *S. coelicolor* most closely matches with VanB type. This resistance is conferred by *vanHAX* genes which are orthologous to those in *Enterococci* (Hong, *et al.*, 2004). The expression of these genes are induced by the TCS VanRS. In *S. coelicolor* two additional genes were identified in the regulon, *vanK* and *vanJ*. The function of the encoded proteins has been described in section 1.3.2.3. In summary, resistance is caused by a change in the terminal peptide of peptidoglycan precursors which reduces binding by vancomycin about 1000-fold.

	<i>S. lividans</i>	<i>S. viridochromogenes</i>	<i>S. scabiei</i>	<i>S. viceus</i>	<i>S. avermitilis</i>	<i>S. griseoflavus</i>	<i>S. venezuelae</i>	<i>S. griseus</i>	<i>S. hygroscopicus</i>	<i>S. pristinaespiralis</i>	<i>S. roseosporus</i>	<i>S. albus</i>	<i>S. clavuligerus</i>	<i>Kitasatosporabetae</i>
<i>vanS</i>														
<i>vanR</i>														
<i>vanJ</i>														
<i>vanK</i>														
<i>vanH</i>														
<i>vanA</i>														
<i>vanX</i>														

Figure 4.1: Conservation of *vanRS* regulon within Streptomycineae based on ActinoBLAST results using *S. coelicolor* as reference (Chandra and Chater, 2014). Boxes filled in magenta show presence of homologue.

The *van* genes are not well conserved within *Streptomyces* as shown in figure 4.1. The TCS encoding genes are more conserved than the resistance genes. As HGT typically results in the maintenance of genes clustered together, it seems unlikely that these genes were acquired through HGT. However, as conservation of TCSs is extremely hard to validate as speciation can result in vast changes of certain structural regions of the two proteins and not others, these orthologues may not be true orthologues and instead a TCS which shares similar structure. Figure

4.1 shows that paralogues of VanRS are found in *S. venezuelae*, but this species is sensitive to vancomycin and does not possess the resistance genes *vanJKHAX* (Marcone, *et al.*, 2010; Chandra and Chater, 2014).

It is important to understand VanS and its mechanism of interaction. It is through this understanding that methods which prevent vancomycin binding to VanS could be developed to bypass resistance and allowing vancomycin's continual effective use against infections. As VanS is not the sole phospho-donor to VanR, the deletion of VanS causes the bacteria to constitutively express the *van* genes. Therefore, antagonising VanS may simply prevent dephosphorylation of VanR and hence cause the bacteria to constitutively express the *van* genes.

As previously discussed (section 1.3.2.3), VanS is thought to bind to a complex formed between vancomycin and an intermediate of cell wall biosynthesis such as lipid II. However, the studies conducted by Koteva, *et al.*, 2010, Kalan, *et al.*, 2013 and Kwun, *et al.*, 2013 did not show definitively whether vancomycin alone was sufficient to activate VanS. In the study by Kwun, *et al.*, 2013, desleucyl vancomycin which does not bind to the peptidoglycan unit sequence of L-Ala-D-iso-Gln-L-Lys-D-Ala-D-Ala, is unable to bind due to the *N*-methyl-leucine removal from vancomycin. From molecular dynamics simulations, it has been shown that this terminal leucine (Leu) is required to form heptapeptide aglycon structure of vancomycin (Wang, *et al.*, 2018). The structural change of the glycopeptide may be the cause of VanS not recognising the glycopeptide as opposed to the VanS not binding due of complex formation with the peptidoglycan unit.

To investigate the interaction mechanism between vancomycin and VanS, the aim is to purify the protein and reconstitute it into liposomes before analysing its phosphorylated state when exposed to vancomycin directly without the presence of any other cellular proteins or cell wall biosynthesis components such as lipid II. To enable this characterisation, VanS must first be purified. This chapter demonstrates the complexities and obstacles encountered during the purification of the membrane protein VanS.

4.3 Results

4.3.1 Generation of VanS overexpression vector

Two different cloning strategies were adopted to yield two different expressed tagged versions of VanS. The expression vector pGS-21a (Genscript) possesses coding sequences for two hexa-His tags and a GST tag. Cloning *vanS* between the *NcoI* and *HindIII* sites result in expression of a N-terminal His and GST tagged VanS (His-GST-VanS), whereas, cloning between the *NdeI* and *HindIII* sites result in expression of a C-terminal His tagged VanS (VanS-His). Both the *NdeI* and *HindIII* sites are located within the multi-cloning site of pGS-21a but *NdeI* is located upstream and overlaps with the start codon. This strategy is shown in figure 4.2A. The addition of a His tag allows later affinity purification. As VanS is a membrane bound protein, the transmembrane domain is highly hydrophobic, the addition of the GST tag may aid in solubilising the protein. The vector encodes an enterokinase recognition site between the GST and His tags and VanS allowing cleavage of both tags post purification. To this end, the *vanS* gene was amplified from the cosmid H66 of *S. coelicolor* using primer pairs RL001/002 (*NcoI* and *HindIII* overhangs) and RL003/004 (*NdeI* and *HindIII* overhangs). These fragments were subcloned into pGemT-easy. The cloning region of pGemT-easy is within an α -peptide coding region of β -galactosidase allowing blue/ white colony screening. White colonies were selected and subsequent to vector extraction, this was sequenced using universal primers T7 and SP6 for confirmation of *vanS* sequence, before cloning into the pGS-21a. The resulting overexpression vector of His-GST-VanS was named pRL100 and VanS-His overexpression vector pRL101. To verify the success of the cloning, the vectors were digested with *NcoI/HindIII* (pRL100) and *NdeI/HindIII* (pRL101). The expected fragment size of *vanS* from pRL100 digestion is 1097bp and from a pRL101 digestion is 1095bp. These sizes correspond well with the smaller fragments seen in Figure 4.2B. Sequencing analysis, using T7 and SP6 primers, of these showed a silent mutation in the first construct (His-GST-VanS) of Leu-156 where the codon CTG has mutated to CTT. There were no mutations found in *vanS* of pRL101. Both vectors were transformed into *E. coli* overexpression strain BL21 and taken forward into overexpression trials. Strain RL100 possesses pRL100 and RL101 possesses pRL101.

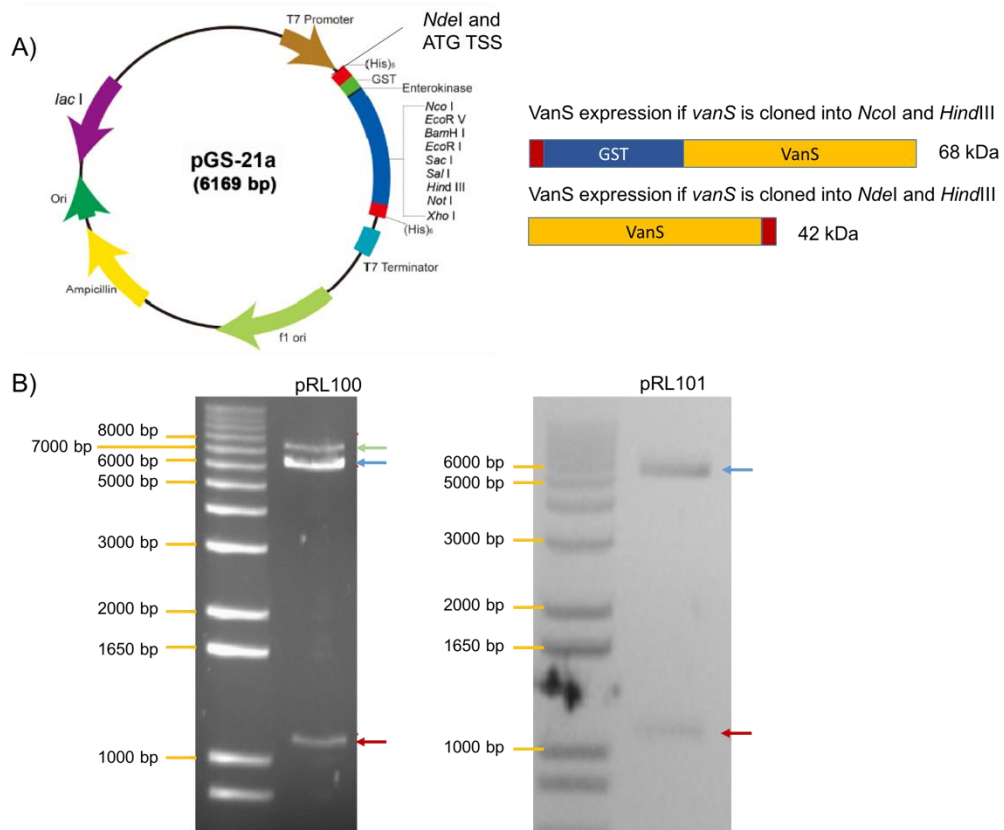


Figure 4.2: Cloning of *vanS* into pGS-21a. A) Overexpression vector pGS-21a (Genscript) with its multi-cloning site containing *Nco*I and *Hind*III which when cloned into yields a N-terminal His and GST tagged *VanS* and when cloned into *Nde*I and *Hind*III yields a C-terminally tagged *VanS* once expressed. The *Nde*I site overlaps with the transcriptional start site (TSS). The red boxes represent the hexa-His tags; B) Restriction digest of *vanS* (expected size of 1100 bp) from pGS-21a. pRL100 refers to N-terminally hexa-His tagged *vanS* and pRL101 refers to C-terminally hexa-His tagged *vanS*. Red arrow denotes excised *vanS*, blue arrow denotes linear pGS-21a and green arrow denotes undigested pRL100 vector.

4.3.2 Overexpression of *VanS*

Induction trials were carried out to identify the optimal IPTG concentration for induction. In these trials, concentrations ranged from 0 mM to 2 mM. Following 4hrs of induction by IPTG, the cells were harvested, lysed and analysed through SDS-PAGE (Figure 4.3A and B). As a positive control, BL21 containing the vector pET-28a-AntA (Seipke, *et al.*, 2014), which overexpresses a His tagged AntA protein from the expression vector of pET-28a, was used. The protein samples were not equalised prior to loading, however from looking at the intensity of the Coomassie stained acrylamide gels, most of the samples look to be of similar

concentrations, with the exception of lane 7 (1 mM) of the His-GST-VanS overexpression (Figure 4.3A) which has a weaker intensity. Taking the intensity of the bands as a reference of total protein loaded into consideration, VanS expression levels did not seem to change in the concentrations tested. In further experiments 1 mM of IPTG was used due its common use in overexpression of proteins from the vector pGS-21a (Schiffer and Hölting, 1999; Chen, *et al.*, 2007; Heydari Zarnagh, *et al.*, 2015).

The overexpression of His-GST-VanS with the expected size of 68 kDa matches with the reference ladder sizing (Figure 4.3A), however, the overexpressed VanS-His which is expected to be 42 kDa does not match up in size to the reference ladder proteins (Figure 4.3B). Instead, the overexpressed protein appears to be around the range of 27-30 kDa. Using the 1 mM IPTG collected sample from both proteins overexpression, an anti-His protein immuno-blot was carried out which is shown in figure 4.3C. This was carried out to determine whether the overexpression bands highlighted in figures 4.3A and B are indeed His tagged. The protein immuno-blot confirmed this to be the case. The difference in size of VanS-His may be caused by a number of reasons. As charges and salt concentrations can change the migration of a protein on acrylamide gels subjected to SDS-PAGE, these indicated size of VanS-His, may not be solely due to protein degradation or truncation. However, the bands which have run further on the gel which tested His tag positive on the protein immuno-blot does suggest degradation.

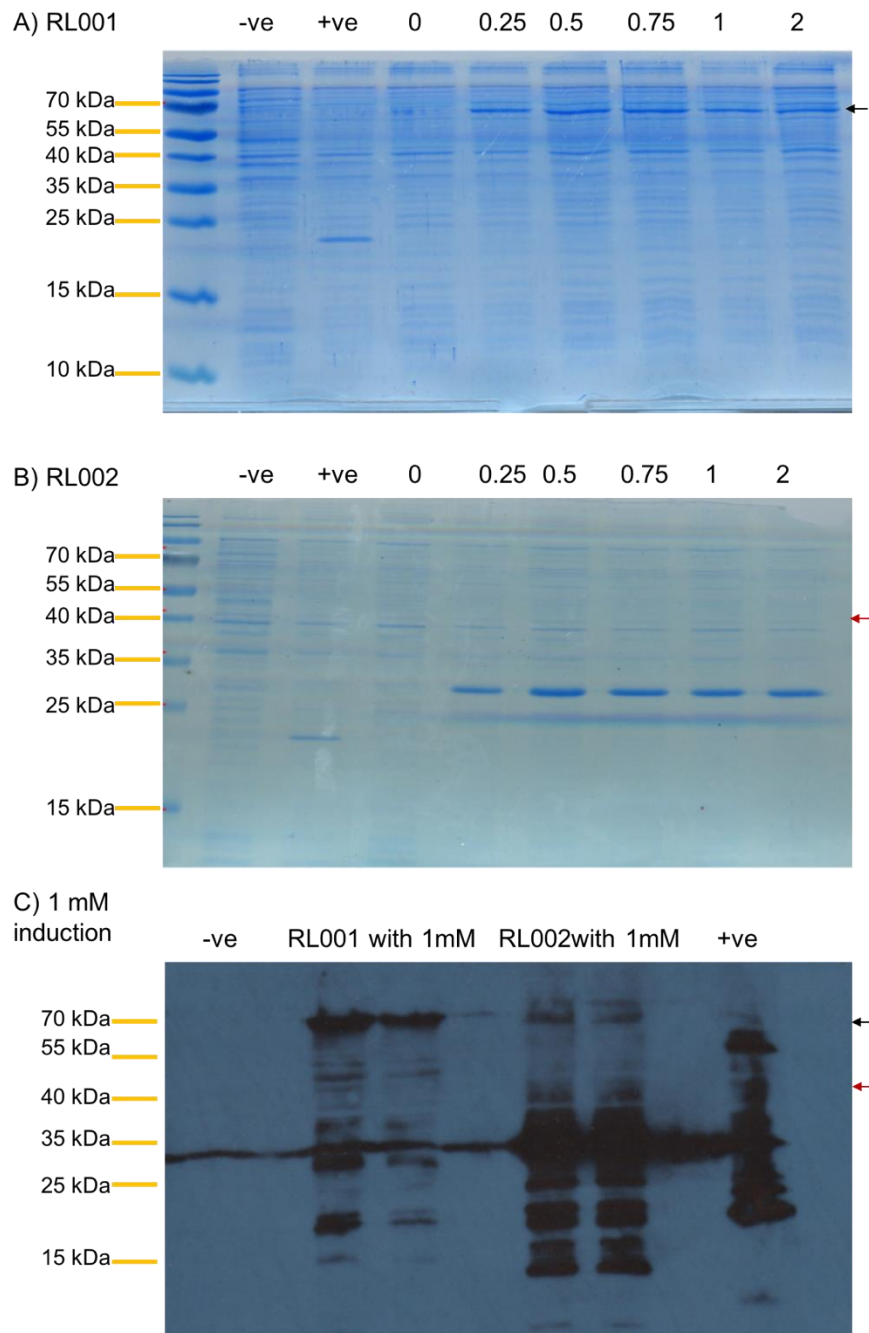


Figure 4.3: Overexpression of VanS after 4 hrs of induction using IPTG ranging from 0 mM to 2 mM. A) Coomassie stained SDS-PAGE gel of His-GST-VanS overexpression in RL001 (BL21 pRL100); B) Coomassie stained SDS-PAGE gel of of His-GST-VanS overexpression in RL002 (BL21 pRL101). For both A) and B) lanes from left to right are BL21 pGS-21a (-ve control), BL21 pET-28a-AntA (+ve control), RL001/2 induced with 0 mM, 0.25 mM, 0.5 mM, 0.75 mM, 1 mM or 2 mM IPTG. C) Western blot analysis of VanS overexpression from RL001 and RL002 using HRP conjugated His antibody. Lanes from left to right are BL21 pGS-21a (-ve), RL001 induced with 1 mM IPTG, 10-fold dilution of RL001 with 1 mM IPTG, RL002 with 1 mM IPTG induction, 10-fold dilution of RL002 with 1 mM IPTG, BL21 pET-28a-AntA (+ve). Arrows denote expected migration of VanS proteins at 68 kDa (Blue for His-GST-VanS) and 42 kDa (Red for VanS-His). Band running through whole gel ~30 kDa is likely caused by intensity luminescence refracting off the film covering gels in the exposure process.

4.3.3 Truncation of VanS-His

To determine the size of expressed VanS-His, the protein was purified from RL002 and mass spectrometry was performed. Before purification the fraction which Van-His resided in, insoluble or soluble, was determined. After overexpression, 5 ml cells were lysed and ultra-centrifugated as described in section 2.3.3.3. The soluble protein fraction (supernatant) and insoluble protein fraction (pellet resuspended with 0.5% sarkosyl buffer) was compared after SDS-PAGE (Figure 4.4). To solubilise the protein the detergent sarkosyl was selected as sarkosyl was successfully used previously in a study purifying the cytoplasmic domains of VanS (Hutchings, *et al.*, 2006). The protein was identified both in the insoluble and soluble fractions but predominantly in the soluble. This was interesting because VanS-His is expected to be insoluble due to it being a membrane bound protein.

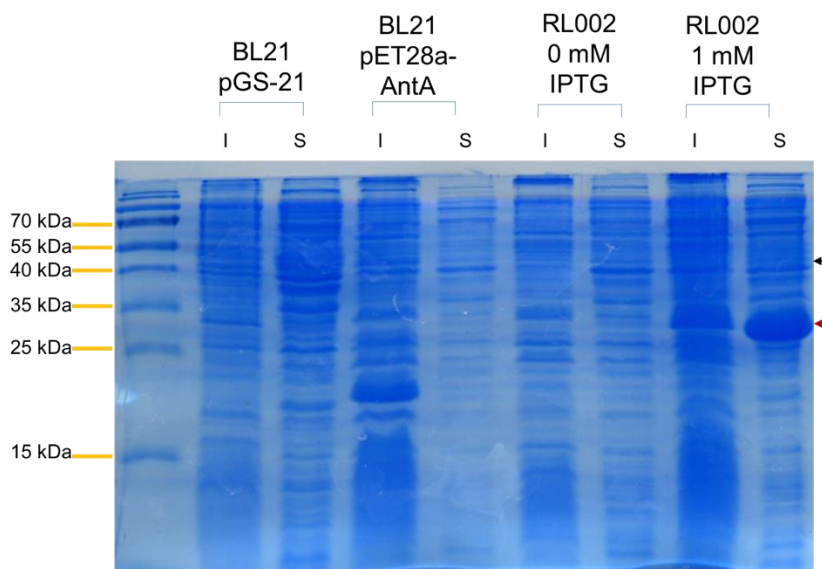


Figure 4.4: SDS-PAGE analysis of VanS-His fraction location through ultracentrifugation of lysate to pellet insoluble protein. Supernatant, containing soluble proteins was extracted (soluble fraction) and pellet was resuspended in Tris buffer containing 0.5% sarkosyl (insoluble fraction) before pelleting of cell debris. Lanes from left to right excluding protein size reference ladder are BL21 pGS-21a insoluble fraction, BL21 pGS-21a soluble fraction, BL21 pET-28a-AntA insoluble fraction, BL21 pET-28a-AntA soluble fraction, RL002 0 mM IPTG insoluble fraction, RL002 0 mM IPTG soluble fraction, RL002 1mM IPTG insoluble fraction, RL002 1 mM IPTG soluble fraction. Black arrow shows expected size of VanS-His and red arrow shows overexpression of VanS-His.

Having identified the fraction containing VanS-His, RL002 was cultured in 1 L flasks (4 L total), induced for VanS overexpression for 4 hrs before harvesting. The cells were lysed under high pressure generated by passing through a French

Press twice. The lysate was ultra-centrifuged at 42,000 rpm for an hour before the supernatant (soluble protein fraction) was loaded onto a Ni²⁺ His-Trap and purified through fast protein liquid chromatography (FPLC). The elution of which is displayed in figure 4.5. As the protein is eluted from the column with the increase of imidazole concentration, the UV absorbance increases. A selection of these samples which spanned the peak were analysed through SDS-PAGE. The results show clean protein fractions with little to no contamination or immediate degradation. This was also reflected in the western blot which is more sensitive than Coomassie staining (data not shown).

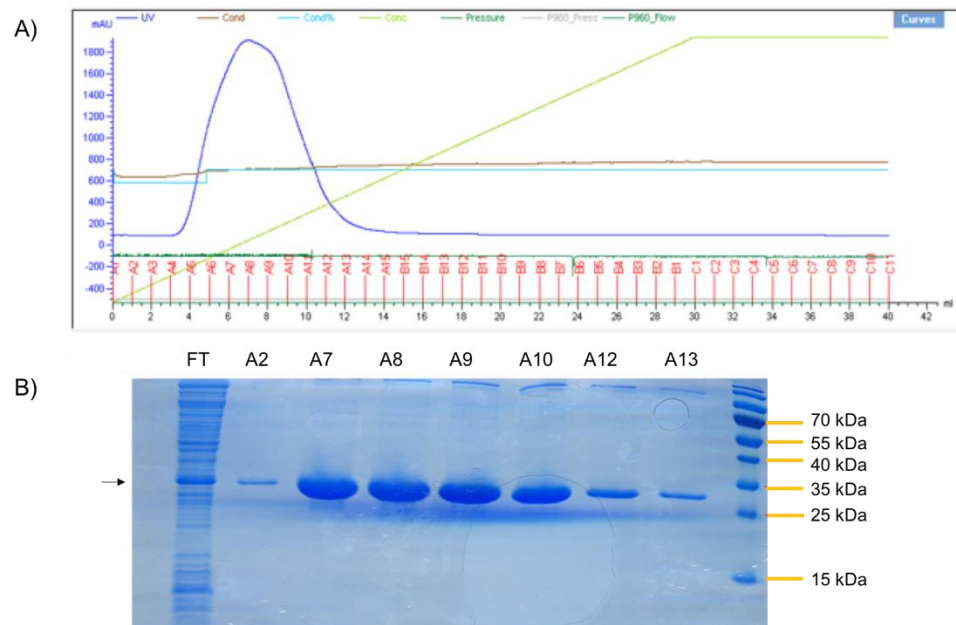


Figure 4.5: Purification of VanS-His from the soluble protein fraction through use of FPLC. A) Purification elution profile. Lime green line displays the gradient of imidazole concentration in each fraction of the elution, with 300 mM as the maximum. Dark blue line represents the UV absorbance in mAU as the protein is eluted from the column which is presented in the Y axis. Collected fractions are listed in the X axis. B) Eluted fractions from the purification process analysed through SDS-PAGE. The lanes from left to right are flow through protein was loaded on the column, fraction A2, A7, A8, A9, A10, A12, A13. Arrow denotes VanS-His purified protein of expected size 42 kDa.

Intact mass spectrometry was conducted using the purified protein from fraction A3 (Figure 4.6). The different peaks show the relative abundance of the protein isoforms different sizes of the truncated protein. Two peaks were most dominant representing two proteins of 31.476 kDa and 31.781 kDa of size. The N-terminal part of of VanS composed of the sensor domain and the TM domain may be the band located in the supernatant fraction of figure 4.4.

The amino acid sequence of VanS-His was assessed to determine the cleavage site and whether this was a specific protease recognition site. Based on the mass of the protein, the cleavage site is most likely to be located between amino acids L-89 and A-90 (Figure 4.7). The sequence surrounding this site was also probed and it was found that many proteases could target this region including chymotrypsin, CNBr pepsin, proteinase K and thermolysin. However, none of these proteases were found to be specific to that site.

As these proteases were non-specific, mutations were designed, changing one or two amino acids at this cleavage site to determine whether this was sufficient to prevent targeted cleavage. These VanS mutations include L89V, A91G and LA90:91VG. These mutated *vanS* genes were synthesised by Genscript. To the mutated *vanS* genes, His tags were added to both terminals independently using primer pairs RL029/30 for N terminal and RL032/33 for C-terminal. These were cloned into pGS-21a giving rise to the overexpression vectors pRL102-104 for N-terminally His-tagged L89V, A91G and LA90:91VG VanS variants, respectively and pRL105-107 for C-terminally His-tagged L89V, A91G and LA90:91VG VanS variants, respectively. Following cloning of hexa-His tagged *vanS* sequences into overexpression vector pGS-21a, these were also confirmed through sequencing with universal primers T7 and T7 term. These vectors were subsequently transformed into BL21. After induction of overexpression, the harvested cells were analysed through SDS-PAGE to determine whether the designed mutations had prevented targeted cleavage (Figure 4.8). Unfortunately, protein cleavage was observed using all generated strains, so efforts were focused on the His-GST-VanS protein.

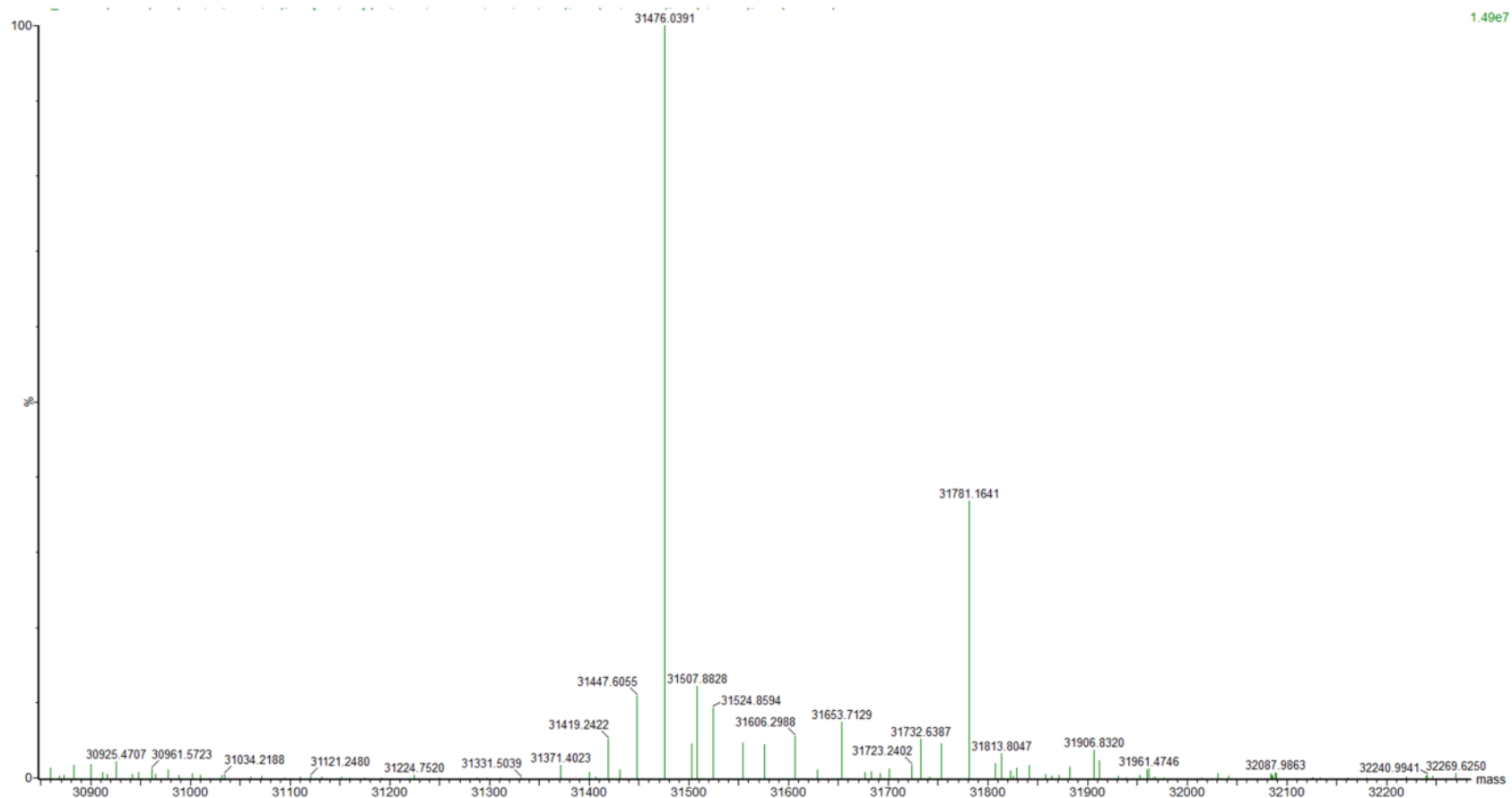


Figure 4.6: Intact mass spectrometry of VanS-His protein expressed from pRL101 vector in BL21. Mass spectrometry was carried out on protein purified from fraction A3 from the purification shown in figure 4.5. The deconvoluted spectrum measured peak masses are 31476.04 and 31781.2. Y axis shows relative abundance of protein and X axis shows the size of the protein isoform. Expected full-length protein size is 42 kDa.

incorporated into the membrane and in the lysis process remaining being attached to the fragmented membrane or being packaged into inclusion bodies within BL21.

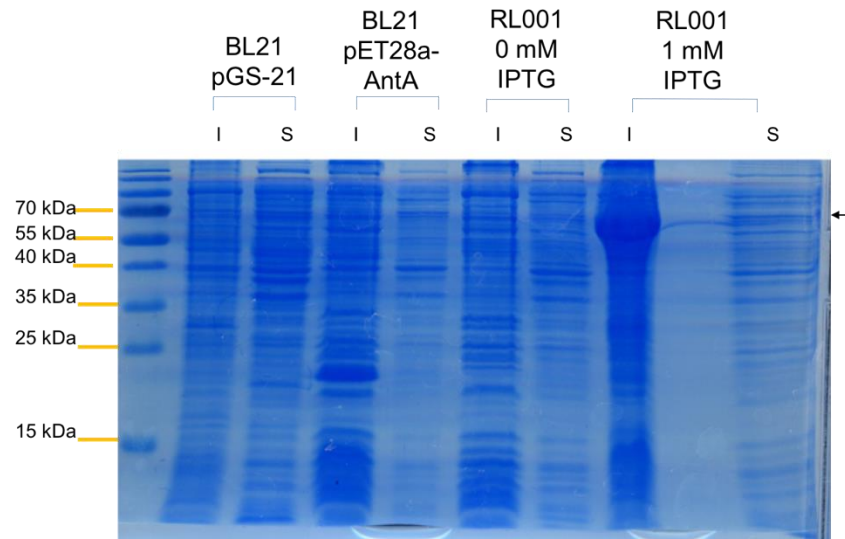


Figure 4.9: SDS-PAGE analysis of His-GST VanS fraction location through ultracentrifugation of lysate to pellet insoluble protein. Supernatant, containing soluble proteins was extracted (soluble fraction) and pellet was resuspended in Tris buffer containing 0.5% sarkosyl (insoluble fraction) before pelleting of cell debris. Lanes from left to right excluding protein size reference ladder are BL21 pGS-21a insoluble fraction, BL21 pGS-21a soluble fraction, BL21 pET-28a-AntA insoluble fraction, BL21 pET-28a-AntA soluble fraction, RL001 0 mM IPTG insoluble fraction, RL001 0 mM IPTG soluble fraction, RL001 1mM IPTG insoluble fraction overflow, RL001 1 mM IPTG soluble fraction.

Knowing the protein was located in the insoluble fraction, after ultracentrifugation of lysate, the supernatant was discarded and pellet was resuspended in Tris buffer containing 0.5% sarkosyl overnight before pelleting cell debris and loading onto the Ni^{2+} column and carrying out FPLC. Protein was washed with buffer A before elution with a sloping shallow gradient increase of imidazole, before a sharp incline of imidazole concentration to rid the column of all bound proteins (Figure 4.10A). The elution generated one peak. The collected fractions spanning this peak were loaded onto acylamide gels and subjected to SDS-PAGE and Western blot analysis (Figure 4.10B). In the purification, a large amount of protein was present in the flow through inferring that the column was either saturated with protein or was unable to bind. Despite this, a lot of protein was still able to be purified. The purification yielded less pure protein than for truncated VanS-His as many smaller protein bands were seen in both the Coomassie stained gel and the protein immuno-blot.

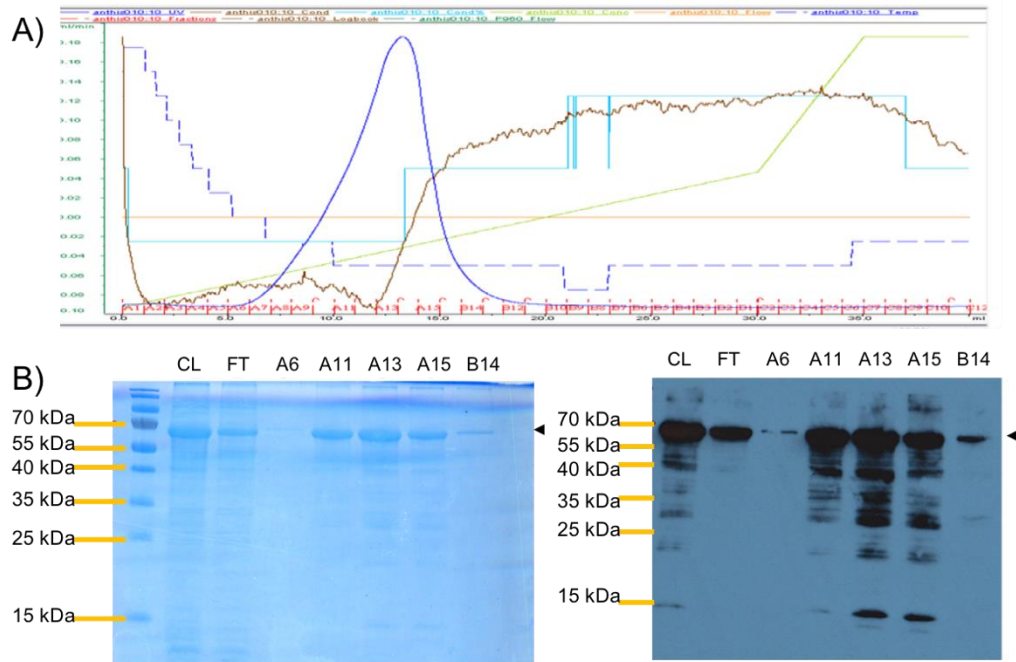


Figure 4.10: Purification of His-GST-VanS from the insoluble protein fraction through use of FPLC. A) Purification elution profile. Lime green line displays the gradient of imidazole concentration in each fraction of the elution (300 mM maximum). Dark blue line represents the UV absorbance in mAU as the protein is eluted from the column which is presented in the Y axis. Collected fractions are listed in the X axis. B) Eluted fractions from the purification process analysed through SDS-PAGE and consequent anti-His immune blotting. The lanes from left to right are resuspended insoluble protein of crude lysate (CL), flow through (FT), A6, A11, A13, A15, B14. Arrow denotes His-GST-VanS purified protein which was expected to be 68 kDa.

To remove the degraded protein, pooled fractions (A10-B14) was loaded onto a size exclusion column, where larger proteins traveled through the column faster and smaller proteins migrated through the column slower. This is due to smaller proteins being trapped in the differently sized pores of the gel matrix whereas larger proteins would not. The elution profile is shown in Figure 4.11A. The eluted protein fractions spanning the dual peak (B3-C3) were again analysed through gel electrophoresis and anti-His immuno-blotting (Figure 4.11B). Visualising the protein showed that whilst the amount of degraded protein had been reduced, the fractions still contained degraded protein. This shows that the protein was constantly undergoing degradation. The buffers used during elution did not stabilise the protein.

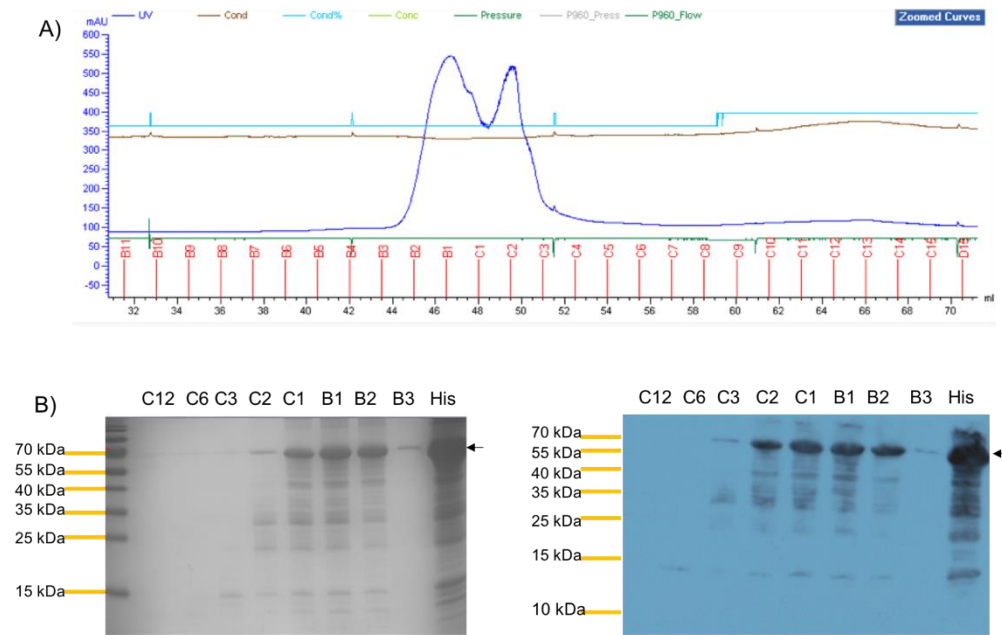


Figure 4.11: Purification of His-GST-VanS through size exclusion. Protein first purified through His-affinity FPLC then further purified by feeding through a Superdex 75 prepgrade gel filtration column. A) purification profile. Dark blue line shows the UV absorbance as protein was eluted and the collected fractions are shown in the X axis. B) Coomassie blue stained acrylamide gel image after SDS-PAGE and subsequent Western blot using His antibodies. Lanes from left to right for B) and C) are fractions spanning the peak of A) C12, C6, C3, C2, C1, B1, B2, B3, His-GST-VanS after His affinity FPLC purification before loading onto the gel filtration column. Arrows shows expected band of His-GST-VanS.

To troubleshoot the issue of degradation different buffers were tested in the purification process. This included changing the different components, concentrations and pH. The different buffers used have been listed in table 4.1. The buffering components tested were Tris, PBS and HEPES which buffer within the range of the tested pH's (7.3 - 8) which were chosen based on the isoelectric point of His-GST-VanS of 6.77. Further to this, different concentrations of NaCl were trialled (ranging from 10 mM – 500 mM) to assess whether different ionic strengths would affect the stability of the protein. Additionally, DTT, a reducing agent, glycerol, a cryoprotectant and EDTA, a chelator of ions which inhibits proteases which require bivalent ions to function, were all added in hopes to stabilise the protein, however, these changes made no noticeable difference.

Table 4.1: Buffer composition of the different buffers used in different His affinity FPLC purifications of His-GST-VanS, where solubilisation buffer refers to buffer used to resuspend pellet after ultracentrifugation of lysate, buffer 1 refers to buffer used to wash protein on His-trap column and also used in elution mixed with buffer 2 which contains imidazole.

Solubilisation buffer	Buffer 1	Buffer 2
PBS, 1% sarkosyl	PBS, 0.5 sarkosyl	PBS, 0.5 sarkosyl, 300mM imidazole
50mM Tris, 10mM NaCl, 0.5% sarkosyl, 0.5mM EDTA (pH7.3)	50mM Tris, 10mM NaCl, 0.5% sarkosyl, 0.5mM EDTA (pH7.3)	50mM Tris, 10mM NaCl, 0.5% sarkosyl, 0.5mM EDTA, 300mM imidazole (pH7.3)
50mM Tris, 10mM NaCl, 0.5% sarkosyl, 0.5mM EDTA (pH8)	50mM Tris, 10mM NaCl, 0.5% sarkosyl, 0.5mM EDTA (pH8)	50mM Tris, 10mM NaCl, 0.5% sarkosyl, 0.5mM EDTA, 300mM imidazole (pH8)
*50mM Tris, 150mM NaCl, 1% sarkosyl (pH8)	*50mM Tris, 150mM NaCl, 0.5% sarkosyl, 10% glycerol (pH8)	*50mM Tris, 150mM NaCl, 0.5% sarkosyl, 10% glycerol, 300mM imidazole (pH8)
50mM Tris, 250mM NaCl, 1% sarkosyl (pH7.3)	50mM Tris, 250mM NaCl, 0.5% sarkosyl, 10% glycerol (pH7.3)	50mM Tris, 250mM NaCl, 0.5% sarkosyl, 10% glycerol, 300mM imidazole (pH7.3)
50mM Tris, 250mM NaCl, 0.5% sarkosyl (pH7.3)	50mM Tris, 250mM NaCl, 0.2% sarkosyl, (pH7.3)	50mM Tris, 250mM NaCl, 0.2% sarkosyl, 300mM imidazole, (pH7.3)
50mM Tris, 250mM NaCl, 0.5% sarkosyl (pH8.0)	50mM Tris, 250mM NaCl, 0.2% sarkosyl, (pH8.0)	50mM Tris, 250mM NaCl, 0.2% sarkosyl, 300mM imidazole, (pH8.0)
50mM Tris, 500mM NaCl, 0.5% sarkosyl (pH8.0)	50mM Tris, 500mM NaCl, 10% glycerol, 0.5% sarkosyl (pH8.0)	50mM Tris, 500mM NaCl, 10% glycerol, 0.5% sarkosyl, 300mM imidazole (pH8.0)
50mM Tris, 150mM NaCl, 10% glycerol, 0.5mM EDTA, 1% sarkosyl (pH8.0)	50mM Tris, 150mM NaCl, 10% glycerol, 0.5% sarkosyl (pH8.0)	50mM Tris, 150mM NaCl, 10% glycerol, 0.5% sarkosyl, 300mM imidazole (pH8.0)
50mM HEPES, 150mM NaCl, 10mM DTT (pH 8.0)	50mM HEPES, 150mM NaCl, 10% glycerol, 0.5% triton X-100 (pH8.0)	50mM HEPES, 150mM NaCl, 10% glycerol, 0.5% triton X-100, 300mM imidazole (pH8.0)
50mM HEPES, 500mM NaCl, 1% sarkosyl, 10mM DTT (pH 8.0)	50mM HEPES, 500mM NaCl, 10% glycerol, 0.5% sarkosyl (pH8.0)	50mM HEPES, 500mM NaCl, 10% glycerol, 0.5% sarkosyl, 300mM imidazole (pH8.0)
*50mM Tris, 150mM NaCl, 1% Triton X-100 (pH8)	*50mM Tris, 150mM NaCl, 0.5% Triton X-100, 10% glycerol (pH8)	*50mM Tris, 150mM NaCl, 0.5% Triton X-100, 10% glycerol, 300mM imidazole (pH8)

All buffers contained a cocktail of protease inhibitors

pH of buffers measured at 4°

* buffers tested in figure 4.11

The only buffer component switch which made a difference to the stability was use of the detergent Triton X-100 instead of sarkosyl. The comparison between sarkosyl and Triton X-100 purification and storage (buffer composition in table 4.1) is shown in figure 4.12. From the Coomassie blue stained gels of purifications of His-GST-VanS using both sarkosyl and Triton X-100 looked very impure, however, from analysis with Western blotting, it can be seen that no His-tagged protein was collected in the the two purified protein fractions (F5 and F6) tested for

Triton X-100. Instead the protein was located in the flow through fraction. This suggests that the protein was unable to bind to the His-trap column. It can however be seen that His-GST-VanS in the flow through was experiencing much less degradation in the Triton X-100 buffer than sarkosyl buffer as fewer bands are seen. However, following recommendations of manufacturers, use of Triton X-100 between 0.1-1% should not affect binding of proteins to the column.

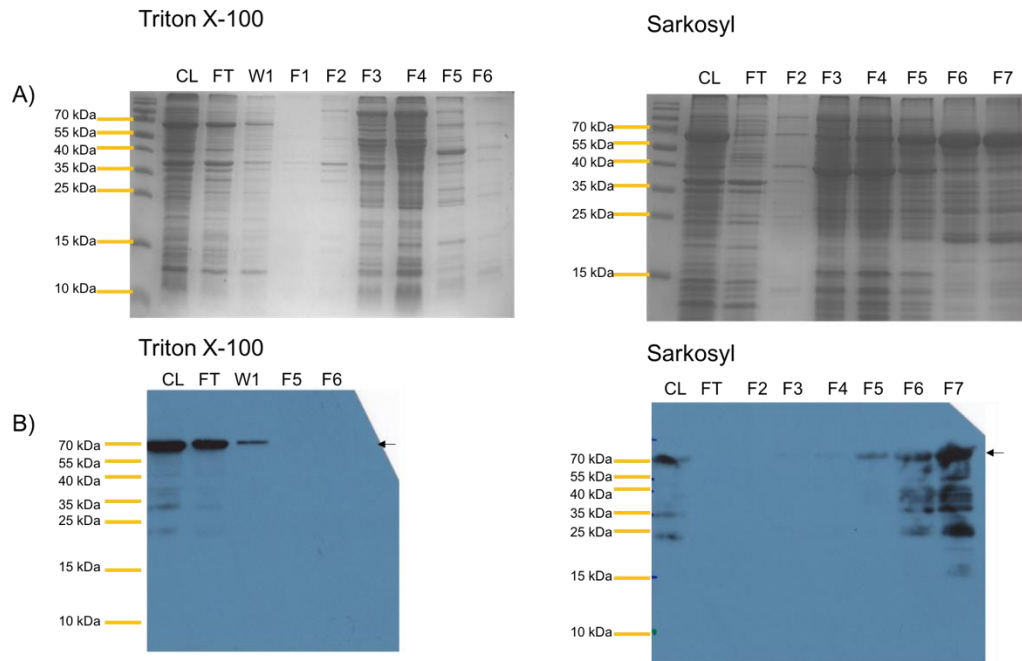


Figure 4.12: Effects of Triton X-100 and sarkosyl on the purification of His-GST-VanS. Purification by use of His affinity FPLC. A) SDS-PAGE analysis; B) Anti-His protein immuno-blot. The different lanes labeled are CL= crude lysate where post lysis and ultracentrifugation, pellet has been resuspended in detergent overnight; FT refers to flow through from His-trap column; W1 is the first wash of column after lysate has been loaded; F1-F7 refer to fractions taken from elution step. Arrows denote expected band of His-GST-VanS.

During the purification, the elution gradient used was also altered. Two of these include the initial use of 5-10 mM of imidazole in the first 10 fractions (10 ml) with the aim to wash off some of the weakly bound proteins before gradually increasing to 300mM to elute the more specifically bound proteins. The gradation profile was also changed to an incremental profile, where an increase of 10 mM imidazole was made which continued for 3 ml before another 10 mM increase until a concentration of 300 mM imidazole was reached. This was done to try to separate the different proteins. However, in these attempts, whilst some of the protein was washed off in every step change or gradation, the bound protein continued to degrade.

Further to these changes in buffer compositions, physical changes made included culturing shaking speed (200, 220 and 250 rpm) and temperature of growth (37°C and 30°C). None of these changes made a noticeable difference in reducing degradation of protein, only amount of protein produced by RL001.

In addition to using BL21 as an overexpression strain, other strains were also tested. *E. coli* C41, C43 and Rosetta were also used. C41 and C43 were selected as they have been shown to be effective for use in overexpression of toxic and membrane bound proteins (Lucigen; Miroux and Walker, 1996; Dumon-Seignovert, *et al.*, 2004). Rosetta was used as it allows expression of proteins encoded by rare codons for *E. coli* including AGG, AGA, AUA, CUA, CCC and GGA, which are used in His-GST-VanS (Novogen). The expression of VanS from C41 and C43 is shown in Figure 4.13. Overexpression from strain C43 results in the lowest level of protein degradation of the three strains tested. Overexpression from Rosetta (data not shown) did not alter the level of degradation in comparison to BL21. Consequent overexpression was carried out using strain C43. However, with all the changes made, His-GST-VanS was not able to be kept stable after purification. Whether the protein was stored at RT, 4°C, -20°C or -80°C, also made little difference in degradation.

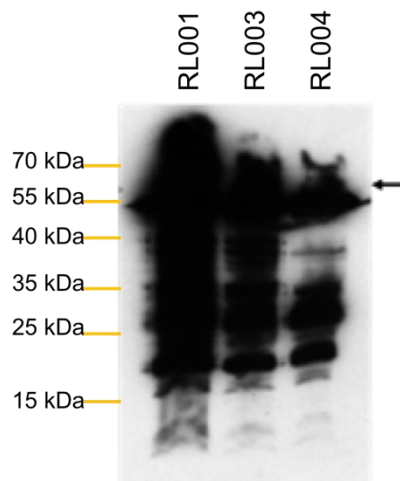


Figure 4.13: Overexpression of His-GST-VanS from vector pRL100 in different expression strains of *E. coli*. After 4 hours of induction using 1 mM IPTG induced overexpression, cells were harvested and analysed through Anti-His immune blotting. Strains tested were RL001, RL003 (C41 pRL100) and RL004 (C43 pRL100). Arrow denotes positioning of 68 kDa protein band.

4.3.5 Cleavage of GST and His tag

While optimising protein purification and storage, attempts at cleaving the GST tag from the existing purified samples was tested so assess if removal would improve the stability of the protein. An enterokinase site (DDDDK) is situated between the GST tag and VanS. Purified proteins were buffer exchanged using Millipore filtration spin columns (Amicon) to enterokinase compatible buffer and in the process concentrated. An aliquot containing 10 μg protein was removed and incubated with 5U of Enterokinase overnight at 37°C. The sample was analysed for GST cleavage (Figure 4.14A). However, the GST tag was found to still be attached to the protein with both temperature treatments. If the enterokinase treatment was successful, a band of 40 kDa and 28 kDa would be seen in the Coomassie stained gel. However, there is no difference between the protein alone lanes and the protein with added enterokinase lanes. This was repeated using varying amounts of enterokinase (Figure 4.14B). As the image shown is an anti-His immune blot, if cleavage have been successful, less of the His-GST-VanS band should be seen and instead a band at 28 kDa should be seen. In the last two lanes where 20 μg of protein was loaded, a band at ~28 kDa is seen but this seems to match the degradation band seen in the controls of protein and protein with enterokinase buffer. Therefore, from these results enterokinase cleavage has been unsuccessful.

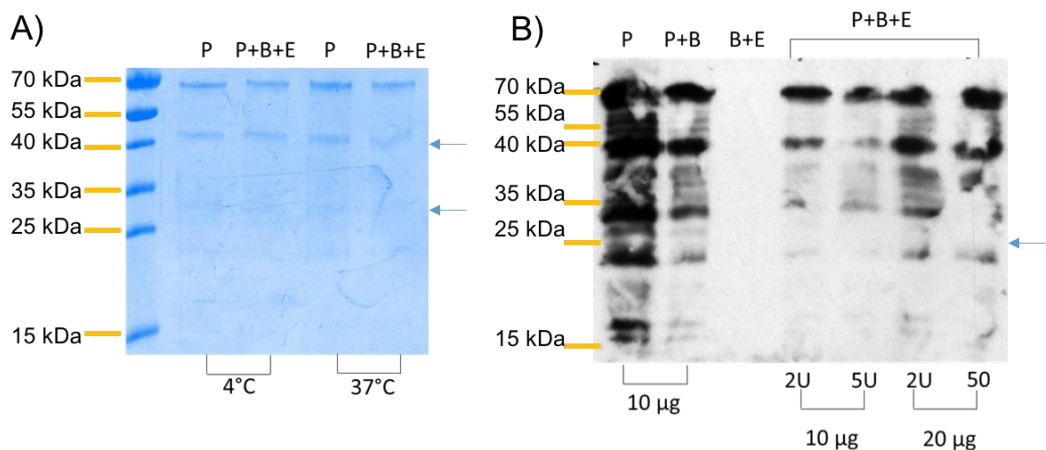


Figure 4.14: His-GST-VanS (10 μg) incubation with enterokinase to cleave GST tag from VanS under different conditions. A. Overnight incubation at 4°C and 37°C with 5U enterokinase. B. Incubation using different ratios of purified protein to enzyme. P is the protein (His-GST-VanS) only, P + B refers to the protein and buffer, B + E is buffer and enterokinase, and P + B + E refers to protein, enterokinase buffer and enterokinase. The arrows denote expected size of His-GST-VanS and His-GST and VanS if enterokinase cleavage is successful.

4.4 Discussion

His-tagged VanS was heterologously overexpressed in *E. coli* (Figure 4.3). However, full-length VanS could not be purified or stored stably without degradation. It is interesting to note that the truncated VanS-His contains only the cytoplasmic domains. In 2006, Hutchings, *et al.*, purified the cytoplasmic region of VanS (c-VanS) by expressing codons 85-365. In this work, the truncated protein has lost the N-terminal amino acids encoded by codons 1-88. As only the cytoplasmic region remains, this explains why this protein was stable as demonstrated in figure 4.4.

Generation of the VanS variant proteins did not prevent protein cleavage (Figure 4.6). If this site is targeted specifically by proteases, further amino acid changes may be necessary to change the protease recognition site and hence protease cleavage.

Another possibility is that VanS-His expression may have begun not from the start codon which was part of the *NdeI* restriction site but the methionine two codons upstream from the predicted cleavage site. If this is the case the calculated molecular weight of this protein is 31.680 kDa, which falls between the two major peaks (31.476 and 31.781) from the intact mass spectrometry. To explore this possibility a change in the methionine could have been made, however, further changes could have adversely affected signal transduction from sensor to HAMP to Dhp domain. Consequently, further work was focused on His-GST-VanS. GST tags have been known to prevent targeting by proteases and to help solubilise proteins (Terpe, 2003). In this case however, VanS remained largely in the insoluble fraction (Figure 4.9).

After initial purification of His-GST-VanS through a Ni²⁺ affinity column (Figure 4.10), it was further purified through a size filtration column. However, whilst some of the smaller proteins were removed, many bands were still evident in figure 4.11. This was concluded to be due to degradation and as such, a series of purifications using different buffers were trialed to optimise purification and storage conditions. However, none of the tested conditions significantly improved the stability of His-GST-VanS other than Triton X-100.

Triton X-100 is a non-ionic detergent which is widely used for protein purification for its less denaturing properties. At <1%, both detergents are far below their critical micelle concentration. The use of the latter detergent may not have solubilised GST-His-VanS as it was not successfully bound to the His-Trap column. It is unclear why the protein did not bind to the column during purification when the detergent was changed as other studies have shown that under those conditions, protein could be purified (Parks, *et al.*, 1994; Lemercier, *et al.*, 2003). Recently, a study has shown that sarkosyl, Triton X-100 and CHAPS can be mixed in the purification of proteins and with the use of the three improves native protein folding (Tao, *et al.*, 2018). Furthermore, it has also been shown that the detergent *n*-Dodecyl β -D-maltoside (DDM) is effective in the purification of SKs. The SK, RegB from *Rhodobacter sphaeroides* (Potter, *et al.*, 2002) and VanS from *E. faecalis* (Hussain, *et al.*, 2016) have been purified using this detergent. The use of DDM and the mix of the three detergents could be tested if work is continued on VanS purification.

In addition to optimising buffers, three other overexpression strains were tested in hopes that degradation within the cell could be minimised. *E. coli* overexpression strains BL21, C41 and C43 and Rosetta were all tested. Of these, only C43 demonstrated any visible improvement in terms of reducing protein degradation. C41 and C43 are both derivatives of BL21 that were originally selected for their ability to tolerate the overexpression of membrane proteins which would normally be toxic in other cell types (Miroux and Walker, 1996). Whilst VanS overexpression was not lethal, it potentially was toxic leading to truncation of VanS-His. The use of *E. coli* C43 may have either reduced the level of expression of His-GST-VanS and hence reducing the amount of degradation or secluded the proteins in inclusion bodies (Miroux and Walker, 1996). Another expression strain which could be tested in future work could be heterologous expression not in *E. coli* but a *Streptomyces* strain such as *S. albus* which has a reduced genome and has been used for overexpression of secondary metabolites (Baltz, 2011; Kallifidas, *et al.*, 2018).

The difficulty and challenge of purifying membrane bound proteins such as SKs are due to the mix of hydrophobic and hydrophilic regions and has been the

reason for relatively few SKs being purified and crystallised for characterisation. In many studies, cytoplasmic domains have been purified to characterise the interaction between the SK and RR (Wright, *et al.*, 1993; Hutchings, *et al.*, 2006). As demonstrated here and by Hussain, *et al.*, 2016, VanS is extremely sensitive to buffer constituents and pH. Whilst purification of VanS has been achieved, it was from *E. faecalis* which is of type A vancomycin resistance and shares only 24% identity with VanS_{Sc}. Furthermore, VanS_{Sc} was significantly less stable than the proteins in both studies by Potter, *et al.*, 2002 and Hussain, *et al.*, 2016.

To purify stable VanS_{Sc} changing the expression host may be a good method to reduce the degradation within the cell and implementation of either DDM or the mix of CHAPS, sarkosyl and Triton X-100 may improve stability of the protein once extracted from the cell. In addition, to reduce the time between lysis of cell and use of protein for further investigative experiments, VanS-His would be the preferred expressed protein as no further treatment would be needed (i.e. enterokinase treatment to remove GST tag). If the heterologous host is *S. albus*, the truncation may not occur. The protein is also more likely to be correctly folded which may be a cause of the degradation. In summary, to enable further experiments to determine the interaction between VanS and vancomycin, the expression and purification of VanS would need to be optimised before this work can begin.

5. Rewiring TCS Systems; A SK jigsaw puzzle

5.1 Chapter overview

TCSs play an important role in bacteria, whatever the phylum, clade or family. In *Streptomyces*, many TCSs have been shown to feed into the regulation of secondary metabolite biosynthesis. The study of TCSs in the last 30 years has provided an insight into the mechanism of SK and RR interaction and the role these TCSs may play, often finding homologues in different species. However, due to their diversity, it remains near impossible to predict the activating signal for SKs, as has been demonstrated in the two previous chapters. This chapter presents work on the development of a tool to activate expression of silent pathways (e.g. cryptic antibiotic biosynthetic gene clusters) through activation of RRs by non-cognate SK signalling. Dhp domains and residues within those Dhp domains of two *S. coelicolor* SKs, AfsQ2 and VanS, were exchanged in an attempt to rewire their signaling pathways. The results from this work indicate that introduction of the chimeras into *S. coelicolor* and *S. venezuelae* cause antibiotic production, however, the results do not definitively show that this is a direct cause of the chimeras.

5.2 Introduction

TCSs typically possess highly modular structures as described in section 1.1. The classical membrane bound SK has an extracellular or periplasmic sensing domain, signal transduction domains (e.g. TM, HAMP and PAS, etc.) and signaling domains of the kinase core. As to the RR, there is a REC domain and an effector domain. With this highly modular structure, over the years of research, these domains of different TCSs have been edited together in different configurations to rewire TCS. In early work by Perraud, *et al.*, (1998), through exchanging the domains of the two phosphotransfer proteins EvgS and BvgS, it was shown that the terminal Hpt domain conferred specificity to the phosphorylated RRs. Since then much work has been carried out on rewiring TCSs.

A chimeric SK composed of the photoreceptor domain of the phytochrome Cph1 from *Synechocystis* fused to the intracellular domains of the SK EnvZ from *E. coli*, proved to be functional in *E. coli* (Levskaya, *et al.*, 2005). In this study, a

lacZ reporter was engineered to be under the control of an OmpR regulated promoter. Consequently, under red light, the modified bacteria turned black from the produced β -galactosidase hydrolysing S-gal (3,4-cyclohexenoesculetin- β -D-galactopyranoside) in the culture medium.

In another study, the cytoplasmic chemoreceptor FrzCD of *Myxococcus xanthus* was rewired with the nitrate SK, NarX of *E. coli* (Xu, *et al.*, 2007). The sensory domain of NarX was fused to the signaling module of FrzCD. These chimeras were then introduced into *E. coli*. In the absence of nitrate, the cells expressing the chimera demonstrated similar reversal frequency as wild-type, whereas, in the presence of nitrate, the chimera expressing cells showed a 10-fold reduced reversal frequency (Xu, *et al.*, 2007).

TCSs can also be rewired not through exchange of domains but through exchange of specific residues. The interaction between SKs and their cognate RRs is regulated temporally, spatially and at the molecular level to prevent undesired cross-talk between SKs (Laub, *et al.*, 2007; Garcia Vescovi, *et al.*, 2010; Salazar and Laub, 2015). In chapter 3, the conservation of TCSs was discussed alongside the evolution of new TCSs. As *Streptomyces* have gained most of their TCSs through LSE involving duplication events whether of genes, operons or arms of chromosomes (Alm, *et al.*, 2006), the build up of changes either at the nucleotide level or through domain shuffling, causes new TCSs to evolve in this method. For the TCS to continue functioning, the SK and RR pairing on the interaction level and not location in genome, must be retained. Skerker, *et al.*, (2008) reasoned that the residues responsible for the specificity between the partner proteins must coevolve for the interaction to be sustained, meaning that if a residue in one protein involved in the specificity is mutated, a corresponding mutation in the cognate partner protein must occur, to maintain the partnership or the strength of binding. The interaction between the two proteins is between three domains of these proteins, the CA and Dhp domains of the SK and the REC domain of the RR. The research conducted by Skerker, *et al.*, (2008) identified two clusters of residues in each component, both sites situated above and below the active site of phosphotransfer where the two components interact as modeled on the phosphotransfer proteins Spo0F and Spo0B. In their work, two closely related SKs,

EnvZ and RstB were rewired. Changing as few as three residues in EnvZ to match those of RstB was sufficient to change phosphotransfer of EnvZ to OmpR, the cognate RR of EnvZ, instead to RstA, the cognate RR of RstB.

These studies show that rewiring of SKs can be a successful means of changing the cellular circuitry to both activate the production of desirable products or be incorporated into other biological networks as an ‘on’ and ‘off’ switch. In *Streptomyces*, many TCSs have been identified which are implicated in antibiotic regulation. TCSs have also been identified in cryptic BGCs identified through genome mining, however, the activating signals for these are largely unknown. For instance, in the BGC of phthoxazolin A in *S. avermitilis*, there is a HK and a paired TCS (Suroto, *et al.*, 2018). Rewiring of the SKs in these TCSs could be a means of activating these cryptic pathways to activate secondary metabolite production.

5.3 Results

The two SKs chosen for rewiring were VanS and AfsQ2, both described in section 1.3. VanS was chosen as the sensor and AfsQ2 was chosen for output signaling to AfsQ1.

AfsQ1, the cognate RR of AfsQ2 is a global regulator conserved in the genus *Streptomyces*. It was first identified when a large fragment encoding *afsQ1* from *S. coelicolor* was cloned into *S. lividans*, inducing production of actinorhodin, undecylprodigiosin and A-factor (Ishizuka, *et al.*, 1992). Since that discovery, AfsQ2 has been shown to be activated in MM with 75 mM glutamate (Shu, *et al.*, 2009). AfsQ1 has also been shown to negatively regulate nitrogen metabolism through competitive binding to the promoters of *glnA* and *nirB* with GlnR, an orphan RR (Wang, *et al.*, 2013B).

VanS is the cognate SK of VanR, which modulates the expression of vancomycin resistance genes in response to vancomycin. At the time this research began, few TCSs within *Streptomyces* had known signaling activators. Of those known, few were suitable for this study as a sensor due to their involvement in antibiotic regulation, therefore, PhoPR and AbsA1/A2 were unable to be used in this study.

In the successful event of rewiring VanS and AfsQ2, the addition of vancomycin would result in AfsQ1 being phosphorylated by the chimera, leading to antibiotic production, which would serve as a visual indicator in *S. coelicolor* because actinorhodin and undecylprodigiosin are both pigmented antibiotics.

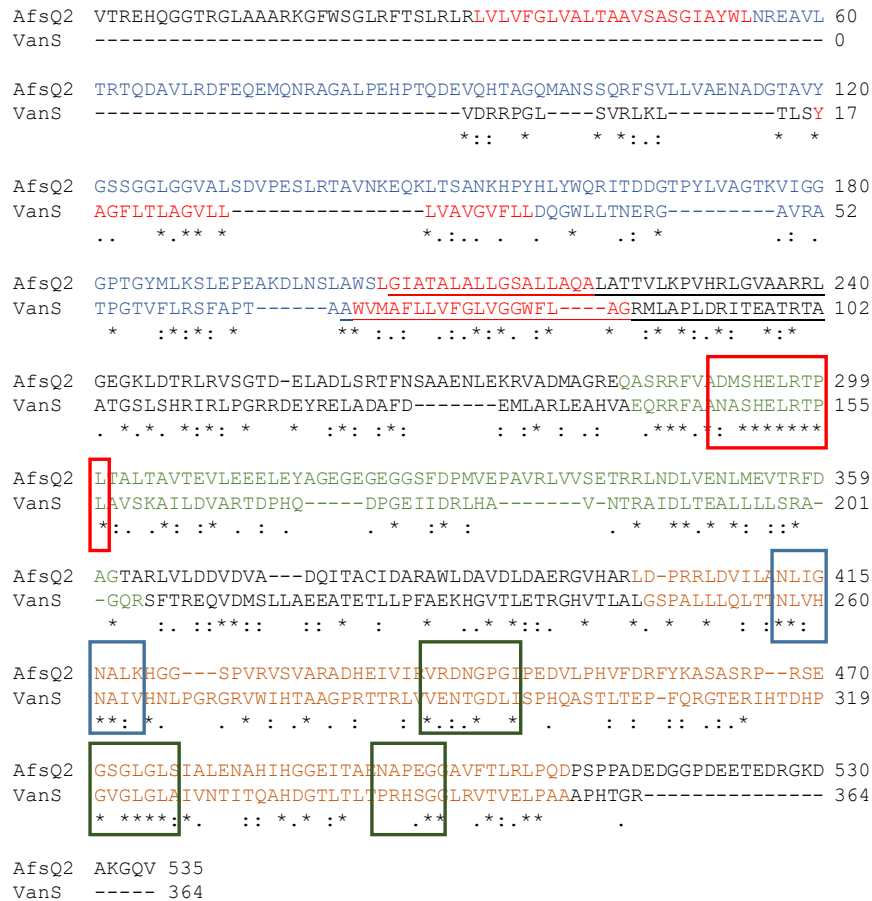


Figure 5.1: Alignment of SKs AfsQ2 and VanS of *S. coelicolor* using Clustal Omega. * refers to conservation of residue, : refers to conservation of strongly similar properties, . refers to conservation of weakly similar properties. The domains are highlighted as follows, blue text denotes sensor domains, red text denotes TM helices (as predicted by ExPASy TMPred), underlined text denotes HAMP domain (as predicted by P2RP; Barakat, *et al.*, 2013), green text denotes Dhp domain and orange/brown text denotes CA domain. The different boxes highlight the conserved regions, with the red boxes showing the H box, the blue boxes showing the N box and the green boxes showing boxes G1, G2 and G3.

Figure 5.1 shows the alignment of both protein sequences using Clustal Omega. Through aligning the two proteins, whilst the sensor domains are highly dissimilar, in keeping with the different stimuli both proteins recognise, both proteins share the basic intracellular domain structure. Both VanS and AfsQ2 are classical SKs which have two TM helices which anchor the protein to the membrane. The sensor domain is situated between these two domains. Using

ExPASy TMPred and P2RP, both SKs were identified to have HAMP domains which overlap with the second TM domain within the proteins. Within the kinase core, in addition to the highly conserved H, G and N boxes, there is a good level of similarity between the two proteins. Protein BLAST (NCBI) analysis of just the kinase core (Dhp and CA domains) shows 28% amino acid identity and 40% similarity between the two proteins. Whilst the proteins are not highly similar, other studies have shown that rewiring SKs of the same class can create functional chimeras. In Skerker, *et al.*, (2008), EnvZ and RstB kinase core shares a similar level of similarity at 26% identity and 52% similarity.

5.3.1 Design of Chimeras

Having decided on VanS as the sensor and AfsQ2 as the output of the chimeric SK, the next task was to design the chimeras. There are a number of means through which the chimeras could be designed including changing of domains as demonstrated in work by Perraud, *et al.*, (1998) or changing of residues within the Dhp domain as demonstrated by Skerker, *et al.*, 2008. In this study, 5 different chimeras were designed as illustrated in figure 5.2.

The first SK chimera, henceforth referred to as Chim1, was designed with the extracellular domain (sensor domain) and TM helices of VanS but the intracellular domains of AfsQ2. In Chimera 2 (Chim2), the Dhp domain of VanS was replaced by the Dhp domain of AfsQ2. Both of these chimeras have changes at the domain level because exchanges of SK domains has been shown to be effective in rewiring protein function. However, as both VanS and AfsQ2 sense extracellular stimuli, the converted signal must pass through the protein into the cell. Whether these domains are compatible has not been previously tested. Therefore, further chimeras were designed to minimise the changes made to the SKs. Chimeras 3-5 (Chim3-5) were designed with only changes to residues within the Dhp domain. Figure 5.2 shows the residues which were changed based on the work conducted by Skerker *et al.*, 2008, who evaluated the importance of Dhp domain residues in determining the interaction specificity between SKs and RRs. Chim3 possesses the fewest residue changes (A157T, V158A, I162V). Chim4 possesses the same residue changes as Chim3 with the additional substitution of

R180E and Chim5 has the most changes including those of Chim4 and additionally H137R, V138E, Q141S and N147D. These specific changes were selected as the substitutions in Chim3 were the corresponding residues changed in the study by Skerker, *et al.*, 2008 which allowed the complete change of EnvZ from phosphorylating OmpR to RstA instead. In that research, other residues were identified to have a high covariation which was termed mutual information. These residues were also changed in Chim5. As the different sequences of the proteins are likely to affect the folding of the proteins, the interface formed between these two TCSs may be different to that of those tested in the study. These changes were made to maximise the potential of these chimeras for successful rewiring.

The expression of Chim1 and Chim2 were designed to be under the control of *vanRS* promoter (*pvanRS*) which is an inducible promoter. In the presence of vancomycin, VanR, from the native VanRS system, upregulates expression from this promoter. The inducible promoter was chosen to maintain expression of the chimeras at a basal level like VanRS in *S. coelicolor*, under non-induced conditions. The expression of Chimeras 3-5 were under the control of the constitutive promoter of *ermE** (*permE**; Bai, *et al.*, 2015). The use of two different promoters was to ensure the chimeras were expressed and at a functional level without affecting bacterial activity through expression levels. Between the promoters and the chimera sequences is a *NdeI* restriction site for use if either promoter was ineffective. All five chimeras were tagged with hexa-His (Chim1 and Chim2) or StrepII (Chim3-5). Chimera sequences are available in supplementary material (S3).

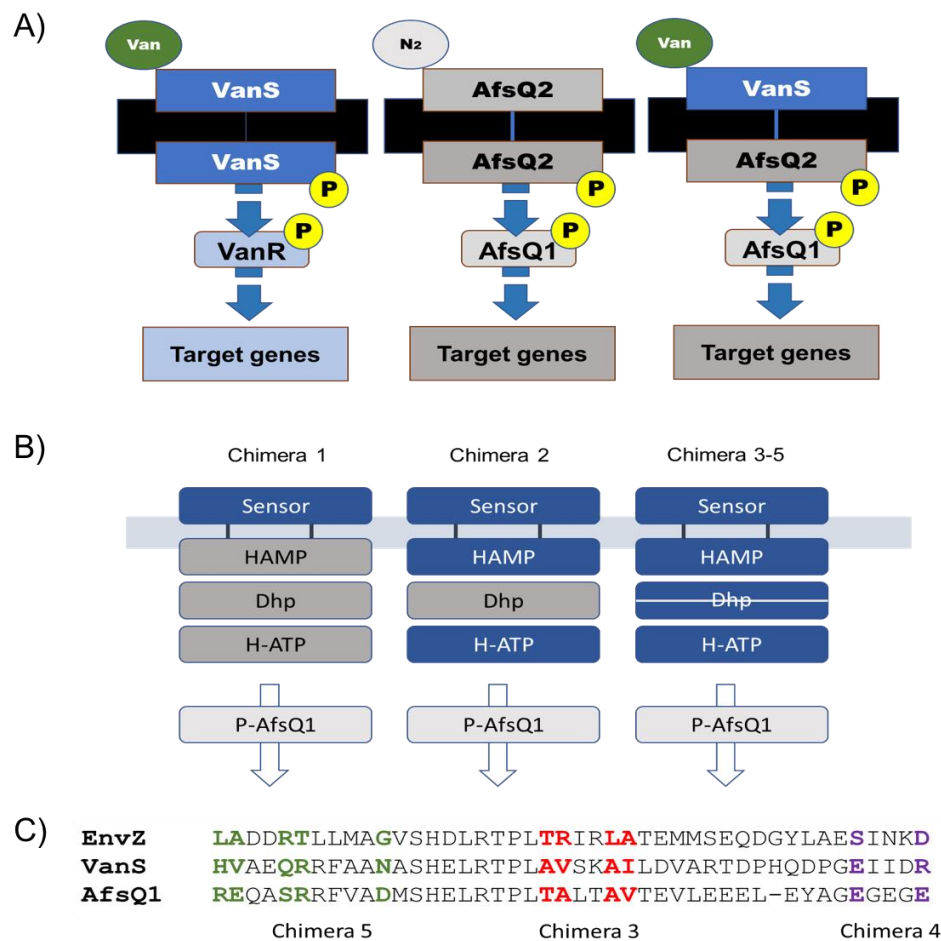


Figure 5.2: Design of VanS-AfsQ2 chimera SKs. A) Schematic of the two TCSs VanSR and AfsQ1/Q2 alongside with designed chimera, demonstrating the desired result. B) Schematic of the designs of the chimeras, where Chimera 1 and 2 have been altered by exchanges of domains and Chimeras 3-5 have residue changes only in the Dhp domain of VanS. C) Residue changes in the Dhp domain of Chim 3-5. These residue changes have been highlighted in the alignment. Chimera 3 possesses changes highlighted in red, Chimera 4 possesses the changes highlighted in red and purple and Chimera 5 has all the changes highlighted in red, purple and green. EnvZ has been shown in the alignment as a comparison between the residues changed between EnvZ and RstB in the rewiring work carried out by Skerker, *et al.*, (2008).

5.3.2 Cloning and Expression

All the chimeric SK encoding sequences were synthesized by Genscript. Both *chim1* and *chim2* were cloned into integration vector pAU3-45 (Bignell, *et al.*, 2005) into the *XbaI* and *EcoRI* sites using primers RL005F, RL006R and RL007R (Table 2.3). Cloning was confirmed by carrying out a restriction digest (Figure 5.3) in addition to sequencing using primer pair pAU3-45F/R (Table 2.3). These vectors were named pRL111 (*chim1*) and pRL112 (*chim2*). Chim3-5 were synthesised and cloned into the integration vector pMS82 (Gregory, *et al.*, 2003)

by Genscript into the *Hind*III and *Kpn*I site. These were subsequently named pRL113 (*chim*3), pRL114 (*chim*4) and pRL115 (*chim*5). Both of these integration vectors, pAU3-45 and pMS82, integrate into the chromosome at different sites, pAU3-45 integrates the ϕ C31 site and pMS82 into the ϕ BT1 site. Integration into either of these sites in *S. coelicolor* does not cause a change to wild-type phenotype.

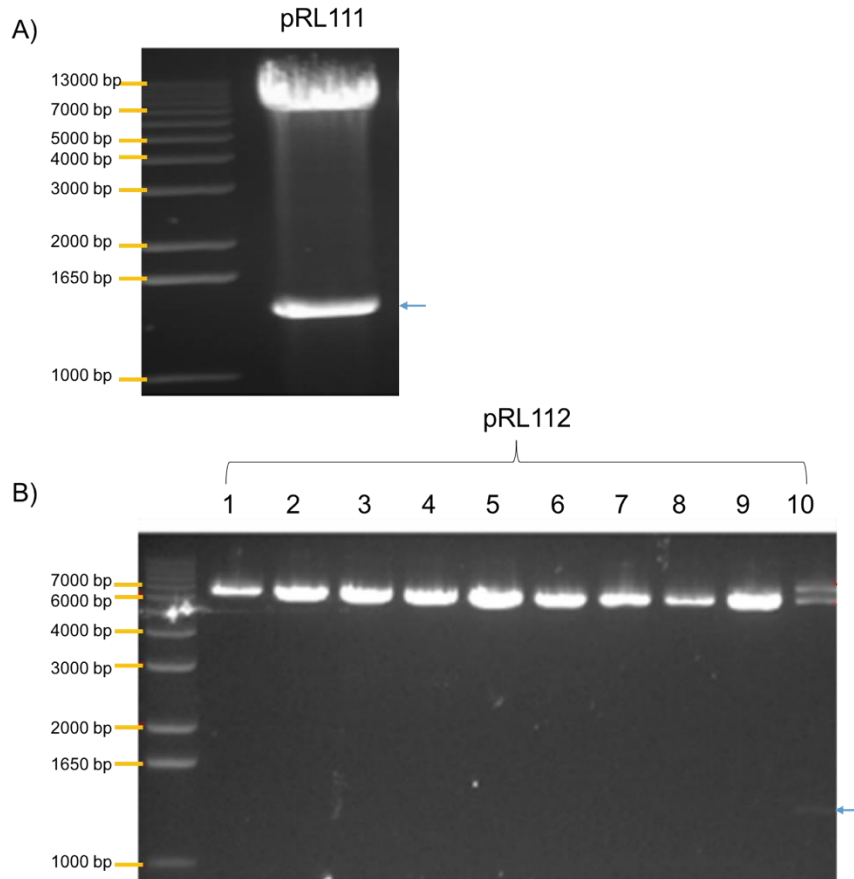


Figure 5.3: Confirmation of cloning A) *chim*1 and B) *chim*2 into pAU3-45 through restriction digest with *Xba*I and *Eco*RI. The expected sizes of *chim*1 and *chim*2 fragments are 1412 bp and 1349 bp, respectively. Arrow depicts the excised chimera fragments.

The chimeras were conjugated into *S. coelicolor* M145 possessing both VanRS and AfsQ1/Q2. These strains are referred to as M145::*Chim*1-5. The genomic DNA was then extracted, and the integration of the chimeras was confirmed through PCR using the sequencing primers pAU3-45F/R for *Chim*1 and *Chim*2 and pMS82F/R for *Chim*3-5 (Figure 5.4).

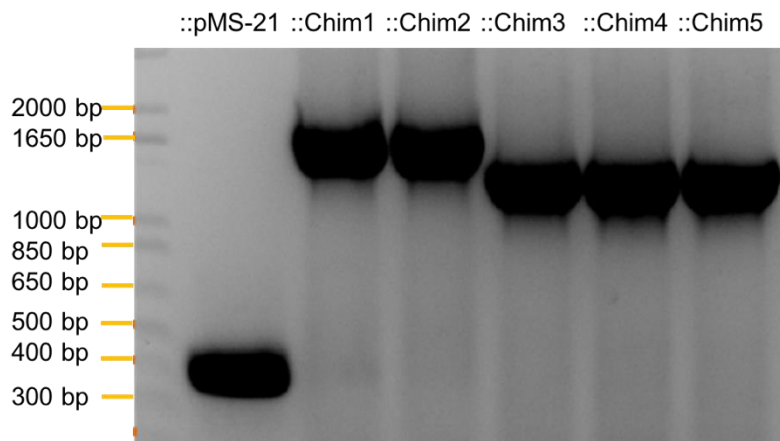


Figure 5.4: PCR confirmation of chimeras (Chim1-5) integrated into *S. coelicolor* M145 genome. The amplification of *chim1* (expected size of 1541 bp) and *chim2* (expected size of 1478 bp) were carried using primers pAU3-45F/R. The amplification of *chim3*, *chim4* and *chim5* and the empty vector pMS82 were carried out using pMS82F/R. The expected size of the amplified fragments for *chim3,4* and 5 is ~1500 bp.

Having confirmed their integration, the expression of the chimeras was then tested. To measure their expression, strains were cultured for 3 days on SFM, atop cellophane disks, and protein immuno-blot were carried out on lysed mycelia. Expression of chimeras in M145 is demonstrated in figure 5.5. The expression of Chim1 and 2 are both dependent on vancomycin which can be seen in figure 5.5A where with no vancomycin, a protein band cannot be seen. Chim3-5 protein however, can be seen with or without the addition of vancomycin as their expression is under the control of the constitutive *ermE** promoter. From the blot it is unclear why there are two faint bands of similar size for Chim3-5 proteins. The difference in size is marginal and would therefore not be dimer formation. This could be caused by shifting of the film during immuno-blotting or be caused by migration differences between the chimeras with ATP or ADP attached to the CA domain or phosphate group bound to the conserved His residue (Brunelle & Green, 2014). Whilst SDS denatures proteins, whether these chimeras had been completely denatured or whether the His residue could still bind phosphate, cannot be determined here.

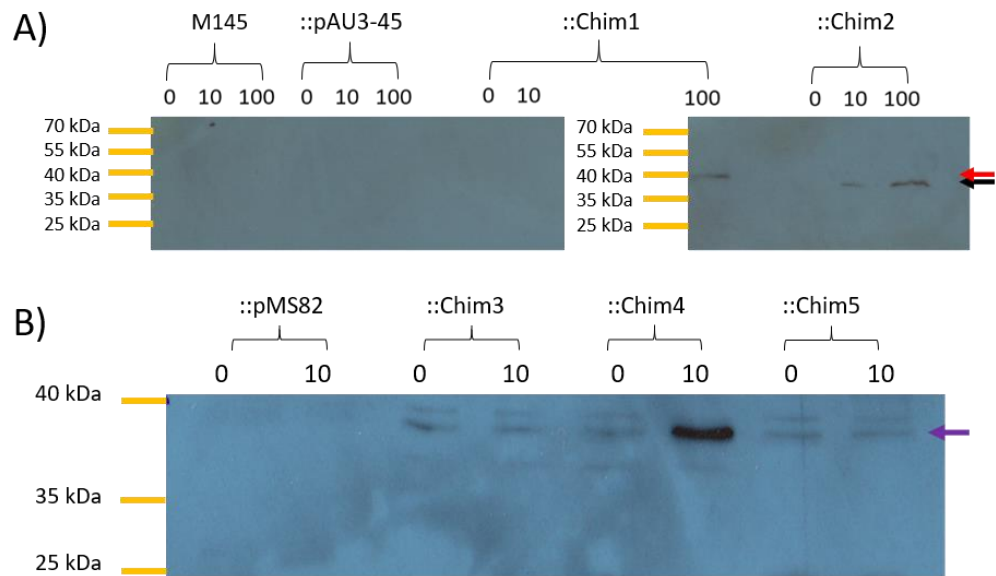
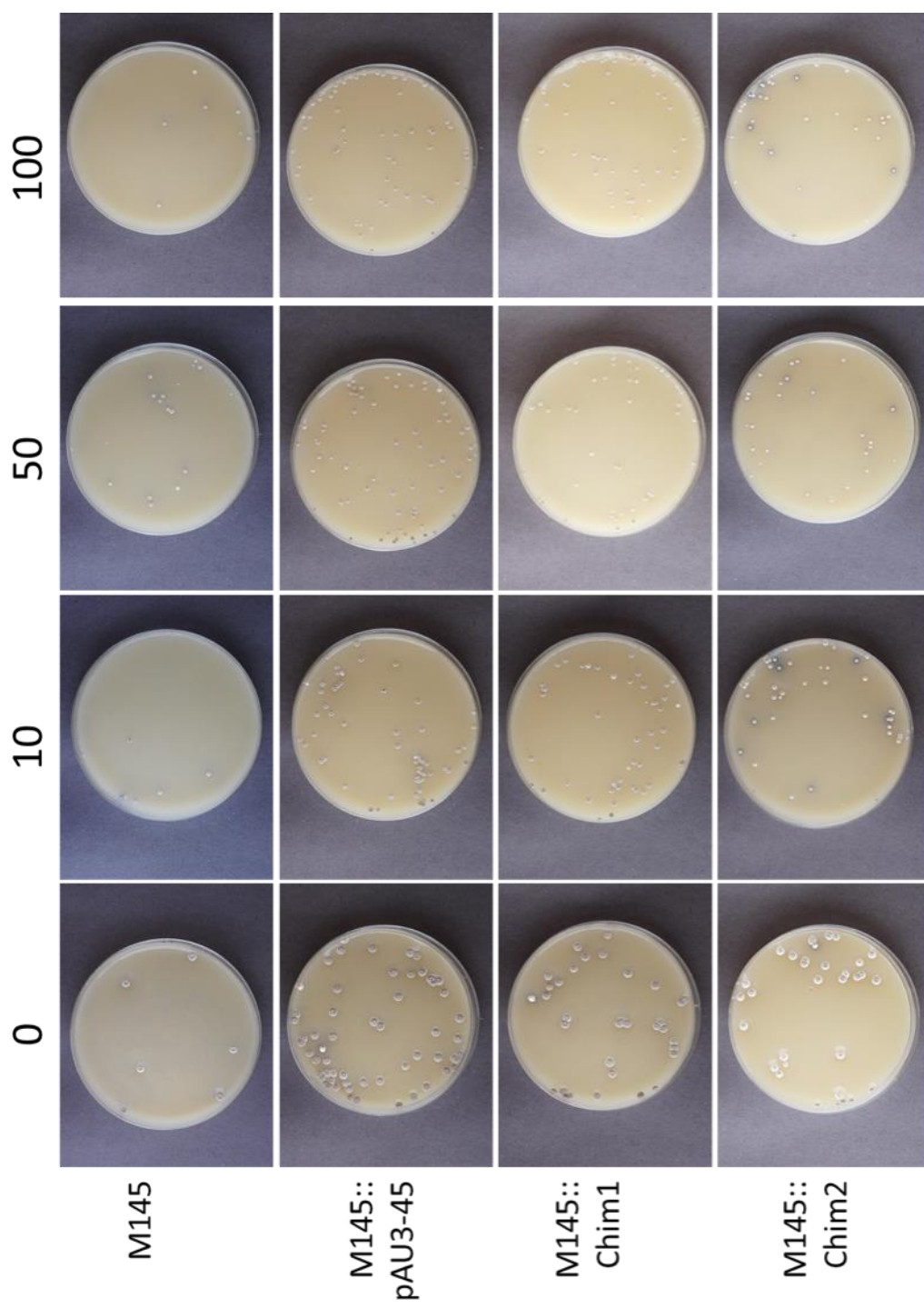


Figure 5.5: Expression of chimeras in M145 with different concentrations of vancomycin. Mycelia was harvested after 3 days of growth on SFM. A) Anti-His was used to visualise Chim1 and 2 proteins. B) Anti-StrepII was used to visualise Chim3-5 proteins. All concentrations in $\mu\text{g/ml}$. Red arrow represents Chim1 (42.7 kDa), black is Chim2 (41 kDa) and purple is Chim3-5 (39.5 kDa).

5.3.3 Phenotype in *S. coelicolor*

To determine whether the chimeras elicited any effect on *S. coelicolor* M145, all the strains were grown on SFM agar with different concentrations of vancomycin for 5 days (Figure 5.6). AfsQ1 positively regulates actinorhodin and undecylprodigiosin by modulating expression of SARPs within both clusters. With vancomycin addition, functional chimeras are expected to illicit antibiotic production through phosphorylation of AfsQ1. After 5 days, M145::Chim1 did not produce any visible actinorhodin or undecylprodigiosin on plates with or without vancomycin, regardless of the dilution of spores (data not shown). M145::Chim2 strains produced actinorhodin when grown in the presence of vancomycin. This effect was more prominent when colonies were in closer proximity. As seen in figure 5.6, when colonies are diffuse, actinorhodin is not produced.



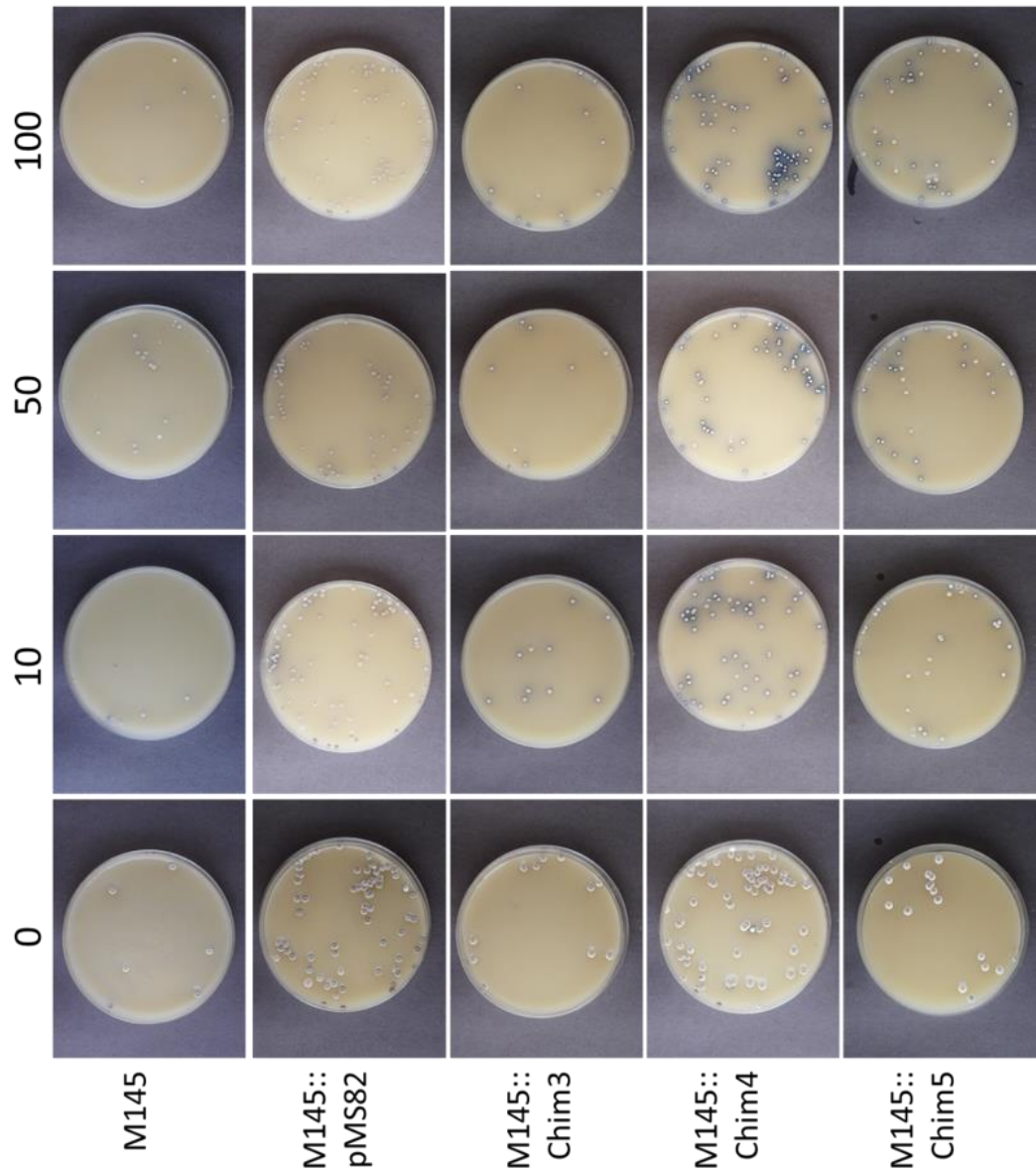


Figure 5.6: *S. coelicolor* M145 strains containing Chim1-5 grown on SFM with different concentrations of vancomycin (0, 10, 50 and 100 µg/ml) for 5 days at 30°C.

M145::Chim2-Chim5 showed visible production of actinorhodin, however M145::Chim1 did not. There was also some production of actinorhodin by M145::pMS82 colonies by some colonies located at the edges of the plate. It is unclear whether the cause of the production here is from the presence of the vector integration, the vancomycin, density of colonies or through other factors. As this production looks to be less than strains containing the chimeras (M145::Chim3-5) and not uniformly across the plates, the production of actinorhodin by the strains

possessing the chimeras, was thought to not be caused by pMS82 integration into the ϕ BT1 site.

Across all the strains, the higher concentrations of vancomycin (50 and 100 μ g/ml) did not seem to visibly increase the amount of actinorhodin produced. This may be because increasing vancomycin levels does not lead to an increase in *vanRS* promoter activity above a certain threshold, i.e. 10 μ g/ml of vancomycin.

As chimeras were introduced into a wild-type *S. coelicolor* background, antibiotic production could be caused by native AfsQ1/2 signalling of AfsQ1. The chimera strains were hence grown on MM supplemented with a low level of glutamate (7.5 mM) as the sole nitrogen source to negate affects of AfsQ1 phosphorylation by AfsQ2, to test whether the chimeras elicited antibiotic production independent of AfsQ2. Figure 5.7 shows the growth of the M145 strains with Chim3 and Chim4 because these produced the most actinorhodin when grown on SFM agar. Growth on MM supplemented with vancomycin for 11 days did not result in the production of actinorhodin which is exported from the cells and seeps into the media. As AfsQ1 is a pleiotrophic regulator, colony morphology was then focused on to see whether there were any notable differences between the strains in the presence of vancomycin.

AfsQ1 positively regulates *bldM*, which encodes an ARR that is activated by the sigma factor σ^{BldN} during aerial hyphae formation (Molle and Buttner, 2000). BldM forms homodimers and heterodimers with WhiI to regulate two groups of regulatory genes. Group I genes which are typically expressed earlier in growth is regulated by BldM homodimers include *smeA-sffA*, *whiB* and *whiE* which are involved in sporulation (Al-Bassam, *et al.*, 2014). AfsQ1 is also thought to negatively regulate *whiD*, which is a homologue of *whiB*, which is expressed early in sporulation (Wang, *et al.*, 2013B). Therefore, if AfsQ1 is phosphorylated from germination, precocious sporulation would be expected.

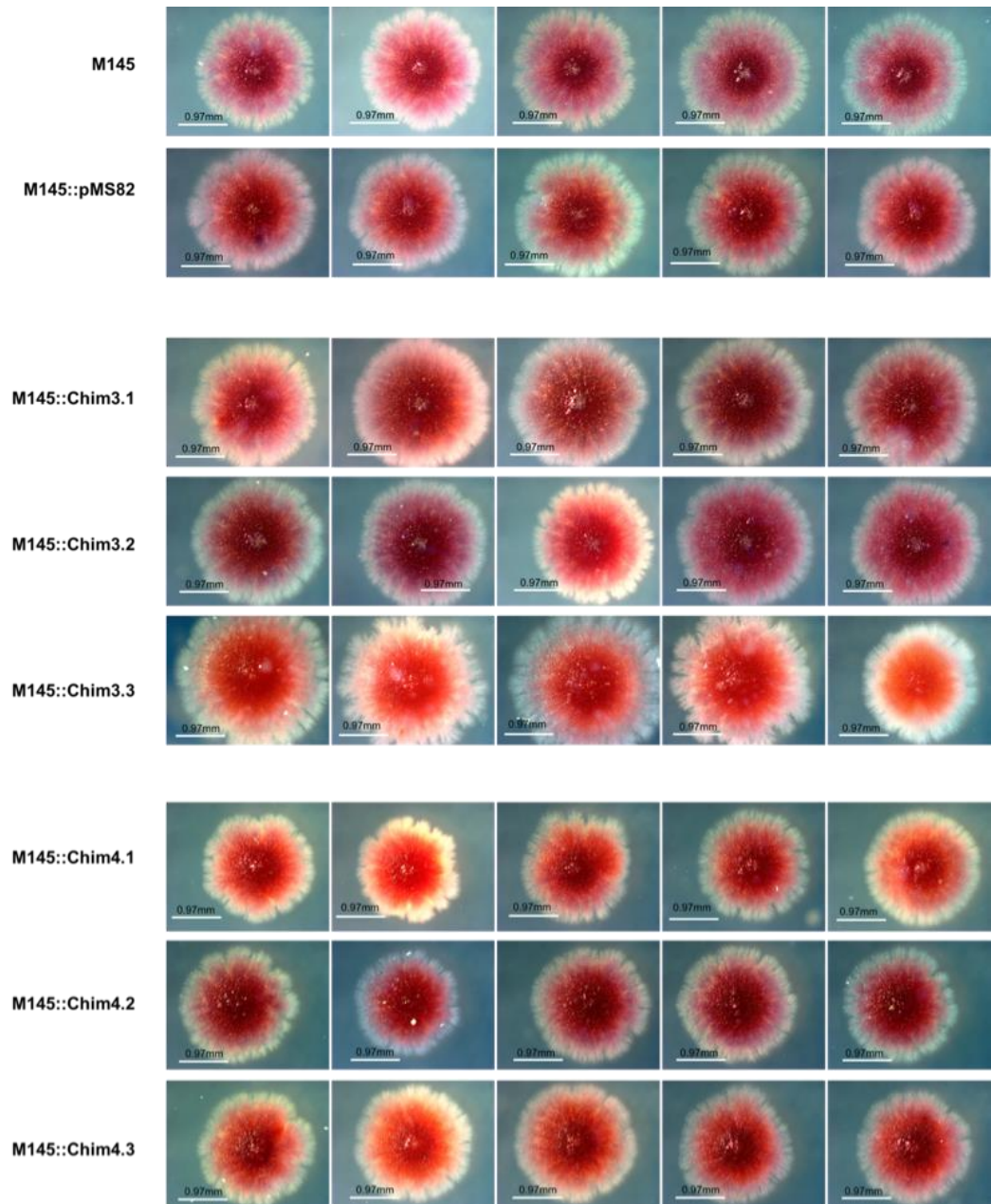


Figure 5.7: Effect of chimeras on M145 colony morphology after 11 days of growth on MM supplemented with low levels of glutamate (7.5 mM) as sole nitrogen source and vancomycin (10 μ g/ml).

Wild-type M145 and M145::pMS82 both display a blurred ‘fluffy’ phenotype caused by the aerial hyphae on MM media. Conversely, M145::Chim3 and M145::Chim4 displays concentrated aerial hyphae growth in the peripheries of the colonies but the central regions of the colonies have a bald ‘shiny’ phenotype. As vancomycin is present in the media from the beginning of growth, the central parts of the colony which formed first may have undergone sporulation during early

hyphal development, consequently resulting in sporulation with short hyphae. To determine this scanning electron microscopy could be carried out.

5.3.4 Effects on other *Streptomyces* spp.

AfsQ1/Q2 is highly conserved in *Streptomyces* but not in other Actinobacteria classes (Figure 3.5). The study carried out by Daniel-Ivad, *et al.*, (2017) showed that phosphomimetic allele AfsQ1 could activate antibiotic production in different *Streptomyces* isolates. Whilst this requires only AfsQ1 binding to AfsQ1 target promoter sequences, the induced antibiotic production in some isolates showed that this was compatible. The chimeras we thus expressed heterologously in other *Streptomyces* species. As the chimeras were generated using *S. coelicolor* proteins, the similarity of the AfsQ proteins were analysed. Figure 5.9 shows that the AfsQ proteins of *S. coelicolor* are identical to those in *S. lividans*. The only difference is that there is no overlap in the stop and start codons of *afsQ2* and *afsQ3* (which encodes an accessory lipoprotein). *S. venezuelae* AfsQ proteins however, possessed lower identity and there was an even lower identity with the AfsQ homologues of *S. formicae*. The same was also true for the divergently encoded SigQ protein.

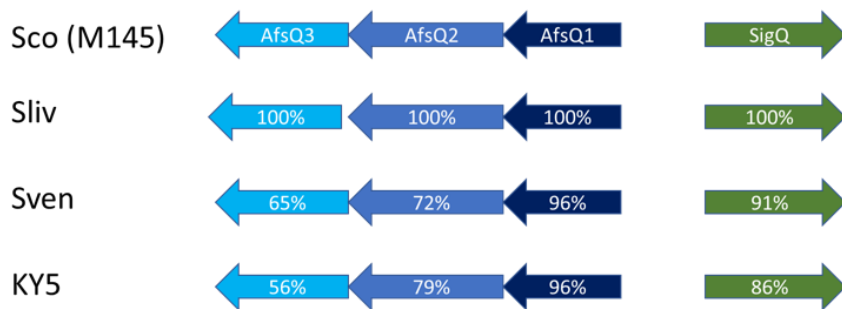


Figure 5.8: Comparison of homologues of AfsQ operon with SigQ across four *Streptomyces* species (*S. lividans* (Sliv), *S. venezuelae* (Sven) and *S. formicae* (KY5)) against *S. coelicolor* (Sco). Amino acid identity was measured through use of NCBI BLASTp alignment.

As the identity of AfsQ_{Sco} genes were not the same as AfsQ_{Sven/KY5} genes, the genes were aligned to identify where the differences were. Figure 5.9 shows the alignment between AfsQ1 and AfsQ2 across the three species. *S. lividans* was not aligned due to the 100% identity match with *S. coelicolor*. Across the AfsQ2 homologues, most of the differences between the proteins were identified in the sensor domain, which would not affect the chimeras' function as this has been

substituted for the VanS sensor. However, within the Dhp domain, AfsQ1_{Sven} and AfsQ1_{KY5} have missing residues compared to AfsQ1_{Sco}. These residues form part of D α 2. This region includes two of the residues changed in Chim4 and Chim5. These differences in residues are highlighted in figure 5.10, which shows the alignment of the region of residues changed within the Dhp domain for Chim3-5. Based on the crystal model of Spo0B and Spo0F (Skerker, *et al.*, 2008), this region of missing residues does not include any residues which are located at the interface, however, as the two glutamates (shown in purple) are within this region, interaction between chimeras and AfsQ1 within these species may be affected. However, analysis of AfsQ1 in the three species (Figure 5.10) reveals only 6 residue differences within the REC domain. Comparison of these 6 residues with residues modeled to be at the interface of Spo0F and Spo0B shows that none of these are at the interface (Skerker, *et al.*, 2008). Furthermore, none of these residues were calculated to have a high covariation score (Skerker, *et al.*, 2008). Therefore, even with the changes in sequences, there does not seem to have been any corresponding changes in the RR, suggesting that the altered residues in the SK may not affect AfsQ1 binding.

B)

```

Sco   ---VPSLLLIEDDDAIRTALELSLRQGHRVATAASGEDGLKLLREQRPDLIVLDVMLPG 57
Sven  MLPVPFLLLIEDDDAIRTALELSLSRQGHRVATAATGEDGLQLLREQRPDLVLDVMLPG 60
KY5   ---VPSLLLIEDDDAIRTALELSLRQGHRVATAATGEDGLKLLSEQRPDLIVLDVMLPG 57
      *****:*****:*****:* * *****:*****

Sco   IDGFVCCRIRRTDQLPIIILLTARNDDIDVVVGLESGADDYVVKPVQGRVLDARIRAVLR 117
Sven  IDGFVCCRIRRTDQLPIIILLTARSDDIDVVVGLESGADDYVVKPVQGRVLDARIRAVLR 120
KY5   IDGFVCCRIRRTDQLPIIILLTARNDDIDVVVGLESGADDYVVKPVQGRVLDARIRAVLR 117
      *****.*****.*****.*****.*****

Sco   RGERESTDSASFGSLVIDRSAMTVTKNGEDLQLTPTELRLLELSRRPGQALSRRQQLLRL 177
Sven  RGERESTDSATYGSGLVIDRSAMTVTKNGEDLQLTPTELRLLELSRRPGQALSRRQQLLRL 180
KY5   RGEREANDAATFGSLVIDRAAMTVTKNGEDLQLTPTELRLLELSRRPGQALSRRQQLLRL 177
      *****:.*:.*:*****:*****.*****.*****

Sco   VWEHDYLGDSRLVDACVQRLRAKVEDVPSSPTLIRTVRGVGYRLDPPQ 225
Sven  VWEHDYLGDSRLVDACVQRLRAKVEDVPSSPTLIRTVRGVGYRLDPA 228
KY5   VWEHDYLGDSRLVDACVQRLRAKVEDVPSSPTLIRTVRGVGYRLDTPQ 225
      ***** *

```

Figure 5.9: Protein sequence alignment of A) AfsQ2 and B) AfsQ1 homologues from *S. coelicolor* (Sco), *S. venezuelae* (Sven) and *S. formicae* (KY5) using Clustal Omega. The domains of AfsQ2 are highlighted as follows, blue text denotes sensor domains, red text denotes TM helices (as predicted by Expsy TMPred), underlined text denotes HAMP domain (as predicted by P2RP; Barakat, et al., 2013), green text denotes Dhp domain and yellow text denotes CA domain. The REC domain of AfsQ1 is shown in purple and the DNA binding domain in orange.

```

AfsQ2 (Sco/Sliv) REQASRRFVADMSHELRTPLTALTAVTEVLEEELEYAGEGEGE
AfsQ2 (Sven)    REESSRRFVADMSHELRTPLTALTAVTEVLEDE-----
AfsQ2 (KY5)    RDEASRRFVADMSHELRTPLTAITAVTEVLEEELD-----AE

```

Figure 5.10: Alignment of the Dhp domain region where changes were made between Chim3-5 between AfsQ2 homologues of *S. colicolor* and *S. lividans* (Sco/Sliv), *S. venezuelae* (Sven) and *S. formicae* (KY5). Altered residues between the chimeras are colour coded. Red residues are altered residues in Chim3; Chim4 residues altered are those in red and purple and Chim5 altered residues are the green, purple and red residues.

The chimeras were first conjugated into *S. lividans*. Unlike *S. coelicolor*, actinorhodin biosynthesis in *S. lividans* is silent. AfsQ1 was first identified when actinorhodin was produced after AfsQ1_{Sco} was heterologously expressed in *S. lividans* (Ishizuka, et al., 1992). Figure 5.11 and 5.12 both show that the chimera SKs had no effect on antibiotic production in *S. lividans*; the biosynthetic pathways remained silenced. Different concentrations of vancomycin were tested to assess whether a higher concentration of vancomycin would activate production. Figures 5.11 and 5.12 shows growth of *S. lividans* strains with 10 and 50 µg/ml, respectively. A higher concentration of vancomycin, 100 µg/ml was also tested (data not shown), however the tested concentrations displayed no change in phenotype. Analysis of colony morphology also did not display any differences

between wild-type strains or with the chimeras when grown with vancomycin. As the sequence between AfsQ1_{Sco} and AfsQ1_{Sliv} are identical, this lack of phenotype may be due to signaling of chimera SK to AfsQ1. However, in work conducted by Ishizuka, *et al.*, (1992), AfsQ1 was introduced through plasmids meaning higher copy numbers and expression levels of AfsQ1. As the levels of AfsQ1 here remain low, there may be another mechanism silencing the system.

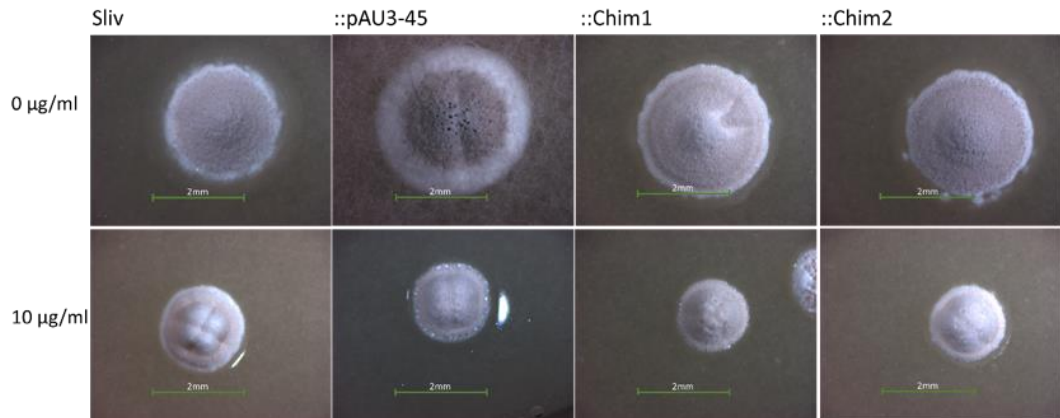


Figure 5.11: The effects of Chim1 and Chim2 in *S. lividans* with and without vancomycin (10 µg/ml). Strains were grown on SFM agar for 7 days. All scale bars show 2 mm. Sliv refers to *S. lividans*, ::pAU3045 refers to *S. lividans* with empty vector pAU3-45 integrated, ::Chim1 and ::Chim2 refer to *S. lividans* with *chim1* and *chim2* integrated at the ϕ C31 site.

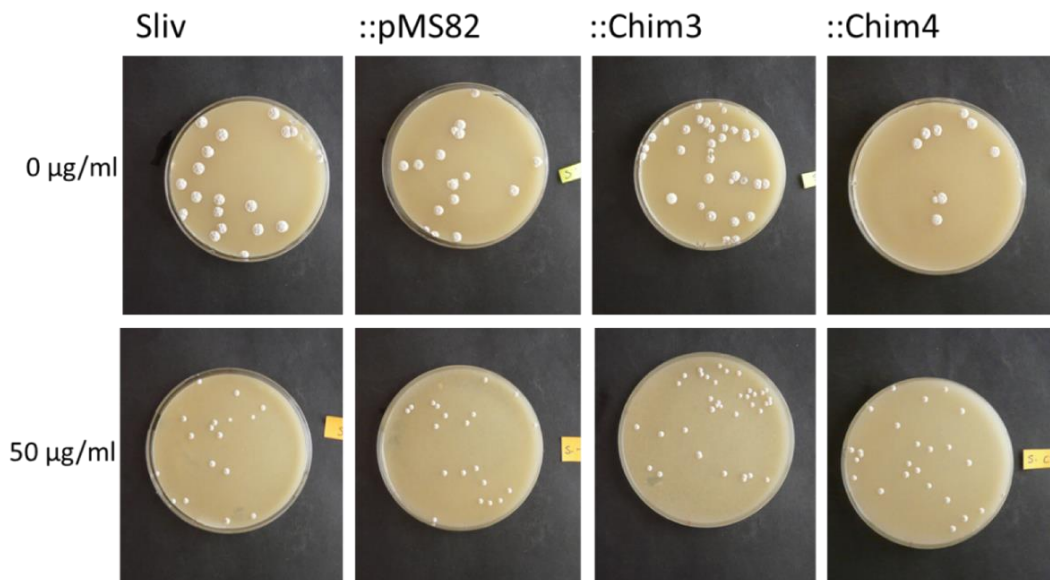


Figure 5.12: The effects of Chim3 and Chim4 on *S. lividans* with and without vancomycin (50 µg/ml). Strains cultured on SFM for 7 days. Sliv refers to *S. lividans*, ::pMS82 refers to *S. lividans* with empty vector pMS82 integrated, ::Chim3 and ::Chim4 refer to *S. lividans* with *chim3* and *chim4* integrated at the ϕ BT1 site.

Chim3-5 were then conjugated into *S. venezuelae* and *S. formicae* KY5. Unlike *S. coelicolor* and *S. lividans*, neither *S. venezuelae* or *S. formicae* KY5 have

vancomycin resistance. Furthermore, as Chim1 and Chim2 are integrated at ϕ C31 site through pAU3-45, these were not integrated into *S. venezuelae* due to integration at this site in the genome causing a developmental defect. Chim1 and Chim2 were also not used due to earlier results in *S. coelicolor* showing greater production on antibiotics in strains containing Chim3 and Chim4.

Due to *S. formicae* KY5 and *S. venezuelae* possessing no resistance against vancomycin, different concentrations of vancomycin were tested on these strains to elucidate the highest non-lethal concentration of vancomycin which could be used on these strains. The highest concentration was identified to be 0.5 μ g/ml.

Neither strain produces actinorhodin or undecylprodigiosin, which could be used as indicators of successful rewiring. Consequently, bioassays were instead carried out to identify whether antibiotic production was activated by chimeras with the addition of vancomycin. The interaction between *S. venezuelae* and *S. formicae* KY5 strains with different indicator strains can be seen in figure 5.13 and 5.14, respectively.

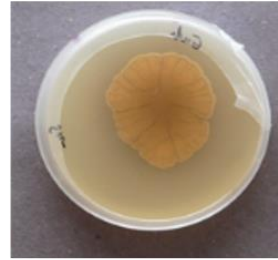
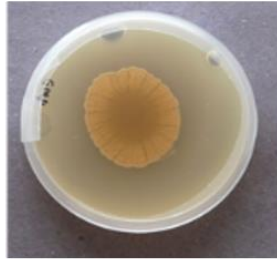
E. coli Top 10 and *C. albicans* (clinical isolate) were used as indicators for chloramphenicol production against *S. venezuelae* strains. Sven::Chim3 grown with vancomycin showed the greatest level of *E. coli* inhibition in both assays. Although less clear with *C. albicans*, compared to wild-type and other strains, the area surrounding Sven::Chim3 was clearest, despite being hazy, showing low level inhibition. This is interesting as *C. albicans* is not susceptible to chloramphenicol even at 200 mg/ml (Joseph, *et al.*, 2015). This hazy zone may be due to other bioactives produced by *S. venezuelae* such as watasemycin, which is part of the 2-Hydroxyphenylthiazolines family on non-ribosomal natural products (Inahashi, *et al.*, 2017). Against *E. coli* both Sven::Chim4 and Sven::Chim5 showed inhibition with Sven::Chim4 displaying a smaller zone of inhibition than Sven::Chim3 but larger than Sven::Chim5.

A) *E. coli*

0 $\mu\text{g/ml}$

0.5 $\mu\text{g/ml}$

Sven



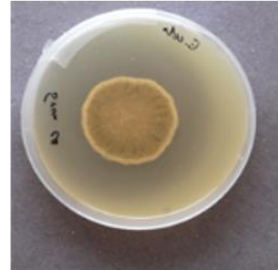
::pMS82



::Chim3



::Chim4



::Chim5



B) *C. albicans*

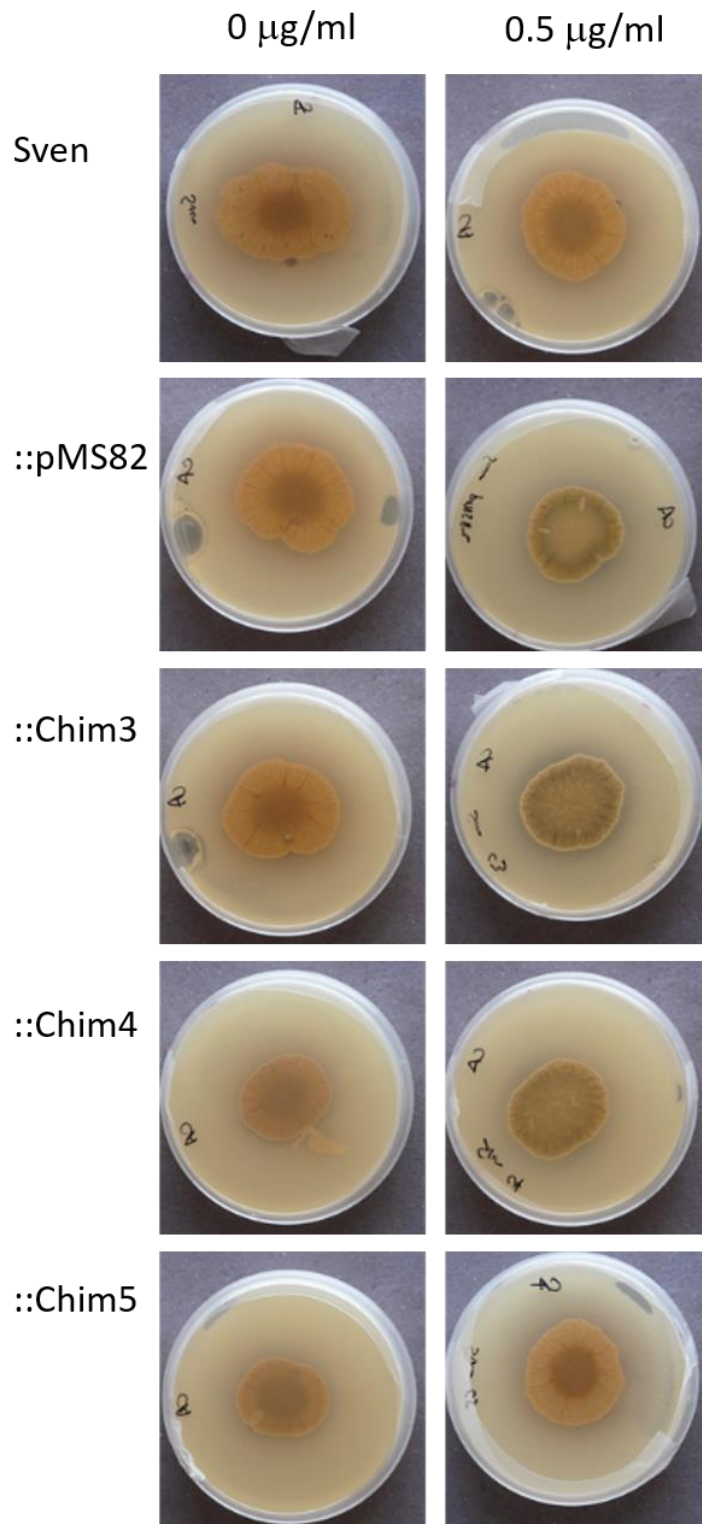


Figure 5.13: Analysis of bioactivity of *S. venezuelae* strains containing Chim3-5 against (A) *E. coli* Top 10 and (B) *C. albicans* (clinical isolate). *S. venezuelae* strains were spotted on to the MYM plate with (0.5 $\mu\text{g/ml}$) and without vancomycin and grown for 3 days before indicator strains were inoculated into SNA and overlaid onto the plate around the growing *Streptomyces*.

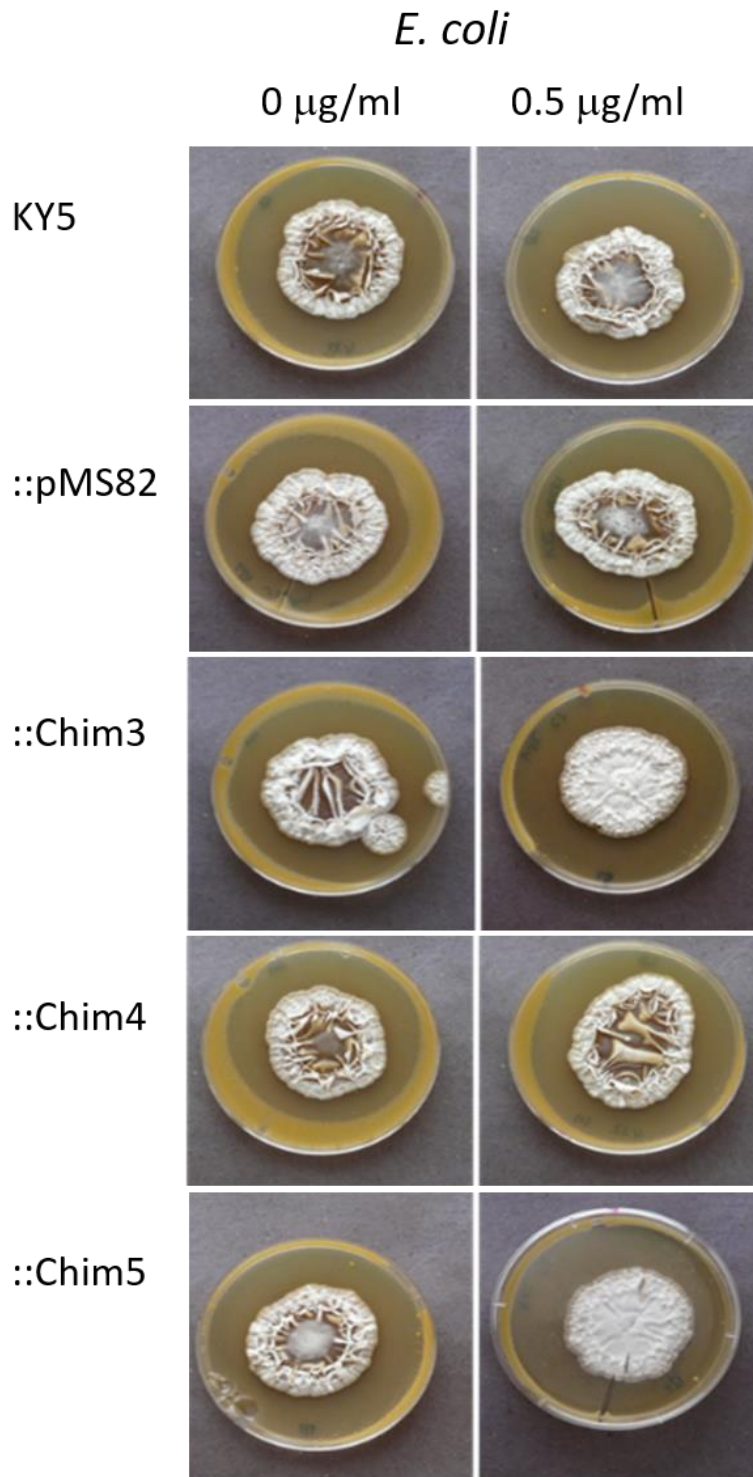


Figure 5.14: Analysis of bioactivity of *S. formicae* KY5 strains containing Chim3-5 against *E. coli* Top10. KY5 strains were spotted on to the MYM plate with (0.5 $\mu\text{g/ml}$) and without vancomycin and grown for 7 days before indicator strains were inoculated into SNA and overlaid onto the plate around the growing *Streptomyces*.

As this is a qualitative assay, LCMS was carried out using the media surrounding the growing biomass to attain the exudates to assess whether any new compounds were produced. After culturing the cells (*S. venezuelae* wild-type, Sven::pMS82 and Sven::Chim3) on solid MYM media for 5 days, the media surrounding the live mass was excised and soaked in acetonitrile overnight before vacuum drying. Dried samples were sent for LCMS analysis which showed no differences between the samples, however, the time between sending the samples and sample analysis was over a month at 4°C which could have resulted in degradation of samples if any compounds are unstable. Therefore, these results do not show definitively that chloramphenicol or jadomycin or other bioactives are not produced in a chimera dependent manner in response to vancomycin.

Bioassays carried out with *S. formicae* were difficult to assess as even without chimeras *S. formicae* inhibited growth of *E. coli* Top10 and *C. albicans* (clinical isolate). Inhibition of *E. coli* is presented in Figure 5.14, which shows a marginal increase in the zones of inhibition around KY5::Chim3 and KY5::Chim4 on plates with vancomycin than plates without, however, the difference is very similar to that of wild-type.

From the bioassays, the *S. venezuelae* strains demonstrated the greatest bioactivity with the integration of chimeras. Surprisingly, the chimeras did not activate antibiotic production in *S. lividans*. As SKs often possess phosphatase activity in addition to kinase activity, phosphorylated AfsQ1 (by the chimeras) could be dephosphorylated again by native AfsQ2 due to lack of AfsQ2 signal. Therefore, we reasoned that deletion of the *afsQ2* gene may improve the activity of the rewired systems. Research by Rodriguez, *et al.*, (2013) who complemented an *afsQ1/Q2* double mutant with a copy of *afsQ1* showed this was not sufficient to restore the reduced antibiotic production phenotype, indicating that AfsQ2 is the sole phospho-donor of AfsQ1. Therefore, we reasoned that with deletion of *afsQ2*, the sole phospho-donor of AfsQ1 will be the chimeric SKs and AfsQ2 will not be available to dephosphorylate AfsQ1.

5.3.5 Deletion of *afsQ2*

Deletions of *afsQ2* were made in *S. coelicolor* M145, *S. lividans* and *S. venezuelae*. To generate these mutants, the CRISPR/Cas9 vector pCRISPomyces2 (Cobb, *et al.*, 2015) was used. As *afsQ1/Q2/Q3* possess overlapping start and stop codons, in frame deletions were made to prevent disruption of downstream genes and subsequent polar effects. Flanking sequences (~1600 bp) of *afsQ2* were amplified and assembled into the pCRISPomyces-2 vector containing the protospacers previously inserted (Table 2.3). Δ *afsQ2* strains were confirmed through PCR analysis before sequencing of an amplified fragment including 200bp up- and downstream of the recombined region. Figure 5.15 shows the PCR confirmation of *S. coelicolor* Δ *afsQ2* (M145 Δ *afsQ2*). Three sets of PCRs were carried out to confirm the mutation. For *S. coelicolor*, flanking PCRs were carried out using RLO0129F/131R which amplified ~250 bp 5' and 3' of AfsQ2. Internal PCRs were carried out using RLO130F/131R which amplifies from within AfsQ2 to 100 bp 5' of AfsQ2. The third PCR was carried using one primer outside to the original homology region and one in the flanking arm (RLO129F/133R). Of the four independent strains tested, strain 1 tested positive (mutant genotype) for all three PCRs and mutant 4 for two of these PCRs. Both were sequenced using confirmation primers RLO0129F-135R, which showed only mutant 1 to be correct. This strain was taken forward and the chimeras (Chim3-4) were introduced into this Δ *afsQ2* background. This was also carried out for *S. lividans* Δ *afsQ2* (Sliv Δ *afsQ2*) and *S. venezuelae* Δ *afsQ2* (Sven Δ *afsQ2*). In these deletions two and three independent deletions were successfully made and confirmed, respectively. Only Chim3 and Chim4 were introduced into these backgrounds as the bioassays showed Chim 3 and Chim4 to have the greatest effect on the *Streptomyces* species tested.

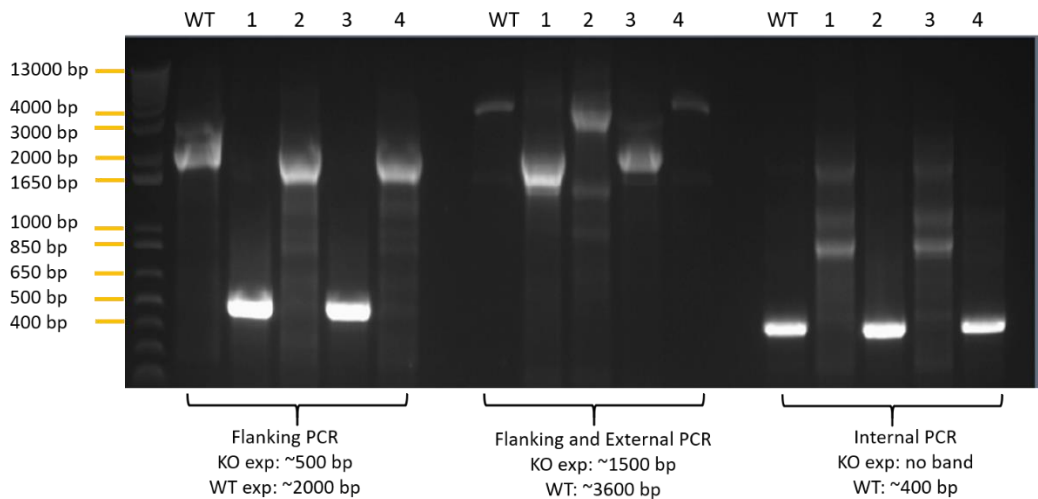


Figure 5.15: PCR confirmation of *S. coelicolor* M145 Δ *afsQ2*. Three sets of PCRs were carried out in the analysis, flanking PCR where primers amplify the region surrounding *afsQ2* (RLO0129F/131R), internal PCR where one primer is situated within *afsQ2* (RLO0130F/131R) and a third PCR where one primer is within the homology region originally amplified and one primer is outside of this region (RLO0129F/133R). The expected (exp) sizes of these PCRs are shown. WT refers to M145, and 1-4 refer to the four independent apramycin sensitive strains tested.

Before testing the effects of the chimeras in the *afsQ2* deletion strains, M145 Δ *afsQ2* was compared to M145 wild-type under low and high levels of glutamate to assess whether without AfsQ2, antibiotics would be produced when grown in high nitrogen levels (Figure 5.16). The strains were grown in triplicate in MM supplemented with 7.5 or 75 mM glutamate as the sole nitrogen source. The results from these triplicates were not reproducible. The wild-type strain showed less variation than the deletion strain. M145 consistently produced actinorhodin when grown in MM with 75 mM glutamate. Under low nitrogen conditions, a varying amount of actinorhodin was produced with the supernatant of one looking pale blue, another clear and the third a purple shade. However, in all three, the level of actinorhodin is decisively lower than the triplicate exposed to high glutamate levels, consistent with findings by Shu, *et al.*, (2009). In the deletion strain, varying levels of antibiotics were produced whether in a low or high concentration of nitrogen. The same result was also seen whether strains were grown in flasks aerated by springs (Figure 5.16) or glass beads (data not shown). Without AfsQ2, AfsQ1 should not be phosphorylated (Shu, *et al.*, 2009). Therefore, the inconsistency could be due to other systems feeding into the network. The TCS GluR/K described in section 1.3.1.2 was found to specifically bind glutamate and

not glutamine. In response to glutamate levels, it positively regulates antibiotic production. Without AfsQ2 phosphotransfer, AfsQ1 will not antagonise GlnR binding, therefore glutamine will be synthesised from glutamate. These two ongoing pathways may be the cause of the inconsistency of antibiotic production. Additionally, despite the volume of media, and concentration of added components being the same, there may still be slight differences between the flasks inducing the differences. All strains were then grown on plates together to reduce differences of conditions between individual flasks.

The chimeras in both the M145 wild-type and Δ *afsQ2* background were spotted (5 μ l of spores) onto MM supplemented with 7.5 and 75 mM glutamate, with (10 μ g/ml) and without vancomycin (Figure 5.17). In Figure 5.17, an overexpression AfsQ1 strain was used to test whether AfsQ1 could be phosphorylated within the cell if overexpressed, however, it was later determined that the construct was incorrect and it was not used further.

In this experiment, with low levels of nitrogen (7.5 mM glutamate), both M145 and M145 Δ *afsQ2* strains, with and without chimeras were expected to not produce antibiotics, as AfsQ1 is not activated, which is observed. M145 strains grown in MM with high levels of nitrogen (75 mM glutamate) were expected to produce antibiotics. Here all the M145 strains have a pink hue which could be actinorhodin or undecylprodigiosin. M145 wild-type produces a higher level of antibiotics than the other strains (::pMS82, ::Chim3 and ::Chim4). Growth of the M145 Δ *afsQ2* strains in 75 mM glutamate was expected to not illicit antibiotic production, however, as seen from figure 5.16, without the AfsQ pathway, the the growth of the strains is highly variable. However, relative to M145 strains, all M145 Δ *afsQ2* produce less antibiotics under high nitrogen conditions.

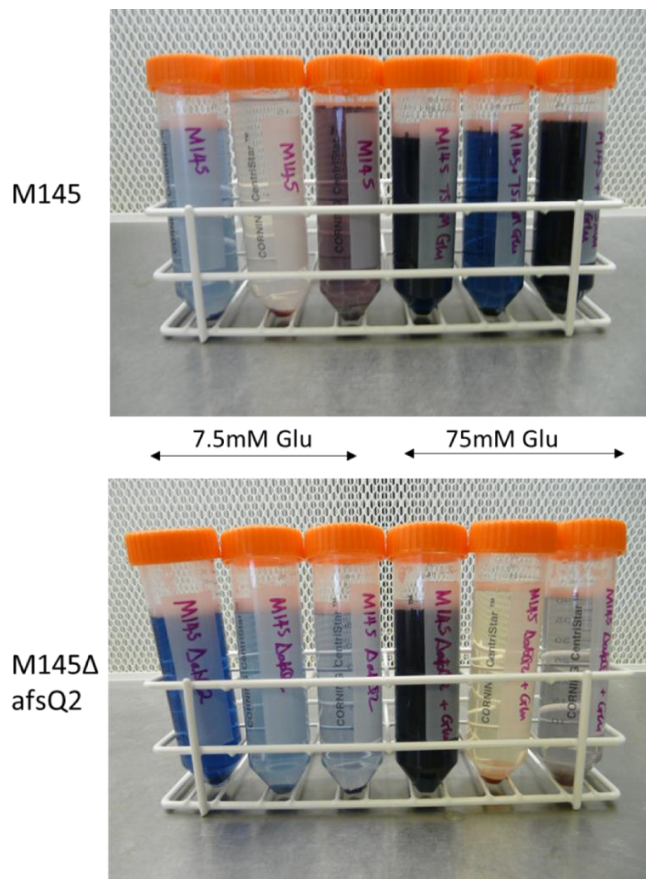


Figure 5.16: Growth of M145 and M145 Δ *afsQ2* in MM in triplicate with low (7.5 mM) and high (75 mM) levels of glutamate for 24 hrs. Cultures (50 ml) were grown in 250 ml conical flasks, aerated with springs.

Under low glutamate and added vancomycin conditions, all strains produced a low level of antibiotics except M145 Δ *afsQ2*. This also holds true under higher glutamate concentration, M145 Δ *afsQ2* is the only tested strain to not produce any pigmented antibiotics. Both M145 Δ *afsQ2* and M145 Δ *afsQ2*::pMS82 were expected to produce none or very low levels of antibiotics across all the tested conditions, whereas the strains containing chimeras, if rewiring was successful, would produce a greater amount of antibiotics in conditions with vancomycin. There is a marginal difference between the colour intensity between M145 Δ *afsQ2* strains without and with chimeras, in the low glutamate with antibiotics plates. The strains expressing chimeras are slightly a darker pink and hence appear to be producing more antibiotics. However, comparing M145 Δ *afsQ2* to M145 Δ *afsQ2*::pMS82, the latter is evidently producing more antibiotics. This is also reflected in these strains grown under high nitrogen levels and with added vancomycin.

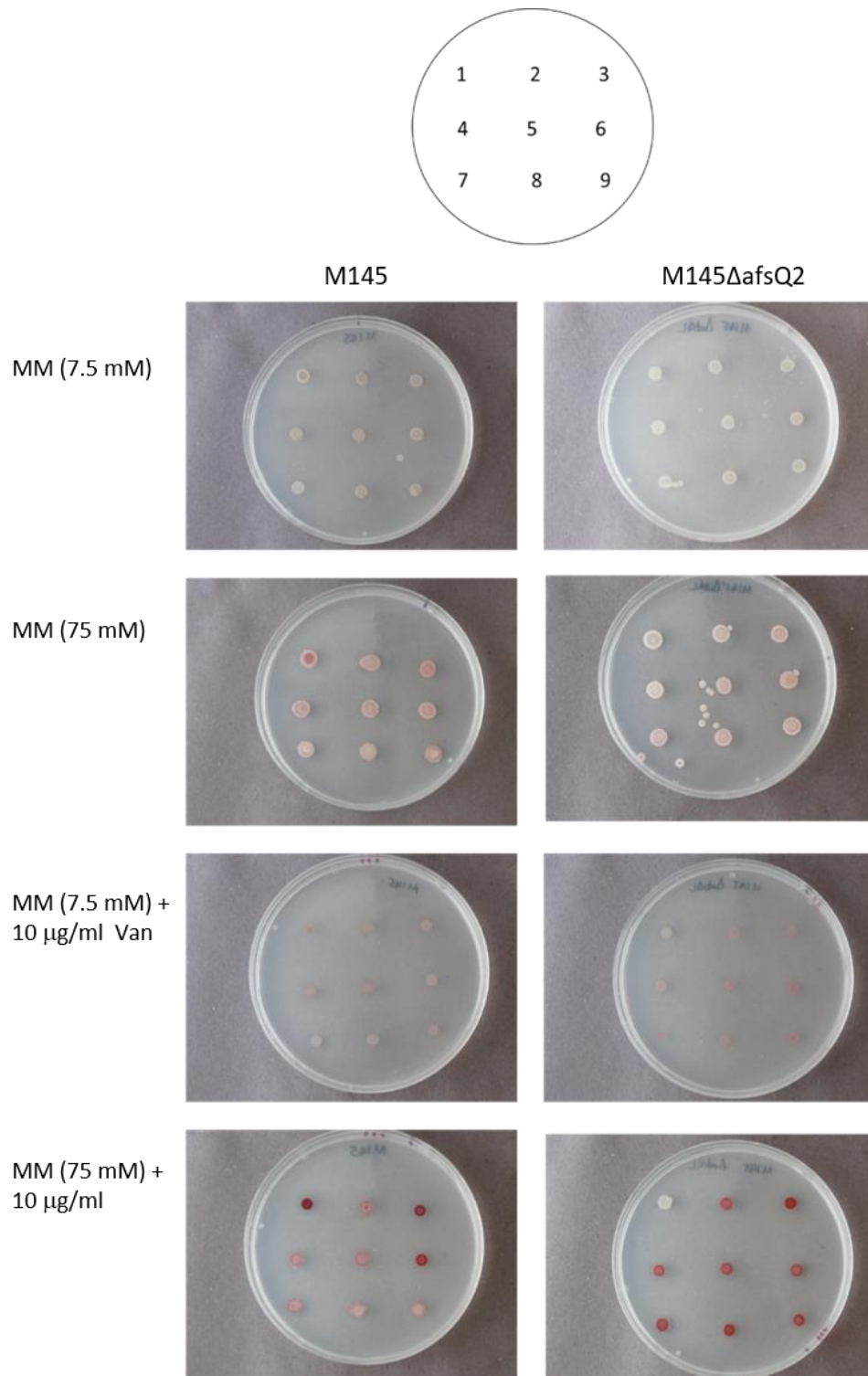


Figure 5.17: *S. coelicolor* M145 and isogenic Δ *afsQ2* strains cultured on MM supplemented with 7.5 mM and 75 mM of glutamate as sole nitrogen source with 0 and 10 μ g/ml. All strains were spotted (5 μ l) onto plates in the same orientation as schematic. The numbers are represented as follows: 1 = M145 (WT or Δ *afsQ2*), 2 = ::pMS82, 3 = ::truncated *afsQ1*(*ermE**), 4-6 = ::Chim3 (independent strains), 7-9 = ::Chim4 (independent strains).

This shows that integration of either pMS82 or integration into the ϕ BT1 site in *S. coelicolor* has an effect on antibiotic production. The ϕ BT1 site within *S. coelicolor* is within the gene *sco4848*. This gene encodes a *Streptomyces* conserved 70 amino acid integral membrane protein of unknown function (Gregory, *et al.*, 2003; Chandra and Chater, 2014). The vector possesses a HygR cassette and part of the AprR cassette promoter. For this reason, pSS170 (Schlimpert, JIC, unpublished) was recently generated to reduce the levels of expression from *aprR* cassette promoter. It is unknown whether it is disruption of *sco4848* or the vector integration itself that is causing this up-regulation in antibiotic production.

Of the strains grown in high nitrogen levels with vancomycin, M145 Δ *afsQ2*::Chim4 are marginally darker than other strains in that condition with the Δ *afsQ2* background. In the wild-type background, M145::Chim4 produces less antibiotics than M145, M145::Chim3 or M145::pMS82. This is a contradicting result as if this was solely due to issues with the integration vector, M145::Chim4 and M145::pMS82 would be expected to present the same phenotype. With the high nitrogen levels, AfsQ2 should be phosphorylating AfsQ1. This phenotype should be independent of AfsQ signaling; however, a similar result is not seen in the Δ *afsQ2* background.

Focusing on strains containing Chim4, these strains were then grown on individual plates to assess the phenotypes of the individual colonies. These strains were grown with and without vancomycin and with low or high levels of glutamate as the sole nitrogen source in MM. Figure 5.18 shows only M145 Δ *afsQ2* strains grown with low nitrogen levels with vancomycin. For all the test conditions, see supplementary material, S4. The individual colonies look very similar. M145 Δ *afsQ2*::Chim4 colonies are slightly larger than M145 Δ *afsQ2* and M145 Δ *afsQ2*::pMS82. M145 Δ *afsQ2*::Chim4 colonies are also larger than those in the wild-type background (Supplimentary material, S4). If Chim4 is phosphorylating AfsQ1, the AfsQ1 would negatively regulate nitrogen metabolism, which would infer small colonies. However, AfsQ1 also positively regulates *SCO2978* and *pstS* which are involved in carbon and phosphate metabolism, which could result in larger colonies.

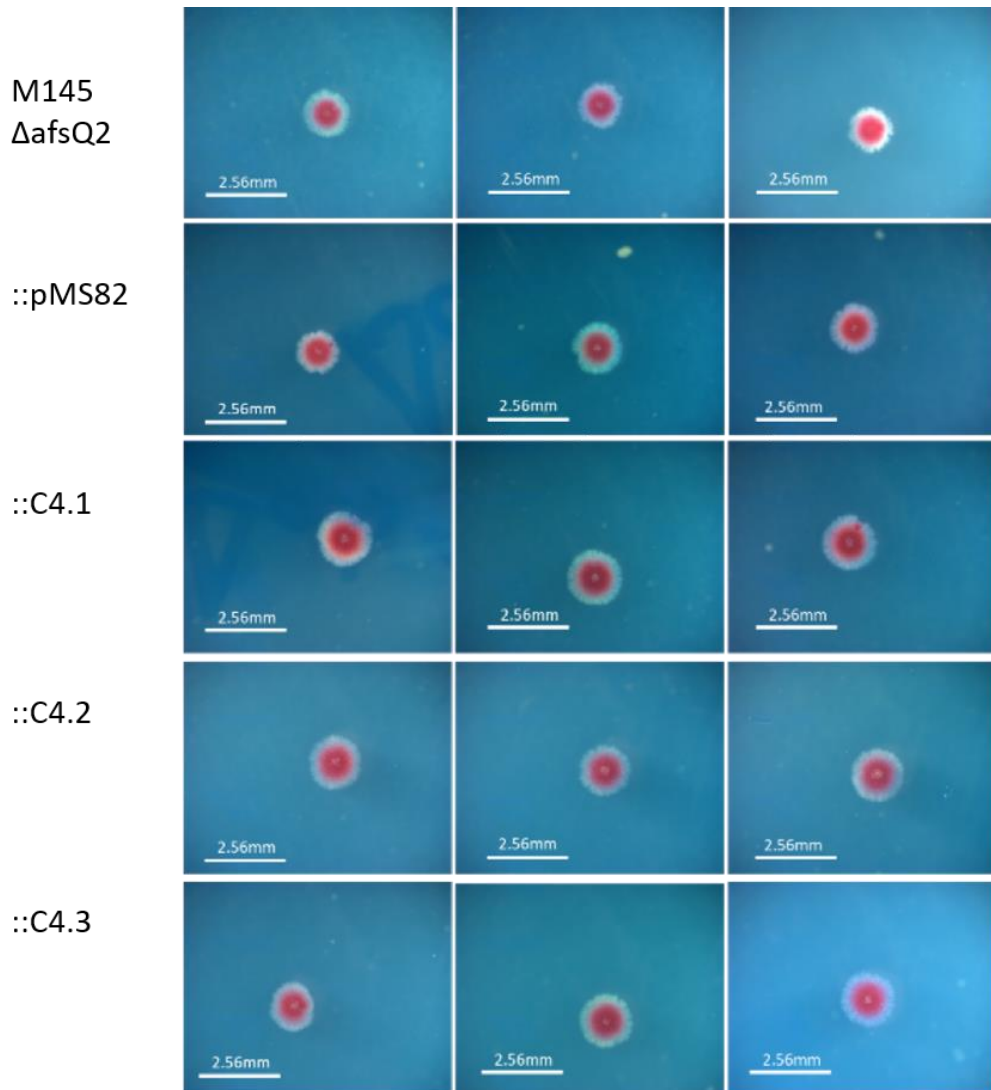


Figure 5.18: Colony morphology comparison of Chim4 in *S. coelicolor* M145 Δ *afsQ2* (M145 Δ *afsQ2*) grown on MM for 9 days with 7.5mM glutamate with 10 μ g/ml vancomycin. C4.1-3 refer to isogenic strains. Three colonies are shown per plate. Each plate contained approximately 15-30 colonies.

Having analysed the affects of the chimeras in *S. coelicolor* strains M145 and M145 Δ *afsQ2*, *S. lividans* and *S. venezuelae* strains with the *afsQ2* deletion were investigated. Despite deletion of *afsQ2*, *S. lividans* strains with or without the chimeras integrated display no effect in any of the tested conditions of high and low nitrogen levels, with or without vancomycin.

Bioassays carried out using the *S. venezuelae* strains (Sven and Sven Δ *afsQ2*) showed that Sven Δ *afsQ2* had greater bioactivity against *E. coli* and *B. subtilis* than wild-type *S. venezuelae* when vancomycin was added (Figure 5.19).

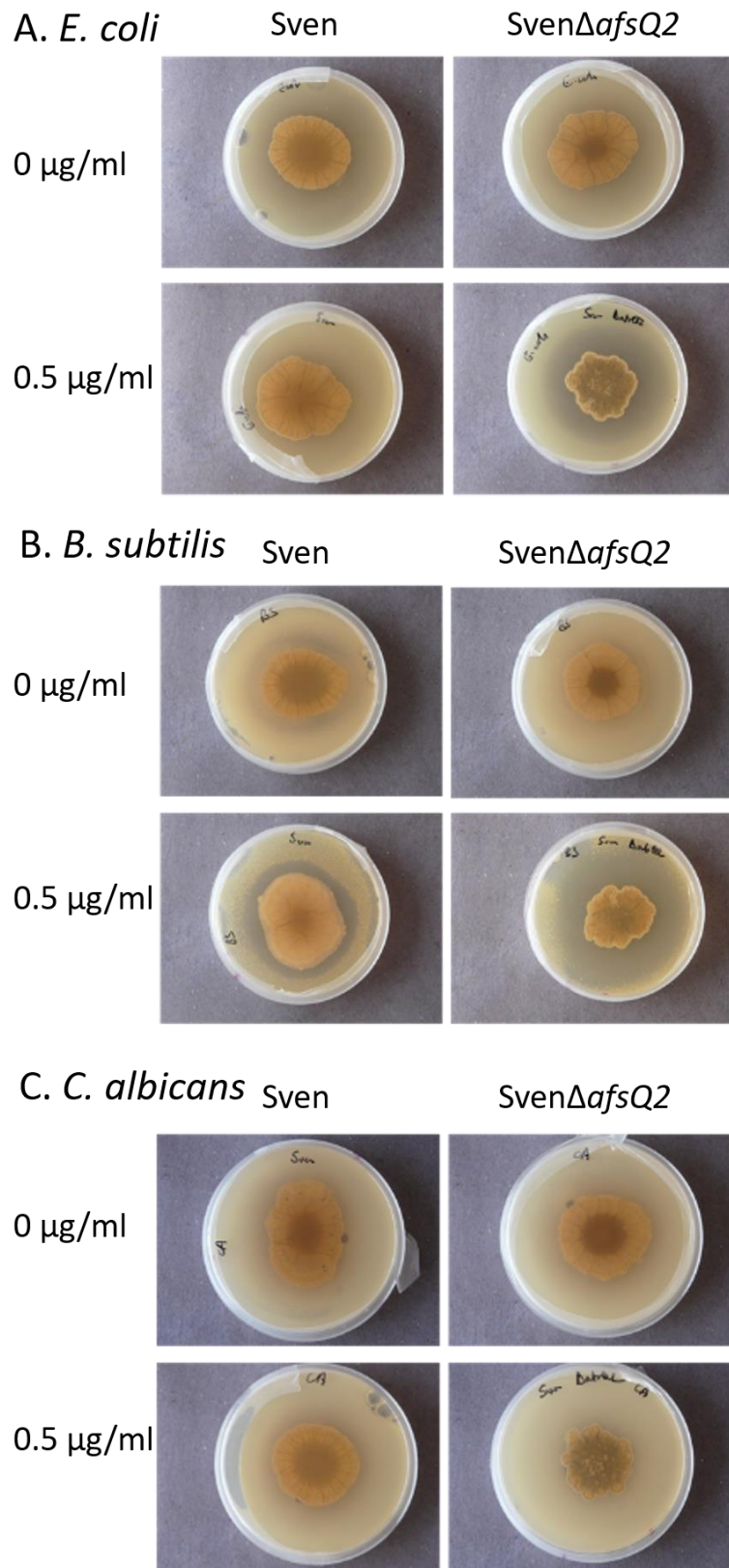


Figure 5.19: Bioassay comparison of *S. venezuelae* and isogenic Δ *afsQ2* grown on MYM with (10 μ g/ml) and without vancomycin. *S. venezuelae* strains were spotted on to the plate and grown for 3 days before indicator strains were inoculated into SNA and overlain.

As *S. venezuelae* does not contain the vancomycin resistance genes, the stress of vancomycin, even below the MIC, could be sufficient to activate antibiotic production which AfsQ1 may negatively regulate. It is unknown whether this is chloramphenicol, jadomycin or another bioactive compound. As antibiotics are thought to be used in signaling as well as improve competitiveness of the producing bacteria, the induction of antibiotic production by low levels of antibiotics is not unexpected (Sengupta, *et al.*, 2013). Interestingly, the difference in the zone of inhibition is much larger for the *Sven* Δ *afsQ2* strain than wild-type strain.

From these experiments, pMS82 integration into ϕ BT1 in *S. coelicolor* has been shown to be unsuitable. These phenotype studies were carried out to determine whether the chimeras have been successfully rewired. As there is a high level of cross regulation within nitrogen sensing and regulation, through phenotypic analysis, it is hard to determine whether the chimeras are functionally pairing with AfsQ1. Therefore, further analyses will need to be carried out to determine whether the chimeras are able to phosphorylate AfsQ1.

5.3.6 *in vitro* analysis of phosphor-transfer between chimera SKs and AfsQ1

To characterise whether the chimeras are able to phosphorylate AfsQ1, an *in vitro* phospho-transfer assay was planned, whereby the cytoplasmic regions of the chimeras would be incubated with ATP and AfsQ1 to determine whether there is a transfer of phosphoryl-group between the two proteins, as other studies have previously carried out (Laub, *et al.*, 2007; Skerker, *et al.*, 2008).

The cytoplasmic regions of the chimeras were overexpressed and purified. To do so, codons 105- 399 of Chim1 (AfsQ2; using primers RLO035F/36R and RLO039F/40R), 104-377 of Chim2 (RLO037F/38R and RLO041F/42R), and 104-364 of Chim3-5 (RLO037F/38R and RLO041F/42R) and VanS (RLO037F/38R and RLO041F/42R) as well as full-length VanR (RLO049F-52R), and AfsQ2 (RLO25F-28R; Table 2.3) were amplified. The primers used to amplify these domains included hexa-His tags for use in purification. These were cloned into the overexpression vector pGS-21a between *Nde*I and *Hind*III and heterologously expressed in *E. coli* BL21. Figure 5.20 shows the PCR confirmation of these constructs where one primer (RLO147F) binds to the vector and the other primer

binds within the gene (RLO144F-146F). Following PCR confirmation, these were further sequenced using universal primers T7 and T7term. Despite *vanR* PCR amplification not producing a specific band, sequencing results showed it to be correct. In the figure, *c-afsQ2* refers to *c-chim1* which are both the same.

Following confirmation of the vectors, these were transformed into *E. coli* BL21. These overexpression strains were named RLOE followed by the overexpressed protein, i.e RLOEVanR strains overexpress VanR.

The overexpression of proteins was induced using 1 mM IPTG. After 4 hrs of induction, cells were harvested and lysed before analysis through SDS-PAGE and Western blotting (Figure 5.21). Two of the proteins were not overexpressed, *c-AfsQ2* and *c-VanS*. After further testing, issues with the vector backbone were identified and these overexpression strains were remade and assessed (Figure 5.22).

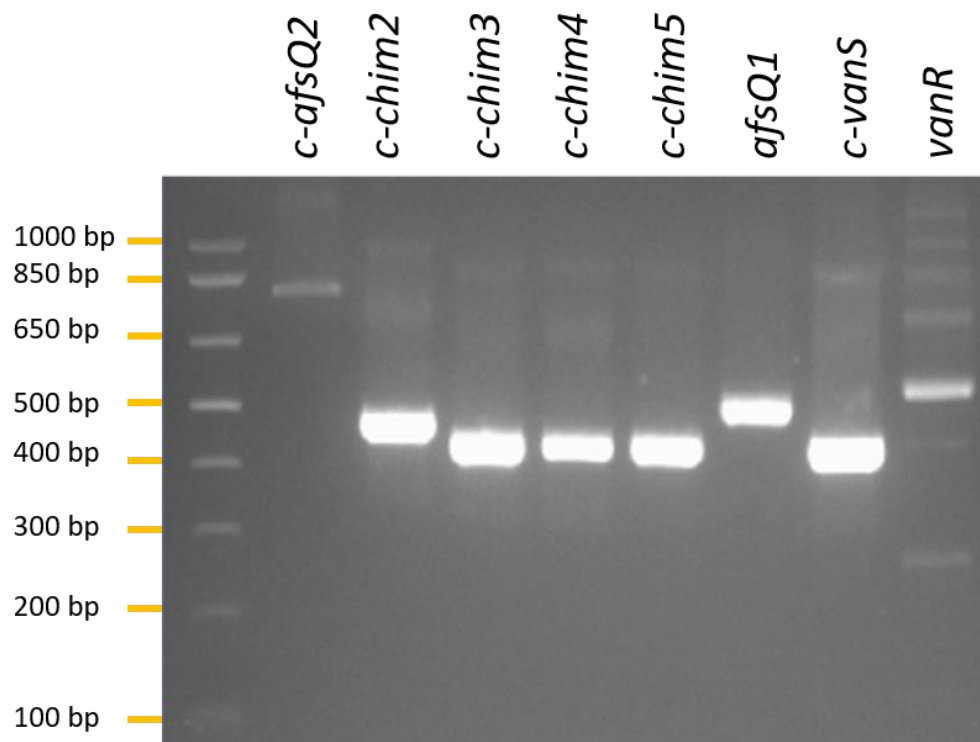


Figure 5.20: Confirmation of overexpression vectors. Primer RLO147F was used in all the amplifications and binds to the T7 promoter of pGS-21a. This was paired with primers amplifying from within the gene inserted. For *c-afsQ2* (expected (exp) size: 750 bp), primer RLO144R was used; *c-chim2* (exp size: 465 bp), *c-chim3*- *c-chim5* (exp size: 423 bp) and *c-vanS* (exp size: 423 bp), primer RLO144aR was used, for *afsQ1* (exp size: 520 bp), primer RLO146R and for confirming *vanR* (exp size: 552 bp), primer RLO145R was used.

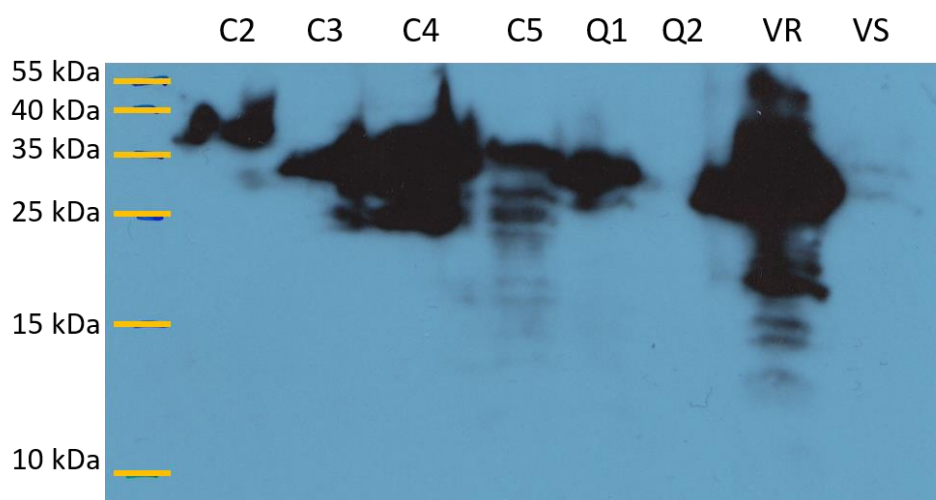


Figure 5.21: Anti-His immuno-blot analysis of the overexpression of cytoplasmic regions of SKs, AfsQ2 (Q2), VanS (VS) and chimeras (C2-5) and RRs, VanR (VR) and AfsQ1 (Q1). The expected sizes of each from the first lane (C2) to lane 8 (VS) are as follows: 30.83 kDa, 30.31 kDa, 30.3 kDa, 30.31 kDa, 26.03 kDa, 32.78 kDa, 25.7 kDa, 30.34 kDa. Cultures of each overexpression strain were induced with 1 mM IPTG and induced for 4 hrs before harvesting of cells.

Whilst c-Chim2 and AfsQ1, were expressed, they migrated through the gel at a slower pace than expected for their size. The expected size of the c-Chim2 and AfsQ1 are 30.83 and 26.03 kDa, respectively, however, the bands displayed in figure 5.21, shows the proteins to be ~38 kDa and 30 kDa. Furthermore, the VanR proteins seemed to run through the gel poorly. As this was a cell lysate, it is possible there was too much protein loaded leading to this effect on these samples. Another possibility for the incorrect sizing is the properties of these proteins. As not all proteins run to the correct size in SDS-PAGE gels, these may be correct (Rath, *et al.*, 2009).

The other proteins were successfully expressed. However, as seen previously in Chapter 4 with the purification of full-length VanS, not all the proteins here appear stable. Further analysis was carried out to assess whether this is degradation within the cell or unstable even after purification.

As stated above, new vectors were constructed for c-VanS and c-AfsQ2 overexpression and transformed into BL21. As before, these were induced for 4hrs with 1 mM IPTG. From carrying out anti-His immuno-blotting, it can be seen that these vectors are overexpressing the protein even without induction. This would may be due to a mutation in the vector, whether in the T7 promoter or the *lacI* promoter, as earlier overexpression trials did not show expression of proteins

before induction. However, the *lac* promoter is well known for having leaky transcription (Penumetcha, *et al.*, 2010). These vectors were not remade, as they were still able to express the desired proteins.

Two different isogenic strains of RLOEAfsQ2 were tested for the overexpression of c-AfsQ2. In the last lane of figure 5.22, there is a protein band for a protein <130 kDa. Due to overexpression of c-AfsQ2, the protein may have formed higher order structures or aggregates which were not dissociated in the boiling process or treatment with SDS. This strain was discarded, and the other strain used.

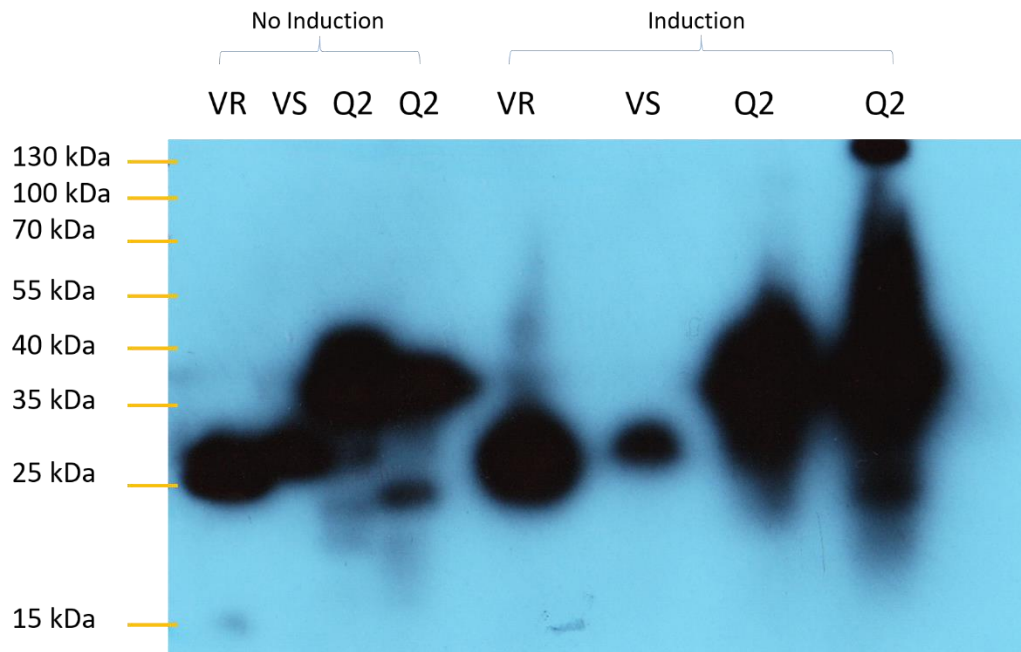


Figure 5.22: Anti-His immuno-blot analysis of the overexpression of cytoplasmic regions of SKs, AfsQ2 (Q2), VanS (VS) and RR, VanR (VR). Two AfsQ2 overexpression strains were used, both overexpressing N-terminally His-tagged cAfsQ2. The expected sizes of each overexpressed protein is 25.7 kDa (VanR), 30.34 kDa (c-VanS) and 32.78 kDa (c-AfsQ2). Cultures of each overexpression strain were induced with 1 mM IPTG and induced for 4 hrs before harvesting of cells.

Having tested the ability of the strains to overexpress the proteins, these proteins were purified. As only cytosolic domains of the SKs were expressed alongside cytosolic RRs, after lysis, the supernatant containing the soluble protein fraction was used in the purification. After purifying the proteins through His-affinity FPLC, a small aliquot of the protein was removed and prepared with SDS Laemmli sample buffer, whilst the remaining had glycerol added to 10% concentration and snap frozen. After storage overnight at -20°C, these were thawed

on ice and also prepared before analysis carrying out SDS-PAGE and Western blot (Figure 5.23).

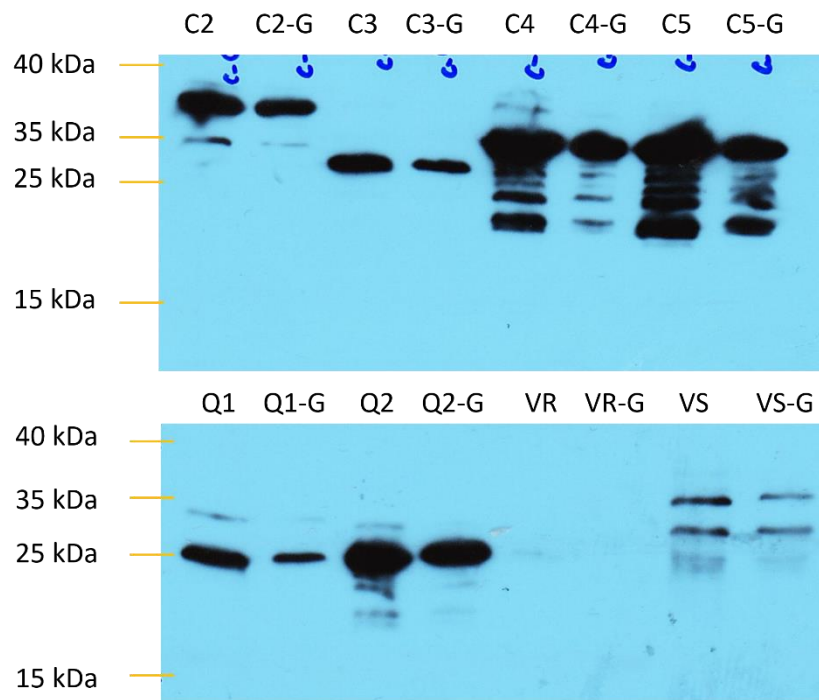


Figure 5.23: Purified protein from His-affinity FPLC. Purified samples were snap frozen and stored at -20°C without and with 10% glycerol (G). Proteins purified are c-Chim2 (C2; 30.83 kDa), c-Chim3 (C3; 30.31 kDa), c-Chim4 (C4; 30.3 kDa), c-Chim5 (C5; 30.31 kDa), AfsQ1 (Q1; 26.03 kDa), c-AfsQ2 (Q2; 32.78 kDa), VanR (VR; 25.7 kDa) and VanS (VS; 30.34 kDa).

Except from VanR, all other proteins were able to be purified. Albeit, the level of VanS purified protein is much lower than the other samples based on the intensity of the immuno-blot. The protein was lost in the purification process as SDS-PAGE analysis (data not shown) and anti-His immuno-blotting (Figures 5.21 and 5.22) of overexpression of VanR in comparison to the chimeras was of a similar level after 4 hrs of induction. VanS overexpression was low in figure 5.22 which is reflected in the purified protein here in figure 5.23.

Of the purified proteins, Chim2, Chim3, AfsQ1 and AfsQ2 are fairly stable, however, Chim4 and Chim5 show a high degree of degradation. As there is no further degradation bands smaller than ~ 20 kDa, these proteins are likely to have reached a stable state. To remove the degradation, c-Chim4 and c-Chim5 could be purified further through size exclusion. Interestingly, Chim3, Chim4 and Chim5 are expected to be of a very similar size and as there are only a few residues

difference between these three proteins, the size difference between c-Chim3 to c-Chim4 and c-Chim5 infers truncation rather than a difference in SDS binding and hence migration. This may explain the stability of c-Chim3.

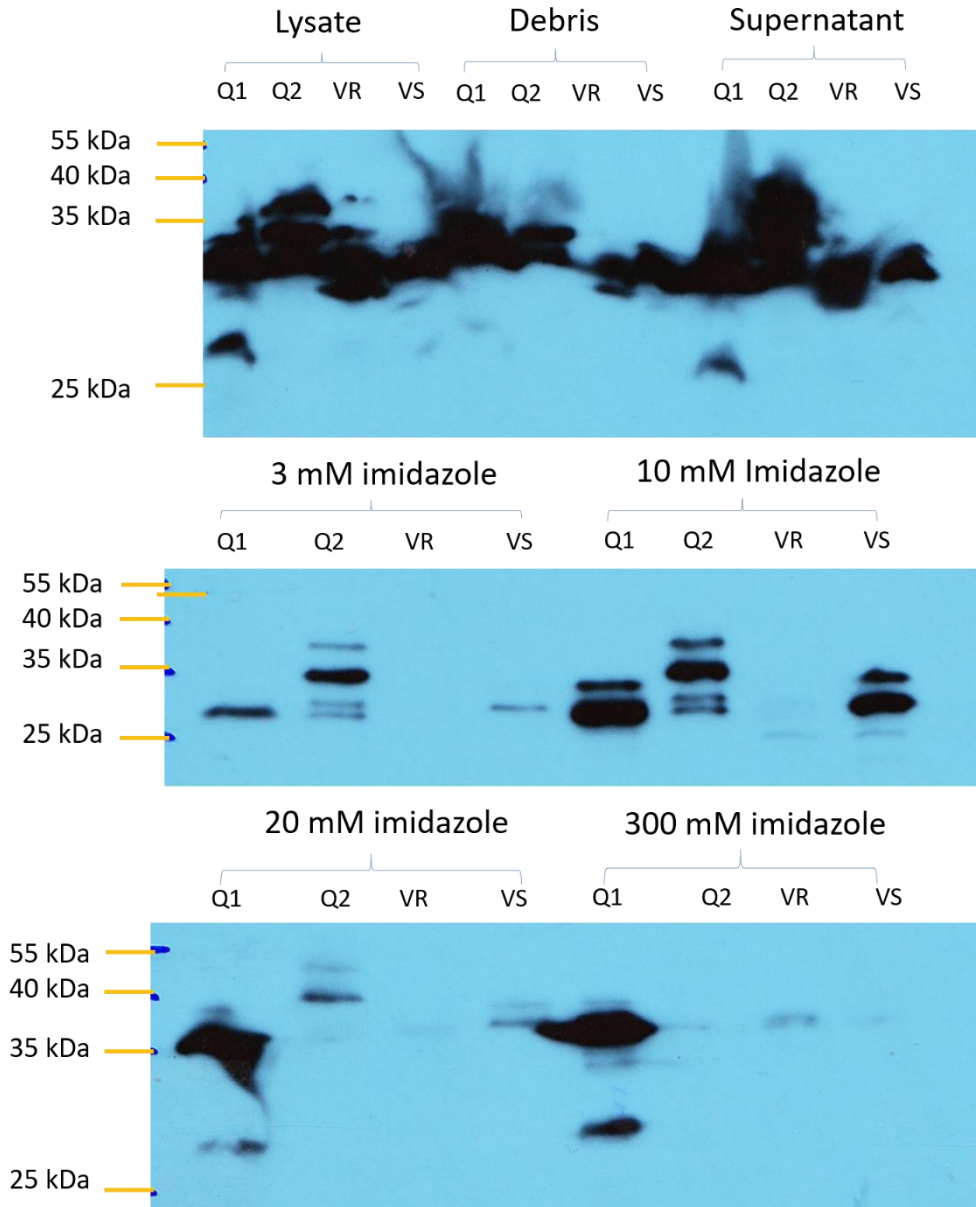


Figure 5.24: Collected fractions from overexpression and purification of AfsQ1 (Q1), c-AfsQ2 (Q2), VanR (VR) and c-VanS (VS) analysed through anti-His immuno-blot. After 1 mM IPTG overexpression induction for 4 hrs, harvested cells were lysed through passage through French press twice (1000 psi). The cell debris was separated from the soluble proteins through centrifugation (10 mins, 10000 rpm, Accupsin 1R with a Ch. 007379 rotor), the supernatant was loaded on the His-Trap column. Column and protein was washed with 40 ml buffer (no imidazole) before eluting with buffer containing different concentrations of imidazole.

Following from this round of purification, due to the low concentration of VanR and VanS purified, the process was repeated. AfsQ1 and c-AfsQ2 were purified alongside as a comparison between samples and to obtain more protein. Figure 5.24 shows that VanR was overexpressed but almost none was purified. As the protein was identified in the supernatant and not in any of the eluted fractions containing imidazole, the protein may not have bound to the column or was bound weakly and hence during wash steps, was removed from the column. The binding of the protein to the column may be affected by the secondary structure of the protein. Further purifications were carried out to purify VanR, with changes in buffer concentration. VanR was able to be purified but in very low amounts. Unlike VanR, c-VanS was able to be purified.

From these purification attempts, many issues were encountered including potential truncation of c-Chim3, instability of c-Chim4 and c-Chim5 and low concentrations of VanR. As such another approach was taken in an endeavor to deduce whether AfsQ1 is phosphorylated by the chimeras.

5.3.7 *in vivo* analysis of phosphotransfer between chimera SKs and AfsQ1

To decipher whether the chimeras are able to phosphorylate AfsQ1, a Phos-tag assay was used. Phos-tagTM is a tag which binds to phosphate groups of a phosphorylated protein with weak affinity. As proteins run through an acrylamide gel, phosphorylated proteins migrate through slower than those without the phosphate group. This means that the phosphorylation would be carried out on full-length protein and *in vivo* and thus allowing clarification of whether the protein, as a whole, senses vancomycin and consequently phosphorylates AfsQ1.

In order to detect the phosphorylative status of AfsQ1 and the chimeras by Phos-tag, all proteins require tagging. As Chim 3 and 4 were both Strep II tagged, 3X FLAG tag was decided upon to identify AfsQ1; 3XFLAG tag was selected over other tags due to studies using 3XFLAG tags in *S. venezuelae* for ChIP-Seq analysis of the RR MtrA, which demonstrated no unspecific binding (Som, *et al.*, 2017).

5.3.7.1 CRISPR/Cas9 3XFLAG- tag *afsQ1*

To add a FLAG tag to AfsQ1, a second copy of *afsQ1* could be integrated into the genome. However, if the native copy was not removed, native AfsQ1 would not be tagged, thus reducing the Phos-tag signaling. Furthermore, as shown earlier, integration into the genome may result in changes to antibiotic production and changes in growth behaviour. Instead direct FLAG tagging of the native copy by CRISPR/Cas9 editing was opted for to maintain native levels of the protein and ensure all AfsQ1 in the cell was FLAG tagged. Following from the phenotypic assays as *S. venezuelae* strains possessing the chimeras, showed greater bioactivity when exposed to vancomycin, *S. venezuelae* was use in this assay to test for phosphorylation.

```
ATGGACTACAAGGACCACGACGGCGACTACAAGGACCACGACATCGACTACAAGGACGAT
GACGACAAGCTGCCCGTGCCCTTTCTGTTGCTGATCGAGGACGACGACGCCATCCGCACG
GCCCTCGAACTCTCCCTGTCACGGCAGGGCCACCGGGTGGCCACCGCCGCGACCGGTGAG
GACGGCCTCCAGCTGCTGCGCGAGCAGCGGCCCGACCTGGTCGTGCTCGACGTCATGCTG
CCCGGCATCGACGGCTTCGAGGTCTGCCGGCGCATCCGCCGCACGGACCAGTTGCCGATC
ATCCTGCTGACCGCGCGCAGCGACGACATCGACGTGGTGGTGGGCTGGAGTCCGGCGCC
GACGACTACGTCGTCAAGCCGGTGCAGGGCCGCGTCTCGGACGCCCGCATCAGGGCCGTA
CTGCGGCGCGGGGAGCGGGAGTCGACGGATTCCGGCGACGTACGGCTCCCTCGTCATCGAC
CGGTCCGCGATGACGGTCACCAAGAACGGCGAGGACCTCCAGCTCACCCCGACCGAGCTG
CGACTGCTCCTGGAGCTGAGCCGCCGGCCGGTTCAGGCGCTCTCCCGGCAGCAGTTGCTG
CGACTCGTGTGGGAGCACGACTACCTCGGCGACTCGCGGCTCGTCGACGCCTGTGTGCAG
CGGCTGCGCGCCAAGGTGGAGGACGTGCCGTCTCGCCGACGCTCATCCGTACCGTGCCG
GGCGTCCGGCTACCGGCTGGACGTCCCTGCGTGA
```

Figure 5.25: Gene sequence of *afsQ1* after insertion of a N-terminal 3 X FLAG tag (red) through CRISPR/Cas9 editing. The protospacer used is shown in green and PAM sequence in bold blue text. To remove the recognised cleavage sequence of Cas9, the PAM sequence was altered 33G>A generating a silent mutation. The amplification of the *afsQ1*, insertion of FLAG sequence and mutation was conducted using primers RLOCC009F-14R and Gibson Assembled into p-CRISPRomyces-2.

ChIP-seq analysis to elucidate the regulon of MtrA was carried out by Som, *et al.*, (2017), using a N-terminally His-tagged MtrA, demonstrating no disruption in development in liquid growth or growth on agar plates, consequently, *afsQ1* was N-terminally 3XFLAG tagged. To edit the genome using CRISPR/Cas9, a DSB is generated by Cas9 through the recognition of a binding site provided by the protospacer as a template, followed immediately by a PAM sequence. To prevent further cleavage following recombination, the protospacer sequence or PAM must be altered. Figure 5.25 shows *afsQ1* following insertion of the 3XFLAG tag. A

silent mutation was added to the homology sequence by changing the PAM sequence from AGG to AAG. The amplification of the homology region with the insertion of the FLAG tag and mutation of PAM sequence was carried out using primers RLOCC009F-14R (Table 2.3). Following conjugation of the assembled vector into *S. venezuelae* wild-type, isogenic strains with the FLAG insertion were verified through amplification of the flanking region of *afsQ1*, 500 bp 5' and 250 bp 3' of the originally amplified homology region using primers RLO102F/R. This amplicon sequence was verified through sequencing with primers RLO102F-106R which showed the same *afsQ1* gene sequence as shown in figure 5.25. This strain was named F-AfsQ1.

To test the expression of F-AfsQ1, the strain was grown in liquid MYM and samples were taken at time-points of 8, 12, 16 and 20hrs, corresponding to germination, vegetative growth, onset of aerial hyphal formation and sporulation (Bush, *et al.*, 2013). After lysing the samples, an immuno-blot was carried out using anti-FLAG antibodies (Figure 5.26). This was conducted in duplicate. It was not possible to load equal amounts of total protein as the 8 and 12 hr time points yielded very low biomass. Consequently, a greater volume was used for these samples to compensate the low biomass, with 3 ml taken from the initial 50 ml for the first time point, 2ml for the second and 1ml for the final two time points. Whilst, the total protein was not consistent between the duplicates, F-AfsQ1 is produced and is the expected size of 28 kDa. Even though this assay does not show the time-point which AfsQ1 is expressed to the highest level, chimera phosphotransfer is caused by vancomycin and not nitrogen levels. In addition to showing that FLAG tagged AfsQ1 is successfully expressed, the blot does not show any non-specific binding of Flag antibodies or evidence of additional FLAG-tagged proteins in *S. venezuelae*.

To assess whether the addition of the FLAG tag resulted in changes to the strain, F-AfsQ1 and *S. venezuelae* wild-type were grown in liquid MYM over 2 days and the growth curve and rate was calculated (Figure 5.27). Figure 5.27 shows that the growth of the *S. venezuelae* is not affected by the FLAG tag addition to AfsQ1. Subsequently, the expression constructs for Chim3 and Chim4 were integrated into the strain through the ϕ BT1 site.

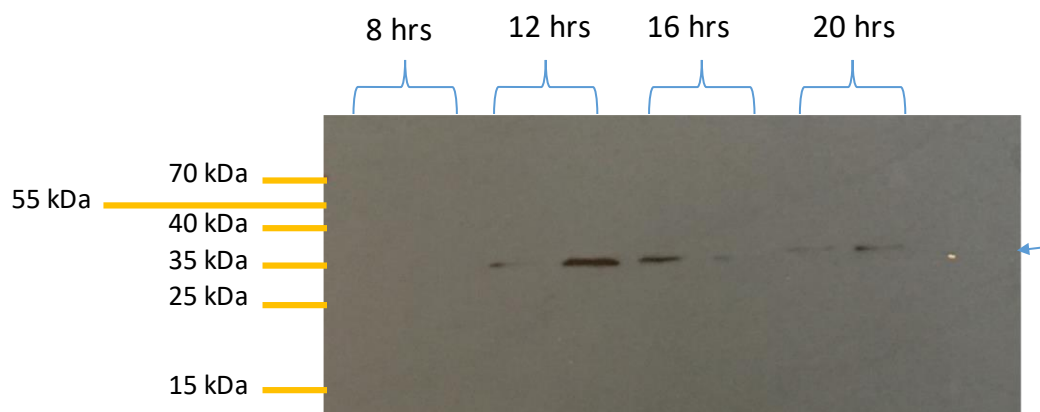
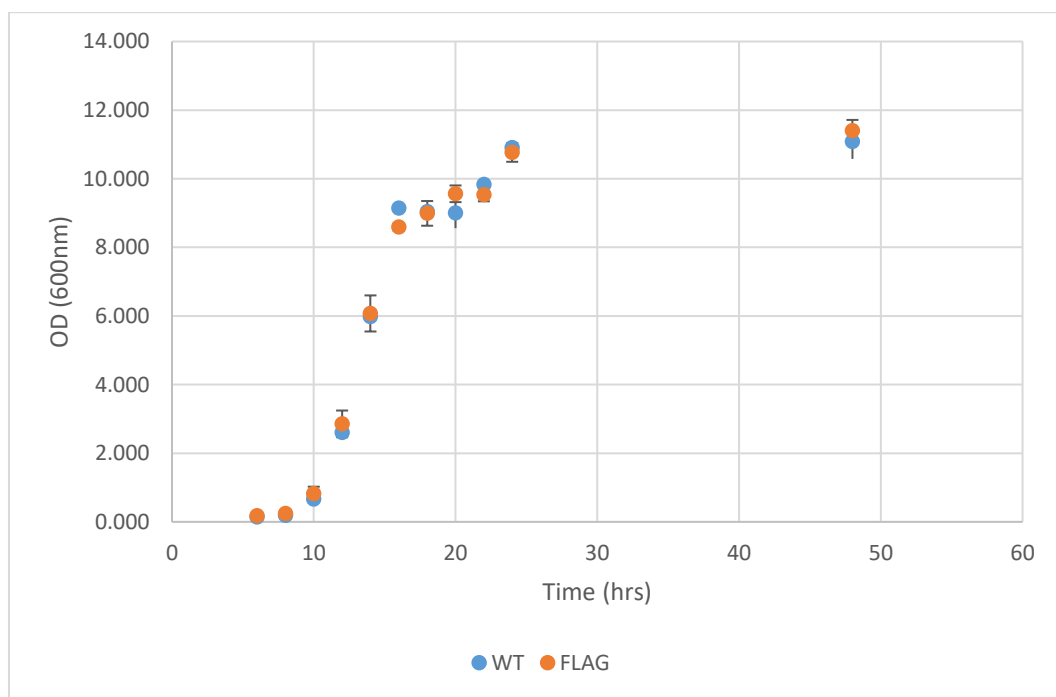


Figure 5.26: Immuno-blot using M2 anti-FLAG antibodies to visualise 3XFLAG tagged AfsQ1 expression over 20 hrs of growth in liquid MYM, where samples were removed every 4 hrs from 8hrs after inoculation. This was carried out in duplicate. Arrow shows represents expected size of AfsQ1 (28 kDa).



Strain	Growth Rate (exponential phase- μ)	
	phase- μ	Duplication time (hrs)
Sven	0.497	1.395
F-AfsQ1	0.466	1.499

Figure 5. 27: Growth curve of *S. venezuelae* wild-type (WT) and F-AfsQ1 (FLAG) in MYM over 48 hrs. Non capped error bars are wild-type and capped are F-AfsQ1. Error bars show standard error. An OD_{600} below 1 was measured using 1 ml sample in a 10 mM path length cuvette. From this growth rate and duplication time were calculated. Samples with an OD_{600} of above 1 were measured through diluting the sample and scaling up. Cultures and samples were taken in triplicate. The growth rate and duplication time are both not significantly different (One-sample T-test; $p < 0.05$, $|t|$ (growth rate) = $1.042 < 4.303$; $|t|$ (duplication) = $1.087 < 4.303$).

5.3.7.2 Phos-tag Assay

To test whether AfsQ1 is phosphorylated by the chimeras in the presence of vancomycin, F-AfsQ1 strains were cultured on MM supplemented with 7.5 mM glutamate to reduce phosphorylation by native AfsQ2. Mycelia was harvested after a day of growth. As strains grown on vancomycin grew slower than those without, to harvest enough mycelia, twice the number of plates of mycelia were harvested. These mycelia were lysed through sonication before the protein concentration was equalised. This proved difficult for samples of mycelia grown with vancomycin. Despite harvesting mycelia from 5 times the number of plates, the volume of mycelia was considerably less. This is reflected in the Coomassie stained SDS-PAGE acrylamide gels which show different levels of protein per lane in figure 5.28.

These samples were loaded on to a Phos-tag acrylamide gel and SDS-PAGE was carried out, followed by anti-FLAG immuno-blotting. Figure 5.28B shows protein bands at two positions in the gel. Phosphorylated proteins run through the gel slower than non-phosphorylated proteins due to interaction with the Phos-tagTM which possesses Mg²⁺ ions. The two bands therefore represent the phosphorylation state of the protein. Though figure 5.28B shows two protein bands which have migrated at different rates across the gel, it is difficult to determine which bands relate to which lanes due to gel distortion. The Phos-tagged SDS-PAGE gels were stained with Coomassie blue following the semi-dry transfer (data not shown) which revealed much of the protein to still be present in the gel. Furthermore, unlike the acrylamide gels without Phos-tag, lanes were not clear but instead distorted, mirroring the Western blot image (Figure 5.28B). All gels were made the day of running gel electrophoresis to maintain integrity of gels. To prevent interference through use of protein ladders, protein ladders had MgCl₂ added or were omitted.

As said above, much of the protein remained on the gel after transfer. To determine whether any of the protein had transferred onto the membrane, these were incubated with Ponceau stain, which showed some of the protein to have transferred but indeed the majority remained on the gel. Using the stained Phos-tag gel and membrane lines were drawn onto the film (Figure 5.28B) to separate the lanes but despite these, the individual lanes are still difficult to see.

In the process of optimising the transfer, changes in voltage, length of time of transfer and buffer components were all altered, however, efficient protein transfer remained unachievable.

Moreover, due to poor transfer from gel to membrane, to visualise any signal, films were exposed for over an hour. This has caused smearing from the chemicals used for exposing and developing, further complicating analysis of the data.

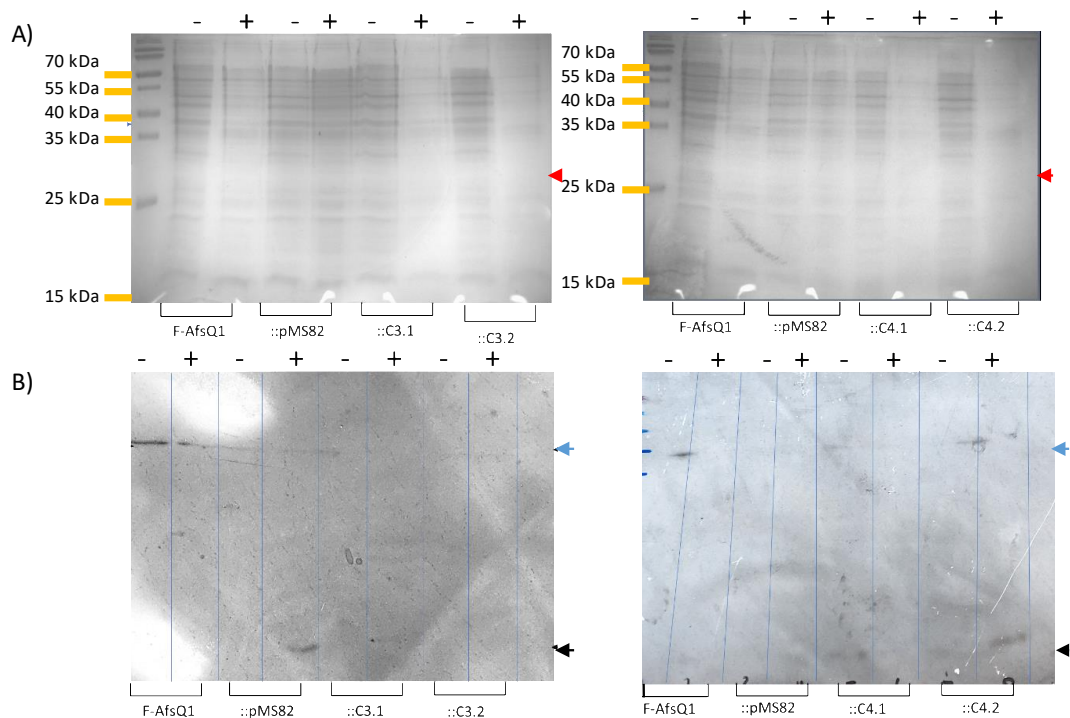


Figure 5.28: Analysis of phosphorylation state of AfsQ1 in F-AfsQ1 background with Chim3 and Chim4 in the presence and absence of vancomycin. Strains were grown on MM with 7.5 mM glutamate as sole nitrogen source. The – and + refer to growth with vancomycin (0.5 μ g/ml) or without. A) Coomassie stained SDS-PAGE acrylamide gel of whole cell lysate of samples. Red arrows show expected position of protein of AfsQ1. B) Western blot (anti-FLAG) Phos-tagged SDS-PAGE. Blue arrows show phosphorylated AfsQ1 and Black arrow shows unphosphorylated AfsQ1.

5.3.8 Quantifying Gene Expression

Both *in vivo* and *in vitro* assessment of AfsQ1 phosphorylation experiments require optimisation to further the studies. Another means of testing whether AfsQ1 is activated, is through analysis of expression of AfsQ1 target genes. To this end, the gene expression of target genes was quantified. Increased expression of

positively regulated target genes under vancomycin conditions would indicate activation of AfsQ1.

To determine if AfsQ1-dependent gene expression is induced by the addition of the chimeras, qRT-PCR was carried out to characterise the expression of three genes which are regulated by AfsQ1. The three target genes chosen are *sigQ*, which has been shown to be directly regulated by AfsQ1 and is divergently expressed from the *afsQ1* promoter (Wang, *et al.*, 2012), *actII-ORF4* and *redZ*, which both encode SARPs of actinorhodin and undecylprodigiosin biosynthesis, respectively. The housekeeping gene *hrdB*, which encodes an essential sigma factor, was used as an internal control.

To investigate the regulation of the chimeras, *S. coelicolor* M145 Δ *afsQ2* strains were selected over the wild-type strains to avoid dephosphorylation through AfsQ2. M145 Δ *afsQ2*, M145 Δ *afsQ2*::pMS82, M145 Δ *afsQ2*::Chim3 and M145 Δ *afsQ2*::Chim4 were grown on cellophane disks on top of MM agar plates (with 7.5 mM glutamate) for 3 days before removing the mycelia from the surface. After lysing samples, RNA was extracted and treated with multiple rounds of DNase (including both DNaseI and Turbo DNase) to remove genomic DNA. The RNA was then first-strand reverse transcribed into cDNA. To generate a standard curve, the primers designed for qRT-PCR were used to amplify template DNA from genomic DNA which was purified and used for standards. Figure 5.29 shows the standards amplification plots from each of the targets. All demonstrate clear gradation between the different numbers of copies of template DNA added. With a 10-fold increase between each standard with a lowest of 10 copies and the highest of 10000000 copies. The 10 copy standard was omitted from each of these due to partial overlapping with the negative standard of water. Figure 5.30 shows the plotting of these standards in blue with the line of best fit. The points in orange are all the data points which fit along this line of best fit. All the data points were clustered together showing the transcript level of target genes between tested samples are within a 10-fold range. Thresholds were decided by eye to omit any noise.

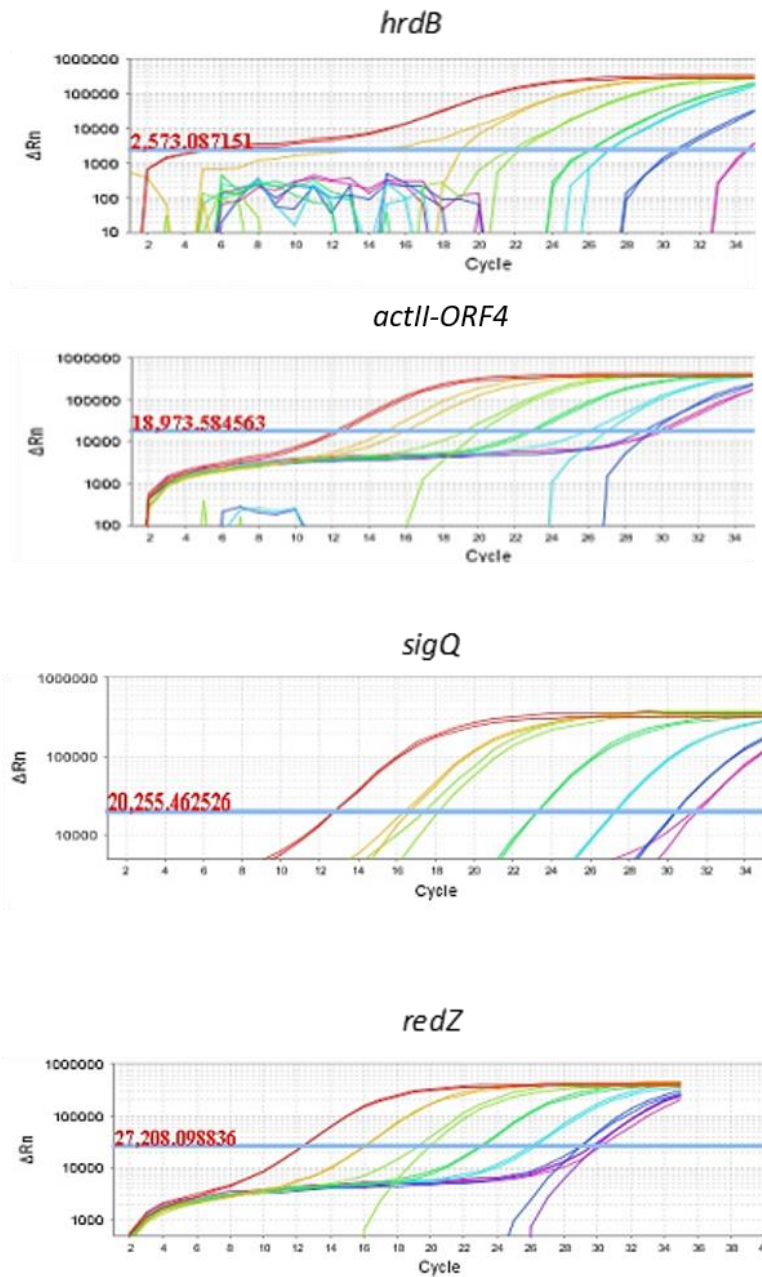


Figure 5.29: Amplification plots generated from standards for each of the targets (*sigQ*, *actII-ORF4* and *redZ*) and also the reference gene (*hrdB*). Standards used were amplification of targets using primers RLO161F-168R (Table 2.3). All standards were <400 bp. From the size of amplicon, the number of copies of DNA was calculated. Standards used ranged from 10000000 to 10 copies of DNA. Standards were carried out in duplicate and each standard is represented by one coloured line in each graph. With red lines representing 10000000 copies, orange showing 1000000 copies, light green showing 100000 copies, green showing 10000 copies, cyan showing 1000 copies, blue showing 100 copies, purple showing 10 copies and magenta showing just water. The horizontal line shows the threshold value, which was decided by eye to omit noise.

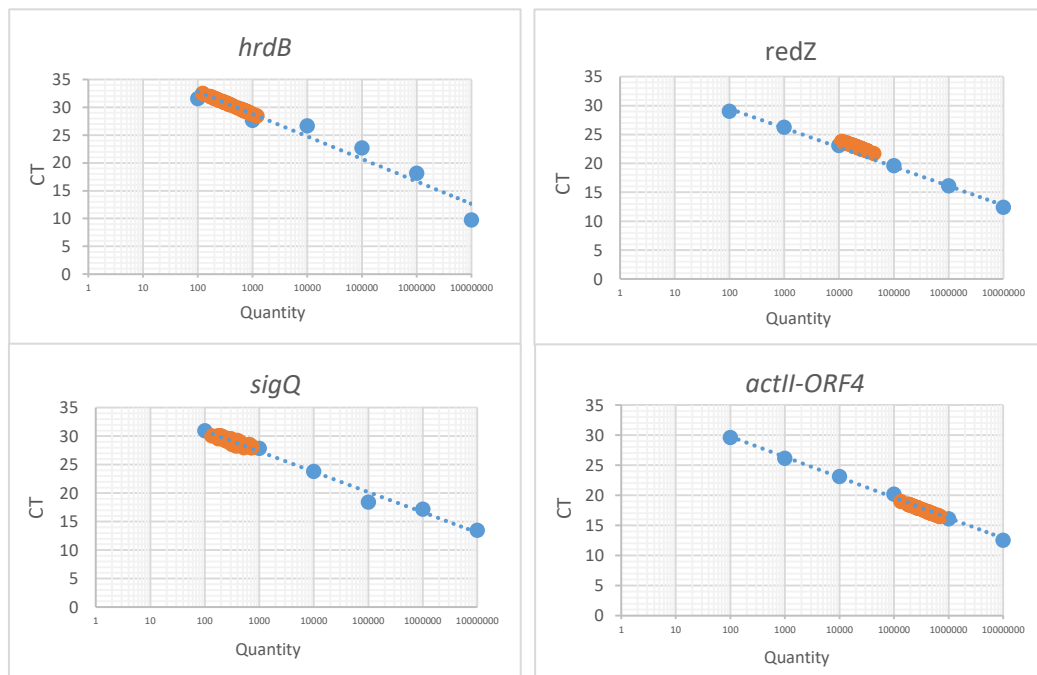


Figure 5.30: CT values were plotted against the number of copies from standards (blue). Lines of best fit were drawn. Orange points represent the data points of the non-standard (purified cDNA) samples. Each purified cDNA sample was amplified in triplicate. Standards were obtained from diluting amplified *hrdB*, *redZ*, *sigQ* and *actII-ORF4* using primers RLO161F-168R (Table 2.3) from 10000000 to 10 copies.

Threshold cycle values (see 2.2.5.2) were converted into copy numbers in reference to the set threshold and also the standard linear trendline equation. The data were then analysed to determine if there were any outliers. The median value of the triplicate of copy numbers was calculated and the exclusion point was set at 1.5 times the median value. From this, each target mean average value was then divided by the reference *hrdB* value before plotting as seen in Figure 5.31.

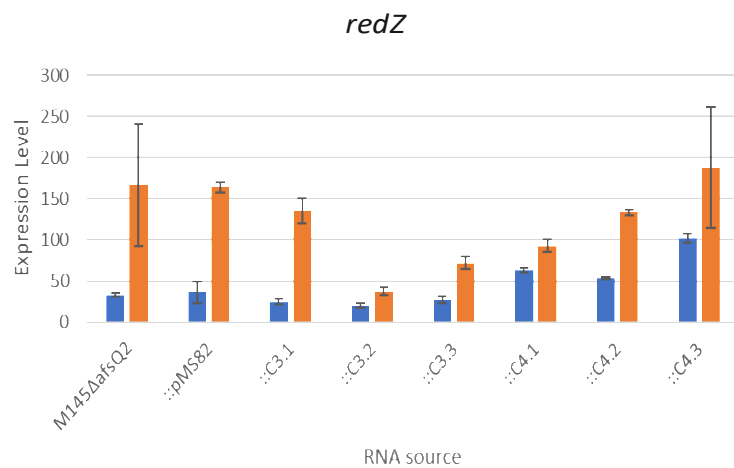
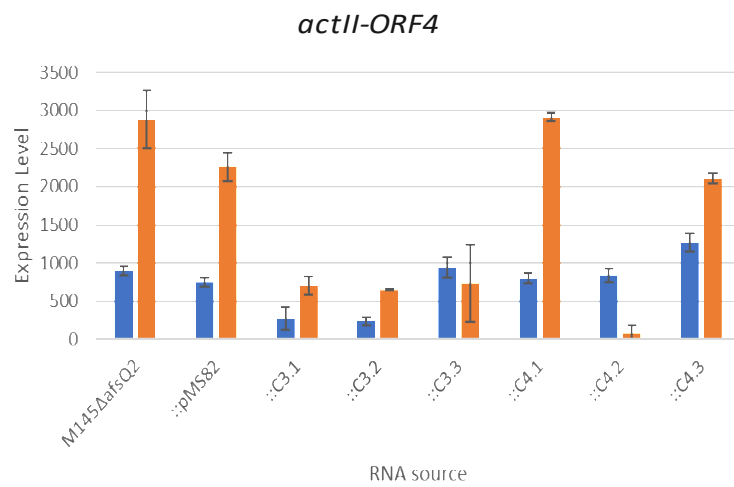
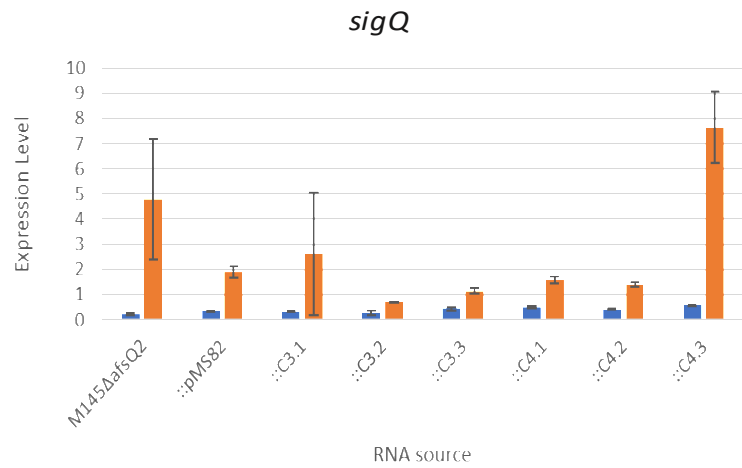


Figure 5.31: Comparison of the expression of targets: *sigQ*, *actII-ORF4* and *redZ* in M145ΔafsQ2 strains with and without chimera proteins when grown in the absence (blue bars) or presence of vancomycin (10 μg/ml; orange bars). Errors bars show are standard deviation of the samples expression levels. Expression levels is shown as fold change as normalised to *hrdB* expression.

Analysis of the expression data shows that with the addition of vancomycin, the expression of each of the targets increases in all the strains with the exception of M145 Δ *afsQ2*::Chim3.3 and M145 Δ *afsQ2*::Chim4.2 for target *actII-ORF4*. In the former, the standard deviation for expression level in vancomycin conditions is very high. This demonstrates a high level of variation in sample data. In the latter, both samples (with and without vancomycin) show lower standard deviations, showing that expression of *actII-ORF4* was indeed lower with vancomycin than without. This shows that vancomycin triggers many regulatory pathways and not simply the VanRS network resulting in resistance genes expression. The addition of vancomycin, as seen in the phenotypic assays, caused antibiotic production not just in strains possessing chimeras but also those without. This makes measuring gene expression levels of target genes very difficult the expression of many if not all the targets are affected by vancomycin.

From the qRT-PCR analysis, it remains ambiguous as to whether the chimeras are phosphorylating AfsQ1 in the presence of vancomycin. As vancomycin could be a large source of stress on the system, this may cascade different networks of regulation. Other targets could be used instead of SARPs as it is known that many regulatory pathways feed into SARP expression regulation. The expression of AfsQ1 or AfsQ2 could be a possible target choice, if AfsQ1 phosphorylation results in positive feedback.

The expression of *hrdB* may also be affected by vancomycin. Whilst *hrdB* is widely used in *Streptomyces* as a reference gene for gene expression analysis (Li, *et al.*, 2015A; Martínez-Burgo, *et al.*, 2015), it has been shown that *hrdB* expression can alter during the course of growth and is not always constant (Otani, *et al.*, 2013; Tabib-Salazar, *et al.*, 2013; Li, *et al.*, 2015A). Therefore, the use of *hrdB* as a reference gene may also need to be reconsidered. Another point to consider is the PCR efficiency. As the internal control (*hrdB*) is used to calculate expression of the target genes (*actII-ORFIV*, *redZ* and *sigQ*), the PCR efficiencies need to be relatively similar. The PCR efficiency can be calculated through analysis of the standards CT values (y axis) plotted against the log cDNA dilution. From the slope of the line of best fit (m), the PCR efficiency (E) can be calculated, where $m = -$

($1/\log E$) (Mygind, *et al.*, 2002; Schmittgen and Livak, 2008). Table 5.1 shows the PCR efficiencies of the 4 amplified genes. The protocol suggests that for an accurate comparison, the efficiencies of amplified targets should be within 10% of the reference gene and all efficiencies should be between 1.8-2.2 (Schmittgen and Livak, 2008).

In the presented data, the comparison of expression fold change of the three targets have been calculated in reference to *hrdB* levels in the cDNA samples. This may not have been an accurate measure due to the difference in PCR efficiency. The PCR conditions would need to be optimised for *hrdB* in order for its PCR efficiency to fall within this range and also to be within 10% of the target genes PCR efficiency. Assessment of whether *hrdB* expression is affected in response to vancomycin and the optimisation of *hrdB* PCR efficiency would need to be carried out before determining whether the results shown here are relevant.

Table 5. 2: PCR efficiencies of the genes amplified including reference gene (*hrdB*) and tested genes (*sigQ*, *redZ* and *actII-ORFIV*). PCR efficiency calculated according to protocol of Mygind, *et al.*, 2002.

Gene amplified	PCR efficiency
<i>hrdB</i>	1.768
<i>sigQ</i>	1.907
<i>actII-ORFIV</i>	1.977
<i>redZ</i>	1.992

5.4 Discussion

From the work presented in this chapter, it is hard to conclude whether rewiring of VanS with AfsQ2 has been successful or not. The assays in *S. coelicolor* and *S. venezuelae* with Chim3 and Chim4 revealed an increase in antibiotic production, with *S. coelicolor* grown on SFM agar demonstrating production of actinorhodin and on MM agar, production of either undecylprodigiosin or actinorhodin. However, in figure 5.17, where strains were spotted onto MM with 7.5 and 75 mM glutamate, with and without vancomycin it could be seen that

integration of pMS82 into the ϕ BT1 in *S. coelicolor* causes changes to the phenotype when exposed to vancomycin. To prevent polar effects, the chimeras could replace the SK with the output signal, which in this case would be AfsQ2 as AfsQ1 is the desired RR to be phosphorylated. This would prevent polar effects, and the expression of both chimera and RR would be a 1:1 ratio.

From the bioassays using *E. coli* Top10 and *C. albicans* as indicator strains (Figure 5.13), a bioactive or bioactives are being produced. This suggests that the chimeras are functioning in *S. venezuelae*, indicating it is transferable from one species to another within the *Streptomyces* genus despite differences in protein identity. The bioactive could be chloramphenicol, jadomycin or other compounds. Whilst this bioactive was not able to be identified through LCMS, the samples may have degraded in the delay between sample collection and running, this could hence be repeated. Compounds could directly be harvested from cells rather than from the media. This method of analysis has been demonstrated when isolating microcin B17 from producing *E. coli* strains (Sinha Roy, *et al.*, 1999).

Moreover, further analysis could be carried out with the *S. venezuelae* Δ afsQ2 strains to investigate whether greater zones of inhibitions are seen. LCMS could also be carried out to quantify the difference in antibiotics produced, if any. As previous work in *S. coelicolor* gave insights into the regulon of AfsQ1, the AfsQ1 regulon in *S. venezuelae* is not known. Further research into whether AfsQ1 regulates antibiotic production in *S. venezuelae* is necessary. With the 3X FLAG-AfsQ1 strain, ChIP-Seq analysis would be the next step to ascertain whether the regulon of AfsQ1 in *S. venezuelae* is similar to that of *S. coelicolor*. It has been shown that production of chloramphenicol and jadomycin are both regulated by JadR1. More recent research has shown that within the chloramphenicol biosynthesis cluster, there is a transcriptional regulator, CmlR. Fernández-Martínez, *et al.*, (2014) showed that deletion of *cmlR* abolishes chloramphenicol production. Potentially AfsQ1 could regulate *cmlR* but identification of binding sites using ChIP-seq is required to see if AfsQ1 directly activates chloramphenicol production.

However, where the assays in this work resulted in antibiotic production for in *S. venezuelae* and *S. coelicolor*, antibiotic production was not activated in *S.*

lividans, despite there being 100% identity between AfsQ1/Q2_{Sco} and AfsQ1/Q2_{Sliv}. As antibiotic production is silent in *S. lividans*, the lack of production with the chimeras present is not necessarily an indication of unsuccessful rewiring. Ishizuka, *et al.*, 1992, showed that by inserting an extra copy of *afsQ1* into *S. lividans*, antibiotic production was triggered. However, as the chimeras are SK chimeras rather than RR chimeras, the AfsQ1 levels would remain the same. After growing *S. lividans* in excess nitrogen (75mM glutamate), there was still no activation of antibiotics even though this should naturally induce AfsQ1 activation. This suggests that phosphorylated AfsQ1 at native levels is insufficient to activate antibiotic production or that AfsQ1 is not active in *S. lividans*. Wang, *et al.*, showed that AfsQ1 regulates expression of *sigQ* but does not induce expression of the *afsQ1/Q2/Q3* operon and hence levels of AfsQ1 should stay relatively constant throughout development.

Verifying phosphotransfer proved a difficult task both for *in vitro* analysis as protein purification proved a challenge and *in vivo analysis* where protein in Phos-tag gels would not transfer onto membranes easily. Whilst both forms of analysis would show whether AfsQ1 can be phosphorylated by the chimeras, *in vivo* phosphotransfer assays would inform whether the proteins, AfsQ1 and chimera SKs, are compatible without interference of other proteins; whilst the *in vivo* phosphotransfer would show whether within the biological system, where many other factors could affect phosphotransfer, whether the proteins would interact. Therefore, there is merit in optimising both forms of analyses.

In the case of *in vitro* studies, the purification of the SKs, both wild-type and chimeras, and the RRs would first need to be optimised. As expression of many of the proteins did not need induction (figure 5.22), the high level of expression may have been toxic to cells or have been misfolded, and hence led to degradation. The overexpression constructs could be regenerated to test this. Additionally, overexpression of these proteins could be trialled using different strains to assess whether the protein is more stable. These strains could include *E. coli* C41 and C43 (Miroux and Walker, 1996), which has been shown to improve protein expression when recombinant proteins are toxic (Dumon-Seignovert, *et al.*, 2004) or use of a *Streptomyces* expression host (Kallifidas, *et al.*, 2018). Other

conditions could also be changed including detergents used and post induction growth temperature lowering for example. Additionally, to further purify the SKs and RRs, after elution from a His-affinity column, proteins could be loaded onto a size exclusion column for further separation of proteins and contaminants through size. AfsQ1 and VanR could also be purified through a heparin sepharose column due to their DNA binding properties, however whether their phosphorylation state affects their binding affinity would need to be tested.

In the case of the Phos tagTM assay, it is imperative to optimise the transfer of proteins from the gel to membrane. In the process of optimisation, different voltages and buffer compositions have been tested. This could be more extensively tested with more vigorous methods of removing the salt from the gel after running. Furthermore, to reduce distortion of lanes, lower running voltages and at colder temperatures could be tested in addition to use of precast gels.

From figure 5.22B, it is interesting to note that even at low nitrogen levels there is phosphorylation of AfsQ1. As the signal for AfsQ2 has not been identified, it is possible that in the low nitrogen level conditions tested, AfsQ1 is still phosphorylated by AfsQ2 but at a lower level than under high nitrogen conditions. Further controls that could be incorporated is culturing cells with excess nitrogen so as to see AfsQ1 in the phosphorylated state. Furthermore, into the F-AfsQ1 strain, chimeras which are His tagged could be integrated. After immunoblotting with one antibody, this could be stripped and repeated with the other to test whether both chimeras and AfsQ1 are phosphorylated under the tested conditions.

Another technique that could be carried out is through purifying 3X FLAG AfsQ1 through immunoprecipitation and use of phospho-protein stains. This technique would still allow identification of the phosphorylation state and proportion of phosphorylated versus unphosphorylated AfsQ1.

In addition to the phosphorylation state, expression of AfsQ1 target genes were analysed using qRT-PCR. The selected genes include *actII-ORF4* and *redZ* which are known to be regulated by multiple transcription factors. Consequently, *sigQ* was also selected as a target because it is divergent from the *afsQ123* operon and activated by AfsQ1. It is however not known whether this operon is also regulated by other transcription factors. In the absence of vancomycin, *sigQ*

expression was consistently low in all samples. However, in the presence of vancomycin, expression was greatly increased in all samples. This was greatest in M145 Δ *afsQ2*, M145 Δ *afsQ2*::pMS82, M145 Δ *afsQ2*::C3.1 and M145 Δ *afsQ2*::C4.3. This was not expected in the M145 Δ *afsQ2* and M145 Δ *afsQ2*::pMS82 as without AfsQ2 to phosphorylate AfsQ1, it was expected that *sigQ* levels would not change. As another control, a phosphomimetic *afsQ1* allele (Daniel-Ivad, *et al.*, 2017) could be incorporated. As AfsQ1 would be permanently phosphorylated, the target genes would be expressed or repressed constitutively. If this strain was then exposed to vancomycin, any additional changes in cell would be independent of AfsQ1. As a comparison this would demonstrate the maximum transcriptional regulation asserted by AfsQ1. With this *sigQ* expression should be constant with or without vancomycin if AfsQ1 is indeed the sole regulator of *sigQ*. It would also be interesting to test this with a lower level of vancomycin as it was used with *S. venezuelae* strains. Additionally, as this was carried out on solid media containing vancomycin, this could be repeated where vancomycin was added to liquid medium at a later stage.

Another point to consider is whether the chimeras are phosphorylating VanR or other RRs within *Streptomyces* instead of AfsQ1. If the chimeras, SKs and RRs could be purified, the phosphotransfer assay would be a good means to test whether VanR or AfsQ1 binds to the chimeras. The kinase core of the RRs of *S. coelicolor* could be analysed to determine whether other RRs share similar residues to those changed between the chimeras. In the purification trials carried out here,

As discussed earlier, in work conducted by Skerker, *et al.*, (2008), the change of three residues was sufficient to change the specificity of EnvZ phosphotransfer switch to RstA rather than its cognate RR OmpR. However, the research also showed that changes of these subset of residues for other SKs including PhoQ and PhoR showed only a partial switch of phosphotransfer where EnvZ phosphorylated OmpR and the other RRs, PhoR and PhoB, respectively. This showed that additional residues may be involved in specificity that the covariation analysis had not discovered. This partial switch over may also have manifested here where AfsQ1 and VanR are both being phosphorylated by the chimeric SKs

Chim3-5. However, a phosphotransfer assay would need to have been successfully carried out to determine this.

In a recent study, the sensor domain of the chemoreceptor Tar was fused to the Dhp domain of EnvZ creating the chimeric SK Taz which regulates the phosphorylation state of OmpR (Landry, *et al.*, 2018). In addition to changing the output signal of Tar, the research showed that in changing residue T436 to S or V could lower the activation threshold signal, therefore making the sensor more sensitive to lower concentrations of the activating signal which is aspartate for Taz (Landry, *et al.*, 2018). It is unknown whether the VanS elements of the chimeras 3-5 have phosphatase activity with AfsQ1. This could potentially be tested by carrying out a phosphotransfer assay in reverse. AfsQ1 could be incubated first with [γ 32P]ATP before addition of chimeras. If the phosphate group is removed, the chimeras would have phosphatase activity. If the VanS parts of the chimeras do have phosphatase activity, corresponding residues could be changed and tested to analyse whether a lower vancomycin concentration could be used to activate chimera activity, and thus reduce the stress on the cell.

From this work, and work carried out by other studies (Haas, *et al.*, 2005; Santos-Beneit, *et al.*, 2014; Hesketh, *et al.*, 2015), it is known that vancomycin exerts high levels of stress in both susceptible and resistant bacteria and results in change in expression of hundreds of genes including *sigE* and *whiB* (Santos-Beneit, *et al.*, 2014; Hesketh, *et al.*, 2015). In *S. coelicolor*, despite resistance, exposure to vancomycin causes colonies to grow more slowly. If work were to continue on rewiring of TCSs in *Streptomyces*, as relatively few TCSs have been characterised over the last few years of this research, and thus, other suitable SKs for rewiring are not available, well characterised SKs of other bacterial families could substitute VanS. From the well characterised model organism *E. coli*, the SK QseC could be a potential candidate. It shares 28% identity with AfsQ2 of *S. coelicolor* and *S. lividans* (Supplementary material S2). Both are classic SKs with a sensor domain, a HAMP domain, a Dhp domain and a CA domain. P2RP analysis shows QseC possesses 15 helices and 11 strands and AfsQ2 has 14 helices and 11 strands (Barakat, *et al.*, 2013). The difference in the number of helices is caused by the additional TM helices in QseC (2 TM helices) in comparison to the one in AfsQ2.

QseC sensed autoinducers (AI-3) produced by gut microflora (Clarke, *et al.*, 2006). This autoinducer would need to be tested against *S. coelicolor* or *S. lividans* to ensure antibiotic production is not induced. Another potential sensor to rewire with AfsQ2 is the photoreceptor used in the study by Levskaya *et al.* The receptor is not a SK but has already been shown to be compatible in rewiring with another SK (Levskaya, *et al.*, 2005). If rewiring is successful, red light would switch on antibiotic production. However, another SK (Sven15_6349; see table 3.1) possesses a phytochrome domain which infers involvement in light sensing too. However, this may not be involved in light sensing within the same spectrum.

Rewiring of TCSs can be applied to further applications that switching on cryptic clusters for antibiotic production for clinical purposes. The library of bioactive and non-bioactive secondary metabolites produced by *Streptomyces* could be utilised in other industries. As *Streptomyces* can also colonise plant roots, rewiring the biological circuitry could also be a means to improve crop growth. Different *Streptomyces* strains could be engineered to produce a concoction of different compounds for plant growth promotion as well as inhibit growth of parasites. Following the example of Levskaya, *et al.*, (2005), engineering the bacteria to produce β -galactosidase, a similar concept could be implemented as an indicator for a particular condition. For instance, under low water, low nutrients, high toxicity or high levels of other bacteria, resulting in either biological response by the engineered strains or through the indication (e.g. colour change or production of light) alerts the farmer to supply the necessary response.

6. Summary and Discussion

The work presented across the three previous chapters share the aim of building on our understanding of how *Streptomyces* comprehend their environment and translate this information into an appropriate response, via the signal transduction pathway of TCSs. To this end, three projects have been undertaken.

In the first (chapter 3), a library of TCS operon deletions has been generated. Whilst not all TCSs have been successfully deleted thus far, it has created a platform to begin characterising the TCSs of *S. venezuelae*. In preliminary screens, SVEN15_3170/71 has been shown to be linked to tunicamycin resistance. SVEN15_3169 encodes the protein TmrB, which binds to tunicamycin and confers resistance in *B. subtilis* (Noda, *et al.*, 1992). $\Delta 3170/71$ was shown to be susceptible to tunicamycin activity where *S. venezuelae* wild-type is resistant. From assessment of dRNA-seq data, *sven15_3169-71* is shown to be transcribed as a single leader less transcript. Combining this data suggests that upon tunicamycin stimulus, the RR SVEN15_3170 upregulates expression the operon. However, complementation of these genes is necessary to determine whether any polar effects were asserted in deleting *sven15_3170/71*.

In this instance, the regulon was predicted through analysis of adjacent genes. For the majority of the TCSs, regulons are not easily identifiable from analysis of neighbouring genes. TCSs can regulate genes situated anywhere within the genome as demonstrated by both MtrA and AfsQ1, two global regulators shown to modulate expression of genes involved in development and primary and secondary metabolism (Wang, *et al.*, 2013B; Som, *et al.*, 2016; Som, *et al.*, 2017). To characterise these TCSs, high throughput screening could be carried out to identify whether specific conditions could elicit a change in phenotype. These changes could include changes in pH, salinity, nutrients, temperature or co-culturing with other bacteria.

Another means of characterising the mutants could be to introduce a phosphomimetic allele. For some TCSs, this may prove to be lethal as demonstrated by Daniel-Ivad, *et al.*, (2016), when a phosphomimetic allele of AfsQ1_{Sco} was not viable in some of the tested wild isolates. For viable strains, use of a phosphomimetic allele would mean not needing to first identify the activating

signal. In parallel to introduction of the phosphomimetic RR allele, the native RR allele could also be introduced into the TCS deletion background to assess whether without the presence of the HK, the RR is able to be phosphorylated or active in the unphosphorylated state. These could be tested through qRT-PCR and phosphorylation assays such as using the Phos-tag assay as presented in chapter 5, if optimised.

To analyse the regulation exerted by the TCSs of *Streptomyces*, another approach to utilising these deletion strains is through analysis of the gene expression levels by microarrays as used by Oshima, *et al.*, 2002 in studying *E. coli* TCS deletion strains or through ChIP-Seq which would provide higher resolution and sensitivity. This could be carried out under different conditions, timepoints of the lifecycle or in combination with strains with a phosphomimetic RR allele or native RR as mentioned above.

In summary, generation of the TCS operon deletion library has laid the groundwork for future characterisation of the TCSs of *S. venezuelae*, allowing us not to just understand what signals trigger a response but also to build on our understanding of the cross regulation in the very complex system of *Streptomyces*. Building the understanding of TCSs of *Streptomyces* could be a means to activate natural product production but also to better characterise TCSs which may be essential in *Streptomyces* or in closely related pathogenic species. This point is particularly highlighted in the case of MtrA in *M. tuberculosis* which was found to be essential (Zahrt and Deretic, 2000).

In addition to characterising the individual TCS operon deletion mutants, the effects of deleting multiple TCSs could also be investigated. It was shown in *M. tuberculosis* that the deletion of *trcXY*, *kdpDE*, *trcS* and *devR* which encodes two TCSs, a SK and a RR, respectively, increased virulence. Where, *M. tuberculosis*, has increased virulence with multiple deletions of TCSs, It would be interesting to assess whether in *Streptomyces*, the same would lead to growth defects or change of growth behaviour such as the change from the vegetative and aerial growth described in the section 1.2.2 to exploratory growth, which is stimulated by fungal interactions from their production of volatile organic compounds (Jones and Elliot, 2017). Other behaviours previously unseen may be

caused. Furthermore, it would be interesting to assess whether the species is viable without any TCSs. This could be tested either through systematic deletion or through use of inhibitors which specially sequester autophosphorylation or ATPase activity of SKs have been identified (Velikova, *et al.*, 2016).

In the Chapter 4, work carried out to purify VanS, with the ultimate aim of discovering whether vancomycin resistance is activated in a VanRS dependent manner through direct binding of the glycopeptide to the SK, through an intermediate or as a complex, has been presented. Though VanS was not able to be purified during the course of the project, recent studies have shown that with use of the detergent DDM, VanS from *E. faecalis* can be purified and maintained stably (Hussain, *et al.*, 2016). Though VanS of the two species is not the same, sharing only 24% identity (NCBI BLASTp), this sheds new light on VanS purification and future possibilities to continue this project. Purified VanS could then be reconstituted into liposomes and exposed to vancomycin and its phosphorylation state be assessed. Additionally, to further determine its binding, crystallography and other techniques such cryo-EM could be carried out with the aim of determining the structure and show the binding of vancomycin or the complex it may form.

Finally, in the third project, presented in chapter 5, where two SKs were rewired with the aim of showing that native signalling can be bypassed and thus rewiring can be tool to activate antibiotic biosynthesis or expression of cryptic genes. The rewiring of AfsQ2 and VanS yielded ambiguous results as to whether the chimeras could phosphorylate AfsQ1 and hence activate downstream antibiotic biosynthesis, with vancomycin stimulus. Vancomycin has been shown to induce global changes of expression in *M. tuberculosis* (Povvedi, *et al.*, 2009), and in *E. faecium* (Ramos, *et al.*, 2015), although, *M. tuberculosis* is not resistant, *E. faecalis* possesses vanA-type resistance. In the latter species, both genes relating to resistance and metabolism showed changes in expression. Here in the case of *Streptomyces*, vancomycin causes a much smaller colony phenotype despite resistance. Vancomycin may well also alter the expression profile making it difficult to determine whether expression of AfsQ1 regulatory targets are altered due to vancomycin or AfsQ1. Therefore, as suggested in Chapter 5, to determine

whether AfsQ1 is activated through a rewired chimera SK, a change in the sensor domain would be necessary.

In changing the elements of the chimeras, other output signalling SKs could also be selected over AfsQ1. Many TCSs are located in antibiotic biosynthetic clusters. The BGC of formicamycins for instance, which have been shown to be bioactive against VRE, MRSA and *B. subtilis*, produced by *S. formicae* (Qin, *et al.*, 2017; Holmes, *et al.*, 2018), also contains two TCSs. In future work, these two TCS may be good candidates for rewiring in combination with a SK of a TCS either not found in *Streptomyces* species, to prevent cross-regulation, or one where the stimulus has a less profound effect on growth as vancomycin.

The study of TCSs in *Streptomyces* allows us to better understand how they decipher the constant changes in their environment and also to develop better means of accessing the abundant natural products this genus of bacteria produces. The work presented here showcases the complexity and challenges encountered in working with these organisms and signalling systems and also serves as a platform for further work to build on our current knowledge of TCSs and streptomycetes.

References

- Aguilar, P.S., Cronan, J.E. & de Mendoza, D., 1998. A *Bacillus subtilis* Gene Induced by Cold Shock Encodes a Membrane Phospholipid Desaturase. *Journal of Bacteriology*, 180(8), pp.2194–2200.
- Ainsa, J.A., Parry, H.D. & Chater, K.F., 1999. A response regulator-like protein that functions at an intermediate stage of sporulation in *Streptomyces coelicolor* A3(2). *Molecular microbiology*, 34(3), pp.607–619.
- Airola, M. V. *et al.*, 2010. Structure of Concatenated HAMP Domains Provides a Mechanism for Signal Transduction. *Structure*, 18(4), pp.436–448.
- Al-Bassam, M.M. *et al.*, 2014. Response Regulator Heterodimer Formation Controls a Key Stage in *Streptomyces* Development D. B. Kearns, ed. *PLoS Genetics*, 10(8), p.e1004554.
- Allenby, N.E.E. *et al.*, 2012. Diverse control of metabolism and other cellular processes in *Streptomyces coelicolor* by the PhoP transcription factor: genome-wide identification of in vivo targets. *Nucleic Acids Research*, 40(19), pp.9543–9556.
- Alm, E., Huang, K. & Arkin, A., 2006. The Evolution of Two-Component Systems in Bacteria Reveals Different Strategies for Niche Adaptation. *PLOS Computational Biology*, 2(11), p.e143.
- Anderson, T.B., Brian, P. & Champness, W.C., 2001. Genetic and transcriptional analysis of *absA*, an antibiotic gene cluster-linked two-component system that regulates multiple antibiotics in *Streptomyces coelicolor*. *Molecular Microbiology*, 39(3), pp.553–566.
- Antoraz, S. *et al.*, 2015. Toward a new focus in antibiotic and drug discovery from the *Streptomyces arsenal*. *Frontiers in Microbiology*, 6, p.461.

Arias, P., Fernández-Moreno, M.A. & Malpartida, F., 1999. Characterization of the Pathway-Specific Positive Transcriptional Regulator for Actinorhodin Biosynthesis *Streptomyces coelicolor*; A3(2) as a DNA-Binding Protein. *Journal of Bacteriology*, 181(22), p.6958 LP-6968.

Arthur, M. *et al.*, 1993. Characterization of Tn1546, a Tn3-related transposon conferring glycopeptide resistance by synthesis of depsipeptide peptidoglycan precursors in *Enterococcus faecium* BM4147. *Journal of bacteriology*, 175(1), pp.117–127.

Ausmees, N. *et al.*, 2007. SmeA, a small membrane protein with multiple functions in *Streptomyces* sporulation including targeting of a SpoIIIE/FtsK-like protein to cell division septa. *Molecular Microbiology*, 65(6), pp.1458–1473.

Baba, T. *et al.*, 2006. Construction of *Escherichia coli* K-12 in-frame, single-gene knockout mutants: the Keio collection. *Molecular Systems Biology*, 2, p.2006.0008-2006.0008.

Bai, C. *et al.*, 2015. Exploiting a precise design of universal synthetic modular regulatory elements to unlock the microbial natural products in *Streptomyces*. *Proceedings of the National Academy of Sciences*, 112(39), p.12181 LP-12186.

Baker, M.D. & Neiditch, M.B., 2011. Structural Basis of Response Regulator Inhibition by a Bacterial Anti-Activator Protein. *PLOS Biology*, 9(12), p.e1001226.

Baltz, R.H., 2011. Strain improvement in actinomycetes in the postgenomic era. *Journal of industrial microbiology & biotechnology*, 38(6), pp.657–666.

Baraquet, C. *et al.*, 2006. TorT, a member of a new periplasmic binding protein family, triggers induction of the Tor respiratory system upon trimethylamine N-oxide electron-acceptor binding in *Escherichia coli*. *The Journal of biological chemistry*, 281(50), pp.38189–38199.

Barakat, M., Ortet, P. & Whitworth, D.E., 2013. P2RP: a web-based framework for the identification and analysis of regulatory proteins in prokaryotic genomes. *BMC Genomics*, 14(1), pp.269.

Barke, J. *et al.*, 2011. A mutualistic microbiome: How do fungus-growing ants select their antibiotic-producing bacteria? *Communicative & Integrative Biology*, 4(1), pp.41–43.

Barrett, J.F. & Hoch, J.A., 1998. Two-Component Signal Transduction as a Target for Microbial Anti-Infective Therapy. *Antimicrobial Agents and Chemotherapy*, 42(7), pp.1529 LP-1536.

Becker, G., Klauck, E. & Hengge-Aronis, R., 2000. The response regulator RssB, a recognition factor for sigmaS proteolysis in *Escherichia coli*, can act like an anti-sigmaS factor. *Molecular microbiology*, 35(3), pp.657–666.

Bem, A.E. *et al.*, 2015. Bacterial Histidine Kinases as Novel Antibacterial Drug Targets. *ACS Chemical Biology*, 10(1), pp.213–224.

Bérdy, J., 2005. Bioactive Microbial Metabolites. *The Journal of Antibiotics*, 58, p.1.

Bhate, M.P. *et al.*, 2015. Signal Transduction in Histidine Kinases: Insights from New Structures. *Structure*, 23(6), pp.981–994.

Biarnes-Carrera, M., Breitling, R. & Takano, E., 2015. Butyrolactone signalling circuits for synthetic biology. *Current Opinion in Chemical Biology*, 28, pp.91–98.

Bidart, G.N. *et al.*, 2012. Manipulation of the Anoxic Metabolism in *Escherichia coli* by ArcB Deletion Variants in the ArcBA Two-Component System. *Applied and Environmental Microbiology*, 78(24), pp.8784–8794.

Bignell, D.R.D. *et al.*, 2005. Expression of *ccaR*, encoding the positive activator of cephamycin C and clavulanic acid production in *Streptomyces clavuligerus*, is dependent on *bldG*. *Antimicrobial agents and chemotherapy*, 49(4), pp.1529–1541.

Bignell, D.R.D. *et al.*, 2010. *Streptomyces scabies* 87-22 Contains a Coronafacic Acid-Like Biosynthetic Cluster That Contributes to Plant–Microbe Interactions. *Molecular Plant-Microbe Interactions*, 23(2), pp.161–175.

Bignell, D.R.D., Fyans, J.K. & Cheng, Z., 2013. Phytotoxins produced by plant pathogenic *Streptomyces* species. *Journal of Applied Microbiology*, 116(2), pp.223–235.

Bijlsma, J.J.E. & Groisman, E.A., 2003. Making informed decisions: regulatory interactions between two-component systems. *Trends in Microbiology*, 11(8), pp.359–366.

Bijlsma, J.J.E. & Groisman, E.A., 2005. The PhoP/PhoQ system controls the intramacrophage type three secretion system of *Salmonella enterica*. *Molecular Microbiology*, 57(1), pp.85–96.

Blat, Y. & Eisenbach, M., 1994. Phosphorylation-dependent binding of the chemotaxis signal molecule CheY to its phosphatase, CheZ. *Biochemistry*, 33(4), pp.902–906.

Blat, Y. & Eisenbach, M., 1996. Oligomerization of the Phosphatase CheZ Upon Interaction with the Phosphorylated Form of CheY: the signal protein of bacterial chemotaxis. *Journal of Biological Chemistry*, 271(2), pp.1226–1231.

Bobek, J. *et al.*, 2004. Activation and expression of proteins during synchronous germination of aerial spores of *Streptomyces granaticolor*. *Proteomics*, 4.

Bobek, J. *et al.*, 2014. Changes in activity of metabolic and regulatory pathways during germination of *S. coelicolor*. *BMC Genomics*, 15(1), pp.1173.

Bobek, J., Šmídová, K. & Čihák, M., 2017. A Waking Review: Old and Novel Insights into the Spore Germination in *Streptomyces*. *Frontiers in Microbiology*, 8, pp.2205.

- Borland, S., Prigent-Combaret, C. & Wisniewski-Dye, F., 2016. Bacterial hybrid histidine kinases in plant-bacteria interactions. *Microbiology (Reading, England)*, 162(10), pp.1715–1734.
- Bongiorni, C. *et al.*, 2005. Synergistic Regulation of Competence Development in *Bacillus subtilis* by Two Rap-Phr Systems. *Journal of Bacteriology*, 187(13), pp.4353–4361.
- Brocker, M. & Bott, M., 2006. Evidence for activator and repressor functions of the response regulator MtrA from *Corynebacterium glutamicum*. *FEMS Microbiology Letters*, 264(2), pp.205–212.
- Brockman, H., Pini, H., & Plotho, O. v., 1950. Actinomycete pigments. I. Actinorhodin, a red antibiotically active pigment from actinomycetes, *Chem. Ber.* 83, pp. 161-167.
- Brian, P. *et al.*, 1996. Global negative regulation of *Streptomyces coelicolor* antibiotic synthesis mediated by an *absA*-encoded putative signal transduction system. *Journal of Bacteriology*, 178(11), pp.3221 LP-3231.
- Brown, N.L. *et al.*, 2003. The MerR family of transcriptional regulators. *FEMS microbiology reviews*, 27(2–3), pp.145–163.
- Brunelle, J.L. & Green, R., 2014. Chapter Twelve - One-dimensional SDS-Polyacrylamide Gel Electrophoresis (1D SDS-PAGE). In J. B. T.-M. in E. Lorsch, ed. *Laboratory Methods in Enzymology: Protein Part C*. Academic Press, pp. 151–159.
- Bugg, T.D.H. *et al.*, 1991. Molecular basis for vancomycin resistance in *Enterococcus faecium* BM4147: biosynthesis of a depsipeptide peptidoglycan precursor by vancomycin resistance proteins VanH and VanA. *Biochemistry*, 30(43), pp.10408–10415.

- Bush, M.J. *et al.*, 2013. Genes Required for Aerial Growth, Cell Division, and Chromosome Segregation Are Targets of WhiA before Sporulation in *Streptomyces venezuelae*. Y. V Brun, ed. *mBio*, 4(5).
- Calogero, S. *et al.*, 1994. RocR, a novel regulatory protein controlling arginine utilization in *Bacillus subtilis*, belongs to the NtrC/NifA family of transcriptional activators. *Journal of Bacteriology*, 176(5), pp.1234–1241.
- Capra, E.J. & Laub, M.T., 2012. The Evolution of Two-Component Signal Transduction Systems. *Annual review of microbiology*, 66, pp.325–347.
- Capstick, D.S. *et al.*, 2007. SapB and the chaplins: connections between morphogenetic proteins in *Streptomyces coelicolor*. *Molecular Microbiology*, 64(3), pp.602–613.
- Carpenter, E.J., Lin, S. & Capone, D.G., 2000. Bacterial Activity in South Pole Snow. *Applied and Environmental Microbiology*, 66(10), pp.4514–4517.
- Casino, P., Miguel-Romero, L. & Marina, A., 2014. Visualizing autophosphorylation in histidine kinases. *Nature communications*, 5, pp.3258.
- Celler, K. *et al.*, 2016. Cross-membranes orchestrate compartmentalization and morphogenesis in *Streptomyces*. *Nature Communications*, 7, p.ncomms11836.
- Cetinkaya, Y., Falk, P. & Mayhall, C.G., 2000. Vancomycin-resistant enterococci. *Clinical microbiology reviews*, 13(4), pp.686–707.
- Chandra, G. & Chater, K.F., 2014. Developmental biology of *Streptomyces* from the perspective of 100 actinobacterial genome sequences M. Smith, ed. *Fems Microbiology Reviews*, 38(3), pp.345–379.
- Chater, K.F., 2016. Recent advances in understanding *Streptomyces*. *F1000 Research*, 5, pp.2795.

- Chen, C.W. *et al.*, 2002. Once the circle has been broken: dynamics and evolution of *Streptomyces* chromosomes. *Trends in genetics: TIG*, 18(10), pp.522–529.
- Chen, D. *et al.*, 2007. Expression of recombinant protein encoded by LOC387715 in *Escherichia coli*. *Protein expression and purification*, 54(2), pp.275–282.
- Chen, S. *et al.*, 2016. Roles of two-component system AfsQ1/Q2 in regulating biosynthesis of the yellow-pigmented coelimycin P2 in *Streptomyces coelicolor* D. Clarke, ed. *FEMS Microbiology Letters*, 363(15), p.fnw160.
- Cheng, R.R. *et al.*, 2014. Toward rationally redesigning bacterial two-component signaling systems using coevolutionary information. *Proc Natl Acad Sci U S A*, 111(5), ppE563-71.
- Cheung, J. & Hendrickson, W.A., 2009. Structural Analysis of Ligand Stimulation of the Histidine Kinase NarX. *Structure (London, England: 1993)*, 17(2), pp.190–201.
- Cheung, J. & Hendrickson, W.A., 2010. Sensor Domains of Two-Component Regulatory Systems. *Current opinion in microbiology*, 13(2), pp.116–123.
- Cho, H.Y. & Kang, B.S., 2015. Two component signaling systems in *Mycobacterium tuberculosis*. *Bio Design*, 3(1), pp. 1-13.
- Čihák, M. *et al.*, 2017. Secondary Metabolites Produced during the Germination of *Streptomyces coelicolor*. *Frontiers in Microbiology*, 8, p.2495.
- Clark, C.A. & Matthews, S.W., 1987. Histopathology of sweet potato root infection by *Streptomyces ipomoea*. *Phytopathology*, 77, pp.1418–23.
- Clarke, M.B. *et al.*, 2006. The QseC sensor kinase: a bacterial adrenergic receptor. *Proceedings of the National Academy of Sciences of the United States of America*, 103(27), pp.10420–10425.

- Cobb, R.E., Wang, Y. & Zhao, H., 2015. High-efficiency multiplex genome editing of *Streptomyces* species using an engineered CRISPR/Cas system. *ACS synthetic biology*, 4(6), pp.723–728.
- Coombs, J.T. & Franco, C.M.M., 2003. Isolation and Identification of Actinobacteria from Surface-Sterilized Wheat Roots. *Applied and Environmental Microbiology*, 69(9), p.5603 LP-5608.
- Cordovez, V. *et al.*, 2015. Diversity and functions of volatile organic compounds produced by *Streptomyces* from a disease-suppressive soil. *Frontiers in Microbiology*, 6, p.1081.
- Cornforth, D.M. & Foster, K.R., 2015. Antibiotics and the art of bacterial war. *Proceedings of the National Academy of Sciences of the United States of America*, 112(35), pp.10827–10828.
- Cousin, C. *et al.*, 2013. Protein-serine/threonine/tyrosine kinases in bacterial signaling and regulation. *FEMS Microbiology Letters*, 346(1), pp.11–19.
- Crowe, J.H., Crowe, L.M. & Chapman, D., 1984. Preservation of Membranes in Anhydrobiotic Organisms: The Role of Trehalose. *Science*, 223(4637), p.701 LP-703.
- Cui, C. *et al.*, 2018. A novel two-component system modulates quorum sensing and pathogenicity in *Burkholderia cenocepacia*. *Molecular Microbiology*, 108(1), pp.32–44.
- Daniel-Ivad, M. *et al.*, 2017. An Engineered Allele of afsQ1 Facilitates the Discovery and Investigation of Cryptic Natural Products. *ACS Chemical Biology*, 12(3), pp.628–634.
- Datsenko, K.A. & Wanner, B.L., 2000. One-step inactivation of chromosomal genes in *Escherichia coli* K-12 using PCR products. *Proceedings of the National Academy of Sciences of the United States of America*, 97(12), pp.6640–6645.

Deshmukh, K.B., Pathak, A.P. & Karuppayil, M.S., 2011. Bacterial Diversity of Lonar Soda Lake of India. *Indian Journal of Microbiology*, 51(1), pp.107–111.

Derouaux, A. *et al.*, 2004. Deletion of a Cyclic AMP Receptor Protein Homologue Diminishes Germination and Affects Morphological Development of *Streptomyces coelicolor*. *Journal of Bacteriology*, 186(6), pp.1893–1897.

Den Hengst, C.D. *et al.*, 2010. Genes essential for morphological development and antibiotic production in *Streptomyces coelicolor* are targets of BldD during vegetative growth. *Molecular Microbiology*, 78(2), pp.361–379.

Ditkowski, B. *et al.*, 2013. Dynamic interplay of ParA with the polarity protein, Scy, coordinates the growth with chromosome segregation in *Streptomyces coelicolor*. *Open Biology*, 3(3), p.130006.

Domagala, J. M., *et al.*, (1998). Bacterial Two-Component Signalling as a Therapeutic Target in Drug Design. In B. P. Rosen & S. Mobashery (Eds.), *Resolving the Antibiotic Paradox: Progress in Understanding Drug Resistance and Development of New Antibiotics* (pp. 269–286). Boston, MA: Springer US.

Dumon-Seignovert, L., Cariot, G. & Vuillard, L., 2004. The toxicity of recombinant proteins in *Escherichia coli*: a comparison of overexpression in BL21(DE3), C41(DE3), and C43(DE3). *Protein expression and purification*, 37(1), pp.203–206.

Dun, J. *et al.*, 2015. PapR6, a Putative Atypical Response Regulator, Functions as a Pathway-Specific Activator of Pristinamycin II Biosynthesis in *Streptomyces pristinaespiralis* T. M. Henkin, ed. *Journal of Bacteriology*, 197(3), pp.441–450.

Eguchi, Y. *et al.*, 2007. B1500, a small membrane protein, connects the two-component systems EvgS/EvgA and PhoQ/PhoP in *Escherichia coli*. *Proceedings of the National Academy of Sciences*, 104(47), pp.18712–18717.

Elbein, A.D. *et al.*, 2003. New insights on trehalose: a multifunctional molecule. *Glycobiology*, 13(4), p.17R–27R.

Elliot, M.A. *et al.*, 2003. The chaplins: a family of hydrophobic cell-surface proteins involved in aerial mycelium formation in *Streptomyces coelicolor*. *Genes & Development*, 17(14), pp.1727–1740.

Elliot, M.A. & Flärdh, K., 2012. Streptomycete Spores. *eLS*.

Esnault, C. *et al.*, 2017. Strong antibiotic production is correlated with highly active oxidative metabolism in *Streptomyces coelicolor* M145. *Scientific Reports*, 7(1), p.200.

Evers, S. & Courvalin, P., 1996. Regulation of VanB-type vancomycin resistance gene expression by the VanS(B)-VanR (B) two-component regulatory system in *Enterococcus faecalis* V583. *Journal of bacteriology*, 178(5), pp.1302–1309.

Feng, X., Oropeza, R. & Kenney, L.J., 2003. Dual regulation by phospho-OmpR of *ssrA/B* gene expression in *Salmonella* pathogenicity island 2. *Molecular Microbiology*, 48(4), pp.1131–1143.

Fernández-Martínez, L.T. *et al.*, 2014. New Insights into Chloramphenicol Biosynthesis in *Streptomyces venezuelae* ATCC 10712. *Antimicrobial Agents and Chemotherapy*, 58(12), pp.7441–7450.

Fernández-Moreno, M.A. *et al.*, 1991. The act cluster contains regulatory and antibiotic export genes, direct targets for translational control by the *bldA* tRNA gene of *Streptomyces*. *Cell*, 66(4), pp.769–780.

Fernández-Moreno, M.A. *et al.*, 1994. DNA sequence and functions of the *actVI* region of the actinorhodin biosynthetic gene cluster of *Streptomyces coelicolor* A3(2). *Journal of Biological Chemistry*, 269(40), pp.24854–24863.

Fernández-Piñar, R. *et al.*, 2008. A Two-Component Regulatory System Integrates Redox State and Population Density Sensing in *Pseudomonas putida*; *Journal of Bacteriology*, 190(23), p.7666 LP-7674.

Finn, R.D. *et al.*, 2008. The Pfam protein families database. *Nucleic Acids Res*, 36.

Fischer, G., Decaris, B. & Leblond, P., 1997. Occurrence of deletions, associated with genetic instability in *Streptomyces ambofaciens*, is independent of the linearity of the chromosomal DNA. *Journal of Bacteriology*, 179(14), p.4553 LP-4558.

Fischer, G. *et al.*, 1998. Chromosomal arm replacement generates a high level of intraspecific polymorphism in the terminal inverted repeats of the linear chromosomal DNA of *Streptomyces ambofaciens*. *Proceedings of the National Academy of Sciences*, 95(24), p.14296 LP-14301.

Flårdh, K., Findlay, K.C. & Chater, K.F., 1999. Association of early sporulation genes with suggested developmental decision points in *Streptomyces coelicolor* A3(2). *Microbiology*, 145(9), pp.2229–2243.

Flårdh, K. *et al.*, 2000. Generation of a non-sporulating strain of *Streptomyces coelicolor* A3(2) by the manipulation of a developmentally controlled *ftsZ* promoter. *Molecular Microbiology*, 38(4), pp.737–749.

Flårdh, K., 2003. Essential role of DivIVA in polar growth and morphogenesis in *Streptomyces coelicolor* A3(2). *Molecular Microbiology*, 49(6), pp.1523–1536.

Flårdh, K. & Buttner, M.J., 2009. *Streptomyces* morphogenetics: dissecting differentiation in a filamentous bacterium. *Nat Rev Micro*, 7(1), pp.36–49.

Fleischer, R. *et al.*, 2007. Purification, Reconstitution, and Characterization of the CpxRAP Envelope Stress System of *Escherichia coli*. *Journal of Biological Chemistry*, 282(12), pp.8583–8593.

Fong, I.W. & Drlica, K. eds., *Antimicrobial Resistance and Implications for the 21st Century Emerging Infectious Diseases of the 21st Century* 2007th ed., Springer Science & Business Media.

Forget, S.M. *et al.*, 2017. *Streptomyces venezuelae* ISP5230 Maintains Excretion of Jadomycin upon Disruption of the MFS Transporter JadL Located within the Natural Product Biosynthetic Gene Cluster. *Frontiers in microbiology*, 8, p.432.

Fuchino, K. *et al.*, 2013. Dynamic gradients of an intermediate filament-like cytoskeleton are recruited by a polarity landmark during apical growth. *Proceedings of the National Academy of Sciences of the United States of America*, 110(21), pp.E1889–E1897.

Galperin, M.Y., 2006. Structural Classification of Bacterial Response Regulators: Diversity of Output Domains and Domain Combinations. *Journal of Bacteriology*, 188(12), pp.4169–4182.

Galperin, M.Y., 2010. Diversity of Structure and Function of Response Regulator Output Domains. *Current opinion in microbiology*, 13(2), pp.150–159.

Gao, R., Mack, T.R. & Stock, A.M., 2007. Bacterial Response Regulators: Versatile Regulatory Strategies from Common Domains. *Trends in biochemical sciences*, 32(5), pp.225–234.

Gao, R. & Stock, A.M., 2009. Biological Insights from Structures of Two-Component Proteins. *Annual review of microbiology*, 63, pp.133–154.

Gao R. & Stock AM., 2010. Molecular strategies for phosphorylation-mediated regulation of response regulator activity. *Curr Opin Microbiol*, 13, pp160–167.

Gao, B. & Gupta, R.S., 2012. Phylogenetic Framework and Molecular Signatures for the Main Clades of the Phylum Actinobacteria; *Microbiology and Molecular Biology Reviews*, 76(1), p.66 LP-112.

Gao, R. & Stock, A.M., 2013. Evolutionary Tuning of Protein Expression Levels of a Positively Autoregulated Two-Component System. *PLOS Genetics*, 9(10), p.e1003927.

Gao, R. *et al.*, 2017. Counterbalancing Regulation in Response Memory of a Positively Autoregulated Two-Component System. *Journal of Bacteriology*.

Garcia Vescovi, E., Sciara, M.I. & Castelli, M.E., 2010. Two component systems in the spatial program of bacteria. *Current opinion in microbiology*, 13(2), pp.210–218.

Garg, R.P. & Parry, R.J., 2010. Regulation of valanimycin biosynthesis in *Streptomyces viridifaciens*: characterization of VImI as a *Streptomyces* antibiotic regulatory protein (SARP). *Microbiology*, 156(Pt 2), pp.472–483.

Gerber, N.N. & Lechevalier, H.A., 1965. Geosmin, an Earthy-Smelling Substance Isolated from Actinomycetes. *Applied Microbiology*, 13(6), p.935 LP-938.

Glauert, A.M. & Hopwood, D.A., 1961. The fine structure of *Streptomyces violaceoruber* (*S. coelicolor*). *The Journal of Biophysical and Biochemical Cytology*, 10(4), p.505 LP-516.

Glazebrook, M.A. *et al.*, 1990. Sporulation of *Streptomyces venezuelae* in submerged cultures. *Journal of general microbiology*, 136(3), pp.581–588.

Gomelsky, M., 2011. cAMP, c-di-GMP, c-di-AMP and now cGMP: Bacteria use them all! *Molecular microbiology*, 79(3), pp.562–565.

Gomelsky, M. & Galperin, M.Y., 2013. Bacterial second messengers, cGMP and c-di-GMP, in a quest for regulatory dominance. *The EMBO Journal*, 32(18), pp.2421–2423.

Gomez-Escribano, J.P. *et al.*, 2012. Structure and biosynthesis of the unusual polyketide alkaloid coelimycin P1, a metabolic product of the *cpk* gene cluster of *Streptomyces coelicolor* M145. *Chemical Science*, 3(9), pp.2716–2720.

Goodman, A.L. *et al.*, 2009. Direct interaction between sensor kinase proteins mediates acute and chronic disease phenotypes in a bacterial pathogen. *Genes & Development*, 23(2), pp.249–259.

Gotoh, Y. *et al.*, 2010. Novel antibacterial compounds specifically targeting the essential WalR response regulator. *The Journal Of Antibiotics*, 63, p.127.

- Gottelt, M. *et al.*, 2010. Deletion of a regulatory gene within the *cpk* gene cluster reveals novel antibacterial activity in *Streptomyces coelicolor* A3(2). *Microbiology*, 156(8), pp.2343–2353.
- Goulian, M., 2010. Two-component signaling circuit structure and properties. *Current opinion in microbiology*, 13(2), pp.184–189.
- Gramajo, H.C., Takano, E. & Bibb, M.J., 2018. Stationary-phase production of the antibiotic actinorhodin in *Streptomyces coelicolor* A3(2) is transcriptionally regulated. *Molecular Microbiology*, 7(6), pp.837–845.
- Grangeasse, C., Nessler, S. & Mijakovic, I., 2012. Bacterial tyrosine kinases: evolution, biological function and structural insights. *Philosophical Transactions of the Royal Society B: Biological Sciences*, 367(1602), pp.2640–2655.
- Gregory, M.A., Till, R. & Smith, M.C.M., 2003. Integration site for *Streptomyces* phage phiBT1 and development of site-specific integrating vectors. *Journal of bacteriology*, 185(17), pp.5320–5323.
- Groisman, E.A., 2016. Feedback Control of Two-Component Regulatory Systems. *Annual review of microbiology*, 70, pp.103–124.
- Gupta, R.S. *et al.*, 2013. Molecular signatures for the class *Coriobacteriia* and its different clades; proposal for division of the class *Coriobacteriia* into the emended order *Coriobacteriales*, containing the emended family *Coriobacteriaceae* and *Atopobiaceae* fam. nov., and *Eggerthellales* ord. nov., containing the family *Eggerthellaceae* fam. nov. *International Journal of Systematic and Evolutionary Microbiology*, 63(9), pp.3379–3397.
- Gusa, A.A. & Scott, J.R., 2005. The CovR response regulator of group A streptococcus (GAS) acts directly to repress its own promoter. *Molecular microbiology*, 56(5), pp.1195–1207.
- Gushchin, I. *et al.*, 2017. Mechanism of transmembrane signaling by sensor histidine kinases. *Science (New York, N.Y.)*, 356(6342).

- Gust, B. et al., 2003. PCR-targeted *Streptomyces* gene replacement identifies a protein domain needed for biosynthesis of the sesquiterpene soil odor geosmin. *Proceedings of the National Academy of Sciences of the United States of America*, 100(4), pp.1541–1546.
- Haas, W. et al., 2005. Vancomycin stress response in a sensitive and a tolerant strain of *Streptococcus pneumoniae*. *Journal of bacteriology*, 187(23), pp.8205–8210.
- Haiser, H.J., Yousef, M.R. & Elliot, M.A., 2009. Cell Wall Hydrolases Affect Germination, Vegetative Growth, and Sporulation in *Streptomyces coelicolor*. *Journal of Bacteriology*, 191(21), pp.6501–6512.
- Hardisson, C. et al., 1978. Fine Structure, Physiology and Biochemistry of Arthrospore Germination in *Streptomyces antibioticus*. *Microbiology*, 105(2), pp.203–214.
- Hauptmann, A.L. et al., 2014. Bacterial diversity in snow on North Pole ice floes. *Extremophiles*, 18(6), pp.945–951.
- He, J. et al., 2016. Complete Genome Sequence of *Streptomyces venezuelae* ATCC 15439, Producer of the Methymycin/Pikromycin Family of Macrolide Antibiotics, Using PacBio Technology. *Genome announcements*, 4(3), pp.e00337-16.
- Heermann, R. & Jung, K., 2010. The complexity of the “simple” two-component system KdpD/KdpE in *Escherichia coli*. *FEMS Microbiology Letters*, 304(2), pp.97–106.
- Heichlinger, A. et al., 2011. The MreB-Like Protein Mbl of *Streptomyces coelicolor* A3(2) Depends on MreB for Proper Localization and Contributes to Spore Wall Synthesis. *Journal of Bacteriology*, 193(7), pp.1533–1542.
- Heidelberg, J.F. et al., 2004. The genome sequence of the anaerobic, sulfate-reducing bacterium *Desulfovibrio vulgaris* Hildenborough. *Nat Biotechnol*, p. 22.

- Hempel, A.M. *et al.*, 2008. Assemblies of DivIVA mark sites for hyphal branching and can establish new zones of cell wall growth in *Streptomyces coelicolor*. *Journal of bacteriology*, 190(22), pp.7579–7583.
- Hempel, A.M. *et al.*, 2012. The Ser/Thr protein kinase AfsK regulates polar growth and hyphal branching in the filamentous bacteria *Streptomyces*. *Proceedings of the National Academy of Sciences of the United States of America*, 109(35), pp.E2371–E2379.
- Hense, B.A. & Schuster, M., 2015. Core Principles of Bacterial Autoinducer Systems. *Microbiology and Molecular Biology Reviews*, 79(1), p.153 LP-169.
- Heo, I. *et al.*, 2008. Lin28 Mediates the Terminal Uridylation of let-7 Precursor MicroRNA. *Molecular Cell*, 32(2), pp.276–284.
- Herrou, J. *et al.*, 2010. A structural model of anti-anti-sigma inhibition by a two-component receiver domain: the PhyR stress response regulator. *Molecular microbiology*, 78(2), pp.290–304.
- Herrou, J., Crosson, S. & Fiebig, A., 2017. Structure and function of HWE/HisKA2-family sensor histidine kinases. *Current opinion in microbiology*, 36, pp.47–54.
- Hesketh, A., Deery, M.J. & Hong, H.-J., 2015. High-Resolution Mass Spectrometry Based Proteomic Analysis of the Response to Vancomycin-Induced Cell Wall Stress in *Streptomyces coelicolor* A3(2). *Journal of Proteome Research*, 14(7), pp.2915–2928.
- Heydari Zarnagh, H. *et al.*, 2015. Expression and Purification of a Novel Computationally Designed Antigen for Simultaneously Detection of HTLV-1 and HBV Antibodies. *Iranian journal of allergy, asthma, and immunology*, 14(2), pp.168–178.

Hirsch, C.F. & Ensign, J.C., 1976. Nutritionally defined conditions for germination of *Streptomyces viridochromogenes* spores. *Journal of bacteriology*, 126(1), pp.13–23.

Hoff, G. *et al.*, 2016. Multiple and Variable NHEJ-Like Genes Are Involved in Resistance to DNA Damage in *Streptomyces ambofaciens*. *Frontiers in Microbiology*, 7, p.1901.

Holmes, N.A. *et al.*, 2013. Coiled-coil protein Scy is a key component of a multiprotein assembly controlling polarized growth in *Streptomyces*. *Proceedings of the National Academy of Sciences of the United States of America*, 110(5), pp.E397–E406.

Holmes, N. A., *et al.*, (2018). Complete genome sequence of *Streptomyces formicae* KY5, the formicamycin producer. *Journal of Biotechnology*, 265, 116–118.

Hong, H.-J., Paget, M.S.B. & Buttner, M.J., 2002. A signal transduction system in *Streptomyces coelicolor* that activates the expression of a putative cell wall glycan operon in response to vancomycin and other cell wall-specific antibiotics. *Molecular Microbiology*, 44(5), pp.1199–1211.

Hong, H.-J. *et al.*, 2004. Characterization of an inducible vancomycin resistance system in *Streptomyces coelicolor* reveals a novel gene (*vanK*) required for drug resistance. *Molecular Microbiology*, 52(4), pp.1107–1121.

Hong, H.-J. *et al.*, 2005. The Role of the Novel Fem Protein VanK in Vancomycin Resistance in *Streptomyces coelicolor*. *Journal of Biological Chemistry*, 280(13), pp.13055–13061.

Hong, E. *et al.*, 2007. Structure of an Atypical Orphan Response Regulator Protein Supports a New Phosphorylation-independent Regulatory Mechanism. *Journal of Biological Chemistry*, 282(28), pp.20667–20675.

Hong, K. *et al.*, 2009. Actinomycetes for Marine Drug Discovery Isolated from Mangrove Soils and Plants in China. *Marine Drugs*, 7(1), pp.24–44.

Hoskisson, P.A. & Hutchings, M.I., 2006. MtrAB–LpqB: a conserved three-component system in actinobacteria? *Trends in Microbiology*, 14(10), pp.444–449.

Hoster, F., Schmitz, J.E. & Daniel, R., 2005. Enrichment of chitinolytic microorganisms: isolation and characterization of a chitinase exhibiting antifungal activity against phytopathogenic fungi from a novel *Streptomyces* strain. *Applied Microbiology and Biotechnology*, 66(4), pp.434–442.

Hughes, D.T. & Sperandio, V., 2008. Inter-kingdom signalling: communication between bacteria and their hosts. *Nature reviews. Microbiology*, 6(2), pp.111–120.

Hulko, M. *et al.*, 2006. The HAMP Domain Structure Implies Helix Rotation in Transmembrane Signaling. *Cell*, 126(5), pp.929–940.

Hussain, R. *et al.*, 2016. Purification of bacterial membrane sensor kinases and biophysical methods for determination of their ligand and inhibitor interactions. *Biochemical Society Transactions*, 44(3), pp.810–823.

Hutchings, M.I. *et al.*, 2004. Sensing and responding to diverse extracellular signals? Analysis of the sensor kinases and response regulators of *Streptomyces coelicolor* A3(2). *Microbiology*, 150(9), pp.2795–2806.

Hutchings, M.I., Hong, H.-J. & Buttner, M.J., 2006. The vancomycin resistance VanRS two-component signal transduction system of *Streptomyces coelicolor*. *Molecular Microbiology*, 59(3), pp.923–935.

Inahashi, Y. *et al.*, 2017. Watasemycin biosynthesis in *Streptomyces venezuelae*: thiazoline C-methylation by a type B radical-SAM methylase homologue. *Chemical Science*, 8(4), pp.2823–2831.

Iqbal, M. *et al.*, 2012. Extracting regulator activity profiles by integration of de novo motifs and expression data: characterizing key regulators of nutrient depletion

responses in *Streptomyces coelicolor*. *Nucleic Acids Research*, 40(12), pp.5227–5239.

Ishizuka, H. *et al.*, 1992. A putative two-component regulatory system involved in secondary metabolism in *Streptomyces* spp. *Journal of Bacteriology*, 174(23), pp.7585–7594.

Island, M.D. & Kadner, R.J., 1993. Interplay between the membrane-associated UhpB and UhpC regulatory proteins. *Journal of Bacteriology*, 175(16), pp.5028–5034.

Itoh, T. *et al.*, 2007. Actinorhodin Biosynthesis: Structural Requirements for Post-PKS Tailoring Intermediates Revealed by Functional Analysis of ActVI-ORF1 Reductase. *Biochemistry*, 46(27), pp.8181–8188.

Jakimowicz, D. *et al.*, 2007. Alignment of multiple chromosomes along helical ParA scaffolding in sporulating *Streptomyces* hyphae. *Molecular Microbiology*, 65(3), pp.625–641.

Janausch, I.G., Garcia-Moreno, I. & Udden, G., 2002. Function of DcuS from *Escherichia coli* as a fumarate-stimulated histidine protein kinase in vitro. *The Journal of biological chemistry*, 277(42), pp.39809–39814.

Jing, X. *et al.*, 2010. Crystal Structure and Oligomeric State of the RetS Signaling Kinase Sensory Domain. *Proteins*, 78(7), pp.1631–1640.

Jones, S.E. *et al.*, 2017. *Streptomyces* exploration is triggered by fungal interactions and volatile signals T. Mignot, ed. *eLife*, 6, p.e21738.

Joseph, P. *et al.*, 2002. Regulatory relationship of two-component and ABC transport systems and clustering of their genes in the *Bacillus/Clostridium* group, suggest a functional link between them. *Journal of molecular microbiology and biotechnology*, 4(5), pp.503–513.

- Joseph, M.R.P. *et al.*, 2015. In vitro anti-yeast activity of chloramphenicol: A preliminary report. *Journal de Mycologie Médicale*, 25(1), pp.17–22.
- Kalan, L. *et al.*, 2013. Glycopeptide Sulfation Evades Resistance. *Journal of Bacteriology*, 195(1), pp.167–171.
- Kallifidas, D. *et al.*, 2018. Rational engineering of *Streptomyces albus* J1074 for the overexpression of secondary metabolite gene clusters. *Microbial cell factories*, 17(1), p.25.
- Kaltenpoth, M. *et al.*, 2014. Partner choice and fidelity stabilize coevolution in a Cretaceous-age defensive symbiosis. *Proceedings of the National Academy of Sciences*, 111(17), p.6359 LP-6364.
- Kaspar, S. & Bott, M., 2002. The sensor kinase CitA (DpiB) of *Escherichia coli* functions as a high-affinity citrate receptor. *Archives of Microbiology*, 177(4), pp.313–321.
- Karniol, B. & Vierstra, R.D., 2004. The HWE histidine kinases, a new family of bacterial two-component sensor kinases with potentially diverse roles in environmental signaling. *J Bacteriol*, 186.
- Kato, A., Tanabe, H. & Utsumi, R., 1999. Molecular Characterization of the PhoP-PhoQ Two-Component System in *Escherichia coli* K-12: Identification of Extracellular Mg²⁺-Responsive Promoters. *Journal of Bacteriology*, 181(17), pp.5516–5520.
- Kato, A. & Groisman, E.A., 2004. Connecting two-component regulatory systems by a protein that protects a response regulator from dephosphorylation by its cognate sensor. *Genes & development*, 18(18), pp.2302–2313.
- Kieser, T. *et al.*, 2000. Practical *Streptomyces* Genetics. *John Innes Centre Ltd.*,

Kiehler, B., Haggett, L. & Fujita, M., 2017. The PAS domains of the major sporulation kinase in *Bacillus subtilis* play a role in tetramer formation that is essential for the autokinase activity. *MicrobiologyOpen*, 6(4), p.e00481.

Kim, D. & Forst, S., 2001. Genomic analysis of the histidine kinase family in bacteria and archaea. *Microbiology*, 147, pp.1197-1212.

Kim, Y.J. *et al.*, 2007. pH shock induces overexpression of regulatory and biosynthetic genes for actinorhodin production in *Streptomyces coelicolor* A3(2). *Applied Microbiology and Biotechnology*, 76(5), pp.1119–1130.

Kirby, R. *et al.*, 2012. Draft Genome Sequence of the Human Pathogen *Streptomyces somaliensis*, a Significant Cause of Actinomycetoma. *Journal of Bacteriology*, 194(13), pp.3544–3545.

Kleinschmitz, E.-M. *et al.*, 2011. Proteins encoded by the *mre* gene cluster in *Streptomyces coelicolor* A3(2) cooperate in spore wall synthesis. *Molecular Microbiology*, 79(5), pp.1367–1379.

Koo, B.-M. *et al.*, 2017. Construction and Analysis of Two Genome-scale Deletion Libraries for *Bacillus subtilis*. *Cell systems*, 4(3), pp.291–305.e7.

Koretke, K.K. *et al.*, 2000. Evolution of two-component signal transduction. *Mol Biol Evol*, p.17.

Kostrewa, D. *et al.*, 1991. Three-dimensional structure of the *E. coli* DMA-binding protein FIS. *Nature*, 349(6305), pp.178–180.

Kotowska, M. *et al.*, 2002. Type II thioesterase from *Streptomyces coelicolor* A3(2). *Microbiology (Reading, England)*, 148(Pt 6), pp.1777–1783.

Kotowska, M., Ciekot, J. & Pawlik, K., 2014. Type II thioesterase ScoT is required for coelimycin production by the modular polyketide synthase Cpk of *Streptomyces coelicolor* A3(2). *Acta biochimica Polonica*, 61(1), pp.141–147.

Kresge, N., Simoni, R.D. & Hill, R.L., 2004. Selman Waksman: The Father of Antibiotics. *Journal of Biological Chemistry*, 279(48), pp.e7–e7.

Kroiss, J. *et al.*, 2010. Symbiotic streptomycetes provide antibiotic combination prophylaxis for wasp offspring. *Nature Chemical Biology*, 6, p.261.

Kurth, F. *et al.*, 2014. *Streptomyces*-induced resistance against oak powdery mildew involves host plant responses in defense, photosynthesis, and secondary metabolism pathways. *Molecular plant-microbe interactions: MPMI*, 27(9), pp.891–900.

Kwun, M.J. *et al.*, 2013. In Vivo Studies Suggest that Induction of VanS-Dependent Vancomycin Resistance Requires Binding of the Drug to d-Ala-d-Ala Termini in the Peptidoglycan Cell Wall. *Antimicrobial Agents and Chemotherapy*, 57(9), pp.4470–4480.

Lamp, J. *et al.*, 2013. A *Streptomyces*-specific member of the metallophosphatase superfamily contributes to spore dormancy and interaction with *Aspergillus proliferans*. *FEMS Microbiology Letters*, 342(2), pp.89–97.

Landry, B.P. *et al.*, 2018. Phosphatase activity tunes two-component system sensor detection threshold. *Nature Communications*, 9(1), p.1433.

Larkin, M.A., *et al.*, 2007. ClustalW and ClustalX version 2. *Bioinformatics*, 23(21): pp.2947-2948.

Laub, M.T. & Goulian, M., 2007. Specificity in two-component signal transduction pathways. *Annual review of genetics*, 41, pp.121–145.

Laub, M.T., Biondi, E.G. & Skerker, J.M., 2007. Phosphotransfer Profiling: Systematic Mapping of Two-Component Signal Transduction Pathways and Phosphorelays. In M. I. Simon, B. R. Crane, & A. B. T.-M. in E. Crane, eds. *Two-Component Signaling Systems, Part B*. Academic Press, pp. 531–548.

LeDeaux, J.R., Yu, N. & Grossman, A.D., 1995. Different roles for KinA, KinB, and KinC in the initiation of sporulation in *Bacillus subtilis*. *Journal of Bacteriology*, 177(3), pp.861–863.

Lee, P.-C., Umeyama, T. & Horinouchi, S., 2002. *afsS* is a target of AfsR, a transcriptional factor with ATPase activity that globally controls secondary metabolism in *Streptomyces coelicolor* A3(2). *Molecular Microbiology*, 43(6), pp.1413–1430.

Lee, Y. *et al.*, 2006. Binding study of AfsK, a Ser/Thr kinase from *Streptomyces coelicolor* A3(2) and S-adenosyl-l-methionine. *FEMS Microbiology Letters*, 266(2), pp.236–240.

Lee, H.-N. *et al.*, 2013. Repression of Antibiotic Downregulator WblA by AdpA in *Streptomyces coelicolor*. *Applied and Environmental Microbiology*, 79(13), pp.4159–4163.

Lehr, N.A. *et al.*, 2009. WS-5995 B, an antifungal agent inducing differential gene expression in the conifer pathogen *Heterobasidion annosum* but not in *Heterobasidion abietinum*. *Applied microbiology and biotechnology*, 85(2), pp.347–358.

Lemercier, G., Bakalara, N. & Santarelli, X., 2003. On-column refolding of an insoluble histidine tag recombinant exopolyphosphatase from *Trypanosoma brucei* overexpressed in *Escherichia coli*. *Journal of Chromatography B*, 786(1), pp.305–309.

Leonard, P.G., Golemi-Kotra, D. & Stock, A.M., 2013. Phosphorylation-dependent conformational changes and domain rearrangements in *Staphylococcus aureus* VraR activation. *Proceedings of the National Academy of Sciences*, 110(21), pp.8525–8530.

Letunic, I., Doerks, T. & Bork, P., 2012. SMART 7: recent updates to the protein domain annotation resource. *Nucleic Acids Res*, 40.

- Levine, D.P., 2006. Vancomycin: A History. *Clinical Infectious Diseases*, 42(Supplement_1), pp.S5–S12.
- Levskaya, A. *et al.*, 2005. Engineering *Escherichia coli* to see light. *Nature*, 438, p.441.
- A) Li, S. *et al.*, 2015. Genome-wide identification and characterization of reference genes with different transcript abundances for *Streptomyces coelicolor*. *Scientific Reports*, 5, p.15840.
- B) Li, X. *et al.*, 2015. ScbR- and ScbR2-mediated signal transduction networks coordinate complex physiological responses in *Streptomyces coelicolor*. *Scientific reports*, 5, p.14831.
- Li, L., Jiang, W. & Lu, Y., 2017. A novel two-component system, GluR-K, involved in glutamate sensing and uptake in *Streptomyces coelicolor*. *Journal of Bacteriology*.
- Linares, J.F. *et al.*, 2006. Antibiotics as intermicrobial signaling agents instead of weapons. *Proceedings of the National Academy of Sciences*, 103(51), pp.19484–19489.
- Liu, G. *et al.*, 2013. Molecular Regulation of Antibiotic Biosynthesis in *Streptomyces*. *Microbiology and Molecular Biology Reviews*, 77(1), pp.112–143.
- Lonetto, M.A. *et al.*, 1994. Analysis of the *Streptomyces coelicolor* sigE gene reveals the existence of a subfamily of eubacterial RNA polymerase sigma factors involved in the regulation of extracytoplasmic functions. *Proceedings of the National Academy of Sciences of the United States of America*, 91(16), pp.7573–7577.
- Loria, R., Kers, J. & Joshi, M., 2006. Evolution of Plant Pathogenicity in *Streptomyces*. *Annual Review of Phytopathology*, 44(1), pp.469–487.

Lu, Y. *et al.*, 2011. An Orphan Histidine Kinase, OhkA, Regulates Both Secondary Metabolism and Morphological Differentiation in *Streptomyces coelicolor*. *Journal of Bacteriology*, 193(12), pp.3020–3032.

Mack, T.R., Gao, R. & Stock, A.M., 2009. Probing the Roles of the Two Different Dimers Mediated by the Receiver Domain of the Response Regulator PhoB. *Journal of Molecular Biology*, 389(2), pp.349–364.

MacNeil, D. J., Gewain, K. M., Ruby, C. L., Dezeny, G., Gibbons, P. H., & MacNeil, T. (1992). Analysis of *Streptomyces avermitilis* genes required for avermectin biosynthesis utilizing a novel integration vector. *Gene*, 111(1), pp.61–68.

Marchler-Bauer, A. *et al* (2007) CDD: a conserved domain database for interactive domain family analysis. *Nucleic Acids Res.* 35: D237-40.

Marcone, G.L. *et al.*, 2010. Novel Mechanism of Glycopeptide Resistance in the A40926 Producer *Nonomuraea* sp. ATCC 39727. *Antimicrobial Agents and Chemotherapy*, 54(6), p.2465 LP-2472.

Martin C. *et al.* (2006). The live *Mycobacterium tuberculosis* phoP mutant strain is more attenuated than BCG and confers protective immunity against tuberculosis in mice and guinea pigs. *Vaccine* 24 3408–3419.

Martin, J.F., Rodriguez-Garcia, A. & Liras, P., 2017. The master regulator PhoP coordinates phosphate and nitrogen metabolism, respiration, cell differentiation and antibiotic biosynthesis: comparison in *Streptomyces coelicolor* and *Streptomyces avermitilis*. *J Antibiot*, 70(5), pp.534–541.

Martínez-Burgo, Y. *et al.*, 2015. The Pathway-Specific Regulator ClaR of *Streptomyces clavuligerus* Has a Global Effect on the Expression of Genes for Secondary Metabolism and Differentiation. M. A. Elliot, ed. *Applied and Environmental Microbiology*, 81(19), p.6637 LP-6648.

Mascher, T. *et al.*, 2003. Cell wall stress responses in *Bacillus subtilis*: the regulatory network of the bacitracin stimulon. *Molecular microbiology*, 50(5), pp.1591–1604.

Mascher, T., 2006. Intramembrane-sensing histidine kinases: a new family of cell envelope stress sensors in *Firmicutes* bacteria. *FEMS Microbiology Letters*, 264(2), pp.133–144.

Mascher, T., Helmann, J.D. & Uden, G., 2006. Stimulus Perception in Bacterial Signal-Transducing Histidine Kinases. *Microbiology and Molecular Biology Reviews*, 70(4), pp.910–938.

Matsushika, A. & Mizuno, T., 1998. A dual-signaling mechanism mediated by the ArcB hybrid sensor kinase containing the histidine-containing phosphotransfer domain in *Escherichia coli*. *Journal of Bacteriology*, 180(15), pp.3973–3977.

Mattos-Graner, R.O. & Duncan, M.J., 2017. Two-component signal transduction systems in oral bacteria. *Journal of Oral Microbiology*, 9(1), p.1400858.

McCormick, J.R. & Flärdh, K., 2012. Signals and regulators that govern *Streptomyces* development. *Fems Microbiology Reviews*, 36(1), pp.206–231.

McGuire, J.M., Wolfe, R.N. & Ziegler, D.W., Vancomycin, a new antibiotic. II. In vitro antibacterial studies. *Antibiotics annual*, 3, pp.612–618.

McKenzie, N.L. & Nodwell, J.R., 2007. Phosphorylated AbsA2 Negatively Regulates Antibiotic Production in *Streptomyces coelicolor* through Interactions with Pathway-Specific Regulatory Gene Promoters. *Journal of Bacteriology*, 189(14), p.5284 LP-5292.

Mikulik, K. *et al.*, 1984. RNA and ribosomal protein patterns during aerial spore germination in *Streptomyces granaticolor*. *European Journal of Biochemistry*, 145(2), pp.381–388.

- Mikulík, K. *et al.*, 2002. Expression of proteins and protein kinase activity during germination of aerial spores of *Streptomyces granaticolor*. *Biochemical and biophysical research communications*, 299(2), pp.335–342.
- Miller, M.B. & Bassler, B.L., 2001. Quorum Sensing in Bacteria. *Annual Review of Microbiology*, 55(1), pp.165–199.
- Miroux, B. & Walker, J.E., 1996. Over-production of proteins in *Escherichia coli*: mutant hosts that allow synthesis of some membrane proteins and globular proteins at high levels. *Journal of molecular biology*, 260(3), pp.289–298.
- Mistry, B. V *et al.*, 2008. FtsW Is a Dispensable Cell Division Protein Required for Z-Ring Stabilization during Sporulation Septation in *Streptomyces coelicolor*. *Journal of Bacteriology*, 190(16), pp.5555–5566.
- Mitrophanov, A.Y. & Groisman, E.A., 2008. Signal integration in bacterial two-component regulatory systems. *Genes & Development*, 22(19), pp.2601–2611.
- Mitrophanov, A.Y., Hadley, T.J. & Groisman, E.A., 2010. Positive autoregulation shapes response timing and intensity in two-component signal transduction systems. *Journal of molecular biology*, 401(4), pp.671–680.
- Möker, N. *et al.*, 2004. Deletion of the genes encoding the MtrA-MtrB two-component system of *Corynebacterium glutamicum* has a strong influence on cell morphology, antibiotics susceptibility and expression of genes involved in osmoprotection. *Molecular Microbiology*, 54(2), pp.420–438.
- Molle, V. & Buttner, M.J., 2002. Different alleles of the response regulator gene *bldM* arrest *Streptomyces coelicolor* development at distinct stages. *Molecular Microbiology*, 36(6), pp.1265–1278.
- Molnar, K.S. *et al.*, 2014. Cys-Scanning Disulfide Crosslinking and Bayesian Modeling Probe the Transmembrane Signaling Mechanism of the Histidine Kinase, PhoQ. *Structure*, 22(9), pp.1239–1251.

Monzel, C. *et al.*, 2013. The cytoplasmic PAS_C domain of the sensor kinase DcuS of *Escherichia coli*: role in signal transduction, dimer formation, and DctA interaction. *MicrobiologyOpen*, 2(6), pp.912–927.

Moore, J.O. & Hendrickson, W.A., 2009. Structural Analysis of Sensor Domains from the TMAO-Responsive Histidine Kinase Receptor TorS. *Structure*, 17(9), pp.1195–1204.

Nealson, K.H. & Hastings, J.W., 1979. Bacterial bioluminescence: its control and ecological significance. *Microbiological Reviews*, 43(4), pp.496–518.

Nett, M., Ikeda, H. & Moore, B.S., 2009. Genomic basis for natural product biosynthetic diversity in the actinomycetes. *Natural product reports*, 26(11), pp.1362–1384.

Nguyen, K.T. *et al.*, 2003. Colonial Differentiation in *Streptomyces coelicolor* Depends on Translation of a Specific Codon within the *adpA* Gene. *Journal of Bacteriology*, 185(24), pp.7291–7296. Available at: <http://jb.asm.org/content/185/24/7291.abstract>.

Nguyen, K.T. *et al.*, 2010. Mycobacterial Biofilms Facilitate Horizontal DNA Transfer between Strains of *Mycobacterium smegmatis*. *Journal of Bacteriology*, 192(19), pp.5134–5142.

Nieselt, K. *et al.*, 2010. The dynamic architecture of the metabolic switch in *Streptomyces coelicolor*. *BMC Genomics*, 11(1), p.10.

Nikaido, H. & Takatsuka, Y., 2009. Mechanisms of RND Multidrug Efflux Pumps. *Biochimica et biophysica acta*, 1794(5), pp.769–781.

Ninfa, A.J., 2010. Use of Two-Component Signal Transduction Systems in the Construction of Synthetic Genetic Networks. *Current opinion in microbiology*, 13(2), pp.240–245.

Nishijyo, T., Haas, D. & Itoh, Y., 2001. The CbrA-CbrB two-component regulatory system controls the utilization of multiple carbon and nitrogen sources in *Pseudomonas aeruginosa*. *Molecular microbiology*, 40(4), pp.917–931.

Noda, Y. *et al.*, 1992. TmrB protein, responsible for tunicamycin resistance of *Bacillus subtilis*, is a novel ATP-binding membrane protein. *Journal of Bacteriology*, 174(13), pp.4302–4307.

Noda, Y. *et al.*, 1995. TmrB Protein, Which Confers Resistance to Tunicamycin on *Bacillus subtilis*, Binds Tunicamycin. *Bioscience, Biotechnology, and Biochemistry*, 59(2), pp.321–322.

Noens, E.E.E. *et al.*, 2005. SsgA-like proteins determine the fate of peptidoglycan during sporulation of *Streptomyces coelicolor*. *Molecular Microbiology*, 58(4), pp.929–944.

Novotna, G. *et al.*, 2012. A Novel Membrane Protein, VanJ, Conferring Resistance to Teicoplanin. *Antimicrobial Agents and Chemotherapy*, 56(4), pp.1784–1796.

Oganesyan, V. *et al.*, 2005. Crystal Structure of the “PhoU-Like” Phosphate Uptake Regulator from *Aquifex aeolicus*. *Journal of Bacteriology*, 187(12), pp.4238–4244.

O’Hara, B.P. *et al.*, 1999. Crystal structure and induction mechanism of AmiC-AmiR: a ligand-regulated transcription antitermination complex. *The EMBO Journal*, 18(19), pp.5175–5186.

Ohnishi Y., *et al*, 2005. AdpA, a central transcriptional regulator in the A-factor regulatory cascade that leads to morphological development and secondary metabolism in *Streptomyces griseus*. *Biosci. Biotechnol. Biochem.* 69:431–439

Onaka, H. *et al.*, 2002. Cloning of the staurosporine biosynthetic gene cluster from *Streptomyces* sp. TP-A0274 and its heterologous expression in *Streptomyces lividans*. *The Journal of antibiotics*, 55(12), pp.1063–1071.

- Oshima, T. *et al.*, 2002. Transcriptome analysis of all two-component regulatory system mutants of *Escherichia coli* K-12. *Molecular Microbiology*, 46(1), pp.281–291.
- Otani, H. *et al.*, 2013. An alternative sigma factor governs the principal sigma factor in *Streptomyces griseus*. *Molecular Microbiology*, 87(6), pp.1223–1236.
- Ortet, P. *et al.*, 2012. P2TF: a comprehensive resource for analysis of prokaryotic transcription factors. *BMC Genomics*, 13.
- Paget, M.S., Leibovitz, E. & Buttner, M.J., 1999. A putative two-component signal transduction system regulates *sigmaE*, a sigma factor required for normal cell wall integrity in *Streptomyces coelicolor* A3(2). *Mol Microbiol*, 33.
- Paget, M.S.B. *et al.*, 1999. Evidence that the Extracytoplasmic Function Sigma Factor ζ (E) Is Required for Normal Cell Wall Structure in *Streptomyces coelicolor* A3(2). *Journal of Bacteriology*, 181(1), pp.204–211.
- Parish, T. *et al.*, 2003. Deletion of Two-Component Regulatory Systems Increases the Virulence of *Mycobacterium tuberculosis*. *Infection and Immunity*, 71(3), pp.1134–1140.
- Park, A.K. *et al.*, 2013. Crystal structure of the response regulator spr1814 from *Streptococcus pneumoniae* reveals unique interdomain contacts among NarL family proteins. *Biochemical and Biophysical Research Communications*, 434(1), pp.65–69.
- Parks, T.D. *et al.*, 1994. Release of Proteins and Peptides from Fusion Proteins Using a Recombinant Plant Virus Proteinase. *Analytical Biochemistry*, 216(2), pp.413–417.
- Paul, R. *et al.*, 2008. Allosteric Regulation of Histidine Kinases by Their Cognate Response Regulator Determines Cell Fate. *Cell*, 133(3), pp.452–461.

Pawelczyk, S. *et al.*, 2012. Predicting Inter-Species Cross-Talk in Two-Component Signalling Systems. *PLOS ONE*, 7(5), p.e37737.

Pawlik, K. *et al.*, 2007. A cryptic type I polyketide synthase (*cpk*) gene cluster in *Streptomyces coelicolor* A3(2). *Archives of Microbiology*, 187(2), pp.87–99.

Penumetcha, P., *et al.*, 2010. Improving the Lac system for synthetic biology. *BIOS*, 81(1), pp7-15.

Perego, M., 1998. Kinase–phosphatase competition regulates *Bacillus subtilis* development. *Trends in Microbiology*, 6(9), pp.366–370.

Périchon, B. & Courvalin, P., 2009. VanA-Type Vancomycin-Resistant *Staphylococcus aureus*. *Antimicrobial Agents and Chemotherapy*, 53(11), p.4580 LP-4587.

Perraud, A.-L. *et al.*, 1998. Specificity of the BvgAS and EvgAS phosphorelay is mediated by the C-terminal HPT domains of the sensor proteins. *Molecular Microbiology*, 27(5), pp.875–887.

Perraud, A.-L., Weiss, V. & Gross, R., 1999. Signalling pathways in two-component phosphorelay systems. *Trends in Microbiology*, 7(3), pp.115–120.

Petersen, F. *et al.*, 1993. Germicidin, an autoregulative germination inhibitor of *Streptomyces viridochromogenes* NRRL B-1551. *The Journal of antibiotics*, 46(7), pp.1126–1138.

Plocinska, R. *et al.*, 2012. Septal localization of *Mycobacterium tuberculosis* MtrB sensor kinase promotes MtrA regulon expression. *Journal of Biological Chemistry*. 6;287(28), pp.23887-99.

Plocinska, R. *et al.*, 2014. *Mycobacterium tuberculosis* MtrB Sensor Kinase Interactions with FtsI and Wag31 Proteins Reveal a Role for MtrB Distinct from That Regulating MtrA Activities. *Journal of Bacteriology*, 196(23), pp.4120–4129.

- Potter, C.A. *et al.*, 2002. Expression, Purification and Characterisation of Full-length Histidine Protein Kinase RegB from *Rhodobacter sphaeroides*. *Journal of Molecular Biology*, 320(2), pp.201–213.
- Procópio, R.E. de L. *et al.*, 2012. Antibiotics produced by *Streptomyces*. *Brazilian Journal of Infectious Diseases*, 16, pp.466–471.
- Prost, L.R. *et al.*, 2007. Activation of the bacterial sensor kinase PhoQ by acidic pH. *Molecular cell*, 26(2), pp.165–174.
- Provvedi, R. *et al.*, 2009. Global transcriptional response to vancomycin in *Mycobacterium tuberculosis*. *Microbiology*, 155(4), 1093-102.
- Pullan, S.T. *et al.*, 2011. Genome-wide analysis of the role of GlnR in *Streptomyces venezuelae* provides new insights into global nitrogen regulation in actinomycetes. *BMC Genomics*, 12(1), p.175.
- Purushotham, G. *et al.*, 2015. Mycobacterium tuberculosis oriC sequestration by MtrA response regulator. *Molecular microbiology*, 98(3), pp.586–604. Available at: <http://www.ncbi.nlm.nih.gov/pmc/articles/PMC4700885/>.
- Qin, Z. *et al.*, 2017. Formicamycins, antibacterial polyketides produced by *Streptomyces formicae* isolated from African Tetraponera plant-ants. *Chemical science*, 8(4). pp3218-3227.
- Quintana, E.T. *et al.*, 2008. *Streptomyces sudanensis* sp. nov., a new pathogen isolated from patients with actinomycetoma. *Antonie van Leeuwenhoek*, 93(3), pp.305–313.
- Raghavan, V. & Groisman, E.A., 2010. Orphan and hybrid two-component system proteins in health and disease. *Current opinion in microbiology*, 13(2), pp.226–231.
- Raja, A. & Prabakarana, P., 2011. Actinomycetes and drug-an overview. *American Journal of Drug Discovery and Development*, 1(2), pp.75–84.

Ramesh, A. *et al.*, 2012. The Mechanism for RNA Recognition by ANTAR Regulators of Gene Expression W. F. Burkholder, ed. *PLoS Genetics*, 8(6), p.e1002666.

Ramos, S., *et al.*, 2015. Effect of vancomycin on the proteome of the multiresistant *Enterococcus faecium* SU18 strain. *Journal of Proteomics*, 113, 378–387.

Rampelotto, P.H., 2013. Extremophiles and Extreme Environments. *Life: Open Access Journal*, 3(3), pp.482–485.

Redenbach, M. *et al.*, 1993. The *Streptomyces lividans* 66 chromosome contains a 1 MB deletogenic region flanked by two amplifiable regions. *Molecular and General Genetics MGG*, 241(3), pp.255–262.

Rico, S. *et al.*, 2014. Regulation of the AbrA1/A2 Two-Component System in *Streptomyces coelicolor* and the Potential of Its Deletion Strain as a Heterologous Host for Antibiotic Production. P. Hoskisson, ed. *PLoS ONE*, 9(10), p.e109844.

Riedlinger, J. *et al.*, 2006. Auxofuran, a Novel Metabolite That Stimulates the Growth of Fly Agaric, Is Produced by the Mycorrhiza Helper Bacterium *Streptomyces* Strain AcH 505. *Applied and Environmental Microbiology*, 72(5), pp.3550–3557.

Rigali, S. *et al.*, 2008. Feast or famine: the global regulator DasR links nutrient stress to antibiotic production by *Streptomyces*. *EMBO reports*, 9(7), pp.670–675.

Rivera-Cancel, G. *et al.*, 2014. Full-length structure of a monomeric histidine kinase reveals basis for sensory regulation. *Proceedings of the National Academy of Sciences*, 111(50), p.17839 LP-17844.

Rodríguez-García, A. *et al.*, 2007. Genome-wide transcriptomic and proteomic analysis of the primary response to phosphate limitation in *Streptomyces coelicolor* M145 and in a Δ phoP mutant. *PROTEOMICS*, 7(14), pp.2410–2429.

- Rodríguez, H. *et al.*, 2013. Two-component systems in *Streptomyces*: key regulators of antibiotic complex pathways. *Microbial cell factories*, 12, p.127.
- Rodríguez, H. *et al.*, 2015. The two kinases, AbrC1 and AbrC2, of the atypical two-component system AbrC are needed to regulate antibiotic production and differentiation in *Streptomyces coelicolor*. *Frontiers in Microbiology*, 6, p.450.
- Rothenbücher, M.C. *et al.*, 2006. The Cytoplasmic C-Terminal Domain of the *Escherichia coli* KdpD Protein Functions as a K⁺ Sensor. *Journal of Bacteriology*, 188(5), p.1950 LP-1958.
- Rowland, M.A. & Deeds, E.J., 2014. Crosstalk and the evolution of specificity in two-component signaling. *Proceedings of the National Academy of Sciences*, 111(15), pp.5550–5555.
- Roychoudhury, S. *et al.*, 1993. Inhibitors of two-component signal transduction systems: inhibition of alginate gene activation in *Pseudomonas aeruginosa*. *Proceedings of the National Academy of Sciences*, 90(3), p.965 LP-969.
- Rutledge, P.J. & Challis, G.L., 2015. Discovery of microbial natural products by activation of silent biosynthetic gene clusters. *Nature Reviews Microbiology*, 13, p.509.
- Ryndak, M., Wang, S. & Smith, I., 2008. PhoP, a key player in *Mycobacterium tuberculosis* virulence. *Trends in Microbiology*, 16(11), pp.528–534.
- Ryding, N.J., Anderson, T.B. & Champness, W.C., 2002. Regulation of the *Streptomyces coelicolor* Calcium-Dependent Antibiotic by *absA*, Encoding a Cluster-Linked Two-Component System. *Journal of Bacteriology*, 184(3), pp.794–805.
- Salazar, M.E. & Laub, M.T., 2015. Temporal and evolutionary dynamics of two-component signaling pathways. *Current opinion in microbiology*, 24, pp.7–14.

A) Santos-Beneit, F. *et al.*, 2011. The RNA Polymerase Omega Factor RpoZ Is Regulated by PhoP and Has an Important Role in Antibiotic Biosynthesis and Morphological Differentiation in *Streptomyces coelicolor*. *Applied and Environmental Microbiology*, 77(21), pp.7586–7594.

B) Santos-Beneit, F., Barriuso-Iglesias, M., Fernández-Martínez, L. T., Martínez-Castro, M., Sola-Landa, A., Rodríguez-García, A., & Martín, J. F. (2011). The RNA Polymerase Omega Factor RpoZ Is Regulated by PhoP and Has an Important Role in Antibiotic Biosynthesis and Morphological Differentiation in *Streptomyces coelicolor*. *Applied and Environmental Microbiology*, 77(21), 7586–7594.

Santos-Beneit, F., Rodriguez-Garcia, A. & Martin, J.F., 2013. Identification of different promoters in the *absA1-absA2* two-component system, a negative regulator of antibiotic production in *Streptomyces coelicolor*. *Molecular genetics and genomics: MGG*, 288(1–2), pp.39–48.

Santos-Beneit, F. *et al.*, 2014. Transcriptional response to vancomycin in a highly vancomycin-resistant *Streptomyces coelicolor* mutant. *Future microbiology*, 9(5), pp.603–622.

Satomura, T. *et al.*, 2005. Enhancement of Glutamine Utilization in *Bacillus subtilis* through the GlnK-GlnL Two-Component Regulatory System. *Journal of Bacteriology*, 187(14), pp.4813–4821.

Schär, J., Sickmann, A. & Beier, D., 2005. Phosphorylation-Independent Activity of Atypical Response Regulators of *Helicobacter pylori*. *Journal of Bacteriology*, 187(9), pp.3100–3109.

Schatz, A., Bugle, E. & Waksman, S.A., 1944. Streptomycin, a Substance Exhibiting Antibiotic Activity Against Gram-Positive and Gram-Negative Bacteria. *Proceedings of the Society for Experimental Biology and Medicine*, 55(1), pp.66–69.

Schiffer, G. & Höltje, J.-V., 1999. Cloning and Characterization of PBP 1C, a Third Member of the Multimodular Class A Penicillin-binding Proteins of *Escherichia coli*. *Journal of Biological Chemistry*, 274(45), pp.32031–32039.

Schlimpert, S. *et al.*, 2017. Two dynamin-like proteins stabilize FtsZ rings during *Streptomyces* sporulation. *Proceedings of the National Academy of Sciences*. 114(30):E6176-E6183.

Schütze, E. *et al.*, 2014. Growth of streptomycetes in soil and their impact on bioremediation. *Journal of Hazardous Materials*, 267, pp.128–135.

Seipke, R.F., Kaltenpoth, M. & Hutchings, M.I., 2012. *Streptomyces* as symbionts: an emerging and widespread theme? *FEMS Microbiology Reviews*, 36(4), pp.862–876.

Seipke, R.F., Patrick, E. & Hutchings, M.I., 2014. Regulation of antimycin biosynthesis by the orphan ECF RNA polymerase sigma factor $\sigma_{\text{AntA V}}$. Souza, ed. *PeerJ*, 2, p.e253.

Sekurova, O.N. *et al.*, 2016. Activation of chloramphenicol biosynthesis in *Streptomyces venezuelae* ATCC 10712 by ethanol shock: insights from the promoter fusion studies. *Microbial cell factories*, 15, p.85.

Sengupta, S., Chattopadhyay, M.K. & Grossart, H.-P., 2013. The multifaceted roles of antibiotics and antibiotic resistance in nature. *Frontiers in microbiology*, 4, p.47.

Rico, Sergio *et al.* “Regulation of the AbrA1/A2 two-component system in *Streptomyces coelicolor* and the potential of its deletion strain as a heterologous host for antibiotic production” *PloS one* vol. 9,10 e109844.

Sexton, D.L. *et al.*, 2015. Resuscitation-Promoting Factors Are Cell Wall-Lytic Enzymes with Important Roles in the Germination and Growth of *Streptomyces coelicolor*. *Journal of Bacteriology*, 197(5), pp.848–860.

- Shah, I.M. *et al.*, 2008. A Eukaryotic-like Ser/Thr Kinase Signals Bacteria to Exit Dormancy in Response to Peptidoglycan Fragments. *Cell*, 135(3), pp.486–496.
- Sheeler, N.L., MacMillan, S. V & Nodwell, J.R., 2005. Biochemical Activities of the *absA*; Two-Component System of *Streptomyces coelicolor*; *Journal of Bacteriology*, 187(2), p.687 LP-696.
- Sheldon, P.J., Busarow, S.B. & Hutchinson, C.R., 2002. Mapping the DNA-binding domain and target sequences of the *Streptomyces peucetius* daunorubicin biosynthesis regulatory protein, DnrI. *Molecular Microbiology*, 44(2), pp.449–460.
- Shi, L. *et al.*, 2014. Evolution of Bacterial Protein-Tyrosine Kinases and Their Relaxed Specificity Toward Substrates. *Genome Biology and Evolution*, 6(4), pp.800–817.
- Shor, E. & Chauhan, N., 2015. A Case for Two-Component Signaling Systems As Antifungal Drug Targets. *PLOS Pathogens*, 11(2), p.e1004632.
- Shu, D. *et al.*, 2009. *afsQ1-Q2-sigQ* is a pleiotropic but conditionally required signal transduction system for both secondary metabolism and morphological development in *Streptomyces coelicolor*. *Applied Microbiology and Biotechnology*, 81(6), p.1149.
- Sidote, D.J. *et al.*, 2008. Structure of the *Staphylococcus aureus* AgrA LytTR Domain Bound to DNA Reveals a Beta Fold with a Novel Mode of Binding. *Structure (London, England: 1993)*, 16(5), pp.727–735.
- Skerker, J.M. *et al.*, 2005. Two-Component Signal Transduction Pathways Regulating Growth and Cell Cycle Progression in a Bacterium: A System-Level Analysis A. Arkin, ed. *PLoS Biology*, 3(10), p.e334.
- Skerker, J.M. *et al.*, 2008. Rewiring the specificity of two-component signal transduction systems. *Cell*, 133(6), pp.1043–1054.

- Sola-Landa, A. *et al.*, 2005. Binding of PhoP to promoters of phosphate-regulated genes in *Streptomyces coelicolor*: identification of PHO boxes. *Molecular Microbiology*, 56(5), pp.1373–1385.
- Sola-Landa, A. *et al.*, 2008. Target genes and structure of the direct repeats in the DNA-binding sequences of the response regulator PhoP in *Streptomyces coelicolor*. *Nucleic Acids Research*, 36(4), pp.1358–1368.
- Som, N.F. *et al.*, 2016. MtrA is an essential regulator that coordinates antibiotic production and development in *Streptomyces* species. *bioRxiv*.
- Som, N.F. *et al.*, 2017. The Conserved Actinobacterial Two-Component System MtrAB Coordinates Chloramphenicol Production with Sporulation in *Streptomyces venezuelae* NRRL B-65442. *Frontiers in microbiology*, 8, p.1145.
- Soncini, F.C., Vescovi, E.G. & Groisman, E.A., 1995. Transcriptional autoregulation of the *Salmonella typhimurium* phoPQ operon. *Journal of bacteriology*, 177(15), pp.4364–4371.
- Sorci, L. *et al.*, 2013. Quinolinate Salvage and Insights for Targeting NAD Biosynthesis in Group A Streptococci. *Journal of Bacteriology*, 195(4), pp.726–732.
- Sousa, J.A. de J. & Olivares, F.L., 2016. Plant growth promotion by streptomycetes: ecophysiology, mechanisms and applications. *Chemical and Biological Technologies in Agriculture*, 3(1), p.24.
- Stephenson, K. & Hoch, J.A., 2002. MicroReview Evolution of signalling in the sporulation phosphorelay., pp.297–304.
- Stock, A., Koshland, D.E. & Stock, J., 1985. Homologies between the *Salmonella typhimurium* CheY protein and proteins involved in the regulation of chemotaxis, membrane protein synthesis, and sporulation. *Proceedings of the National Academy of Sciences of the United States of America*, 82(23), pp.7989–7993.

- Stock, A.M., Robinson, V.L. & Goudreau, P.N., 2000. Two-Component Signal Transduction. *Annual Review of Biochemistry*, 69(1), pp.183–215.
- Studier, F.W. & Moffatt, B.A., 1986. Use of bacteriophage T7 RNA polymerase to direct selective high-level expression of cloned genes. *Journal of molecular biology*, 189(1), pp.113–130.
- Suroto, D.A. *et al.*, 2018. Characterization of the biosynthetic gene cluster for cryptic phthoxazolin A in *Streptomyces avermitilis*. *PloS one*, 13(1), pp.e0190973–e0190973.
- Szurmant, H., White, R.A. & Hoch, J.A., 2007. Sensor complexes regulating two-component signal transduction. *Current opinion in structural biology*, 17(6), pp.706–715.
- Tabatabai, N. & Forst, S., 1995. Molecular analysis of the two-component genes, *ompR* and *envZ*, in the symbiotic bacterium *Xenorhabdus nematophilus*. *Molecular microbiology*, 17(4), pp.643–652.
- Tabib-Salazar, A. *et al.*, 2013. The actinobacterial transcription factor RbpA binds to the principal sigma subunit of RNA polymerase. *Nucleic Acids Research*, 41(11), pp.5679–5691.
- Tahlan, K. *et al.*, 2008. Ligand recognition by ActR, a TetR-like regulator of actinorhodin export. *Journal of molecular biology*, 383(4), pp.753–761.
- Takano, E. *et al.*, 2001. A complex role for the gamma-butyrolactone SCB1 in regulating antibiotic production in *Streptomyces coelicolor* A3(2). *Molecular microbiology*, 41(5), pp.1015–1028.
- Tanaka, A. *et al.*, 2007. AfsR Recruits RNA Polymerase to the *afsS* Promoter: A Model for Transcriptional Activation by SARPs. *Journal of Molecular Biology*, 369(2), pp.322–333.

- Tao, H. *et al.*, 2010. Purifying natively folded proteins from inclusion bodies using sarkosyl, Triton X-100, and CHAPS. *BioTechniques*, 48(1), pp.61–64.
- Tarkka, M.T. *et al.*, 2008. Plant behavior upon contact with Streptomycetes. *Plant Signaling & Behavior*, 3(11), pp.917–919.
- Terpe, K., 2003. Overview of tag protein fusions: from molecular and biochemical fundamentals to commercial systems. *Applied Microbiology and Biotechnology*, 60(5), pp.523–533.
- Thomas, K.J. & Rice, C. V., 2014. Revised Model of Calcium and Magnesium Binding to the Bacterial Cell Wall. *Biometals: an international journal on the role of metal ions in biology, biochemistry, and medicine*, 27(6), pp.1361–1370.
- Tiwari, S. *et al.*, 2017. Two-Component Signal Transduction Systems of Pathogenic Bacteria As Targets for Antimicrobial Therapy: An Overview. *Frontiers in Microbiology*, 8, p.1878.
- Tokala, R.K. *et al.*, 2002. Novel Plant-Microbe Rhizosphere Interaction Involving *Streptomyces lydicus*; WYEC108 and the Pea Plant. *Applied and Environmental Microbiology*, 68(5), p.2161 LP-2171.
- Traag, B.A. & van Wezel, G.P., 2008. The SsgA-like proteins in actinomycetes: small proteins up to a big task. *Antonie Van Leeuwenhoek*, 94(1), pp.85–97.
- Trajtenberg, F. *et al.*, 2014. Allosteric Activation of Bacterial Response Regulators: the Role of the Cognate Histidine Kinase Beyond Phosphorylation. *mBio*, 5(6).
- Uchida, T., Miyawaki, M. & Kinashi, H., 2003. Chromosomal Arm Replacement in *Streptomyces griseus*. *Journal of Bacteriology*, 185(3), p.1120 LP-1124.
- Uguru, G.C. *et al.*, 2005. Transcriptional activation of the pathway-specific regulator of the actinorhodin biosynthetic genes in *Streptomyces coelicolor*. *Molecular Microbiology*, 58(1), pp.131–150.

Ulijasz A. T., Weisblum B. (1999). Dissecting the VanRS signal transduction pathway with specific inhibitors. *J. Bacteriol.* 181 627–631.

Ulrich, L.E., Koonin, E. V & Zhulin, I.B., 2005. One-component systems dominate signal transduction in prokaryotes. *Trends Microbiol*, 13.

Utsumi, R. & Igarashi, M., 2012. Two-component signal transduction as attractive drug targets in pathogenic bacteria. *Yakugaku zasshi: Journal of the Pharmaceutical Society of Japan*, 132(1), pp.51–58.

van Wezel, G.P. & McDowall, K.J., 2011. The regulation of the secondary metabolism of *Streptomyces*: new links and experimental advances. *Natural Product Reports*, 28(7), p.1311.

Velikova, Nadya *et al.*, 2016. Putative histidine kinase inhibitors with antibacterial effect against multi-drug resistant clinical isolates identified by *in vitro* and *in silico* screens *Scientific reports* vol. 6 26085.

Verhamme, D.T. *et al.*, 2002. Investigation of *in vivo* cross-talk between key two-component systems of *Escherichia coli*. *Microbiology*, 148(Pt 1), pp.69–78.

Viaene, T. *et al.*, 2016. *Streptomyces* as a plant's best friend? *FEMS Microbiology Ecology*, 92(8), p.fiw119-fiw119.

Vining, L.C., 1992. Secondary metabolism, inventive evolution and biochemical diversity — a review. *Gene*, 115(1), pp.135–140.

Waksman, S.A. & Woodruff, H.B., 1942. Streptothricin, a New Selective Bacteriostatic and Bactericidal Agent, Particularly Active Against Gram-Negative Bacteria. *Proceedings of the Society for Experimental Biology and Medicine*, 49(2), pp.207–210.

Waldburger, C.D. & Sauer, R.T., 1996. Signal detection by the PhoQ sensor-transmitter. Characterization of the sensor domain and a response-impaired mutant

that identifies ligand-binding determinants. *The Journal of biological chemistry*, 271(43), pp.26630–26636.

Wang, L. *et al.*, 2009. Autoregulation of antibiotic biosynthesis by binding of the end product to an atypical response regulator. *Proceedings of the National Academy of Sciences of the United States of America*, 106(21), pp.8617–8622.

Wang, S., (2012). Bacterial Two-Component Systems: Structures and Signaling Mechanisms Bacterial Two-Component Systems: Structures and Signaling Mechanisms. In C.B.T.-P.P in H.H. Huang (Ed.)(p.Ch.1 15). Rijeka: InTech.

A) Wang, C. *et al.*, 2013. Mechanistic Insights Revealed by the Crystal Structure of a Histidine Kinase with Signal Transducer and Sensor Domains. *PLOS Biology*, 11(2), p.e1001493.

B) Wang, R. *et al.*, 2013. Identification of two-component system AfsQ1/Q2 regulon and its cross-regulation with GlnR in *Streptomyces coelicolor*. *Molecular Microbiology*, 87(1), pp.30–48.

Wang, F. *et al.*, 2018. Insights into Key Interactions between Vancomycin and Bacterial Cell Wall Structures. *ACS omega*, 3(1), pp.37–45.

Watanabe, T. *et al.*, 2008. Inhibitors Targeting Two-Component Signal Transduction BT- Bacterial Signal Transduction: Networks and Drug Targets. In R. Utsumi, ed. New York, NY: Springer New York, pp. 229–236.

Watve, M.G. *et al.*, 2001. How many antibiotics are produced by the genus *Streptomyces*? *Archives of Microbiology*, 176(5), pp.386–390.

Weber, T. *et al.*, 2015. antiSMASH 3.0—a comprehensive resource for the genome mining of biosynthetic gene clusters. *Nucleic Acids Research*, 43(W1), pp.W237–W243.

- Weiss, V. & Magasanik, B., 1988. Phosphorylation of nitrogen regulator I (NRI) of *Escherichia coli*. *Proceedings of the National Academy of Sciences of the United States of America*, 85(23), pp.8919–8923.
- White, J. & Bibb, M., 1997. *bldA* dependence of undecylprodigiosin production in *Streptomyces coelicolor* A3(2) involves a pathway-specific regulatory cascade. *Journal of Bacteriology*, 179(3), pp.627–633.
- Widenbrant, E.M. *et al.*, 2007. *Streptomyces coelicolor* Undergoes Spontaneous Chromosomal End Replacement. *Journal of Bacteriology*, 189(24), p.9117 LP-9121.
- Wietzorrek, A. & Bibb, M., 1997. A novel family of proteins that regulates antibiotic production in streptomycetes appears to contain an OmpR-like DNA-binding fold. *Molecular Microbiology*, 25(6), pp.1181–1184.
- Wildermuth, H. & Hopwood, D.A., 1970. Septation During Sporulation in *Streptomyces coelicolor*. *Microbiology*, 60(1), pp.51–59.
- Willemse, J. *et al.*, 2011. Positive control of cell division: FtsZ is recruited by SsgB during sporulation of *Streptomyces*. *Genes & Development*, 25(1), pp.89–99.
- Willey, J.M. *et al.*, 2006. Morphogenetic surfactants and their role in the formation of aerial hyphae in *Streptomyces coelicolor*. *Molecular Microbiology*, 59(3), pp.731–742.
- Williams, R.H.N. & Whitworth, D.E., 2010. The genetic organisation of prokaryotic two-component system signalling pathways. *BMC Genomics*, 11(1), p.720.
- Wojnowska, M. *et al.*, 2013. Autophosphorylation Activity of a Soluble Hexameric Histidine Kinase Correlates with the Shift in Protein Conformational Equilibrium. *Chemistry & Biology*, 20(11), pp.1411–1420.

Wright, Gerard D., *et al.*, 1993. Purification and characterization of VanR and the cytosolic domain of VanS: a two-component regulatory system required for vancomycin resistance in *Enterococcus faecium* BM4147." *Biochemistry* 32(19), pp 5057-5063.

Xie, W. *et al.*, 2010. Structure of the Cytoplasmic Segment of Histidine Kinase Receptor QseC, a Key Player in Bacterial Virulence. *Protein and peptide letters*, 17(11), pp.1383–1391.

Xing, D. *et al.*, 2017. Asymmetric Structure of the Dimerization Domain of PhoR, a Sensor Kinase Important for the Virulence of *Mycobacterium tuberculosis*. *ACS Omega*, 2(7), pp.3509–3517.

Xu, Q. *et al.*, 2007. Chemotaxis mediated by NarX–FrzCD chimeras and nonadapting repellent responses in *Myxococcus xanthus*. *Molecular Microbiology*, 66(6), pp.1370–1381.

Xu, G. *et al.*, 2010. “Pseudo” γ -Butyrolactone Receptors Respond to Antibiotic Signals to Coordinate Antibiotic Biosynthesis. *Journal of Biological Chemistry*, 285(35), pp.27440–27448.

Xu, Y. & Vetsigian, K., 2017. Phenotypic variability and community interactions of germinating *Streptomyces* spores. *Scientific Reports*, 7, p.699.

Yagüe, P. *et al.*, 2016. Subcompartmentalization by cross-membranes during early growth of *Streptomyces* hyphae. *Nature Communications*, 7, p.12467

Yeo, K.J. *et al.*, 2014. Mechanism of the pH-Induced Conformational Change in the Sensor Domain of the DraK Histidine Kinase via the E83, E105, and E107 Residues. *PLOS ONE*, 9(9), p.e107168.

Yepes A, Rico S, Rodríguez-García A, Santamaría RI, Díaz M (2011) Novel Two-Component Systems Implied in Antibiotic Production in *Streptomyces coelicolor*. *PLoS ONE* 6(5): e19980.

- Yu, Z. *et al.*, 2012. Differential regulation of antibiotic biosynthesis by DraR-K, a novel two-component system in *Streptomyces coelicolor*. *Molecular microbiology*, 85(3), pp.535–556.
- Zaburannyi, N. *et al.*, 2014. Insights into naturally minimised *Streptomyces albus* J1074 genome. *BMC Genomics*, 15(1), p.97.
- Zahrt, T.C. & Deretic, V., 2000. An Essential Two-Component Signal Transduction System in *Mycobacterium tuberculosis*. *Journal of Bacteriology*, 182(13), pp.3832–3838.
- Zhang, P. *et al.*, 2017. Deletion of MtrA Inhibits Cellular Development of *Streptomyces coelicolor* and Alters Expression of Developmental Regulatory Genes. *Frontiers in Microbiology*, 8, p.2013.
- Zhang, C.-C., 2018. Bacterial signalling involving eukaryotic-type protein kinases. *Molecular Microbiology*, 20(1), pp.9–15.
- Zhou, L. *et al.*, 2003. Phenotype MicroArray Analysis of *Escherichia coli* K-12 Mutants with Deletions of All Two-Component Systems. *Journal of Bacteriology*, 185(16), p.4956 LP-4972.
- A) Zhou, Z. *et al.*, 2011. ECF sigma factor-associated regulatory networks in *Streptomyces colicolor* A3(2). *2011 IEEE International Workshop on Genomic Signal Processing and Statistics (GENSIPS)*, pp.182–185.
- B) Zhou, Z. *et al.*, 2011. The -omics Era- Toward a Systems-Level Understanding of *Streptomyces*. *Current genomics*, 12(6), pp.404–416.
- Zhou, Z. *et al.*, 2012. Genome plasticity and systems evolution in *Streptomyces*. *BMC bioinformatics*, 13 Suppl 10 (Suppl 10), ppS8–S8.
- Ziegler, M. & Oei, S.L., 2001. A cellular survival switch: poly(ADP-ribosyl)ation stimulates DNA repair and silences transcription. *BioEssays*, 23(6), pp.543–548.

Zschiedrich, C.P., Keidel, V. & Szurmant, H., 2016. Molecular mechanisms of two-component signal transduction. *Journal of molecular biology*, 428(19), pp.3752–3775.

Zhu, H., Sandiford, S.K. & van Wezel, G.P., 2014. Triggers and cues that activate antibiotic production by actinomycetes. *Journal of Industrial Microbiology & Biotechnology*, 41(2), pp.371–386.

Supplementary Material

S 1: All RRs as predicted by P2RP (Barakat, et al., 2013) found within listed *Streptomyces* species as classified by their effector domains.

<i>Streptomyces</i> <i>sp.</i>	OmpR	NarL	CheY	AmiR _NasR	TrxB	LytR	RsbU -like	IclR	Un- class- ified
<i>S. venezuelae</i> NRRL B- 65442	21	42	3	1	1	1	1	0	6
<i>S. coelicolor</i> A3(2)	22	51	2	1	1	1	2	2	5
<i>S. griseus</i> subs. <i>griseus</i> NBRC 12250	24	39	3	1	0	1	4	0	8
<i>S. albus</i> subs. <i>albus</i>	0	1	0	0	0	0	0	0	0
<i>S. avermitilis</i> MA-4680	25	35	2	1	0	1	2	2	5

```

AfsQ2 VTREHQGGTRGLAAARKGFWSGLRFTSLRLRLVLFVGLVALTAAVSASGIAYWLNREAVL 60
QseC -----MKFTQRLSLRVRLTLIFLILASVTWL-LSSFVAWKQTTDNV 40
      . : ***:*:*:*:* : * : : * : . * : :

AfsQ2 TRTQDAVLRDFEQEM-----QNRAGALPEHPTQDEVQHTAGQMANSSQRFVSVLLVAEN 113
QseC DELFDTQLMLFAKRLSTLDLNEINAADRMAQTPNR----LKHGHVDDALTFAIF----T 92
      . * : * * * : . : * * . : : * : . * : : : * : : .

AfsQ2 ADGTAVYGGSSGGLGGVALSDVPESLRTAVNKEQKLTSAKHPYHLYWQRITDDGTPYLVA 173
QseC HDGRMVLND-----GDNGEDI PYSYQREGFAD-GQLVGEDDPWRFVWMTSPDGKYRI-VV 145
      ** * .. * . : * * * : : : . . . * : : * * . * .

AfsQ2 GTKVIGGGPTGYMLKSLEPEAKDLNSLAWSLGIATALALLGSALLAQALATTVLPVHRL 233
QseC GQE-----WEYRE-DMALAIVAGQLIPWLVALPIMLIIM-----MVLLGRELAPLNKL 192
      * : * . : : : * : : * : : . * * * : : *

AfsQ2 GVAARRLGEGKLDTRLRVSGTDELADLSRTFNAAENLEKRVADMAGREQASRRFVADMS 293
QseC ALALRMRD-PDSEKPLNATGV-----PSEVRPLVESLNQLFARTHAMMVRERERTSDAA 245
      . : * * . . : . * . : * . . . * : : * . . * : : * :

AfsQ2 HELRTPLTALTAVTEVLEEELEYAGEGEGEGGSFDPMEPAVRLVVSETRRLNDLVENLM 353
QseC HELRSPLTALKVQTEVAQLSDDDPQARK-----KALLQLHSGIDRATRLVDQLL 294
      **** : ***** . * * : . : : * : : * * * . * : : *

AfsQ2 EVTRFDAGTARLVLDVDDVDVADQIT-----ACIDARAWLDAVDLDAERGVHARL 401
QseC TLSRLDSDLNLQDVAEIPLDLLQSSVMDIYHTAQQAKIDVRLTLNA-----HSIKRTG 348
      : * : * : : : * : * * * . * * * : : :

AfsQ2 DPRRLDVILANLIGNALKHGGSPVRVSVARADHEIVIRVRDNGPGIPEVDLPHVDFRFYK 461
QseC QPLLLSLLVRNLLDNAVRYS PQGSVVDVT--LNADNFIVRDNGPGVTPEALARIGERFYR 406
      : * * . : : * * : * : . * * : : : * * * * : : * : : * * :

AfsQ2 ASASRPRSEGSGLGLSIALENAHIHGGEITAENAPEGGAVFTLRLPQDPSPPADEDGGPD 521
QseC PPGQ--TATGSLGLSIVQRIAKLHG MNVEFGNAEQGGFEAKVSW----- 449
      . . : * * * * * . * : * * : : * * : * * . :

AfsQ2 EETEDRGKDAKGQV 535
QseC ----- 449

```

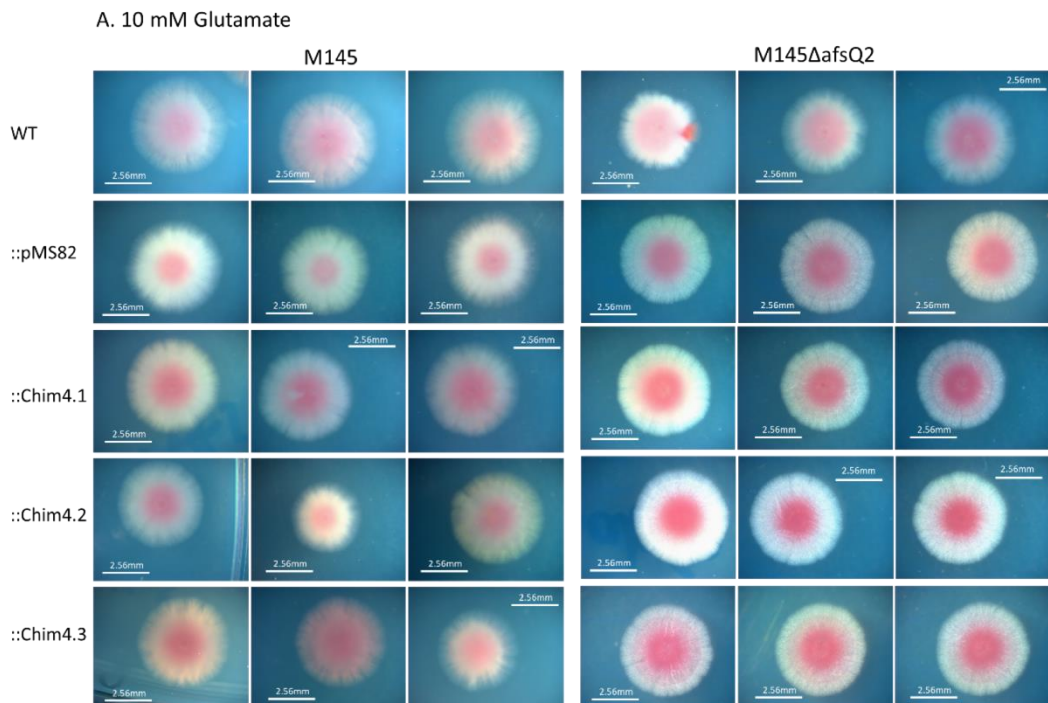
S 2: Alignment of SKs AfsQ2 from *S. coelicolor* and QseC from Enterobacteriaceae (NCBI Ref WP_000673402.1) using Clustal Omega. * refers to conservation of residue, : refers to conservation of strongly similar properties, . refers to conservation of weakly similar properties. The domains are highlighted as follows, blue text denotes sensor domains, red text denotes TM helices (as predicted by ExPasy TMPred), underlined text denotes HAMP domain (as predicted by P2RP; Barakat, *et al.*, 2013), green text denotes Dhp domain and orange text denotes CA domain.

S 3: Sequences of chimeras designed in chapter 5. Chimeras of SKs VanS and AfsQ2 from *S. coelicolor*. Underlined sequences are restriction sites, red sequences are promoters and ribosome binding sites and black text is the chimera sequence.

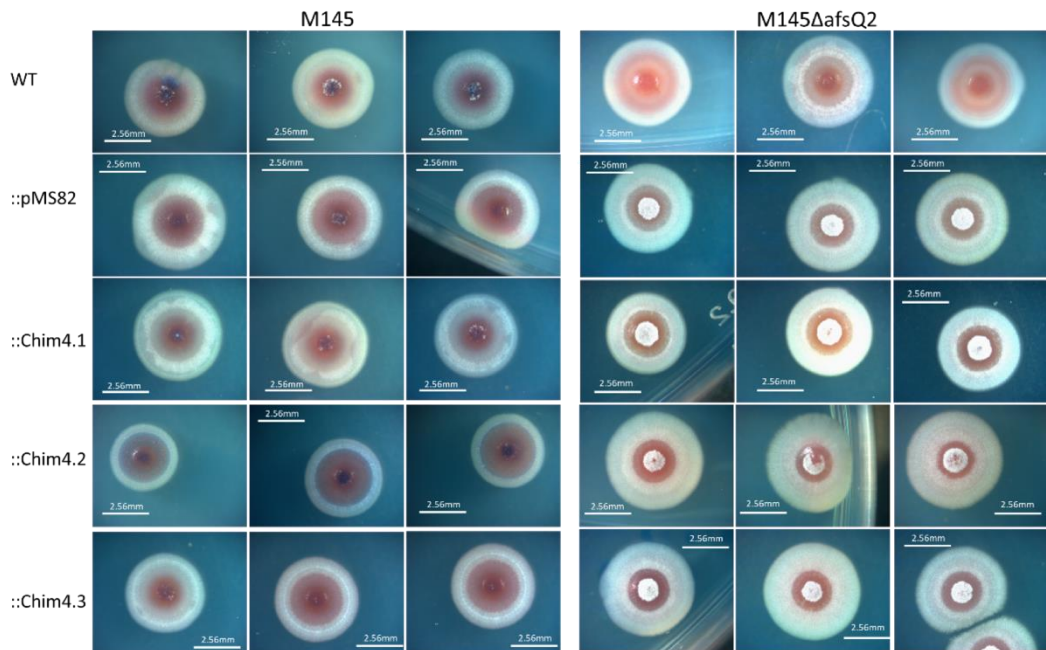
Chimera	Sequence
1	<p><u>TCTAGAGACAGCCGTCTCCGAGCCGGTGTGGCGCCGGTGCGGCCGAC</u> <u>GGTGGTGAGACTGCTGGCGCTGGCGCTGGCGCTGGTGGCGTTGGCAGC</u> <u>GCTGGTGGTGAGGTCTGACGCATACGCCAGTGAACGCGGCAGCGTGT</u> <u>TGCCGGCACGTATGCGGTTTTTCGATATGCCGACGATATGTGGCGACTC</u> <u>GTAATCTCGACCATATGGATAGGCGCCCCGGTCTGAGCGTCCGCCTCA</u> AGCTCACCTCAGCTACGCGGATTCTGACACTCGCGGGCGTCTGC TGCTCGTGGCCGTGGGAGTGTTCCTCCTGGACCAGGGCTGGTTGCTCA CCAACGAACGGGGGGCGGTGAGAGCGACTCCGGGCACAGTCTTCCTT CGCAGTTTCGCCCCACGGCAGCCCTGGGGATCGCCACCGCGCTCGCC CTGCTCGGCTCCGCGCTGCTCGCGCAGGCCCTGGCGACGACCGTGTG AAGCCCGTGCACCGGCTCGGGGTGCGGGCGCGGCGGCTGGGCGAGGG GAAGCTGGACACCCGGCTGCGGGTGTCCGGCACCGACGAACCTGGCCG ACCTGTGCGGACGTTCAACAGTGCCGCCGAGAACCTGGAGAAGCGG GTCGCGGACATGGCGGGGCGGAGCAGGCCCTCGCGGCGCTTCGTGCG GGACATGAGCCACGAGCTGCGTACGCCGCTGACGGCGCTCACCGCGG TGACGGAAGTGTGGAGGAGGAGCTGGAGTACGCGGGCGAGGGCGAG GGGAGGGCGGGAGTTTCGACCCGATGGTCGAGCCCGCGGTGCGGCT GGTGGTGAGCGAGACGCGACGGCTGAACGACCTGGTGGAGAACCTGA TGGAGGTCACCCGCTTCGACGCGGGCACCGCGGGCTGGTCTGGACG ACGTCGACGTCGCGGACCAGATCACCGCCTGCATCGACGCCGGGCT GGCTGGACGCCGTCGACCTGGACGCCGAGCGCGGCGTCCACGCCCGC CTCGACCCGCGCCGGCTGGACGTCATCCTCGCCAACCTGATCGGCAAC GCGCTCAAGCACGGCGGGTCCCGGTCAGGGTGTCCGTGGCGCGGGC GGACCACGAGATCGTCATCCGGGTGCGGGACAACGGTCCCGGCATCC CCGAGGACGTCCTGCCGCACGTCTTCGACCGCTTCTACAAGGCGAGCG CCTCCCGGCCGCGCTCCGAGGGCAGCGGGCTCGGTCTGTCCATCGCCC TGGAGAACGCGCACATCCACGGCGGTGAGATCACCGCGGAGAACGCC CCGAGGGCGGTGCGGTGTTACCCTGCGGCTGCCGCAGGACCCGTCG CCGCCCCCGGACGAGGACGGCGGGCCCGACGAGGAGACCGAGGACCG GGCAAGGACGCGAAGGGACAGGTCTGAGAATTC</p>
2	<p><u>TCTAGAGACAGCCGTCTCCGAGCCGGTGTGGCGCCGGTGCGGCCGAC</u> <u>GGTGGTGAGACTGCTGGCGCTGGCGCTGGCGCTGGTGGCGTTGGCAGC</u> <u>GCTGGTGGTGAGGTCTGACGCATACGCCAGTGAACGCGGCAGCGTGT</u> <u>TGCCGGCACGTATGCGGTTTTTCGATATGCCGACGATATGTGGCGACTC</u> <u>GTAATCTCGACCATATGGATAGGCGCCCCGGTCTGAGCGTCCGCCTCA</u> AGCTCACCTCAGCTACGCGGATTCTGACACTCGCGGGCGTCTGC TGCTCGTGGCCGTGGGAGTGTTCCTCCTGGACCAGGGCTGGTTGCTCA CCAACGAACGGGGGGCGGTGAGAGCGACTCCGGGCACAGTCTTCCTT CGCAGTTTCGCCCCACGGCAGCCTGGGTGTCATGGCGTTTCCTCGGTG TTCGGCCTCGTGGGCGGCTGGTTCCTCGCCGACGCATGCTCGCCCC CTGGACCGCATCACCGAGGCCACCCGCACGGCGGCGACCGGATCCCTC TCCCACCGCATCCGGCTGCCGGGCCGAGGGACGAGTACCGAGA CGCCGATGCCTTCGACGAGATGCTCGCCCGCCTCGAAGCCCACGTGGC CCAGGCTCGCGGCGCTTCGTGCGGACATGAGCCACGAGCTGCGTAC GCCGCTGACGGCGCTCACCGCGGTGACGGAAGTGTGGAGGAGGAGC TGGAGTACGCGGGCGAGGGCGAGGGGGAGGGCGGGAGTTTCGACCCG ATGGTCGAGCCCGCGGTGCGGCTGGTGGTGAGCGAGACGCGACGGCT GAACGACCTGGTGGAGAACCTGATGGAGGTCACCCGCTTCGACGCGG GCTCCTTCACCCGGGAACAGGTGACATGTCCCTCCTCGCGGAGGAAG CCACCGAGACCCTGCTCCCCTTCGCGGAGAAGCACGGTGTACCCCTCG AGACCAGGGGCCACGTAACCCTCGCCCTCGGATCACCGGCCCTCCTCC TCCAACGACCGAACCTCGTCCACAACGCGATCGTCCACAACCTCC</p>

	<p>CCGGCCGGGGCAGAGTCTGGATCCACACCGCCGCGCCGCCCCCGCACC ACGCGGCTCGTCGTCGAGAACACCGGCGACCTGATCAGCCCCACCAG GCCTCGACCCTCACCGAACCTTCCAGCGTGGCACCGAACGCATACAC ACCGACCACCCCGGCGTCGGCCTGGGCCTGGCCATCGTCAACACCATC ACCCAGGCCCATGACGGCACCCCTCACCCACGCCACAGCGGG GGCCTCCGCGTCACGGTGGAGCTGCCCCGCGCCGCTCCGCACACCGGC AGGTGAGAATTC</p>
3	<p><u>AAGCCTGTTGTGGGCTGGACAATCGTGCCGGTTGGTAGGATCCAGCGC</u> <u>ATATGGATAGGCGCCCCGGTCTGAGCGTCCGCCTCAAGCTCACCCCTCA</u> GCTACGCGGGATTCTGACACTCGCGGGCGTCCTGCTGCTCGTGGCCG TGGGAGTGTTCTCTGGACCAGGGCTGGTTGCTACCAACGAACGGG GGGCGGTGAGAGCGACTCCGGGCACAGTCTTCTTCGCAGTTTCGCCC CCACGGCAGCCTGGGTCATGGCGTTCCTCCTGGTGTTCGGCCTCGTGG GCGGCTGGTTCCTCGCCGGACGCATGCTCGCCCCCTGGACCGCATCA CCGAGGCCACCCGCACGGCGGGCACC GGATCCCTCTCCACCGCATCC GGCTGCCGGGCCGACGGGACGAGTACCGAGAACTCGCCGATGCCTTC GACGAGATGCTCGCCCGCCTCGAAGCCACGTGGCCGAACAGCGGGC CTTCGCGGCCAACGCCTCGCACGAGCTGCGCACCCCGCTGACCGCCCTC GAAGGCCGTGCTCGACGTGGCCCCGACCGACCCGACCGACCGCCCG GCGAGATCATCGACCGCCTCCACGCCGTGAACACCAGGGCGATCGAC CTCACCGAGGCCCTGCTCCTGCTCAGCCGCGCCGGCCAGCGCTCCTTC ACCCGGGAACAGGTGACATGTCCCTCCTCGCGGAGGAAGCCACCGA GACCCTGCTCCCCTTCGCGGAGAAGCACGGTGTACCCCTCGAGACCAG GGGCCACGTAACCCTCGCCCTCGGATCACCGGCCCTCCTCCTCAACT GACCACGAACCTCGTCCACAACGCGATCGTCCACAACCTCCCCGGCCG GGCAGAGTCTGGATCCACACCGCCGCGCCGCCCCCGCACCACGCGGCT CGTCGTCGAGAACACCGGCGACCTGATCAGCCCCACCAGGCCTCGAC CCTCACCGAACCTTCCAGCGTGGCACCGAACGCATACACACCGACCA CCCCGGCGTCGGCCTGGGCCTGGCCATCGTCAACACCATCACCCAGGC CCATGACGGCACCCCTCACCCCTACCCACGCCACAGCGGGGGCCTCCG CGTCACGGTGGAGCTGCCCCGCGCCGCTCCGCACACCGGCAGGTGAG GTACC</p>
4	<p><u>AAGCCTGTTGTGGGCTGGACAATCGTGCCGGTTGGTAGGATCCAGCGC</u> <u>ATATGGATAGGCGCCCCGGTCTGAGCGTCCGCCTCAAGCTCACCCCTCA</u> GCTACGCGGGATTCTGACACTCGCGGGCGTCCTGCTGCTCGTGGCCG TGGGAGTGTTCTCTGGACCAGGGCTGGTTGCTACCAACGAACGGG GGGCGGTGAGAGCGACTCCGGGCACAGTCTTCTTCGCAGTTTCGCCC CCACGGCAGCCTGGGTCATGGCGTTCCTCCTGGTGTTCGGCCTCGTGG GCGGCTGGTTCCTCGCCGGACGCATGCTCGCCCCCTGGACCGCATCA CCGAGGCCACCCGCACGGCGGGCACC GGATCCCTCTCCACCGCATCC GGCTGCCGGGCCGACGGGACGAGTACCGAGAACTCGCCGATGCCTTC GACGAGATGCTCGCCCGCCTCGAAGCCACGTGGCCGAACAGCGGGC CTTCGCGGCCAACGCCTCGCACGAGCTGCGCACCCCGCTGACCGCCCTC GAAGGCCGTGCTCGACGTGGCCCCGACCGACCCGACCGACCGCCCG GCGAGATCATCGACGAGCTCCACGCCGTGAACACCAGGGCGATCGAC CTCACCGAGGCCCTGCTCCTGCTCAGCCGCGCCGGCCAGCGCTCCTTC ACCCGGGAACAGGTGACATGTCCCTCCTCGCGGAGGAAGCCACCGA GACCCTGCTCCCCTTCGCGGAGAAGCACGGTGTACCCCTCGAGACCAG GGGCCACGTAACCCTCGCCCTCGGATCACCGGCCCTCCTCCTCAACT GACCACGAACCTCGTCCACAACGCGATCGTCCACAACCTCCCCGGCCG GGCAGAGTCTGGATCCACACCGCCGCGCCGCCCCCGCACCACGCGGCT CGTCGTCGAGAACACCGGCGACCTGATCAGCCCCACCAGGCCTCGAC CCTCACCGAACCTTCCAGCGTGGCACCGAACGCATACACACCGACCA CCCCGGCGTCGGCCTGGGCCTGGCCATCGTCAACACCATCACCCAGGC CCATGACGGCACCCCTCACCCCTACCCACGCCACAGCGGGGGCCTCCG CGTCACGGTGGAGCTGCCCCGCGCCGCTCCGCACACCGGCAGGTGAG GTACC</p>

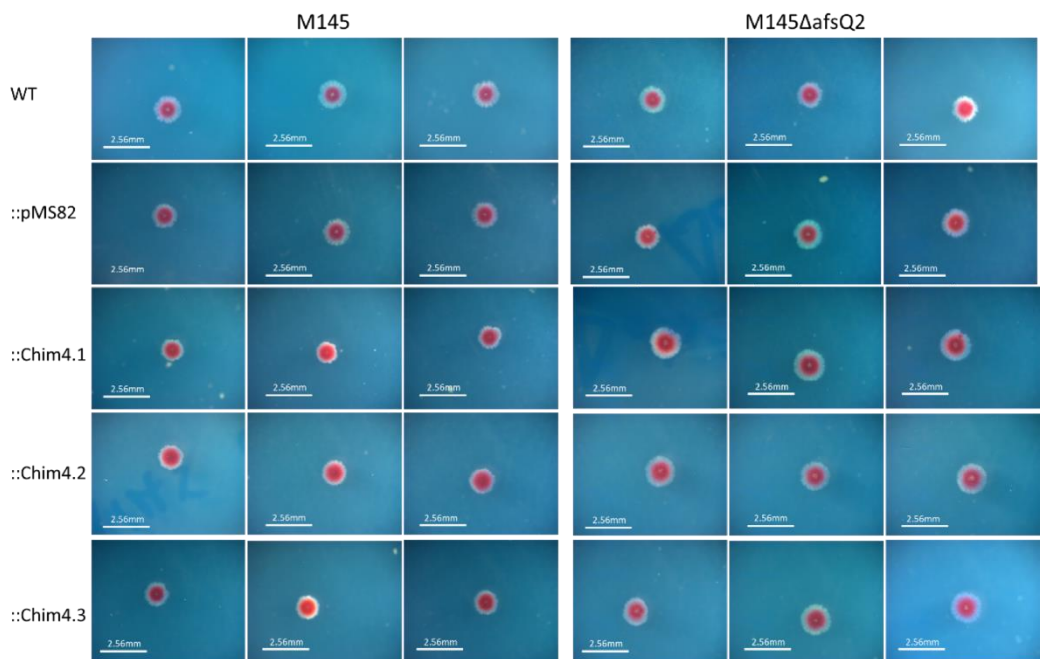
5	<p><u>AAGCCTGTTGTGGGCTGGACAATCGTGCCGGTTGGTAGGATCCAGGC</u> <u>ATATGGATAGGCGCCCCGGTCTGAGCGTCCGCCTCAAGCTCACCTCA</u> GCTACGCGGGATTCTGACTCGCGGGCGTCTGCTGCTCGTGGCCG TGGGAGTGTTCCTCCTGGACCAGGGCTGGTTGCTCACCAACGAACGGG GGGCGGTGAGAGCGACTCCGGGCACAGTCTTCCTTCGCAGTTTCGCCC CCACGGCAGCCTGGGTCATGGCGTTCCTCCTGGTGTTCGGCCTCGTGG GCGGCTGGTTCCTCGCCGGACGCATGCTCGCCCCCTGGACCGCATCA CCGAGGCCACCCGCACGGCGGCGACCGGATCCCTCTCCCACCGCATCC GGCTGCCGGGCCGCAGGGACGAGTACCGAGAACTCGCCGATGCCTTC GACGAGATGCTCGCCCCCTCGAAGCCCGGGAGGCCGAATCGCGGGCG CTTCGCGGCCGACGCCTCGCACGAGCTGCGCACCCCCGCTGACCGCCTC GAAGGCCGTGCTCGACGTGGCCCCGACCGACCCGCACCAGGACCCCG GCGAGATCATCGACGAGCTCCACGCCGTGAACACCAGGGCGATCGAC CTCACCGAGGCCCTGCTCCTGCTCAGCCGCGCCGGCCAGCGCTCCTTC ACCCGGGAACAGGTCGACATGTCCCTCCTCGCGGAGGAAGCCACCGA GACCCTGCTCCCCTTCGCGGAGAAGCACGGTGTACCCTCGAGACCAG GGCCACGTAACCCTCGCCCTCGGATCACCGGCCCTCCTCCTCAACT GACCACGAACCTCGTCCACAACGCGATCGTCCACAACCTCCCCGGCCG GGCAGAGTCTGGATCCACACCGCCGCGCCCGCCCGCACCACGCGGCT CGTCGTCGAGAACACCGGCGACCTGATCAGCCCCACCAGGCCTCGAC CCTACCGAACCCTTCCAGCGTGGCACCGAACGCATACACACCGACCA CCCCGGCGTCGGCCTGGGCTGGCCATCGTCAACACCATCACCCAGGC CCATGACGGCACCCCTACCCCTACCCACGCCACAGCGGGGGCCTCCG CGTACGGTGGAGCTGCCCGGGCCGCTCCGCACACCGGCAGGTGAG <u>GTACC</u></p>
---	---



B. 75 mM Glutamate



C. 10 mM Glutamate with 10 μg/ml vancomycin



S 4: Colony morphology comparison of Chim4 in *S. coelicolor* M145 Δ*afsQ2* (M145Δ*afsQ2*) grown on MM supplemented with glutamate as sole glutamate source for 9 days. C4.1-3 refer to isogenic strains. Three colonies are shown per plate. Each plate contained approximately 15-30 colonies. A. 7.5 mM glutamate B. 75 mM glutamate C. 7.5 mM glutamate and 10 μg/ml vancomycin.